Atomistic mechanism of cholesterol-dependent membrane activity of saponins with different glycosylation positions

糖修飾位置の異なるサポニン類の コレステロール依存的な膜活性機構の精密解析

Raymond Samson Malabed

Department of Chemistry
Graduate School of Science
Osaka University

2018

Atomistic mechanism of cholesterol-dependent membrane activity of saponins with different glycosylation positions

糖修飾位置の異なるサポニン類の コレステロール依存的な膜活性機構の精密解析

A Thesis Submitted to the
Graduate School of Science
Osaka University

In Partial Fulfillment of the Requirements for the Degree of
Doctor of Philosophy (Ph.D.) in Chemistry

By

Raymond Samson Malabed

Department of Chemistry
Graduate School of Science
Osaka University

2018

Abstract

Saponins are naturally occurring amphiphilic compounds derived from various plant and marine organisms. They are mainly composed of a hydrophobic sapogenin backbone which could be of steroid or triterpenoid in origin. On the other hand, the hydrophilic moiety is comprised of sugar groups attached to the sapogenin backbone via an ester or ether linkage. The structure of sapogenin ring and sugar moiety could differ for every saponin. In addition, the attached sugar moiety can also differ in terms of the number of saccharide units, branching of sugars and functionalization of some of its portion. These variations give each saponin a unique structure. Saponins have also been primarily used as foaming agents and ingredients in making soap. The pharmacological value of saponins has been cited in terms of its ability to reduce cardiovascular diseases and prevent cancer. Various saponins have already been subjected to structure-activity relationship studies including digitonin, soyasaponin Bb(I) and glycyrrhizin. These saponins have significant difference in their structures, but one common property is the presence of a sugar moiety attached to the C3 position of sapogenin backbone. However, some unusual saponins have already been isolated in plants such as OSW-1. OSW-1 is a structurally unique steroidal saponin isolated from the bulbs of the lily family *Ornithogalum saundersiae*, and has exhibited highly potent and selective cytotoxicity in tumor cell lines. OSW-1 contains an acylated disaccharide moiety attached to C16 of steroid backbone. This study aimed to investigate the atomistic mechanism for the membrane-permeabilizing activity of OSW-1 in comparison with those of other saponins by using various spectroscopic and microscopic approaches.

The membrane effect and hemolytic activity of OSW-1 were markedly enhanced in the presence of cholesterol. Binding affinity measurements using fluorescent cholestatrienol and solid-state NMR spectroscopy of a 3-*d*-cholesterol probe suggested that OSW-1 interacts with cholesterol in membrane without forming large aggregates while 3-*O*-glycosyl saponin, digitonin, forms cholesterol-containing large aggregates. Furthermore, the fluorescent probes of OSW-1 and lipids were also used in microscopic experiments to observe saponin-induced morphological changes and its effect on membrane integrity. The results suggest that digitonin exhibits detergent properties while OSW-1 promoted pore formation in a similar fashion with soyasaponin Bb(I). I hypothesized that OSW-1 induces formation of barrel stave like pores due to OSW-1/cholesterol interaction and likely causes membrane permeabilization without

destroying the whole membrane integrity. This observation could be partly responsible for its highly potent cytotoxicity.

Table of Contents

Abstract iii

Table of Contents v

List of Abbreviations viii

List of Figures x

Supporting Information List of Figures xii

Appendix List of Figures xii

List of Tables xiii

Supporting Information List of Tables xiii

List of Schemes xiii

Chapter 1
General Introduction

1.1 The Biological Membrane 1
- 1.1.1 Components of Biological Membranes 2
- 1.1.2 Organization of Biological Membranes 5
- 1.1.3 Membrane Dynamics 7
- 1.1.4 Lamellar Phase in Biological Membranes 8
- 1.1.5 Importance of Cholesterol and other Lipids in Membrane 9

1.2 Saponins and other amphiphiles 11
- 1.2.1 Saponins and its amphiphilic properties 12
- 1.2.2 Biosynthesis of saponins 15
- 1.2.3 Modes of interaction of membrane-active compounds 19
  - 1.2.3.1 Interaction of saponins with membrane lipids 23
  - 1.2.3.2 Interaction of saponins with eukaryotic cells 27
- 1.2.4 Biological activities of OSW-1 and other saponins 30

1.3 Methods used to investigate membrane interactions 36
- 1.3.1 NMR Spectroscopy 36
- 1.3.2 Fluorescence microscopic approaches 40
- 1.3.3 Other methods 42

1.4 Aim and Significance of the Study 43

References 45

Chapter 2
Sterol recognition and membrane-permeabilizing activity of saponins deduced from spectroscopic evidences

2.1 Introduction – The unique steroidal saponin OSW-1 51

2.2 Aim and significance 53

2.3 Results 54
2.3.1 Leakage properties of saponins 54
2.3.2 Hemolysis induced by saponins under Chol-depletion and osmotic protection 56
2.3.3 Binding of saponin to Chol in membrane by CTL fluorescence spectroscopy 59
2.3.4 Solid state ^{2}H NMR for investigating saponin/Chol interaction 61
2.3.5 Solid state ^{31}P NMR for investigating membrane integrity 62

2.4 Discussion 64

References 69

Chapter 3
Effect of saponins on membrane permeability and morphology as examined by fluorescence techniques

3.1 Introduction – Utilizing fluorescence probes 73

3.2 Aim and significance of the study 76

3.3 Results 76
3.3.1 Time-course leakage assays 76
3.3.2 Binding isotherm experiments 78
3.3.3 Membrane permeabilization and morphological changes induced by saponins examined by fluorescence microscopy 82
3.3.4 Distribution of DBD-OSW-1 in liposomes and changes in membrane morphology and integrity 87

3.4 Discussion 92

References 96

Chapter 4
General Discussion and Conclusions

4.1 General Discussion 99

4.2 Conclusions 101

Chapter 5
Experimental Section

5.1 Materials 103

5.2 Instrumentation 103

5.3 Experimental Methods 104
5.3.1 Calcein leakage assays 104
5.3.2 Parallel artificial membrane permeation assay (PAMPA) 105
5.3.3 Hemolytic activity under Chol depletion conditions and osmotic protection 107
5.3.4 CTL fluorescence spectroscopy 108
5.3.5 Dynamic light scattering 109
5.3.6 Solid-state ^{2}H NMR 109
5.3.7 Solid-state ^{31}P NMR 110
5.3.8 Fluorescence microscopy 110
5.3.9 Synthesis of Chol-*d* 111

References 112

Supporting Information I 113

Supporting Information II 123

Acknowledgment 129

Appendix 131

Reprint Permissions 135

Publications Related to Thesis 154

List of Abbreviations

Chol	cholesterol
Chol-*d*	3-*d*-cholesterol
Erg	ergosterol
Epichol	epicholesterol
CTL	cholestatrienol
PA	phosphatidic acid
PC	phosphatidylcholine
PE	phosphatidylethanolamine
PS	phosphatidylserine
PI	phosphatidylinositol
SM	sphingomyelin
GSL	glycosphingolipid
GlcCer	glucosylceramide
GalCer	galactosylceramide
LacCer	lactosylceramide
GPI	glycosylphosphatidylinositol
DOPC	1,2-dioleoyl-*sn*-glycero-3-phosphocholine
DMPC	1,2-dimyristoyl-*sn*-glycero-3-phosphocholine
DSPC	1,2-distearoyl-*sn*-glycero-3-phosphocholine
SOPC	1-stearoyl-2-oleoyl- *sn*-glycero-3-phosphocholine
POPC	1-palmitoyl-2-oleoyl- *sn*-glycero-3-phosphocholine
pSM	N-palmitoyl-D-*erythro*-sphingosylphosphorylcholine
sSM	N-stearoyl-D-*erythro*-sphingosylphosphorylcholine
TR-DPPE	Texas Red-1,2-dipalmitoyl-*sn*-glycero-3-phosphoethanolamine
DiI	1,1'-Dioctadecyl-3,3,3',3'-tetramethylindocarbocyanine perchlorate
S_o	solid phase
L_β	lamellar gel phase
L_α	liquid crystalline phase
L_d	liquid disordered phase
L_o	liquid ordered phase
P_β	ripple phase
T_m	transition temperature
MLV	multilamellar vesicle
SUV	small unilamellar vesicle
LUV	large unilamellar vesicle
GUV	giant unilamellar vesicle
NMR	nuclear magnetic resonance
EPR	electron paramagnetic resonance
SS-NMR	solid state nuclear magnetic resonance
^{2}H NMR	deuterium nuclear magnetic resonance
^{31}P NMR	phosphorous-31 nuclear magnetic resonance

Δν	quadrupolar splitting
Δσ	chemical shift anisotropy
S_{mol}	molecular order parameter
FRET	Förster resonance energy transfer
DSC	differential scanning calorimetry
SAR	structure-activity relationship
EC_{50}	half-maximal effective concentration
PAMPA	parallel artificial membrane permeation assay
P_e	effective permeability
CMC	critical micelle concentration
DPH	1,6-diphenyl-1,3,5-hexatriene
AFM	atomic force microscopy
DLS	dynamic light scattering
SEM	standard error of the mean
RBC	red blood cell
MβCD	methyl-β-cyclodextrin
PEG	polyethylene glycol
AMP	antimicrobial peptide
AM	amphidinol
AmB	amphotericin B
TNM-A	theonellamide-A
THP-1	human leukemic monocytic cell line
HeLa	human cervical cancer cell line
HL-60	human promyelocytic leukemia cell line
TIG	human fetal lung fibroblast

List of Figures

Figure 1-1.	A representation of biological membrane	2
Figure 1-2.	Representative structures of main classes of lipids	3
Figure 1-3.	The fluid mosaic model of the structure of cell membranes	6
Figure 1-4.	Movements of lipids in biological membrane	7
Figure 1-5.	Lipid phase in biological membranes	9
Figure 1-6.	Phase diagram for co-existence of phase-separated lipids in ternary system composed of DOPC/CHOL/PSM	11
Figure 1-7.	Examples for a steroid and triterpenic sapogenins	12
Figure 1-8.	Examples of common saponins of plant origin	13
Figure 1-9.	Saponins in aqueous solution	15
Figure 1-10.	Biosynthesis of 2,3-oxidosqualene via mevalonate pathway (MVA)	17
Figure 1-11.	Biosynthesis of steroidal and triterpenoid aglycones from common precursor 2,3-oxidosqualene	18
Figure 1-12.	Structures of common antimicrobial peptides	20
Figure 1-13.	Mechanism of barrel stave pore formation of antimicrobial peptides (AMPs)	21
Figure 1-14.	Mechanism of toroidal pore formation of antimicrobial peptides (AMPs)	21
Figure 1-15.	Carpet or detergent-type mechanism of antimicrobial peptides (AMPs)	22
Figure 1-16.	Mechanism of interaction of α-hederin	26
Figure 1-17.	Mechanism of interaction of 50 μM digitonin at various Chol concentration	31
Figure 1-18.	Structure of OSW-1	32
Figure 1-19.	Images of flowers and bulbs of *Ornithogalum saundersiae*	32
Figure 1-20.	Structure-activity relationship of OSW-1 towards tumor cells	33
Figure 1-21.	Three-dimensional structure of OSW-1	34
Figure 1-22.	Examples of unusual monodesmosidic and bidesmosidic saponins derived from plants and marine organisms	35
Figure 1-23.	^{2}H NMR spectra of sterol probes in the absence and presence of marine sponge cyclic peptide Theonellamide A (TNM-A)	38
Figure 1-24.	^{31}P NMR spectra of phospholipids at different phase	39
Figure 1-25.	Pore-forming properties of α-hederin (40 μM) on GUVs composed of DMPC/Chol (3:1)	41
Figure 1-26.	Effect of addition of 20 μM digitonin in GUVs composed of PC/Chol (80:20) at different incubation period	41
Figure 2-1.	Structure of OSW-1 and 3D space-filling representation of a derivative of OSW-1	51
Figure 2-2.	Structures of common saponins	52

Figure 2-3.	Sterol-dependent calcein-leakage from POPC liposomes by various saponins (100 μM)	55
Figure 2-4.	Hemolytic activity of saponins (300 μM) using non-depleted, cholesterol-depleted and cholesterol-repleted red blood cells	57
Figure 2-5.	Osmotic protection experiments for saponins using 1% (v/v) RBC	58
Figure 2-6.	Fluorescence intensities of cholestatrienol (CTL) at different saponin concentrations	60
Figure 2-7.	^{2}H NMR spectra of POPC/Chol-*d* bilayers in the absence and presence of saponins	62
Figure 2-8.	^{31}P NMR spectra of MLVs consisting of POPC/Chol (9:1) in the absence and presence of saponins	63
Figure 2-9.	Hypothetical mechanism for the membrane-permeabilizing effect of OSW-1 in Chol-containing membranes	68
Figure 3-1.	Common fluorescent probes	75
Figure 3-2.	Structure of OSW-1	75
Figure 3-3.	Time-course calcein leakage by treatment with digitonin and OSW-1	77
Figure 3-4.	Effect of lipid concentration on leakage properties of saponins	79
Figure 3-5.	Determination of $[S]_f$ and *r* as intercepts and slopes, respectively, at different leakage extents for digitonin and OSW-1	80
Figure 3-6.	Binding isotherms of digitonin and OSW-1 at different leakage extents	81
Figure 3-7.	Membrane disruptivity of the saponins	82
Figure 3-8.	Effect of addition of 30 μM OSW-1 in 2:2:1 DOPC/DMPC/Chol GUV	83
Figure 3-9.	Effect of addition of 30 μM digitonin in 2:2:1 DOPC/DMPC/Chol GUV	84
Figure 3-10.	Effect of addition of 30 μM soyasaponin Bb(I) in 2:2:1 DOPC/DMPC/Chol GUV	86
Figure 3-11.	Effect of addition of 30 μM glycyrrhizin in 2:2:1 DOPC/DMPC/Chol GUV	86
Figure 3-12.	Effect of 30 μM OSW-1 in 1:1 DOPC/DMPC GUV	88
Figure 3-13.	Effect of various concentration of OSW-1 in 2:2:1 DOPC/DMPC/Chol (20 mol% Chol)	89
Figure 3-14.	Effect of various concentration of OSW-1 in 9:9:2 DOPC/DMPC/Chol (10 mol% Chol)	90
Figure 3-15.	Effect of various concentration of OSW-1 in 19:19:2 DOPC/DMPC/Chol (5 mol% Chol)	91
Figure 5-1.	PAMPA sandwich set-up	106
Figure 5-2.	Glass slide set-up for electroformation of GUVs	111

Supporting Information List of Figures

Figure S1-1. Structures of trillin, diosgenin, and cholestatrienol 113
Figure S1-2. Average size of cholesterol-containing liposomes after incubation with various concentrations of OSW-1, digitonin, soyasaponin Bb(I), and glycyrrhizin 117
Figure S1-3. ^{2}H NMR spectra of Chol-d in POPC bilayer in the presence of soyasaponin Bb(I) and digitonin at various molar Chol/saponin ratio 119
Figure S1-4. ^{31}P NMR spectra of POPC in POPC/Chol 9:1 bilayers in the presence of soyasaponin Bb(I) and digitonin at various molar Chol/saponin ratio 120
Figure S2-1. Time-course calcein leakage by treatment with soyasaponin Bb(I) 123
Figure S2-2. Determination of $[S]_f$ and r as intercepts and slopes, respectively, at different leakage extents for soyasaponin Bb(I) 124
Figure S2-3. Binding isotherm of soyasaponin Bb(I) at different leakage extents 124
Figure S2-4. Concentration-response curves for digitonin, OSW-1 and soyasaponin Bb(I) at the incubation time of 10 min 125
Figure S2-5. Time-lapse image for 30 μM OSW-1 in 2:2:1 DOPC/DMPC/Chol (20 mol% Chol) 126
Figure S2-6. Time-lapse image for 30 μM OSW-1 in 9:9:2 DOPC/DMPC/Chol (10 mol% Chol) 127
Figure S2-7. Time-lapse image for 30 μM OSW-1 in 19:19:2 DOPC/DMPC/Chol (5 mol% Chol) 127

Appendix List of Figures

Appendix Figure 1. ^{1}H NMR spectrum of Chol in $CDCl_3$ 131
Appendix Figure 2. ^{1}H NMR spectrum of 5-cholesten-3-one in $CDCl_3$ 132
Appendix Figure 3. ^{1}H NMR spectrum of Chol-*d* in $CDCl_3$ 133
Appendix Figure 4. Summary of ^{1}H NMR spectrum of Chol (**1**), 5-cholesten-3-one (**2**) and Chol-*d* (**3**) in $CDCl_3$ 134

List of Tables

Table 2-1.	Calcein leakage activity of liposomes in the presence and absence of various sterols	55
Table 2-2.	Hemolytic activity of saponins under Chol depletion/repletion conditions	56
Table 2-3.	Osmotic protectants utilized for hemolytic assay and their estimated size	58
Table 2-4.	Estimated size of pores induced by saponin addition	58
Table 2-5.	Effect of saponin on size of LUVs (9:1 POPC/Chol)	61
Table 3-1.	EC_{50} of calcein leakage activity by saponins using liposomes composed of 9:1 POPC/Chol.	79
Table 3-2.	Association constant at 50% leakage (K_{50}) and bound saponin/lipid ratio at 50% leakage extent (r_{50}).	81

Supporting Information List of Tables

Table S1-1.	Permeation by saponins in various artificial membrane models	114
Table S1-2.	Influx of calcium in various membrane models	114
Table S1-3.	Determination of the presence of phospholipids in the acceptor wells	115
Table S1-4.	Effect of saponin on size of LUVs (9:1 POPC/Chol)	116

List of Schemes

Scheme 5-1.	Synthesis of Chol-*d*	111

Chapter 1

General Introduction

A wide variety of natural products of animal, plant, fungal and bacterial origin has attracted great attention due to their biological activities. Some of these compounds have been regarded as drug candidates, which could target specific cellular components for treatment and prevention of numerous kinds of diseases. The interesting activity and structural features of the bioactive natural products have led to the investigation of their specific mechanism of action at the molecular level. These bioactive compounds can exhibit their characteristic toxicities via recognition of membrane receptors, including various proteins and lipids found in biomembranes, and exert their activities through a specific mechanism of interaction. In this chapter, the importance of biological membranes and its components on various cellular processes is discussed, including specific interactions with cholesterol (Chol) and surrounding phospholipids. Furthermore, various amphiphiles, with a main focus on saponins, are also covered including its biological activity and membrane interaction. Different methods developed for the study of saponin-membrane interaction are also touched in the latter part of this chapter.

1.1 The Biological Membrane

Biological membranes play a key role in the maintenance of cellular structures and functions.[1] Membranes separate the interior and exterior of the cells and different organelles. Selective passage of various solutes through specific mechanisms allows various cellular processes, initiated through the membrane via signal transduction, cell signaling, etc., although it has also been noted that solutes can directly permeate into the membrane without the aid of channels or transporters.[2,3] Basically, the membrane is composed of three major components such as lipids, proteins and carbohydrates in variable proportions, which serve important roles in several cellular processes.[4,5] Until now, the widely accepted representation, so-called ‘fluid mosaic model” (Fig. 1-1) was first proposed for biological membranes by Singer and Nicholson in 1972, which illustrated the structure and organization of proteins and lipids of the biological membrane, where protein molecules diffuse freely in phospholipid bilayer and are randomly distributed along the membrane surface.[6] This model also suggested the occurrence of

asymmetry of the outer/inner leaflets and lateral mobility within each leaflet.[6,7] Recent developments have presented the existence of important domains called lipid rafts.[7] Since then, the role of lipid rafts on membrane dynamics has attracted a lot of attention leading to various research focusing on the elucidation of the importance of these domains.[8]

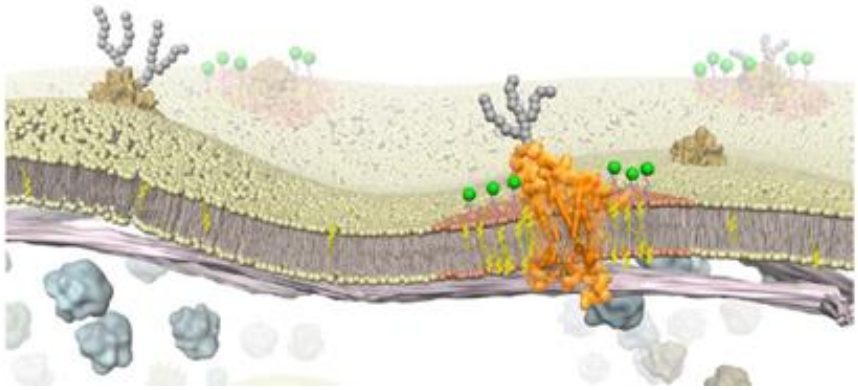

Figure 1-1. A representation of biological membrane. Reprinted with permission from *The Chemical Record*, **2015**.[9] Copyright © (2015) John Wiley and Sons.

Another important feature of biological membranes is high fluidity, which is thought to facilitate cell division. Membrane fluidity is highly affected by temperature and lipid composition.[1,10] The thermotropic behavior of the membrane can also be influenced by the structure of lipids including the chain length, degree of unsaturation, packing of acyl moieties and the presence of the polar headgroup.[1] Furthermore, cholesterol (Chol) and other lipids in membrane are involved in the regulation of its fluidity and permeability. In the following sections, the role of specific membrane components on membrane organization and dynamics are discussed.

1.1.1 Components of Biological Membranes

Biological membranes generally have a common structure characterized by the presence of two layers or leaflets, which act as a barrier for the inner and outer portion of the cell. Biomembranes are composed mainly of lipids, proteins and carbohydrates.[4,5] Lipids play an essential role in diverse cellular processes.[4,11] Several families of lipids have been characterized in the mammalian membrane, which include glycerophospholipids, sphingolipids, and sterols.[4,5] Glycerophospholipids largely have a glycerol backbone and

usually contain two hydrophobic tails that are made up of saturated or *cis*-unsaturated fatty acid chains with varying length and degree of unsaturation.[8] Another important feature of glycerophospholipids is the presence of polar headgroups, which is exposed to the aqueous environment. Glycerophospholipids present in mammalian membranes could be a simple phosphatidic acid (PA), phosphatidylcholine (PC), phosphatidylethanolamine (PE), phosphatidylserine (PS) and phosphatidylinositol (PI).[12] The most common and abundant phospholipid is PC (Fig. 1-2**A**), which often accounts for more than 50% of the phospholipids present in biomembranes.[8] PCs often contain a *cis*-unsaturated alkyl chain, which is mainly responsible for high fluidity of biomembranes at room temperature. PCs can also undergo spontaneous self-organization to form planar bilayers due to their cylindrical geometrical shape. Another common phospholipid in the membrane is PE, which contains a slightly smaller headgroup size as compared to PC and takes a conical molecular shape. Combination of PE and PC in membrane promotes curvature generation in membranes resulting to budding, tubulation, fission, and fusion.[13]

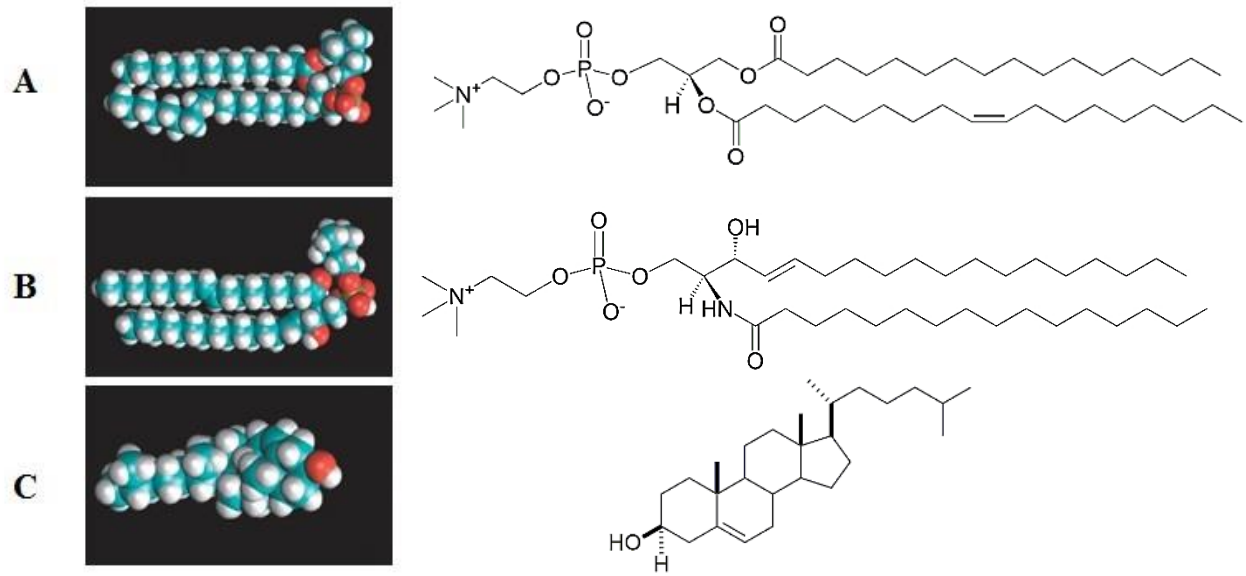

Figure 1-2. Representative structures of main classes of lipids; glycerophospholipid (**A**), sphingomyelin (**B**), and cholesterol (**C**). Reprinted and modified with permission from *Nature Reviews Molecular Cell Biology*, **2008**.[8] Copyright © (2008) Nature Publishing Group.

Another class of lipids that play an important role in membrane function and raft formation is sphingolipids. Sphingolipids generally contain a hydrophobic ceramide backbone composed of sphingosine and fatty acid. Sphingomyelin (SM, Fig. 1-2**B**) and

glycosphingolipids (GSLs) constitute the major sphingolipids in mammalian cells. GSLs can be further classified depending on the kind and number of attached sugar moiety in the headgroup. Common examples of GSLs are glucosylceramide (GlcCer), galactosylceramide (GalCer), lactosylceramide (LacCer) and the gangliosides including GM1, GM2 and GM3.[14] Sphingolipids have saturated or *trans*-unsaturated sphingosine chain. Sphingolipids are also known to cause gel-phase formation due to the tight packing of the fatty acids. However, Chol (Fig. 1-2**C**) eases the gel formation and causes fluidization of the membranes. Chol is the predominant nonpolar lipid found in the mammalian cell membrane. When Chol preferentially mixes with sphingolipids, the resulting mixture causes shielding of Chol by polar headgroups of sphingolipids rather than a preferential interaction between the two species.[15] This effect is referred to as the umbrella model. In current studies, it is suggested that lipid rafts are mainly composed of Chol and SM, which are essential for the formation of liquid ordered (L_o) domains and serve as an important target for several cellular processes including cell signaling, signal transduction and immune responses.[8]

Proteins and carbohydrates are also important components of biological membranes. Carbohydrates (or sugars) are minor components of the membranes and give each type of cell its unique characteristics. Carbohydrates are attached to either proteins or lipids and mostly involved in cellular recognition and metabolism.[4] Proteins act as catalysts, receptors, transporters and anchors in several cellular processes, which simultaneously occur in various types of cell membranes.[16] Proteins can be associated with membrane in various ways depending on its purpose and function.[4] Transmembrane proteins are embedded within the membrane via interaction between hydrophobic regions of the protein and the hydrophobic portions of membrane lipids to extend across the bilayer. Furthermore, these proteins spanning the entirety of the membrane are divided into three different domains. The transmembrane domain is inserted to the membrane and interacts with the hydrophobic chains of lipids in the interior of the bilayer and is secluded away from water molecules. On the other hand, the extracellular and cytosolic domains have hydrophilic properties and are exposed to an aqueous environment. Some transmembrane proteins have α-helical structures, while others can also exist in a β-barrel form. Proteins can also be attached to the membrane via covalent interaction with phospholipids or fatty acyl chains, and are referred to as lipid-anchored proteins. A common example of the lipid-anchored proteins is glycosylphosphatidylinositol (GPI) anchored proteins, which are involved in transport of membrane proteins, cell adhesion, and cell surface protection. GPI-anchored proteins also act as antigens used as cancer markers.[11]

This type of protein is tightly bound to the membrane and can only be extracted through strong treatments such as use of organic solvents and detergents. Lastly, proteins can be classified as peripheral proteins, which are weakly bound to the membrane surface and can be extracted with mild treatment.[2,4,5] Lipids, proteins and carbohydrates are thought to associate to form membrane structure depending on the functions. With the diverse structure and combinations of these membrane components, research on the structure, function and properties of biological membranes are becoming more challenging, and that more advanced and specific techniques should be utilized to characterize the membrane structure.

1.1.2 Organization of Biological Membranes

The focus of this section is placed on the effects of various lipids on the structure and organization of biological membranes. The intrinsic properties of these lipids dictate the structure and functions of biomembranes.[17] In the past years, a great number of scientists have attempted to characterize the organization of biological membranes using available technologies. In the course of these studies, important discoveries have been obtained, providing lines of evidence on the highly organized structures of membranes. These discoveries are attributed to the development of new and more accurate methods, which are described later in this chapter. As early as 1925, Gorter and Grendel proposed that erythrocyte membranes form bimolecular sheets or leaflets composed of lipids.[18] Later on, a model proposed by Davson and Danielli in 1935 suggested that the membrane is covered with proteins.[19] Characterization of this bimolecular sheet progressed until between 1969 and 1970, the nature of this structure has been finally determined and described as a amphipathic membrane lipid complex that forms a lipid bilayer. This discovery has been deemed as the primary lipid-driven organization in membranes.[20] The bilayer structures allow biological membranes to serve as physical boundary between the cellular interior and exterior. However, they found that temperature affects the stability of membranes and attributed it to the characteristic of the fatty acyl chain[4] and that the majority of lipids in biological membranes exist in the fluid phase at 37 °C. In 1972, Singer and Nicolson proposed the renowned fluid mosaic model (Fig. 1-3).[6,7] They described that the existence of fluid phase in biological membranes functions as a solvent for membrane proteins to diffuse freely and distribute randomly across the membrane surface. They also noted that the random distribution of membrane components implies the absence of long-range order in membrane and therefore exhibits lateral homogeneity. Following the fluid mosaic model

hypothesis, studies on the effect of temperature on the behavior of membrane lipids have been done to assess phase behavior of lipid mixtures. They found that temperature affects the lateral organization in biological membranes at a certain degree and that the properties of lipids under various thermal conditions lead to the formation of specific membrane domains, including the lipid raft.[21]

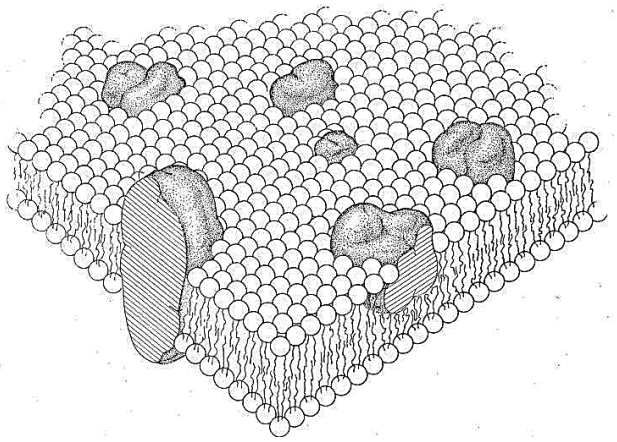

Figure 1-3. The fluid mosaic model of the structure of cell membranes. Reprinted with permission from *Science*, **1972**.[6] Copyright © (1972) The American Association for the Advancement of Science.

Afterwards, continuous efforts have been made to understand the membrane phenomena, underlying the concept of membrane organization. In 1982, scientists hypothesized that the presence of distinct phase in the lipid environment of biological membranes provides evidence on the existence of membrane domains.[22] This finding led to the advent of the lipid raft hypothesis, which is one of the most important findings that researchers need to understand its significant roles and properties in organization of the biological membrane.[23] Scientists are now focusing on a variety of lipid components present in lipid rafts to elucidate their specific contributions to the formation of these domains, as well as to understand their importance in various cellular processes. In the coming years, researchers are looking forward to attaining significant evidence leading to a more concrete understanding about biological membrane related phenomena.

1.1.3 Membrane Dynamics

In the previous section, it was mentioned that the fluid-like structures of biological membranes is one of its important features in the maintenance of the integrity of cells. Next, the dynamic properties of membrane components and its effect to its surroundings are discussed from here. Lipids can undergo several types of motions in membrane at different correlation times (Fig. 1-4).[24] Movement of lipids in membrane can either be one or a combination of lateral and rotational diffusion/wobbling (10^{-7} s to 10^{-8} s), flip-flop mechanism (10^{-3} s to 10^{4} s), leaflet protrusion (10^{-9} s), bond oscillations/vibrations (10^{-12} s) and *gauche-trans* isomerization (10^{-10} s). Additionally, the membrane moves by itself, which is called undulations (10^{-6} to 1 s). To date, occurrence of these motions in membrane have been studied using sophisticated spectroscopic techniques such as nuclear magnetic resonance (NMR), electron paramagnetic resonance (EPR) and fluorescence methods using isotope- or fluorescence-labeled molecular probes. However, these techniques are only advantageous at a specific correlation time and thus, a combination of two or more techniques is recommended for a more accurate understanding of the effects of membrane dynamics on the ordering or disordering of these lipids in membrane.[24] Furthermore, these motions significantly affect the dynamic state of membrane, including lamellar phase separations.

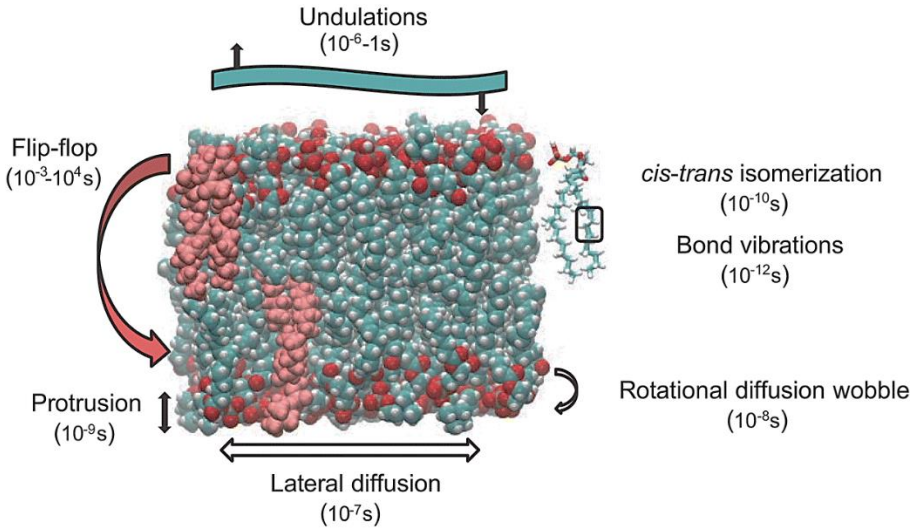

Figure 1-4. Movements of lipids in biological membrane. Reprinted with permission from *Computational Biophysics of Membrane Proteins*, 2016.[25] Copyright © (2017) Royal Society of Chemistry.

1.1.4 Lamellar Phase in Biological Membranes

Various motions of lipids contributes to the overall dynamics of membrane, giving rise to distinguishable lamellar phase and polymorphic states (Fig.1-5).[11] At lower temperature, bilayer membrane takes into the form of solid (S_o) or lamellar gel phase (L_β) (Fig. 1-5**B**). This state is characterized by a tightly packed and highly ordered acyl chains. Although controversies arise regarding the existence of gel phase in membranes, researchers have revealed the occurrence of these structures in both artificial and biological membranes. As discussed earlier, temperature affects the organization of lipids in bilayer membrane. Lipid melts at a certain temperature referred as the phase transition temperature or T_m; above this temperature, bilayer membranes usually take the lamellar liquid crystalline phase (L_α) or liquid disordered (L_d) phase (Fig. 1-5**A**). At this state, the overall structure of the membrane has shown two-dimensional order but lines of evidence have shown the occurrence of disorder in the lipid acyl chain. In contrast, L_α (or L_d) exhibits a higher rate of lipid diffusion and an increase in cross-sectional area of lipid molecules, which render formation of a thinner membrane, while L_β exhibits the higher density of lipids, which causes the formation of a thicker membrane.[11] In addition, the T_m value of certain lipids is affected by the length of acyl chains, the number and position of unsaturation, and the size and ionic states of the headgroup. The pH of a surrounding environment can also influence T_m.[26] In some cases, membranes composed of pure phospholipids exhibits the formation of the ripple phase (P_β), which often occurs as intermediate phase in the L_β to L_α transition.[11,25]

Aside from the structure of phospholipids and the physical conditions that contribute to the properties and T_m of membrane, inclusion of other lipid components also affect the behavior of lipids. Chol is the most important membrane component, which affects the overall property and behavior of membranes. The effect of Chol, as well as other lipid in membrane is discussed in the next section.

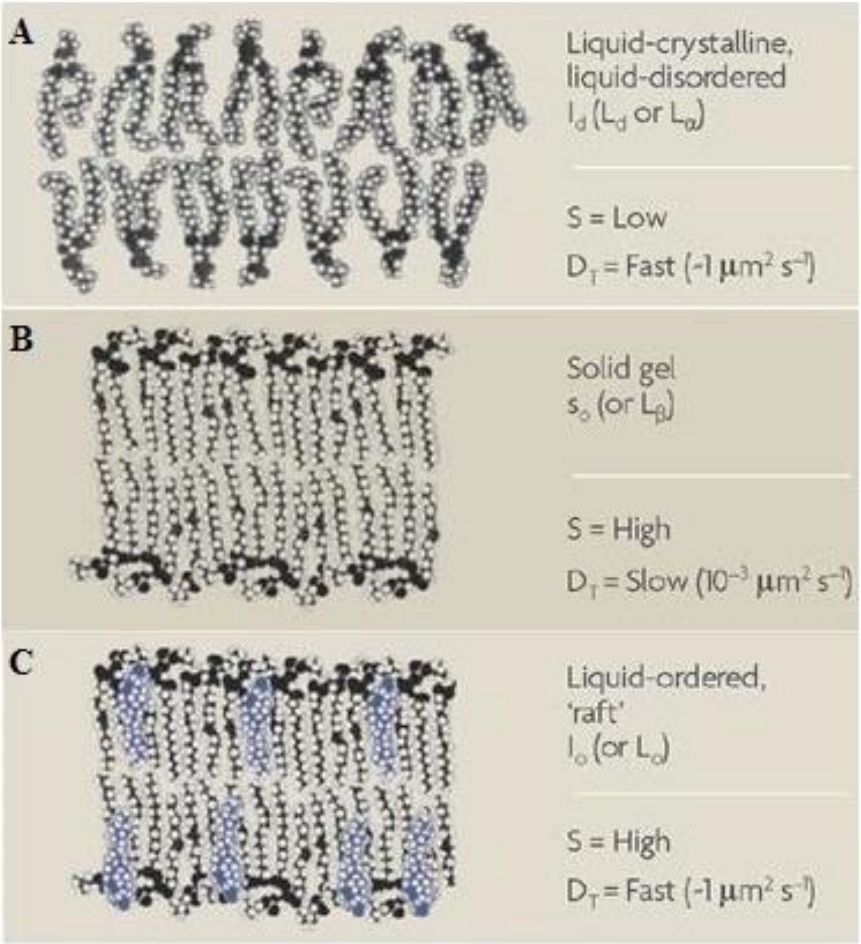

Figure 1-5. Lipid phase in biological membranes. S and D_T denote a molecular order parameter and transversus diffusion rate, respectively. Reprinted with permission from *Nature Reviews Molecular Cell Biology*, **2008**.[8] Copyright © (2008) Nature Publishing Group.

1.1.5 Importance of Cholesterol and other Lipids in Membrane

Despite the fact that the structure of Chol deviates from other membrane lipids , it plays a significant role in keeping the integrity and order of bilayers and serves as a target for membrane interactions (to be discussed in the latter part of the chapter). Chol is composed of the rigid and compact hydrophobic structure with a hydroxy group attached to the 3β-hydroxy position of the steroid A ring.[11] In addition, Chol possesses an over-all planar structure and induces the *gauche-trans* isomerization of acyl chains in phospholipids, favoring the formation of L_α phase. The ordering effect of Chol in L_α phase allows acyl chains to form *trans* arrangement, leading to thickening of the membrane and induced lateral condensation. However, in the gel state (L_β), Chol pushes surrounding lipids away and reduces order, which

is attributed to the presence of alkyl chain in the steroid ring. In short, Chol makes L_α more rigid and L_β more disordered.[27]

The amount of Chol present in membrane could also influence the "fluidity" of membrane. In fact, at a certain threshold, Chol interestingly forms a new phase referred to as the liquid ordered (L_o) phase (Fig. 1-5**C**). This phase is also enriched with phospholipids composed of saturated fatty acyl chains such as sphingomyelin, which is also found to be one of the major components in the lipid raft. However, inclusion of phospholipids with *cis*-unsaturated fatty acyl and renders a less favorable L_o phase formation.[27]

Interestingly, under certain conditions, coexistence of different lamellar domains has been observed in model membranes. This is attributed to the limited solubility of lipid and lipid mixtures in membranes.[17] Different domains in biological membranes have also been found to possess incomplete miscibility which were established in published phase diagrams (Fig.1-6).[28,29] The property of these lipids in membrane has shown the presence of phase separation in model membranes, which could likely exist in biological membranes.[30,31] However, some issues has been raised regarding the relevance of phase separation and whether or not the different membrane systems used could represent the existence of the lipid raft in biological membrane. Phase separation is attributed to the coexistence of both L_o and L_d phase at a critical concentration of lipid components and an inclusion of Chol in the system. Experimental evidence showing the coexistence of these two phases has been observed using Förster resonance energy transfer (FRET), NMR studies[28,32] and differential scanning calorimetry (DSC)[33]. It is also pointed out that the existence of phase separation can mostly be observed in ternary systems composed of Chol, sphingomyelin and phospholipids with unsaturated acyl chain(s),.[34] Some of the studies have also reported that the coexistence of gel phase (L_β) and liquid crystalline (L_α) phase in a binary system composed of two lipids having different transition temperatures (T_m) but pointed out that this type of phase separation may not be observed in eukaryotic membrane due to the presence of Chol in most membranes.[35]

Overall, membrane organization and dynamics are highly dictated by the structure and composition of lipids and the conditions of the surrounding. In fact, numerous studies are still on-going aiming to characterize the relevance of the diverse structure of biological membranes, as well as the existence of lipid rafts. The continuous efforts contributed by scientists open countless opportunities leaning towards the understanding of these membrane phenomena.

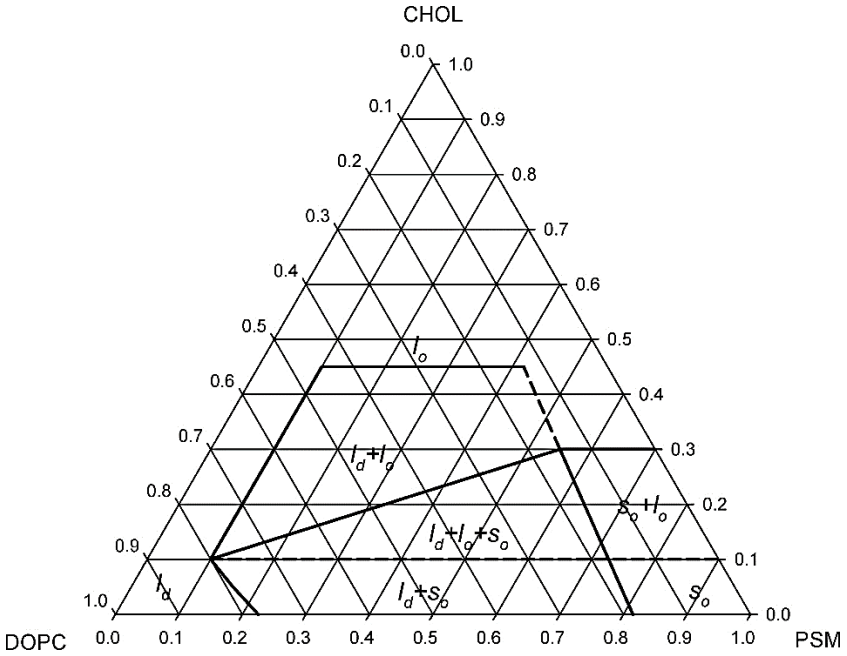

Figure 1-6. Phase diagram for co-existence of phase-separated lipids in ternary system composed of PSM/DOPC/Chol. Reprinted with permission from *Langmuir*, **2011**.[29] Copyright © (2011) American Chemical Society.

1.2 Saponins and other amphiphiles

Quite a few studies have been conducted on the ability of saponins to interact with membrane, which has been considered to be responsible for its biological and pharmacological activities.[36] Researchers have also observed promising anticancer activities in some saponins, which led to the elucidation of their mode of action towards various cell lines.[37] Saponins usually have amphiphilic properties, which are regarded to be responsible for some of their biological activity; lines of evidence concerning the amphiphilic structure and molecular properties of saponins, as well as its effect on membranes are still insufficient and left for further investigations.[38] In this section, the importance of the amphiphilic properties of saponins and their effects on various membrane types, including biological and artificial model systems are discussed.

1.2.1 Saponins and their amphiphilic properties

Saponins are naturally occurring amphiphiles derived from plants and marine organisms, including sea cucumbers.[39] Amphiphiles are compounds that possess both polar and non-polar moieties in structure. Many saponins derived from plants have been used as foaming agents and ingredients in making soaps.[40] Saponins are also known as secondary metabolites that are utilized by plants as defense against variety of predators.[39,41] Most importantly, saponins have been used as a traditional Chinese medicine, because of their pharmacological activities, in particular, prevention of cancer and cardiovascular diseases and nutrients/tonics.[39]

The structures of saponins contain one or more sugar moiety linked to a sapogenin backbone, which are either of steroidal or triterpenic origin (Fig. 1-7).[40,42] Sugars are attached to the sapogenin backbone via an ester or ether linkage in various combinations. Generally, saponins may contain one, two or sometimes more sugar moieties, which are referred to as monodesmosidic, bidesmosidic and polydesmosidic saponins, respectively. In addition, the number and position of sugar attachment also differ in various saponins. Some common sugars that have been found in saponins include D-glucose, D-galactose, L-rhamnose and others.[42] These variations give rise to diverse saponin structures present in different plants.

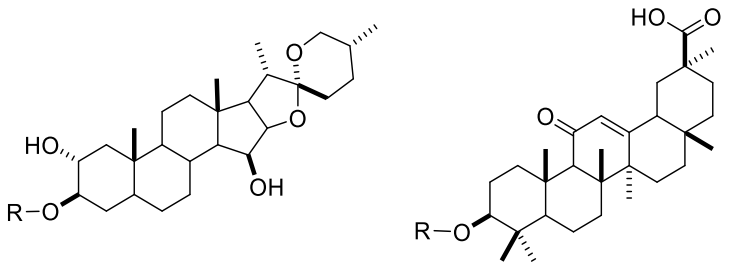

Figure 1-7. Examples for a steroid (*left*) and triterpenic (*right*) sapogenins. The R group represents a sugar moiety attached to the sapogenin backbone via ether or ester linkage.

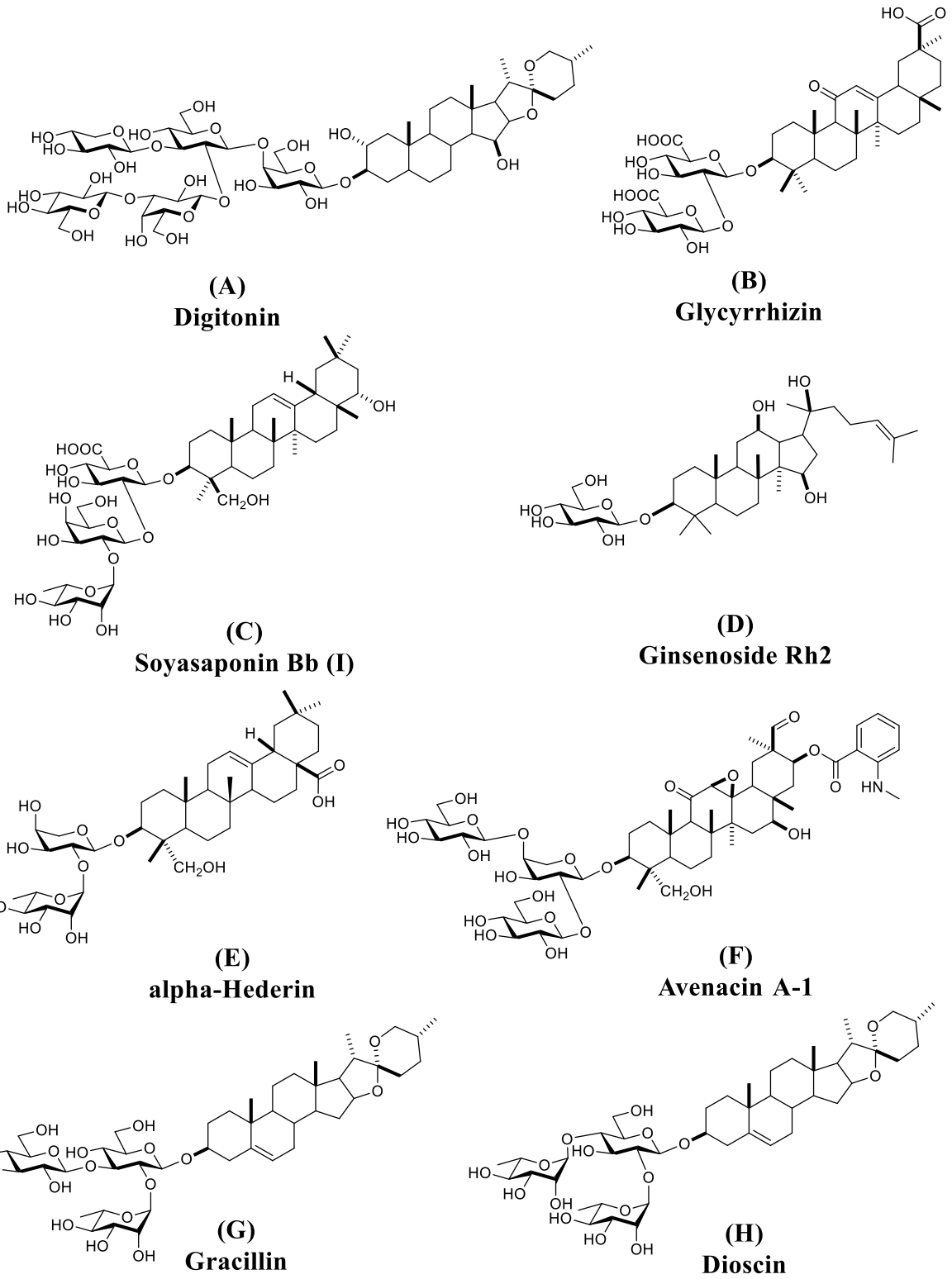

Figure 1-8. Examples of common saponins of plant origin.

Some of saponins have been found to have strong biological activities and regarded as promising drug candidates. Some of the common saponins are summarized in Fig. 1-8.[40,43-48] These saponins have differences in their sapogenin backbones and the variety of sugar moiety attached, but one common characteristic of these saponins is the attachment of sugar moiety at the 3β-OH position of the sapogenin backbone.[47-49] The presence of a sugar moiety at the C3 position is thought to be important for their role in membrane permeabilization, although other factors such as the number of sugar moiety attached to the backbone, the nature of the backbone, and the length of the sugar chains could also influence the observed permeabilizing activity of various saponin models.[49] Specific membrane interactions, as well as structure-activity relationship studies of these saponins are described in the latter part of this chapter.

The amphiphilic nature of saponins has also been found to be critical for its biological activity. The properties of saponins in terms of their amphiphilic structures are discussed from here. As mentioned earlier, saponins are composed of a hydrophobic (sapogenin) and hydrophilic (sugars) interface accounting for their amphiphilicity, and the presence of the highly hydrophilic sugar groups make most saponins soluble in water.[50] Saponins are generally regarded as surface-active agents due to their surfactant activities, which are important factors for manufacture of pharmaceutical drugs, cosmetics and food-related products.[51] Saponins can also form aggregates in solution when their content in water reaches the critical micelle concentration (CMC). Fig. 1-9**A** shows the accumulation of saponins in the air-water interface where the hydrophobic portion is oriented towards the air and the polar head groups reside in the water interface. Other saponins exist as monomers when dissolved in aqueous system (Fig. 1-9**B**) below their CMC. At CMC, formation of molecular aggregates is highly favored (Fig. 1-9**C**) likely due to weak molecular interactions such as van der Waals and hydrophobic interactions, hydrogen bonding between the sugar moieties and often via electrostatic interactions. Most saponins existing as micelles take a spherical shape, although some other notable micellar structures have also been observed such as rod-shaped or worm-like aggregates. Nevertheless, micelles formed by most saponins are viewed as insoluble complex and its formation is affected by the aggregation number, temperature, ionic character and the structure of the saponin itself .[38,50]

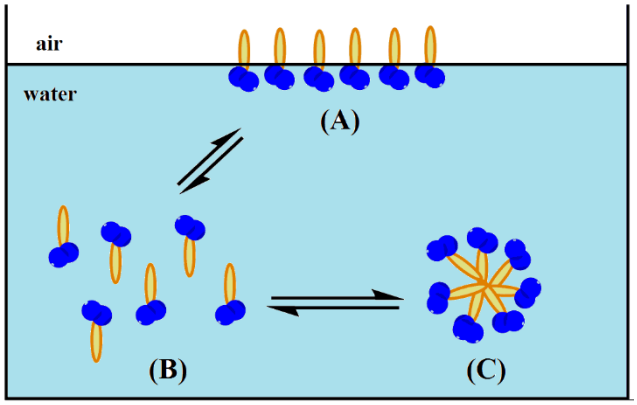

Figure 1-9. Saponins in aqueous solution; (**A**) air-water interface, (**B**) monomers, and (**C**) micellar aggregates[38]

Saponins can also form mixed micellar aggregates especially in the presence of Chol and have larger diameter as compared to micelles of pure saponins.[52] Saponin and Chol can also mix at various proportions to form aggregates with various size, shape and CMC.[38] while their insoluble complexes have also been observed in solutions.[43] Due to the fact that saponins form aggregates with Chol likely via direct interaction, they have been used for the development of drugs that targets cardiovascular diseases including hypercholesterolemia (high Chol levels) by increasing Chol absorption.[40] The amphiphilic nature of saponins may have been thought to be responsible for the membrane permeabilizing activities, but sufficient evidence has not been obtained to support this notion.

1.2.2 Biosynthesis of saponins

The diverse structure and function of saponins have extensively been subjected to a great amount of research regarding their roles in plants, as well as their potential industrial and pharmaceutical uses. Various studies have highlighted the importance of saponin structure on its activity,[52] particularly, the aglycone of the steroid or triterpenoid origin, and the hydrophilic sugar moiety. These structural features of saponin give its amphiphilic properties. Thus, the biosynthetic pathway and intermediates of saponins have attracted researchers' attention. Here an overview of the biosynthesis of saponins is presented, mainly focusing on the two classifications: steroidal and triterpenoid saponins.

Triterpenoid saponins are found to be abundant in dicotyledonous plants, while steroidal saponins mostly accumulate in monocotyledonous plants.[52] Both steroidal and triterpenoid saponins are derived from 2,3-oxidosqualene, which contains 30 carbons in its structure. In synthesis of the precursor, the steroidal aglycone only retains 27 carbons due to loss of three methyl groups in the backbone, while triterpenoid backbone still retains the 30 carbons in its structure.[52] Both steroidal and triterpenoid aglycones originated from isopentylpyrophosphate (IPP) units are produced from the cytosolic mevalonate pathway (MVA) as shown in Fig. 1-10. The MVA pathway begins with the conversion of acetyl CoA to the five-carbon terpene precursor IPP in a multistep process where the enzymes hydroxymethyl-glutaryl-CoA synthase (HGMS) and reductase (HGMR) are used to catalyze each step in the initial biosynthesis. From the precursor IPP, series of isomerization and condensation steps lead to formation of linear precursor squalene, which contains 30 carbons. The epoxidation of squalene further leads to the production of the precursor 2,3-oxidosqualene via action of squalene epoxidase (SQE). Cyclization of 2,3-oxidosqualene proceeds in the presence of oxidosqualene cyclases (OSCs) to yield polycyclic structures, which marks the synthesis of either primary triterpenes, or specialized triterpene structures. The primary steroid precursor is a tetracyclic cycloartenol which is produced by the action of cycloartenol synthase (CAS) on 2,3-oxidosqualene. From the common precursor, which is 2,3-oxidosqualene, various saponins of either steroidal or triterpenoid in origin are generated via series of glycosylation. The gene expression in plants dictates the structure of the saponin that is produced in the natural process. The saponin biosynthesis is depending on what role of the saponin plays especially in response to environmental stimuli and how it is to be transported in different parts of plants. The common biosynthetic scheme for the generation of steroidal and triterpenoid backbones is summarized in Fig. 1-11.

The synthesis of steroidal saponins is brought by series of oxygenation and glycosylation of the Chol backbone to produce either spirostanal or furostanal derivatives containing fused *O*-heterocycles attached to the aglycone core.[53] Other remaining 2,3-oxidosqualene cyclization products serve as precursors for further synthesis of specialized triterpenes. The triterpene aglycone can be modified through a series of oxidation by the action of cyctochrome-P450-dependent monooxygenases (P450s), which could also be responsible for the production of more complex and diverse triterpenoid backbones. Consecutive oxidation at different positions in the triterpene backbone increases overall polarity.

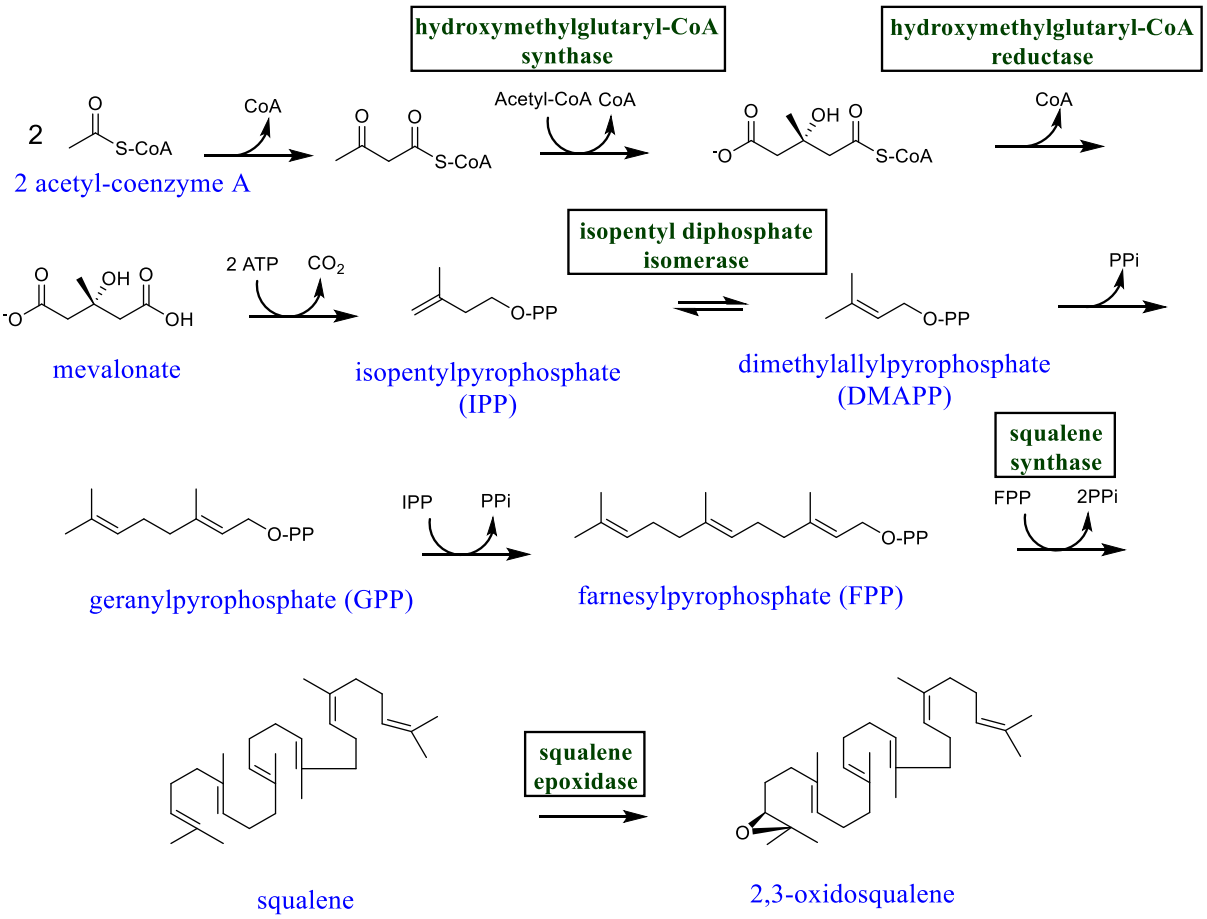

Figure 1-10. Biosynthesis of 2,3-oxidosqualene via mevalonate pathway (MVA)

Furthermore, the number of hydroxy groups relates to the possible number of glycosylations with characteristic sugar units by the action of transferases such as UDP-dependent glucosyltransferases (UGTs), acyltransferases, methyltransferases, etc.; these enzymes also contribute to the production of triterpenoid saponins with diverse structures.[54] The genes involved in the biosynthesis of saponins can be grouped into OSCs, P450s, UGTs and encoding transferases based on their characteristic reactions. The presence of gene clusters is specialized and serves as key factors for the biosynthesis of saponins and other special metabolites.[55] In addition, although the biosynthetic pathway for saponins have already been unraveled, the number of characterized enzymes are still increasing over the decade, which makes the understanding of saponin biosynthesis elusive.

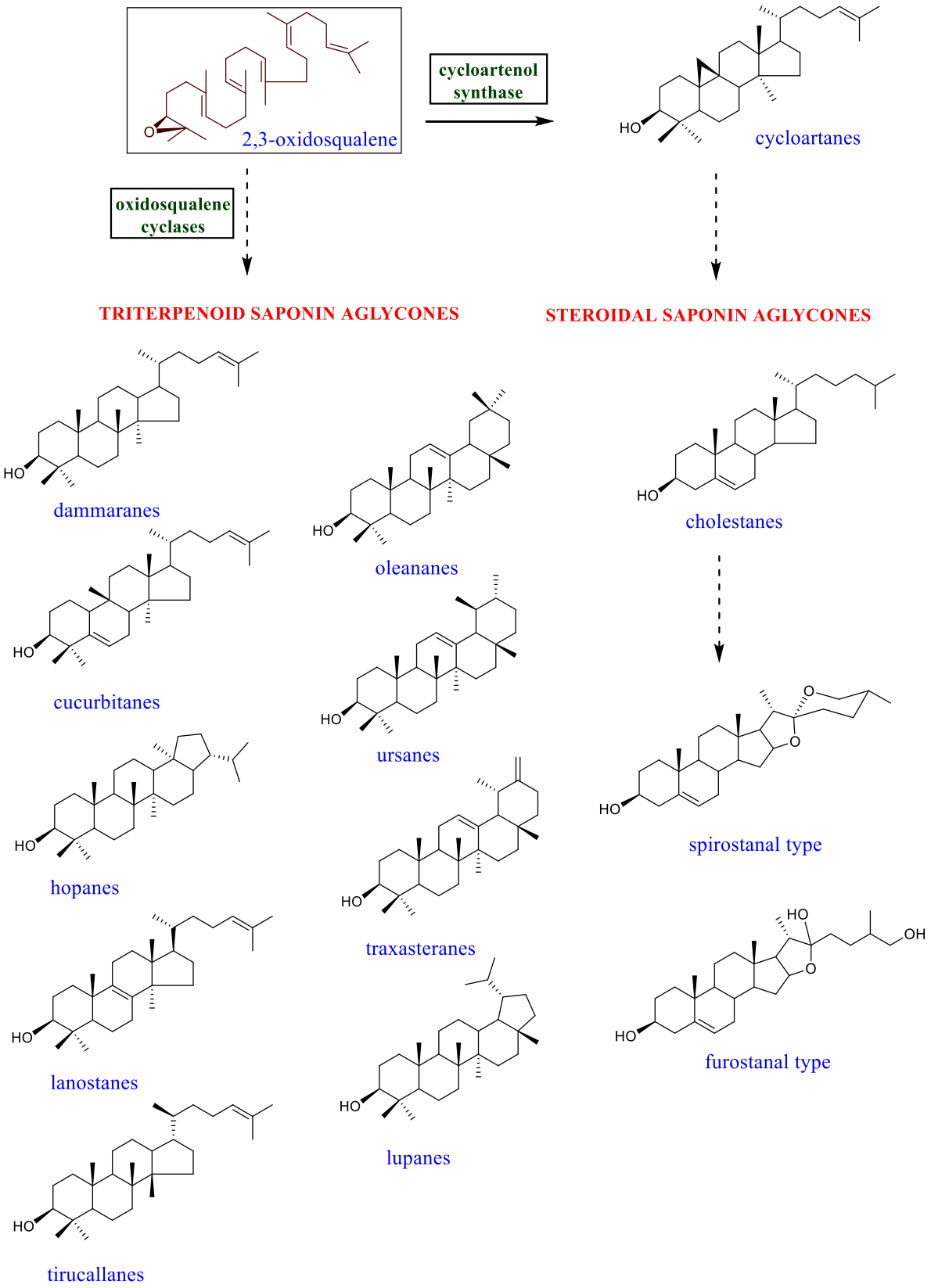

Figure 1-11. Biosynthesis of steroidal and triterpenoid aglycones from common precursor 2,3-oxidosqualene. Blue letters denote the hydrocarbon framework for skeletal structures

1.2.3 Modes of interaction of membrane-active compounds

The amphiphilic character of saponins and other related compounds have been considered to have a significant effect on biological activities towards membrane through direct interactions with specific membrane components.[56] Interaction of these compounds leads to the perturbation of membrane organization, which may result in either pore-formation or considerable membrane disordering and disruption.[57] In general, saponin and other amphiphilic molecules can form transmembrane pores or other membrane defects that lead to significant membrane disordering and permeabilization. The different modes of interactions of these amphiphiles with respect to biological membranes are discussed in this section. The mode of interaction is categorized into two main classes: 1) transmembrane pore models and 2) non-pore models.

First, the famous transmembrane pore models is discussed, which can be further classified into the barrel-stave and toroidal pore models. These models have been proposed in the studies of antimicrobial peptides (AMPs) and extensive controversies surrounding these peptides have been made on their real and specific mode of actions.[58,59] The barrel-stave pore model is described with membrane aggregates that extends to the entire length of a lipid bilayer. The barrel stave pore is characterized by hydrophobic interaction between membrane interior and AMP where the hydrophobic interface of AMP faces to the membrane lipid core and the hydrophilic interface faces to the aqueous lumen.[59] Among several AMPs, one notable example of the barrel stave pore-formers is alamethicin (Fig. 1-12**A**).[58,59] The barrel stave pore-forming mechanism of AMPs is also presented in Fig. 1-13. On the other hand, the toroidal pore model is influenced by the inward induction of curvature by insertion of AMP into membrane as shown in Fig. 1-14.[58] One important characteristic of the toroidal pore is that lipid components and membrane active compounds interact each other upon pore formation.[58,59] Notable examples of AMPs capable of forming toroidal pore are melittin (Fig. 1-12**B**) and magainin (Fig. 1-12**C**), although there were recent debates regarding whether or not these AMPs really form the toroidal pore or may act as barrel stave pore formers.[60] Furthermore, the main difference between these two transmembrane pore models is that the barrel stave model forms a favorable channel in the membrane core where the driving force for peptide penetration is largely due to hydrophobic interactions. On the other hand, the toroidal pore model takes into account the presence of different segments in the membrane bilayer where it can undergo favorable interaction, likely disrupting the hydrophobic domains of the membrane. In addition, formation of toroidal pore is characterized by thinning of the membrane as a consequence of

positive curvature stress caused by embedding AMPs to the polar head group region of the phospholipid. [59]

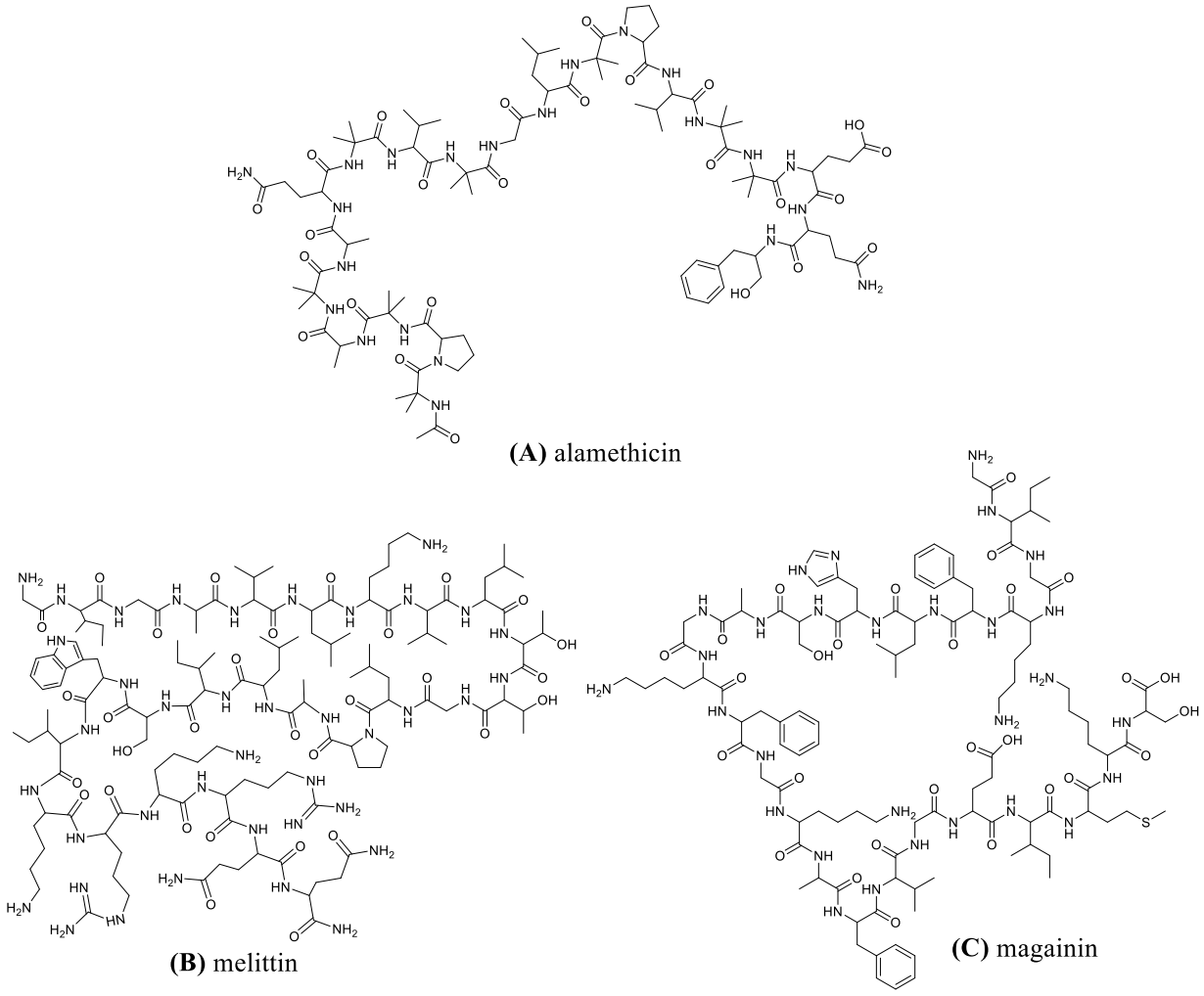

Figure 1-12. Structures of common antimicrobial peptides: (**A**) alamethicin, (**B**) melittin and (**C**) magainin

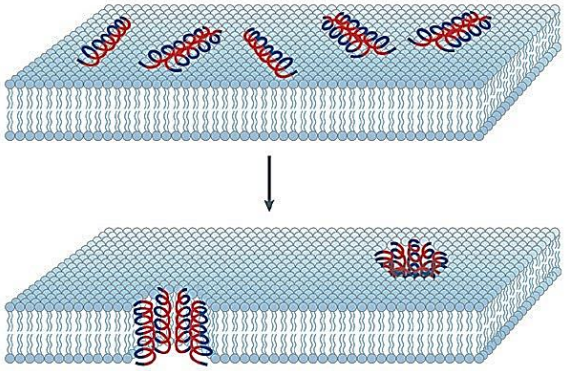

Figure 1-13. Mechanism of barrel stave pore formation of antimicrobial peptides (AMPs). Reprinted with permission from *Nat. Rev. Microbiol.*, **2005**.[58] Copyright © (2005) Nature Publishing Group.

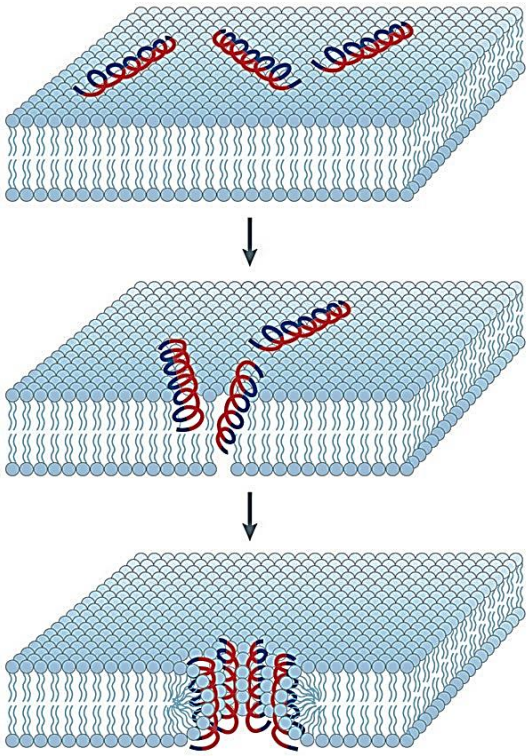

Figure 1-14. Mechanism of toroidal pore formation of antimicrobial peptides (AMPs). Reprinted with permission from *Nat. Rev. Microbiol.*, **2005**.[58] Copyright © (2005) Nature Publishing Group.

Next, the other types of interactions of AMPs that are categorized under the non-pore models are discussed. The most popular non-pore type interaction is known as the carpet model, which is sometimes referred to as the detergent model as shown in Fig. 1-15.[58-60] In this model, membrane active compounds cover the membrane like a carpet in a parallel binding mode at a certain threshold. This is followed by membrane insertion and permeation, which often leads to micellization and membrane disruption. Most AMPs are thought to belong to this model of mechanism.[60] Aside from the carpet mechanism, other models falling under the non-pore forming mechanism has been proposed. Examples of which are the sinking raft model, leaky slit model, charge cluster mechanism and interfacial activity model.[61-63] These models are exclusively observed on specific membrane active compound. Although these mechanisms may also be involved in other amphiphilic compounds, the focus of this study is limited to the three models, barrel stave, toroidal pore and carpet, for describing the mode of action of membrane active amphiphilic compounds, which is further expanded to saponins.

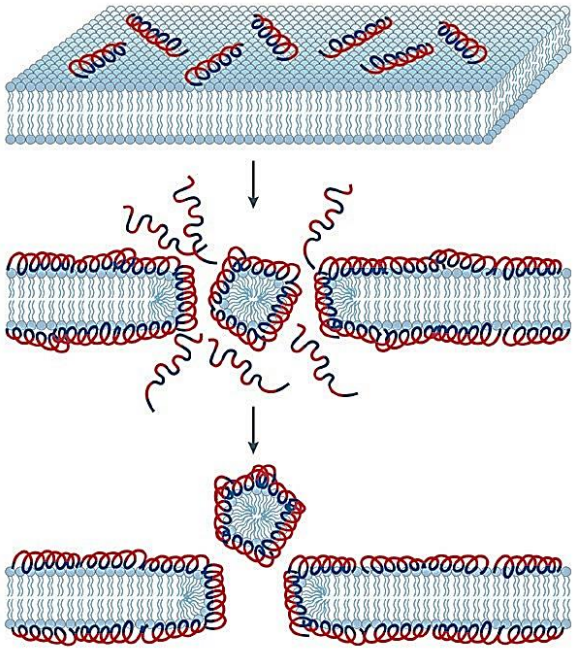

Figure 1-15. Carpet or detergent-type mechanism of antimicrobial peptides (AMPs). Reprinted with permission from *Nat. Rev. Microbiol.*, **2005**.[58] Copyright © (2005) Nature Publishing Group.

1.2.3.1 Interaction of saponins with membrane lipids

As described earlier, saponins can directly interact with Chol and sometimes form mixed micelles. However, other evidence suggested that saponins are also capable of forming mixed micelles with membrane lipids such as Chol and phospholipids.[50] With the addition of phospholipids as a micellar component, formation of other shapes of aggregates have been observed including hexagonal phase, cubic phase, bilayers, etc.[38] The presence of this complex aggregate structures lead to formulation of vaccines for various types of diseases.[50]

In this section, the activity of saponins towards various membrane models is discussed. It has been known that membranes also provide an amphiphilic environment and in effect may attribute to the membrane permeabilizing properties of saponins. The use of artificial membrane models has provided valuable insights into saponin-induced interaction that leads to the elucidation of the mechanism of membrane lysis.[38,50] Furthermore, the mechanism of interaction of common saponins is also described in this section. Among other membrane preparations, supported monolayers serve as a useful tool to study the effect of saponins on phase separation and domain formation. A common approach used to study monolayers is the utilization of the Langmuir-Blodgett films. It was observed that some of the saponins including digitonin and avenacin A-1 are inserted into the monolayer in the absence of Chol.[46,64,65] However, other saponins are found to bind to the monolayer only in the presence of Chol.[66] This was observed in α-tomatine, which in addition, induces a pH-dependent insertion due to a possible protonation to an amino group that increases partition to the aqueous phase.[38] Glycyrrhizin was also noted to bind to the bilayer in the presence of Chol but may only happen at certain surface pressure of the monolayer.[67] Saponins can also induce phase separation and domain formation in monolayer models. Such observations include the effect of glycyrrhizin on lipid phase separation on a ternary lipid system composed of 1:1:1 mole ratio of dioleoylphosphatidylcholine/palmitoylsphingomyelin/cholesterol (DOPC/pSM/Chol). A reduction in the raft size was observed below the CMC of glycyrrhizin. However, above the CMC level, formation of membrane defects characterized by striped regions were observed using Brewster angle microscopy. These striped regions were also found to contain no phospholipid and thought to be responsible for the membrane permeabilizing activity of glycyrrhizin.[38,67]

Aside from monolayer models, bilayer membranes have also been extensively used to study the interaction of saponins with membrane.[38] The bilayer model could reproduce

biological membranes to study saponin-induced membrane permeabilization. Commonly used bilayer preparations include the multilamellar vesicle (MLV), small unilamellar vesicle (SUV), large unilamellar vesicle (LUV) and giant unilamellar vesicle (GUV). These vesicle preparations can be utilized depending on the type of experiments to monitor the effect of saponins. In bilayer models, the effect of saponins was studied both in the absence and in presence of Chol. For example, digitonin and its derivatives prepared by successive removal of sugars attached to the sapogenin were subjected to interaction analysis. They found that digitonin and desglucodigitonin (removal of terminal glucose from digitonin) exhibit interaction with membrane composed of pure phospholipid. However, the observed binding did not lead to their full insertion into the membrane. On the other hand, the addition of Chol to membrane changes the behavior dramatically, where the equimolecular complex of saponin and Chol is formed and induces permanent membrane insertion.[65] With this observation, a three-step mechanism for digitonin-induced membrane interaction in the presence of Chol was proposed as follows: (1) formation of aggregated species in membrane at increasing digitonin/Chol ratio, (2) occurrence of intermediate complex composed of mixture of digitonin-Chol aggregated species and their equimolecular complexes further increased, and (3) formation of equimolecular complex in the bilayer.[38,65,68] Another example of saponin for Chol-dependent activity is α-hederin. It was observed that in pure dimyristoylphosphatidylcholine (DMPC) membrane, α-hederin reduces membrane surface potential. The binding of α-hederin with the membrane is thought to be due to electrostatic interaction between the positively charged polar headgroup of DMPC and the negatively charged carboxyl group in α-hederin.[47,48] On the other hand, in the presence of Chol, α-hederin was able to induce membrane curvature at increasing concentration. The binding of α-hederin to Chol-containing membranes led to the immediate permeabilization and consequent pore formation.[47,48,51]

Next, the effect of saponins on lipid dynamics is discussed. As discussed earlier, the lipids present in membrane undergo various motions at different time scales (*see 1.1.3 Membrane Dynamics*). Techniques such as NMR, EPR and fluorescence spectroscopy are used to study this motion. In addition to the movement of lipids in membrane, Chol is also considered to play a key role in the lipid dynamics. In general, Chol reduces *gauche-trans* isomerization of acyl chains of lipids, their lateral and rotational diffusions in membranes, which result in its membrane ordering effect known as L_o phase.[38] With this property of Chol in membranes, it is assumed that the interaction of saponins with membrane Chol gives rise to a significant effect on the overall membrane dynamics. Likewise, the similarities between the

structure of sapogenin rings and sterol cores may influence membrane dynamics even without saponin-Chol interaction in fluid bilayer systems.[24] The effect of saponins on membrane dynamics in the absence or presence of Chol was determined using the aforementioned methods. It is noted that, in the absence of Chol, lateral diffusion of phosphatidylethanolamine (PE) decreased slightly[46], while the anisotropy for fluorescently labeled lipids and DPH[47,48] generally increased. In addition, the EPR order parameter increases for the pure phospholipid membrane, while a reduction in ^{2}H NMR parameters is also observed in the absence of Chol.[43] In contrast, the presence of Chol reduces the anisotropy of fluorescence labeled lipids, and the order parameters of labeled phospholipids and Chol as revealed by EPR and ^{2}H-NMR experiments.[43,47] The fact that the different techniques correspond to changes in the dynamic behavior of lipids at a certain correlation time or time scale, it is suggested that EPR and fluorescence anisotropy, which are used for molecular movements with the $10^{-8} - 10^{-9}$ s time scale, showed distinguishable effects of saponins on the *gauche-trans* isomerization rate (10^{-10} s) and rotational diffusion rate (10^{-8} s). Both of these dynamic parameters were reduced by saponins even in the absence of Chol, while in the presence of Chol, the opposite is observed indicating the loss of the ordering effect of Chol. For ^{2}H-NMR observations (around 10^{-5} s time scale), an increase in motions between 10^{-6} s 10^{-9} s, which includes rotational diffusion or wobbling, was shown by the reduction in the order parameters regardless of the absence or presence of Chol in the membrane.[38] In addition to saponins' effects on membrane dynamics, the lateral organization of lipids in membrane can be affected by saponin interaction likely due to the formation of saponin-Chol aggregates, which is also responsible for the disruption of specific membrane domains.[65,68]

Lastly, the reported mechanisms of saponin-induced membrane permeabilization for common saponin examples for artificial membrane models are reviewed. The membrane permeabilizing properties of monodesmosidic saponins are reported to proceed in the presence of membrane Chol.[47-49,64] Since then, several modes or mechanisms of interaction have been proposed for different saponins. The membrane-permeabilizing activity of the monodesmosidic saponins is generally accounted for by the following proposed mechanisms. The first mechanism involves the saponin-Chol interaction that leads to formation of equimolecular complexes, and reaches a certain density to induce the formation of a new lipid phase likely due to increased hydrophilic interactions between sugar residues. The equimolecular complex then generates the formation of spherical buds or tubules. The membrane rearrangement continues until it reaches membrane disruption.[49]

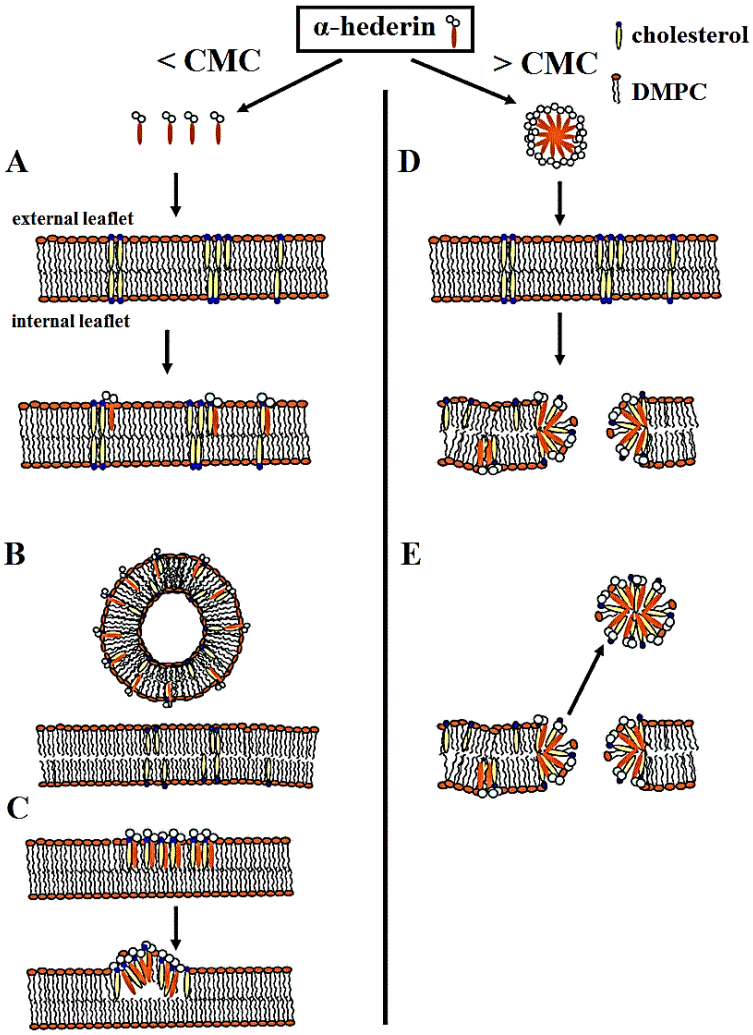

Figure 1-16. Mechanism of interaction of α-hederin, below CMC, (**A**) α-hederin monomers bind to Chol, (**B**) induces vesiculation, (**C**) and lateral phase separation. Above CMC (**D**) α-hederin aggregates forms pore and (**E**) leads to loss of membrane material. Reprinted with permission from *Org. Biomol. Chem.*, **2014**.[38,47,48] Copyright © (2014) Royal Society of Chemistry.

Another mechanism is the toroidal pore formation. In this process, the sugar moiety of saponin tends to interact with one another via hydrophilic interactions, leading to saponin-Chol aggregate and eventually to the formation of the toroidal pore. This mechanism has been observed in avenacin A-1.[46] The third model involves a concentration-dependent membrane permeabilization, which is characterized by membrane curvature generation (Fig. 1-16). This process was proposed for α-hederin, as well as dioscin.[47,48] Below the CMC of α-hederin, monomers binds to the surface of the bilayer generating positive curvature for the outer leaflet. Further aggregation of α-hederin, Chol and phospholipids induce formation of worm-like complexes, which are responsible for the gradual permeabilization as a consequence of membrane defects. In contrast, above the CMC of α-hederin, direct pore formation can be observed leading to loss of membrane material. This process could be attributed to the direct interaction of α-hederin micelles to the membrane containing Chol.[38,47,48] Although these three proposed mechanisms could account for the saponin-induced membrane permeabilization of monodesmosidic saponins, various factors including amphiphilicity, CMC, three-dimensional shape, and Chol affinity can affect the action of individual saponins with membrane.[47,48,51] Continuous efforts to relate the permeabilizing effect of saponins and self-aggregating properties are still being conducted.

1.2.3.2 Interaction of saponins with eukaryotic cell membranes

The effects of saponins on eukaryotic cells with a special focus on the erythrocyte membrane and cancer cell membranes are discussed from here. In this regard, the biological activity of saponins with these cellular types gives additional information on their specific mechanism of interactions. The erythrocyte (red blood cells) membrane is regarded as one of the most effective biological membrane models that can be used to study interactions of membrane active compound; the high Chol content makes it a good candidate for these studies. In fact, the absence of other cellular components, including nucleus, makes the analysis much easier. Due to the ability of saponins to interact with membrane-containing Chol in artificial membranes, saponins are known to exhibit hemolytic effects and cause cell lysis. However, it is still uncertain whether Chol is an important factor for saponin for induction of hemolysis[38], because contradictory results have been reported. Previous studies suggested that saponins are found to aggregate with Chol in the erythrocyte membrane and displaces Chol from the membrane, rendering hemolysis. Other studies disagree with this observation by noting that

Chol does not serve as specific binding sites for saponins.[69] Some studies also demonstrated that some saponins tend to act as osmotic protectants to prevent induction of hemolysis.[38] With regards to the relationship between saponin structure and hemolytic activity, contradicting lines of evidence are also presented as to the importance of the sugar moiety.[38,69] However, it is noted that most steroidal saponins have stronger hemolytic activity compared to triterpenic counterparts and that bidesmosidic saponins tend to have weaker hemolytic activities compared to monodesmosidic saponins.[70,71] Other modifications found in saponins may also have effects on the degree of hemolysis including the number of sugar residues attached in monodesmosidic sapogenins, branching of sugar chains and the presence of carboxylic acid and ester groups in the sugars.

In this section, the activities of these saponins on cancer cell membranes are further discussed. The potential activity of saponins against various types of cancer is mentioned for several occasions in this chapter. In contrast to erythrocytes, the structural features of cancer cells differ significantly. For instance, cancer cells contain nucleus and other cellular organelles, some of which the erythrocytes lack. In addition, the organelles of cancer cells are bound with membranes, which separate it from the cytoplasm. The subcellular membranes are composed of variable lipid and protein compositions, which allow saponins to specifically interact with certain organelles. The ability of saponins to interact with cancer cells can affect membrane dynamics or lateral organization to induce cell lysis. These membrane alterations may lead to either activation or inhibition of proteins surrounding the membrane and may induce the activation of signaling pathways, which may sometimes lead to programmed cell death.[72]

In cancer cells, the effect of saponins on membrane dynamics may vary due to the structural properties and composition of the cancer cells. However, Chol also plays an important role for the modulation of the membrane orders. Furthermore, cancer cell membranes have been found to contain lipid rafts that are thought to be a target of saponins.[38] Interaction of saponins at lipid rafts disrupts the lateral organization of the membrane, which sometimes leads to programmed cell death including apoptosis and autophagy, through an activation of membrane receptors, or with accompanying alteration of ion channel permeability.[73] The effect of saponins on cell death was also observed in necrosis and cell lysis by disruption of the membrane. However, it is necessary to understand the underlying concept to classify the exact mechanism of saponin-induced cell death by considering membrane morphological changes and biochemical properties.[74] Hereon, the different mechanisms involved in saponin-induced

cell death are presented. Saponins can induce formation of blebs, destruction of membrane and increase in cell volume, which are characteristics of necrotic cell death. This mechanism further allows activation of Ca^{2+}-dependent enzymes, some of which induce lysis of cytoskeleton.[38,74] Saponin-induced cell death can also occur via membrane lysis and pore-formation that have been observed in model membranes. These two mechanisms are characterized by increase of Ca^{2+} concentration in the cytosol and further activate the Ca^{2+}-dependent enzymes leading to necrosis.[74] At high saponin concentrations, immediate membrane lysis by hederacolchiside A1 could be observed on electron microscopy.[47,75,76] Experiments involving a release of fluorescence materials from cells have also exhibited the membrane-lysing activities of saponins as a consequence of pore formation, as shown with oleanane-type saponins, digitonin, avicins and *Quillaja* saponins.[38] Moreover, Chol has been suggested to be a key player for the membrane lysis and cell death. The activity of α-hederin towards monocytic cells was seen to decrease significantly when Chol is depleted.[47] Aside from the plasma membrane, saponins also target specific organelles for their lytic activities based on their composition and the susceptibility of these organelles to saponins is influenced by the amount of Chol contents. Another pathway to saponin-induced cell death is apoptosis. This is characterized by chromatin condensation and nucleus fragmentation. In addition, membranes are deformed to blebs and apoptotic bodies. Some of the saponins such as avicins, α-hederin and ginsenoside induce apoptotic cell death that affects the permeabilization of mitochondrial membrane (intrinsic pathway) and/or activation of death receptors at lipid raft domains (extrinsic pathway).[38] Apoptosis can also be accompanied by the release of cytochrome c into the cytosol, which increase in reactive oxygen species (ROS) and Ca^{2+}-influx or opening of a transition pore complex to enhance permeability.[38,77] Lastly, saponins can induce autophagy characterized by vacuole-formation of the cytosol, which leads to auto-digestion. The major proteins involved in autophagy include Atg5, Atg6 and Atg8. Saponins can either cause autophagy such as ginsenoside Rh2 and avicin D, while other saponins induce autophagy in order to prevent apoptosis.[38]

Saponins have been considered as potential cancer treatment drugs due to their ability to induce cytotoxic effects involving various pathways. Studies have also been conducted on the selective activity of saponins to cancer cell lines, but this property can sometimes be defeated by the fact that some saponins also possess cell lysis activity at certain concentrations. Nevertheless, some studies have pointed out that saponins exhibit specific cytotoxicity to some cancer cells and reduced hemolytic potential.[38,78] Scientists have attempted to elucidate a more

accurate mechanism of saponin-induced cytotoxicity to develop pharmaceutical drugs for cancer treatment and related diseases.

1.2.4 Biological activities of OSW-1 and other saponins

In this section, the saponins investigated in this study are discussed with a focus on OSW-1, including their biological activity on selected membrane models and biological systems. It is also worth mentioning that previous studies have partly elucidated their mode of action towards biological membrane. As already described, the structure of saponins plays an important role in biological activities. In this study, well-studied saponins such as digitonin, glycyrrhizin and soyasaponin Bb(I) were used to compare their activity with that of OSW-1. Digitonin (Fig.1-8**A**), which is a monodesmosidic steroidal saponin found in *Digitalis purpurea* and related species,[68] has shown strong hemolytic and membrane permeabilizing activities in a Chol-dependent manner.[65] In a recent paper by Frenkel et al.[68], the mechanism of interaction between digitonin and membrane Chol was investigated, in which digitonin penetrates into membrane containing Chol and elicits the formation of aggregates in the membrane without causing prominent membrane disruption. However, lines of evidence have pointed out that Chol is removed from the hydrophobic core region. The presence of a large sugar moiety in digitonin creates steric hindrance in the aggregates, which induces membrane curvature rise by accumulating in the outer leaflet. The induced curvature further increases membrane permeability. Moreover, it was also pointed out that a certain Chol/digitonin ratio is required to observe this phenomenon. At 0 mol% of Chol in SOPC membrane, no interaction was observed after addition 50 μM of digitonin (Fig. 1-17**A**). On the other hand, increasing Chol concentrations enhanced digitonin interaction at the same concentration. Actually, addition of 5 mol% of Chol elicited insertion of digitonin in the membrane and formation of insoluble complex composed of digitonin, Chol and SOPC (Fig. 1-17**C**), while the presence of 20 mol% Chol in membrane showed full insertion of digitonin to lead to removal of Chol from the membrane core. (Fig. 1-17**B**). [68]

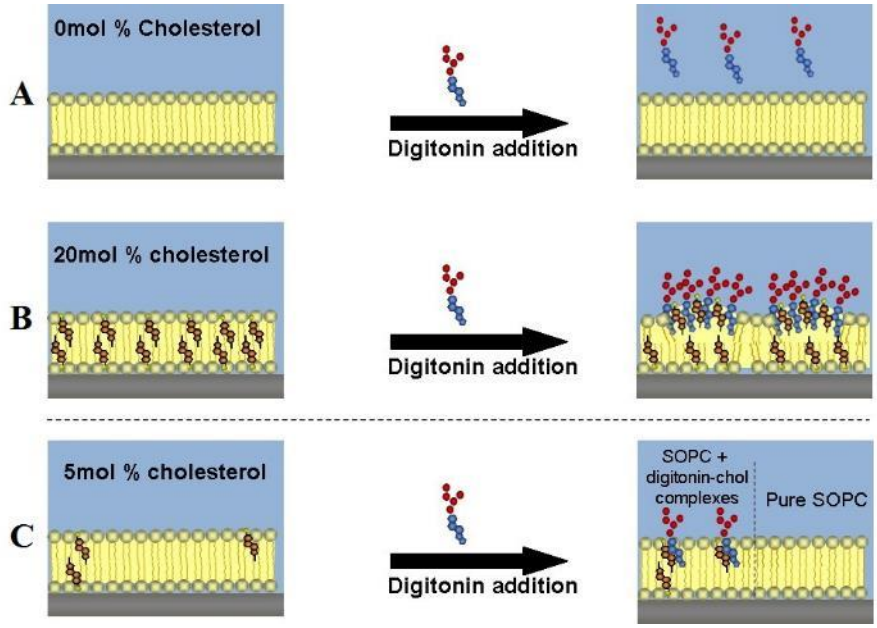

Figure 1-17. Mechanism of interaction of 50 μM digitonin at various Chol concentrations: (**A**) 0 mol% (**B**) 20 mol%, (**C**) 5 mol %. Reprinted with permission from *J. Phys. Chem. B*, **2014**.[68] Copyright © (2014) American Chemical Society.

Glycyrrhizin (Fig. 1-8**B**), which is a monodesmosidic triterpenoid saponin found in the licorice, *Glycyrrhiza glabra* is well known as a natural sweetener. The saponin has been found to exhibit antitumor and anticancer properties.[67] On the other hand, glycyrrhizin exhibits weak or no hemolytic activity, and hardly permeabilizes membrane permeabilizing activity even in the presence of Chol.[76] However, studies on lipid raft models using Langmuir monolayers have suggested that glycyrrhizin increases size of lipid raft domains, which is thought to be important for numerous cellular processes. In addition, these observations can also occur if Chol is present in the monolayer.[67] There have been no concrete mechanism proposed for glycyrrhizin on its membrane permeabilizing activity due to differences in the type of a model used, which gives contrasting results on whether glycyrrhizin has a Chol-dependent membrane activity. Similarly, soyasaponin Bb(I) (Fig. 1-8**C**) is an abundant monodesmosidic triterpenoid saponin present in soybeans, *Glycine max*. Although preliminary studies showed interesting biological properties of this saponin, the mechanism of its potential membrane permeabilizing properties remains elusive. One study suggests that soyasaponin Bb(I) directly interacts with membrane Chol and gives rise to more flexible membrane constituents.[44]

From here, previous studies on OSW-1 (Fig. 1-18), the major saponin interest of this study, is reviewed. OSW-1 is a steroidal monodesmosidic saponin isolated from bulbs of the lily family plant *Ornithogalum saundersiae* (Fig. 1-19).[79] OSW-1 has been first isolated in 1992 by Sashida's group together with other acylated cholestane glycosides. In particular, OSW-1 showed the ability to exhibit exceptionally high cytostatic activity against malignant tumor cells.[79,80] This discovery sparks the start of several studies on OSW-1 and its analogues, including total synthesis and structure-activity relationship studies (SAR), on its potential activity towards cancer cells.

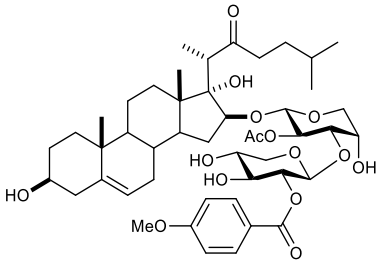

Figure 1-18. Structure of OSW-1

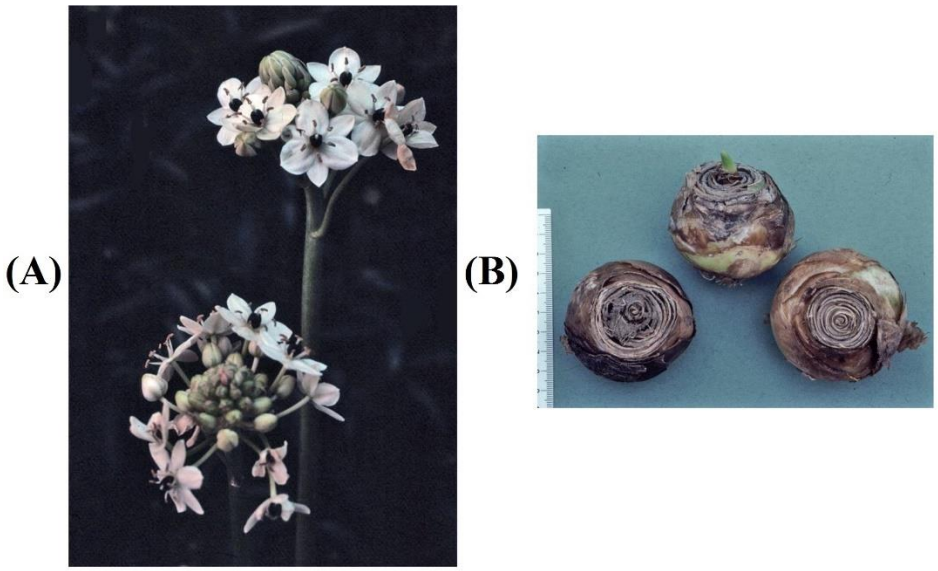

Figure 1-19. Images of (**A**) flowers and (**B**) bulbs of *Ornithogalum saundersiae*. Reprinted and modified with permission from *Chem. Rev.*, **2013**.[79] Copyright © (2013) American Chemical Society.

Among the other saponins examined in this study, OSW-1 shows a unique structural feature. Most saponins have a sugar moiety attached to the C3 position of aglycone, which is necessary for the membrane activity.[38,49] On the other hand, the position of sugar in OSW-1 at C16 position is very unusual for saponins.[79] In addition, OSW-1 contains an acylated sugar moiety (methoxybenzoyl-β-D-xylose and acetyl-α-L-arabinose), which is not common among saponins.[38] The X-ray crystallography of an OSW-1 variant showed the three-dimensional structure bearing hydrophobic clusters due to the presence of the two acyl chains in the disaccharide as well as the sterol side chain, and the overall structure of OSW-1 in a triangular shape (Fig. 1-21).[81] This hydrophobic cluster decreases its hydrophilicity compared to most saponins. However, even if the structure of OSW-1 deviates from common saponins, it has shown high activity and selectivity towards tumor cell lines and this is greatly attributed to the presence of acylated disaccharide moiety and the C16 attachment. The structure-activity relationships on antitumor activity of OSW-1 is summarized in Fig. 1-20.[79] Some important highlights regarding the selectivity of OSW-1 on tumor cells emphasized the importance of these structural features as OSW-1 exhibited powerful cytotoxic effects on HeLa cells (IC_{50} = 0.5 nM) and HL-60 cells (IC_{50} = 0.25 nM). The removal of methoxy-benzoyl group caused a ~40-fold drop in the cytotoxicity index (IC_{50} = 11 nM, HL-60 cells) and successive removal of the acetyl group caused a ~800-fold decrease in the cytotoxicity (IC_{50} = 190 nM, HL-60 cells).[79,82]

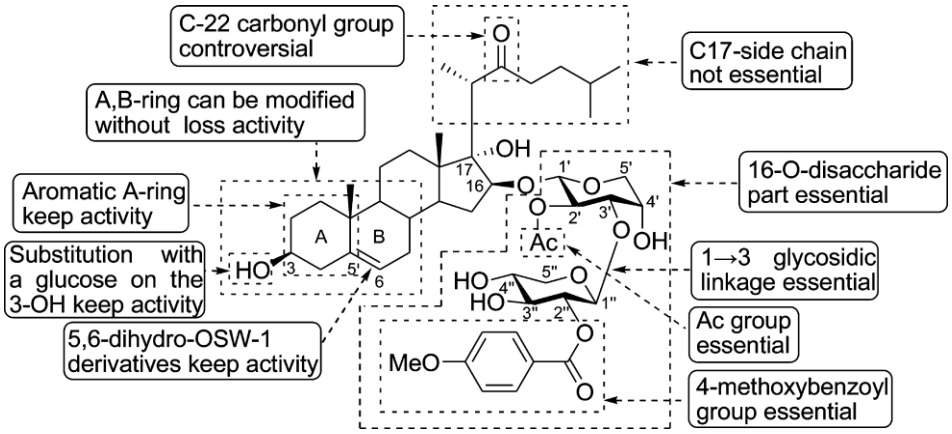

Figure 1-20. Structure-activity relationship of OSW-1 towards tumor cells. Reprinted with permission from *Chem. Rev.*, **2013**.[79] Copyright © (2013) American Chemical Society.

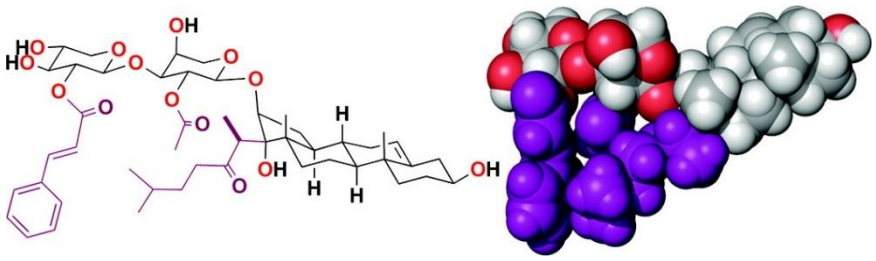

Figure 1-21. Three-dimensional structure of OSW-1. The structure on the left represents it close congener that differs in the acyl group attached to the L-arabinose from that of OSW-1. Reprinted with permission from *Org. Lett.*, **2010**.[81] Copyright © (2010) American Chemical Society.

Although studies have been reported on the mechanism of OSW-1 towards cancer inhibition by targeting oxysterol-binding proteins (OSBP) and OSBP-related protein 4L (ORP4L), which are involved in signal transduction, lipid transport and metabolism, and cancer cell survival[83], little information is known about its mode of interaction with lipid molecules in the biological membrane, specifically with Chol that is the main target of most saponins. In this study, the properties of OSW-1 towards simple membrane models and red blood cells are to be clarified. A mechanism of interaction with model membranes as well as biological membranes is proposed based on its properties at the end of this study.

Aside from OSW-1, other unusual saponins (Fig. 1-22) have also been investigated and compared to the usual saponins containing a sugar moiety attached to the C3 position of the sapogenin.[38,84,85] Interestingly, these saponins have often been isolated from marine organisms and have exhibited membrane-permeabilizing properties. The unusual origin of these saponins serves as a proof on biosynthetic diversity in the structure, function and activity towards biological membranes. First, pavoninins (Fig. 1-22**A** and **B**) have been isolated from the sole of *Pardachirus* spp. by Tachibana's group, and shown to act as a defense secretion for its predators.[84] The saponins have shown ichthyotoxic and shark-repellent activities. The attachment of the sugar moiety in both pavoninins differs from the usual ones, in that the sugar N-acetylglucosamine (GlcNAc) in pavoninin-1 is attached to the C7 carbon of the steroidal backbone; while in pavonin-4, GlcNAc is attached to the C15 of the steroidal backbone. Studies of pavoninins have revealed that membrane perturbation is independent of Chol in membrane. Actually, calcein leakage assays suggested that in the absence of Chol, membrane leakage

could be observed. In addition, a C3 analog of pavoninin (GlcNAc in C3 and carbonyl group in C7) has been synthesized and its activity was compared. The synthetic analog exhibited similar properties to those of pavoninin-1 in terms of Chol-independent membrane perturbation, but showed enhanced leakage activity in membranes composed only of PC.[84] Other unusual saponin reported so far is leucospilotaside B (Fig. 1-22**C**) isolated from *Holothuria leucospilota*, but a few studies have been reported regarding their activities. These saponins have exhibited antifungal and antitumor activities.[85] However, no detailed study has been done to examine the membrane properties of these unusual saponins at the molecular level.

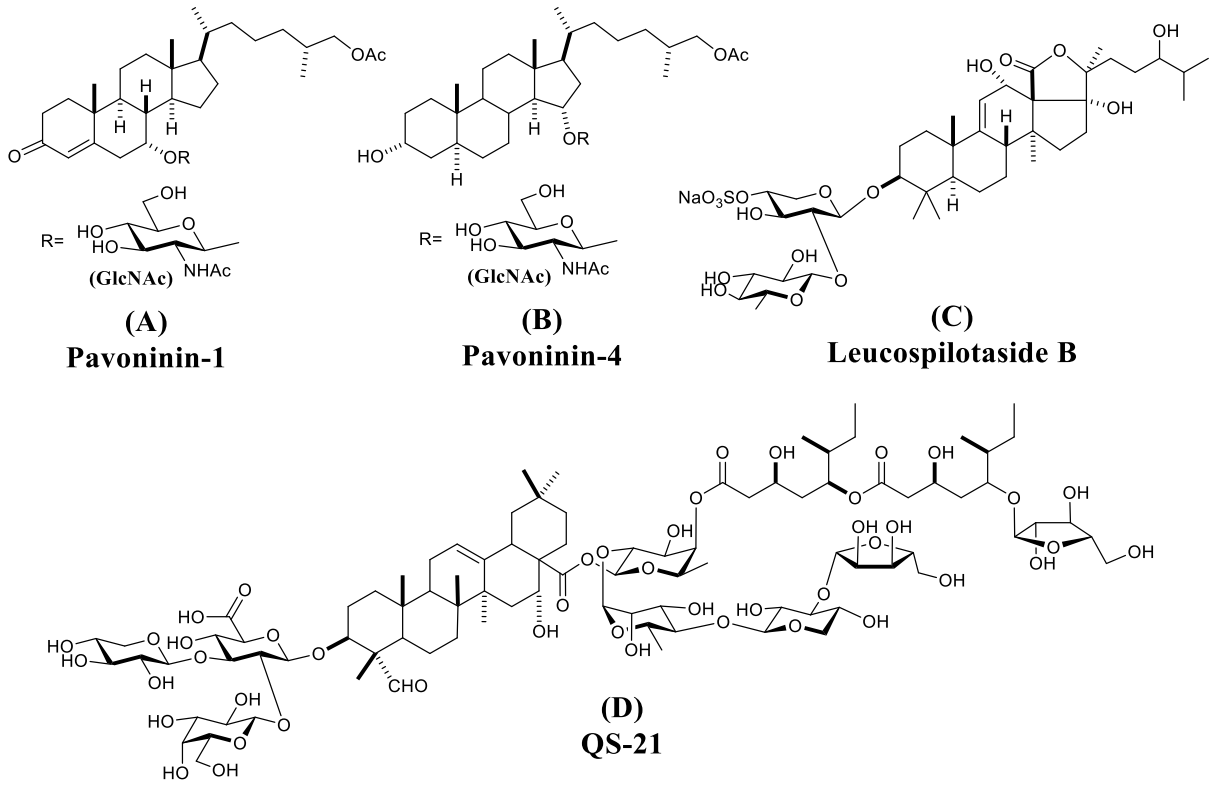

Figure 1-22. Examples of unusual monodesmosidic and bidesmosidic saponins derived from plants and marine organisms.

Aside from the saponins discussed earlier, a bidesmosidic triterpenoid saponin, QS-21 (Fig. 1-22**D**), has been widely studied due to the unique structure and bioactivity. QS-21 is a plant saponin obtained from *Quillaja saponaria* extracts. QS-21 contains an acylated sugar moiety at C3 and a complex sugar moiety at C28. It has been shown that QS-21 exhibits Chol-dependent membrane permeabilization and hemolysis, similar to other *Quillaja* fractions.[38] This fraction has attracted a lot of attention due to its cytotoxicity and potential adjuvant properties for vaccines that target influenza, malaria, hepatitis B, human papillomavirus, HIV/AIDS, tuberculosis, non-small-cell lung carcinoma, melanoma, etc.; but current studies have been limited to a potential human use due to its high toxicity and hemolytic properties.[86]

1.3 Methods used to investigate membrane interactions

An understanding of the important biological and membrane permeabilizing properties of saponins have been much advanced due to great progress in analytical instrumental technologies. Without these instruments, no concept has been established as to how natural products, including saponins, behave in biological systems. Scientists and engineers who have contributed to these technological advancements should be commended for their efforts. Their contributions have significantly brought new insights in very important phenomena occurring in biological systems, as well as in the molecular level mechanism.

In this section, the useful tools to examine important membrane interactions of saponins are presented. Extensive research has already been done on these phenomena using a combination of two or more tools. The focus of this section is on spectroscopic and microscopic techniques that have greatly contributed to an understanding of these interactions including saponin's effect on membrane lateral organization, dynamics and permeabilization.

1.3.1 NMR Spectroscopy

Solid state nuclear magnetic resonance (SS-NMR) spectroscopy has been widely used to study lipid-lipid and lipid-protein interactions in bilayer membranes. SS-NMR has also expanded to study on the effects of natural product towards membrane models. Common membrane models are micelles, bicelles and liposomes with various size and degree of lamellarity.[38,47,65] In the study of saponins, ^{2}H NMR and ^{31}P NMR are frequently used. ^{2}H NMR is commonly used to determine the molecular interaction between Chol and saponins

through the signal broadening and change of the quadrupolar splitting. This technique requires a deuterium probe in which deuterium substitutes the hydrogen at specific positions in the structure.[11,87] Spectrum of deuterated derivatives shows two peaks termed as Pake doublet. The distance (kHz) of this peak separation is called quadrupolar splitting $\Delta\nu_o$, which relates to the time-averaged orientation and wobbling of the vector between the bilayer normal and C–D bond vector. An important parameter in ^{2}H NMR is the molecular order parameter (S_{mol}) which gives information on the wobbling of the labeled site of lipid molecules;[11] usually, ^{2}H NMR is used to study motions due to molecular vibrations and rotations (10^{-7} s to 10^{-8} s)of the C–D bond in membrane bilayers.[11,24,25] The 3-α-deuterated sterol probes (Chol-d_1 and ergosterol-d_1) has been successfully used to analyze their direct interactions with natural products, proteins, peptides and saponins. The direct interaction to the partners significantly reduces the axial rotational rate of Chol-d_1 in membrane, which is often close to the ^{2}H NMR timescale, resulting in the attenuation and broadening of Pake doublet signals; a ^{2}H NMR signal appearing at 0 kHz is usually attributed to residual HOD or deuterated probe forming micelles. (Fig. 1-23).[87] This technique has also been adopted in the study of digitonin-Chol interaction.[38,43] The ^{2}H NMR of Chol-d_6 probe was measured in egg yolk PC at various digitonin-Chol ratio. They found that the interaction of digitonin with Chol proceeds in a concentration-dependent manner. Between 0 and 0.35 digitonin/Chol mole ratio, aggregated species containing digitonin and Chol is present, increasing the mole ratio of digitonin and Chol (0.35 to 0.90) causes the formation of intermediate complex and higher ratios could indicate formation of rigid equimolecular digitonin/Chol complex. Lower mole ratio of digitonin/Chol may have led to the reduction of molecular ordering by Chol-d_6 characterized by the presence of aggregated species as a result of fast exchange between free and Chol bound digitonin. At higher ratios, specifically a 1 to 1 ratio, the formation of the rigid complex results in the immobilization of Chol-d_6.[43] The result of this investigation could lead to an interesting discussion on the activity of saponins in terms of its effect on membrane Chol.

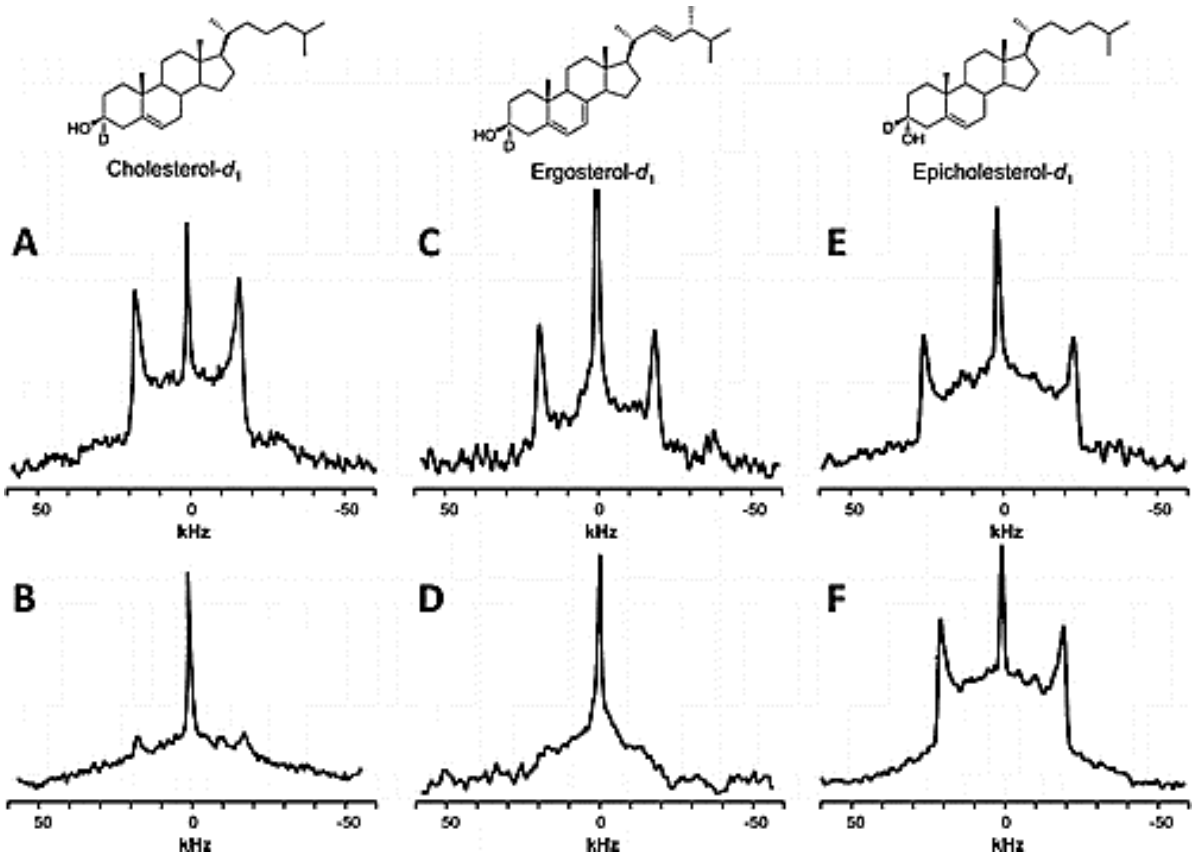

Figure 1-23. ^{2}H NMR spectra of sterol probes (Chol, ergosterol and epicholesterol) in the absence (A, C and E) and presence (B, D and F) of marine sponge cyclic peptide Theonellamide A (TNM-A). Reprinted with permission from *Biochemistry*, **2013**.[86] Copyright © (2013) American Chemical Society.

Another tool applied to study membrane dynamics is ^{31}P NMR, which gives rise to similar information to ^{2}H NMR. Particular difference between them is that ^{31}P NMR provides information on the orientation and dynamics of phospholipid headgroups and effects of natural products on the bilayer such as perturbations and curvature generation even under the conditions that ^{2}H signals become broad.[11] In addition, the structural properties of lipids in hydrated membrane including the phase state can also be characterized by ^{31}P NMR (Fig. 1-24). In other cases, morphological changes induced by natural products could also be determined by analysis of ^{31}P spectra. Regarding saponins, α-hederin was studied with respect to its effect on bilayer organization using a DMPC/Chol model.[47] In these experiments,

additions of α-hederin (10 mol% and 20 mol%) led to phase transition from lamellar phase to hexagonal phase. Increase in temperature from 37°C to 60°C made the hexagonal pattern more pronounced. In addition, a decrease in chemical shift anisotropy, Δσ, upon addition of α-hederin indicates possible membrane disruption leading to the higher mobility and diffusibility of phospholipids.[38,47] Similar NMR studies have also been done with membrane-active peptides regarding their effect on the lamellar structure and membrane morphology.[87] However, they reported that these compounds did not show any significant effects on the membrane lamellar structure or membrane dynamics. The combination of ^{2}H NMR and ^{31}P NMR techniques could provide important information for a better understanding of the effects of saponins on membrane dynamics. However, one of these methods is sometimes not enough to prove the mechanism of interaction of saponins and other natural products.

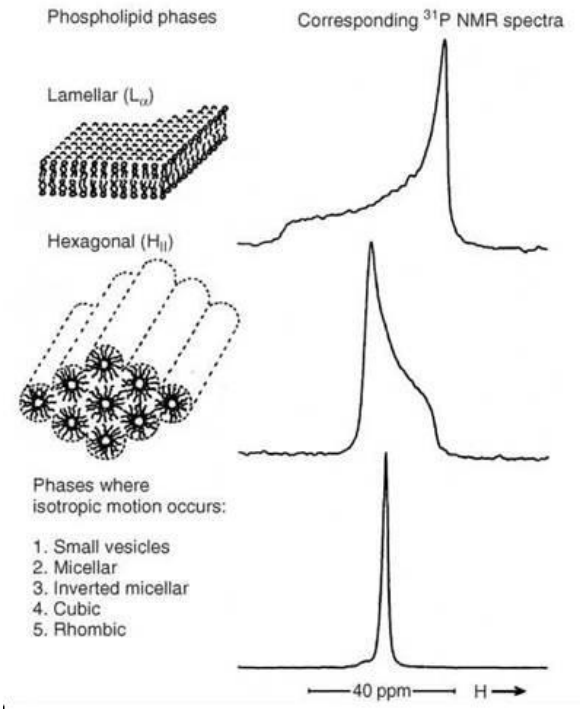

Figure 1-24. ^{31}P NMR spectra of phospholipids at different phase. Reprinted with permission from *The Structures and Properties of Membrane Lipids*, **1989**.[11] Copyright © (1989) Springer.

1.3.2 Fluorescence microscopic approaches

The concept of fluorescent probes has become popular in research on membrane dynamics and permeabilization. Fluorescence spectroscopic techniques have been utilized to determine the anisotropy of fluorescent compounds such as laurdan, cholestatrienol (CTL) and 1,6-diphenyl-1,3,5-hexatriene (DPH) to observe the fluidity and/or polarity in the membrane environment (10^{-10} s).[38] In addition, other fluorescent compounds can also be used to examine the membrane permeabilizing properties of saponins and natural products. In this case, the properties of these dyes are usually examined after addition of compounds into artificial vesicles. In addition, sensitivity to pH, concentration, membrane potential, and the environment surrounding the probe induce changes in their fluorescent properties. Commonly used assays for evaluating membrane permeabilization are the calcein leakage and K^+/H^+ exchange (monitored by lumen pH), for which calcein and BCECF (2',7'-bis-(2-carboxyethyl)-5-(and-6)-carboxyfluorescein) dyes are utilized, respectively.[47,48,88] Usually, LUVs that incorporate a fluorescent dye are used. A release of the dye from the lumen of the LUV to extravesicular solution gives rise to an increase in fluorescence intensity as a result of reduction in self-quenching.

The utilization of fluorescence probes has also expanded to microscopic imaging techniques in which fluorescent-labeled lipids give information on membrane partitioning and morphological changes caused by natural products.[47,48] GUVs are used as membrane models for confocal microscopic observation. In the study of saponins, phospholipids and Chol are usually fluorescently labeled. Probes used in the GUV observations can partition to either the L_o or L_d domain. In the case of the study on α-hederin, GUVs are labeled with Texas Red – DPPE (TR-DPPE), which has the excitation wavelength at 560 nm and the emission at 595 nm and partitions to the L_d domain. In the study, they assessed the time dependent morphological changes upon addition of α-hederin and related compounds. They also observed pore-forming properties of α-hederin, which provided additional information on the mechanism of interaction of this saponin (Fig. 1-25).[47]

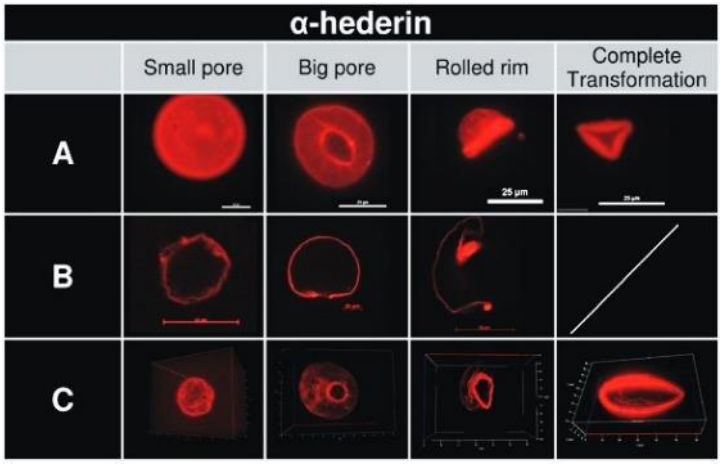

Figure 1-25. Pore-forming properties of α-hederin (40 µM) on GUVs composed of DMPC/Chol (3:1). (A) fluorescence microscopy, (B) confocal microscopy of cross section of one vesicle and (C) confocal microscopy of three-dimensional view of all cross section of an entire vesicle. Reprinted and modified with permission from *Journal of Biological Chemistry*, **2013**.[47] Copyright © (2013) The American Society for Biochemistry and Molecular Biology.

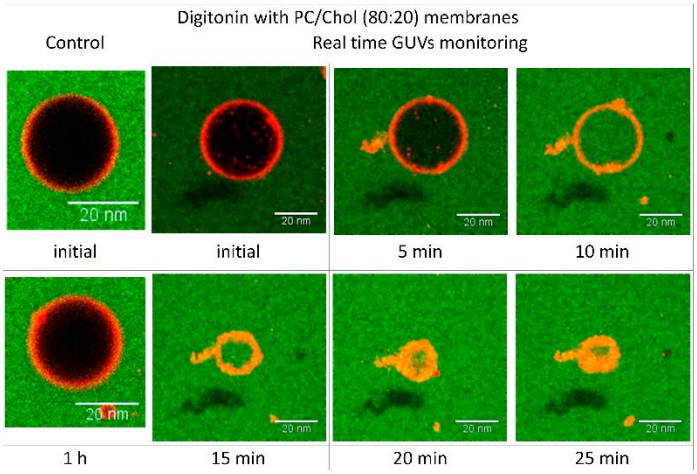

Figure 1-26. Effect of 20 µM digitonin on GUVs composed of PC/Chol (80:20) at different incubation period. Left panel shows control measurement where digitonin is not added in the system. Reprinted with permission from *Molecules*, **2015**.[89] Copyright © (2015) Multidisciplinary Digital Publishing Institute (MDPI).

Study on the membrane disrupting activity of digitonin has also been conducted using fluorescence microscopy (Fig. 1-26).[89] The GUVS are labeled with dioctadecyltetramethyl-indocarbocyanine perchlorate stain (DiI; Ex: 549 nm, Em: 565 nm), while Alexa Fluor 488 (Ex: 495 nm, Em: 519 nm) was used to induce fluorescence in the extravesicular fluid. A time-dependent membrane disruption elicited by digitonin was observed to proceed at a fast rate. When after 10 minutes of incubation, intact GUVs were no longer observed. Membrane disruption is thought to be a consequence of membrane permeabilization and Chol is a main factor for this effect.

Other microscopic techniques have also been used to study saponins such as Brewster angle microscopy in monolayers to evaluate domain formation in α-tomatine and reduction of raft size induced by glycyrrhizin.[66,67] Atomic force microscopy (AFM) has also been used to study co-localization of cofactor for acrosome reaction inducing substance (Co-ARIS), a monodesmosidic saponin, with ganglioside GM1 clusters and its expansion as well as formation of worm-like domains of α-hederin with phospholipids and Chol.[38,48]

1.3.3 Other methods

Other methods have also been used to assess the properties of saponins on membrane especially in the presence of Chol. Dynamic light scattering (DLS) spectroscopy has often been applied to determine the effect of saponins in the size of liposomes and determine whether aggregates or micelles are formed as a consequence of saponin interaction. In α-hederin, the size of Chol-free liposomes is not changed when the saponin is added. On the other hand, when Chol is present in the liposomes, membrane dispersion that may correspond to formation of isotropic and hexagonal phases could be observed upon addition of α-hederin.[47] Similarly, upon addition of digitonin, no effect on size of pure SOPC was observed. However, change in size distribution was observed for SOPC/Chol liposomes.[89]

The influence of Chol on saponins' activity can also be studied in biological systems. Chol depletion experiments can be done to assess the activities on red blood cells and human leukemic monocytic cell line (THP-1). Living cells can be treated with methyl-β-cyclodextrin (MβCD) to extract Chol from the cell membranes. Data on α-hederin have been shown that depletion of Chol markedly reduces the cytotoxicity.[38,47] Lately, research on the effects of saponins has been expanded to more complex biological systems in order to examine their pharmacological properties. This could be achieved by using cancer cell lines and by the assays

to determine saponin's potent activity and selectivity to different cancer cells. However, the complexity of these cells may also lead to uncertainties especially on the role of Chol towards saponin-induced cytotoxicities.[38]

Several techniques that can be used to study saponin interaction and its effect on membranes have been discussed in this section. However, one or a few of these techniques are sometimes not enough to gain desired experimental results. It is also important to use a combination of two or more techniques that could be very useful to achieve the purpose of the research, which compensate the limitations of each technique. In addition, the methods presented here are also utilized in the course of this research and some results thus obtained are reviewed in the other chapters later on.

1.4 Aim and Significance of the Study

The amphiphilic structure of saponins has served an important role in their membrane activity and pharmacological applications. Moreover, amphiphilic drugs must overcome the membrane barrier to enter the cells or organelles to exert its specific pharmacological properties. This could be achieved by penetration or permeation through the bilayer via passive diffusion or via interaction with specific membrane components such as transporter proteins. While saponins have largely exhibited interesting biological activities including cytotoxicity towards tumor cells, the mode of interaction at the atomistic lever has not been clearly established. This study focuses on OSW-1, an unusual saponin isolated from *Ornithogalum saundersiae* due to its highly potent and selective cytostatic properties against various malignant tumor cells. It has been known that OSW-1 specifically binds to a protein target OSBP (oxysterol-binding protein) and OSBP-related protein 4L (ORP4L), which are associated with signal transduction and lipid transport. Recently, these target proteins have also been characterized to have important functions in cancer cell proliferation and survival. Moreover, OSW-1 has been involved in the inhibition of Na^+/Ca^{2+} exchanger 1, which can lead to apoptosis in cancer cells. Despite this discovery, other membrane components, particularly lipids, could also be involved in the exertion of OSW-1's powerful cytotoxicity towards cancer cells. In this study, the elucidation of the mechanism of interaction of OSW-1 with membrane components was attempted, such as phospholipids and Chol. Furthermore, several reports suggest the importance of membrane Chol in order for saponins to exert its activity, which could also be for the case with OSW-1. Since OSW-1 has a unique sugar substitution position,

the mechanism study was carried out in comparison with other typical saponins, including digitonin, soyasaponin Bb(I), and glycyrrhizin, using spectroscopic and microscopic approaches. Structure activity relationship (SAR) studies have also been conducted on various saponins, which suggested that activities of saponins rely on the glycosylation position, size and arrangement (branching) of sugar moiety, and the nature of sapogenin rings. Assays utilizing biological membrane (red blood cells) and artificial model membranes (MLV, LUV and GUV) were carried out to study the effects of saponins on membrane permeability, lipid dynamics and morphology. Effect of Chol on the activity of saponins was also investigated using these assays. Solid-state NMR (SS-NMR) including ^{2}H NMR and ^{31}P NMR were applied to examine membrane dynamics and structural properties of phospholipids in membranes, respectively. These methods have shown valuable information regarding the direct interaction of natural products and membrane-active compounds with membranes composed of deuterium-labelled lipids. Fluorescence probes have also facilitated the study of saponin-Chol interaction as a consequence of binding and aggregation. Furthermore, the fluorescent probes were also used in microscopic studies to observe saponin-induced morphological changes and its effect on membrane integrity.

As of this writing, there are limited studies regarding the properties of OSW-1 towards membrane, even if there have been numerous papers published regarding its potent and selective activity for tumor cells. In addition, other typical saponins were used to establish a comparison with OSW-1's properties. It is also worth mentioning that the structure of OSW-1 deviates from most saponins in terms of sugar attachment in the sapogenin ring and the presence of an acylated sugar moiety. The structural differences of these saponins to establish a clear relationship with their biological properties, and to determine a plausible atomistic mode of interaction towards the membrane is also considered in this study.

References

1. Lodish, H., Berk, A., Zipursky, S.L., Matsudaira, P., Baltimore, D, Darnell, J. Molecular Cell Biology. 4th edition. New York: W. H. Freeman; **2000**. Section 5.3, Biomembranes: Structural Organization and Basic Functions. Available from: https://www.ncbi.nlm.nih.gov/books/NBK21583/

2. Watson, H. Biological membranes, *Essays in Biochemistry*. **2015**, *59*, 43-69.

3. Simons, K., Toomre, D., Lipid rafts and signal transduction, *Nat Rev Mol Cell Biol.* **2000**, *1*, 31-39.

4. Brown, B. S. Biological Membranes. The Biochemical Society, Portland, London, **1996**, p.1

5. Guidotti, G., The composition of biological membranes, *Arch Intern Med.* **1972**, *129*, 194-201.

6. Singer, S.J., Nicholson, G.L. Fluid mosaic model, *Science* **1972**, *18*, 720-731

7. Nicolson, G.L., The fluid—mosaic model of membrane structure: Still relevant to understanding the structure, function and dynamics of biological membranes after more than 40 years, *Biochim. Biophys. Acta* **2014**, *1838*, 1451–1466

8. van Meer, G., Voelker, D.R., Feigenson, G.W., Membrane lipids: where they are and how they behave, *Nat. Rev. Mol. Cell Biol*. **2008**, *9*, 112–124.

9. Murata, M., Sugiyama, S., Matsuoka, S. and Matsumori, N., Bioactive structure of membrane lipids and natural products elucidated by a chemistry-based approach. *Chem. Rec.* **2015**, *15*, 675–690.

10. Nenninger, A., Mastroianni, G., Robson, A., Lenn, T., Xue, Q., Leake, M.C., Mullineaux, C.W., Independent mobility of proteins and lipids in plasma membrane of *Escherichia coli*, *Mol. Microbiol.* **2014**, *92*, 1142-1153.

11. Gennis, R.B., Biomembranes: Molecular Structure and Function, New York: Springer-Verlag, **1989**.

12. Feigenson, G.W., Phase behavior of lipid mixtures, *Nature Chem Biol.* **2006**, *2*, 560-563.

13. Marsh, D., Lateral pressure profile, spontaneous curvature frustration, and the incorporation and conformation of proteins in membranes, *Biophys J* **2007**, *93*, 3884-3899.

14. van Meer, G., Lisman, Q., Sphingolipid transport: rafts and translocators, *J Biol Chem* **2002**, *277*, 25855-25858.

15. Ali, M.R., Cheng, K.H., Huang, J., Ceramide drives cholesterol out of the ordered lipid bilayer phase into the crystal phase in 1-palmitoyl-2-oleoyl-*sn*- glycerol-3-phosphocholine/cholesterol/ceramide ternary mixtures, *Biochemistry* **2006**, *45*, 12629-12638.

16. Voet, D., Fundamentals of Biochemistry: Life at the Molecular Level (4th ed.). Wiley. ISBN 978-1118129180, **2012**.

17. Sonnino, S., Prinetti, A., Lipids and membrane lateral organization, *Frontiers in Physiology* **2010**, *1*, 1-9.

18. Gorter, E., Grendel, F., On bimolecular layers of lipoids on the chromocytes of the blood, *J. Exp. Med.* **1925**, *41*, 439–443.

19. Danielli, J. F.; Davson, H.A., contribution to the theory of permeability of thin films, *Journal of Cellular and Comparative Physiology* **1935**, *5*, 495–508.

20. Steim, J. M., Tourtellotte, M. E., Reinert, J. C., McElhaney, R. N., Rader, R. L., Calorimetric evidence for the liquid-crystalline state of lipids in a biomembrane. *Proc. Natl. Acad. Sci. U.S.A.* **1969**, *63*, 104–109.

21. Lee, A. G., Birdsall, N. J., Metcalfe, J. C., Toon, P. A., Warren, G. B., Clusters in lipid bilayers and the interpretation of thermal effects in biological membranes, *Biochemistry* **1974**, *13*, 3699–3705.

22. Karnovsky, M. J., Kleinfeld, A. M., Hoover, R. L., Klausner, R. D., The concept of lipid domains in membranes. *J. Cell Biol.* **1982**, *94*, 1–6.

23. Simons, K., van Meer, G., Lipid sorting in epithelial cells. *Biochemistry* **1988**, *27*, 6197–6202.

24. Gawrisch, K., The dynamics of membrane lipids, in "The structure of biological membranes", **2005**, CRC Press, LLC, pp. 147-171.

25. Luckey, M., Introduction to the Structural Biology of Membrane Proteins, in "Computational Biophysics of Membrane Proteins", **2016**, RSC Publishing, United Kingdom, pp. 1-18.

26. Lewis, R.N., McElhaney, R.N., Surface charge markedly attenuates the nonlamellar phase-forming propensities of lipid bilayer membranes: calorimetric and (31)P-nuclear magnetic resonance studies of mixtures of cationic, anionic, and zwitterionic lipids, *Biophys J.* **2000**, *71*, 1455-1464.

27. London, E., How principles of domain formation in model membranes may explain ambiguities concerning lipid raft formation in cells, *Biochim. Biophys. Acta – Molecular Cell Research* **2005**, *1746*, 203-220.

28. Heberle, F.A., Wu, J., Goh, S.L., Petruzielo, R.S., Feigenson, G.W., Comparison of three ternary lipid bilayer mixtures:FRET and ESR reveal nanodomains, *Biophys. J.* **2010**, *99*, 3309-3318.

29. Nyholm, K.M.T., Lindroos, D., Westerlund, B., Slotte, J.P., Construction of a DOPC/PSM/Cholesterol phase diagram based on the fluorescence properties of trans-parinaric acid, *Langmuir* **2011**, *27*, 8339–8350.

30. Lindner, R., Naim, H. Y., Domains in biological membranes, *Exp. Cell Res.* **2009**, *315*, 2871–2878.

31. Elson, E. L., Fried, E., Dolbow, J. E., Genin, G. M.,Phase separation in biological membranes: integration of theory and experiment, *Annu. Rev. Biophys.* **2010**, *39*, 207–226.

32. Loura, L.M., Federov, A., Prieto, M., Fluid-fluid membrane microheterogeneity: a fluiorescence resonance energy transfer study, *Biophys. J.* **2001**, *80*, 776-788.

33. McMullen, T.P., Vilcheze, C., McElhaney, R.N., Bitman, R., Diffrential scanning calorimetry study of the effect of sterol side chain length and structure on dioalmitoylphosphatidylcholine thermotropic phase behavior, *Biophys. J.* **1995**, *69*, 169-176.

34. de Almeida, R.F., Federov, A., Prieto, M., Sphingomyelin/phisphatidylcholine/cholesterol phase diagram: boundaries and composition of lipid rafts, *Biophys. J.* **2003**, *85*, 2406-2416.

35. Bagatolli, L.A., Ipsen, J.H., Simonsen, A.C., Mouritsen, O.G., An outlook on organization of lipids in membranes: searching for a realistic connection with the organization of biological membranes, *Prog. Lipid Res.* **2010**, *49*, 378-389.

36. Augustin, J.M., Kuzina,V. Andersen, S.B., Bak, S., Molecular activities, biosynthesis and evolution of triterpenoid saponins, *Phytochemistry* **2011**, *72*, 435-457.

37. Bachran, C., Bachran, S., Sutherland, D., Bachran, D., Fuchs, H., Saponins in tumor therapy, *Mini-Rev. Med. Chem.* **2008**, *8*, 575-584.

38. Lorent, J.H., Quetin-Leclercq, J., Mingeot-Leclercq, M.P., The amphiphilic nature of saponins and their effects on artificial and biological membranes and potential consequences for red blood and cancer cells, *Org. Biomol. Chem.* **2014**, *12*, 8803-8822.

39. Williams, J.R., Gong, H., Lipids Biological activities and syntheses of steroidal saponins: the shark-repelling pavoninins, *Lipids* **2007**, *42*, 77-86.

40. Bruneton, J., Pharmacognosie, Phytochimie, *Plantes Médicinales* **2009**, Lavoisier, Paris, 4 edn,

41. Papadopoulou, K. Melton, R.E., Leggett, M., Daniels, M.J., Osbourn, A.E., Compromised disease resistance in saponin-deficient plants, *Proc. Natl. Acad. Sci. U. S. A.* **1999**, *96*, 12923-12928.

42. Dinda, B., Debnath, S., Mohanta, B.C., Harigaya, Y., Naturally Occurring Triterpenoid Saponins, *Chem. Biodiversity* **2010**, *7*, 2327-2580.

43. Akiyama, T., Takagi, S., Sankawa, U., Inari, S., Saito, H., Saponin-cholesterol interaction in the multibilayers of egg yolk lecithin as studied by deuterium nuclear magnetic resonance: digitonin and its analogs, *Biochemistry* **1980**, *19*, 1904-1911.

44. Murata, M., Houdai, T., Morooka, A., Matsumori, N., Oishi, T., Membrane interaction of soyasaponins in association with their antioxidation effects, *Soy Protein Research, Japan* **2005**, *8*, 81-85.

45. Kim, H.J., Kim, P., Shin, C.Y., A comprehensive review of the therapeutic and pharmacological effects of ginseng and ginsenosides in central nervous system, *Journal of Ginseng Research* **2013**, *37*, 8-29.

46. Armah, C.N., Mackie, A.R., Roy, C., Price, K., Osbourn, A.E., Bowyer, P., Ladha, S., The membrane-permeabilizing effect of avenacin A-1 involves the reorganization of bilayer cholesterol, *Biophys. J.* **1999**, *76*, 281-290.

47. Lorent, J., Le Duff, C.S., Quetin-Leclercq, J., Mingeot-Leclercq, M.P., Induction of highly curved structures in relation to membrane permeabilization and budding by the triterpenoid saponins, α- and δ-Hederin, *J. Biol. Chem.* **2013**, *288*, 14000-14017.

48. Lorent, J., Lins, L., Domenech, O., Quetin-Leclercq, J., Brasseur, R., Mingeot-Leclercq, M.P., Domain formation and permeabilization induced by the saponin α-hederin and its aglycone hederagenin in a cholesterol-containing bilayer, *Langmuir* **2014**, *30*, 4556-4569.

49. Keukens, E.A., de Vrije, T., van den Boom, C., de Waard, P., Plasman, H., Thiel, F., Chupin, V., Jongen, W.M., de Kruijff, B., Molecular basis of glycoalkaloid induced membrane disruption, *Biochim. Biophys. Acta* **1995**, *1240*, 216-228.

50. Israelachvili, J.N., *Intermolecular and Surface Forces* **2011**, Academic Press, Elsevier, Amsterdam, 3rd edn.

51. Bottger, S., Hofmann, K., Melzig, M.F., Saponins can perturb biologic membranes and reduce the surface tension of aqueous solutions: a correlation?, *Bioorg. Med. Chem.* **2012**, *20*, 2822-2828.

52. Moses, T., Papadopoulou, K.K, Osbourn, A., Metabolic and functional diversity of saponins, biosynthetic intermediates and semi-synthetic derivatives, *Crit Rev Biochem Mol Biol.* **2014**, *49*, 439-462.

53. Thakur, M., Melzig, M.F., Fuchs, H., Weng, A., Chemistry and pharmacology of saponins: special focus on cytotoxic properties, *Bot Targets Ther*. **2011**, *1*, 19-29.

54. Thimmappa, R., Geisler, K., Louveau, T., O'Maille, P., Osbourn, A., Triterpene biosynthesis in plants, *Annu Rev Plant Biol.* **2014**, *65*, 225-257.

55. Nützmann, H.W., Osbourn, A., Gene clustering in plant specialized metabolism, *Curr Opin Biotechnol.* **2014**, *26*, 91-99.

56. Schroeder, A., Heller, D.A., Winslow, M.M., Dahlman, J.E., Pratt, G.W., Langer, R., Jacks, T., Anderson, D.G., Treating metastatic cancer with nanotechnology, *Nat. Rev. Cancer* **2012**, *12*, 39-50.

57. Nazari, M., Kurdi, M., Heerklotz, H., Classifying surfactants with respect to their effect on lipid order, *Biophys. J.* **2012**, *102*, 498-506.

58. Brodgen, K.A., Antimicrobial peptides: pore formers or metabolic inhibitors in bacteria?, *Nat. Rev. Microbiol.* **2005**, *3*, 238-250.

59. Wimley, W.C., Describing the mechanism of antimicrobial peptide action with the interfacial activity model, *ACS Chem. Biol.* **2010**, *5*, 905-917

60. Shai, Y., Mode of action of membrane active antimicrobial peptides, *Biopolymers* **2002**, *66*, 236-248.

61. Pokorny, A., Almeida, P.F.F., Kinetics of dye efflux and lipid flip-flop induced by δ-lysin in phosphatidylcholine vesicles and the mechanism of graded release by amphipathic, α-helical peptides, *Biochemistry* **2004**, *43*, 8846-8857.

62. Pokorny, A., Almeida, P.F.F., Permeabilization of raft-containing lipid vesicles by δ-lysin: a mechanism for cell sensitivity to cytotoxic peptides, *Biochemistry* **2005**, *44*, 9538-9544.

63. Epand, R.F., Maloy, W.L., Ramamoorthy, A., Epand, R.M., Probing the "charge cluster mechanism" in amphipathic helical cationic antimicrobial peptides, *Biochemistry* **2010**, *49*, 4076-4084.

64. Gogelein, H., Huby, A., Interaction of saponin and digitonin with black lipid membranes and lipid monolayers, *Biochim. Biophys. Acta* **1984**, *773*, 32-38.

65. Nishikawa, M., Nojima, S., Akiyama, T., Sankawa, U., Inoue, K., Interaction of digitonin and its analogs with membrane cholesterol, *J. Biochem.* **1984**, *96*, 1231-1239.

66. Walker, B.W., Manhanke, N., Stine, K.J., Comparison of the interaction of tomatine with mixed monolayers containing phospholipid, egg sphingomyelin, and sterols, *Biochim. Biophys. Acta, Biomembr.* **2008**, *1778*, 2244-2257.

67. Sakamoto, S., Nakahara, H., Uto, T., Shoyama, Y., Shibata, O., Investigation of interfacial behavior of glycyrrhizin with a lipid raft model via a Langmuir monolayer study, *Biochim. Biophys. Acta* **2013**, *1828*, 1271-1283.

68. Frenkel, N., Makky, A., Sudji, I.R., Wink, M., Tanaka, M., Mechanistic investigation of interactions between steroidal saponin digitonin and cell membrane models, *J. Phys. Chem.* **2014**, *118*, 14632-14639.

69. Lange, Y., Ye, J., Steck, T.L., Activation of membrane cholesterol by displacement from phospholipids, *J. Biol. Chem.* **2005**, *280*, 36126-36131.

70. Segal, R., Milo-Goldzweig, I., The susceptibility of cholesterol-depleted erythrocytes to saponin and sapogenin hemolysis, *Biochim. Biophys. Acta* **1978**, *512*, 223-226.

71. Takechi, M., Tanaka, Y., Haemolytic time course differences between steroid and triterpenoid saponins, *Planta Med.* **1995**, *61*, 76-77.

72. Xu, Z.X., Ding, T., Haridas, V., Connolly, F., Gutterman, J.U., Avicin D, a plant triterpenoid, induces cell apoptosis by recruitment of Fas and downstream signaling molecules into lipid rafts, *PLoS One* **2009**, *4*, e8532.

73. Jacobson, K., Mouritsen, O.G., Anderson, R.G.W., Lipid rafts: at a crossroad between cell biology and physics, *Nat. Cell Biol.* **2007**, *9*, 7-14.

74. Kroemer, G., Galluzzi, L., Vandenabeele, P., Abrams, J., Alnemri, E.S., Baehrecke, E.H., Blagosklonny, M.V., El Deiry, W.S., Golstein, P., Green, D.R., Hengartner, M., Knight, R.A., Kumar, S., Lipton, S.A., Malorni, W., Nunez, G., Peter, M.E., Tschopp, J., Yuan, J., Piacentini, M., Zhivotovsky, B., Melino, G., Classification of cell death: recommendations of the Nomenclature Committee on Cell Death 2009, *Cell Death Differ.* **2009**, *16*, 3-11.

75. Mazzucchelli, G.D., Cellier, N.A., Mshviladzade, V., Elias, R., Shim, Y.H., Touboul, D., Quinton, L., Brunelle, A., Laprevote, O., De Pauw, E.A., Pauw-Gillet, M.C., Pores formation on cell membranes by hederacolchiside A1 leads to a rapid release of proteins for cytosolic subproteome analysis, *J. Proteome Res.* **2008**, *7*, 1683-1692.

76. Gilabert-Oriol, R., Mergel, K., Thakur, M., von Mallinckrodt, B., Melzig, M.F., Fuchs, H., Weng, A., Real-time analysis of membrane permeabilizing effects of oleanane saponins, *Bioorg. Med. Chem.* **2013**, *21*, 2387-2395.

77. Hunter, D.R., Haworth, R.A., The Ca^{2+}-induced membrane transition in mitochondria. III. Transitional Ca^{2+} release, *Arch. Biochem. Biophys.* **1979**, *195*, 468-477.

78. Swamy, S.M.K., Huat, B.T.K., Intracellular glutathione depletion and reactive oxygen species generation are important in alpha-hederin-induced apoptosis of P388 cells, *Mol. Cell. Biochem.* **2003**, *245*, 127-139.

79. Tang, Y., Li, N., Duan, J., Tao, W., Structure, bioactivity, and chemical synthesis of OSW-1 and other steroidal glycosides in the genus *Ornithogalum*, *Chemical Reviews* **2013**, *113*, 5480-5514

80. Kubo, S., Mimaki, Y., Terao, M., Sashida, Y., Nikaido, T., Ohmoto, T., Acylated cholestane glycosides from the bulbs of *Ornithogalum saundersiae*, *Phytochemistry* **1992**, *31*, 3969-3973.

81. Sakurai, K., Fukumoto, T., Noguchi, K., Sato, N., Asaka, H., Moriyama, N., Yohda, M., Three dimensional structures of OSW-1 and its congener, *Org. Lett.* **2010**, *12*, 5732-5735.

82. Zhou, Y., Garcia-Prieto, C., Carney, D.A., Xu, R., Pelicano, H., Kang, Y., Yu, W., Lu, C., Kondo, S., Liu, J., Harris, D.M., Estrov, Z., Keating, M.J., Jin, Z., Huang, P., OSW-1: a natural compound with potent anticancer activity and a novel mechanism of action, *J. Natl. Cancer Inst.* **2005**, *97*, 1781-1785.

83. Burgett, A.W., Poulsen, T.B., Wangkanont, K., Anderson, D.R., Kikuchi, C., Shimada, K., Okubo, S., Fortner, K.C., Mimaki, Y., Kuroda. M., Murphy, J.P., Schwalb, D.J., Petrella, E.C., Cornella-Taracido, I., Schirle, M., Tallarico, J.A., Shair, M.D., Natural products reveal cancer cell dependence on oxysterol-binding proteins, *Nat Chem Biol.* **2011**, *7*, 639-647.

84. Ohnishi, Y., Tachibana, K., Synthesis of pavoninin-1, a shark repellent substance, and its structural analogues toward mechanistic studies on their membrane perturbation, *Bioorg Med Chem.* **1997**, *5*, 2251-65.

85. Gomes, A.R., Freitas, A.C., Rocha-Santos, T.A.P., Duarte, A.C., Bioactive compounds derived from echinoderms, *RSC Adv.* **2014**, *4*, 29365-29382.

86. Zhu, D., Tuo, W., QS-21: a potent vaccine adjuvant. *Natural Products Chemistry & Research*. **2016**, *3*, e113-

87. Espiritu, R.A., Matsumori, N., Murata, M., Nishimura, S., Kakeya, H., Matsunaga, S., Yoshida, M., Interaction between the marine sponge cyclic peptide Theonellamide A and sterols in lipid bilayers as viewed by surface plasmon resonance and solid-state ^{2}H nuclear magnetic resonance. *Biochemistry* **2013**, *52*, 2410-2418.

88. Takano, K., Konoki, K., Matsumori, N., Murata, M., Amphotericin-B induced ion flux is markedly attenuated in phosphatidylglycerol membrane as evidenced by newly developed fluorometric method, *Bioorganic Med. Chem.* **2009**, *17*, 6301-6304.

89. Sudji, I.R., Subbura, Y., Frenkel, N., García-Sáez, A.J., Wink, M., Membrane disintegration caused by the steroid saponin digitonin is related to the presence of cholesterol, *Molecules* **2015**, *20*, 20146-20160

Chapter 2
Sterol recognition and membrane-permeabilizing activity of saponins deduced from spectroscopic evidences

2.1 Introduction – The unique steroidal saponin OSW-1

OSW-1 (Fig. 2-1) is a steroidal saponin first isolated by Sashida's group in 1992 from the bulbs of *Ornithogalum saundersiae*.[1,2] The structure of this saponin differs from the usual ones, such that it contains an acylated disaccharide moiety linked to the C16β-OH position on the D ring of the sapogenin backbone. In most saponins, the sugar moieties are usually attached to the 3β-OH position of the A ring of sapogenin backbone.[3-6] Several studies have been done on the ability of OSW-1 to target various tumor cells with high potency and selectivity, including human HeLa cells and HL-60 cells.[6-8] The cytotoxic properties of OSW-1 have been linked to the presence of acylated disaccharide moiety according to the structure activity relationship (SAR) studies. It has been revealed that removal of methoxybenzoyl and acetyl group in the sugar moiety lead to the reduction of its cytotoxicity to up to ~800-fold.[1] This suggests that the presence of these structures are important for OSW-1 in exerting its biological activity.

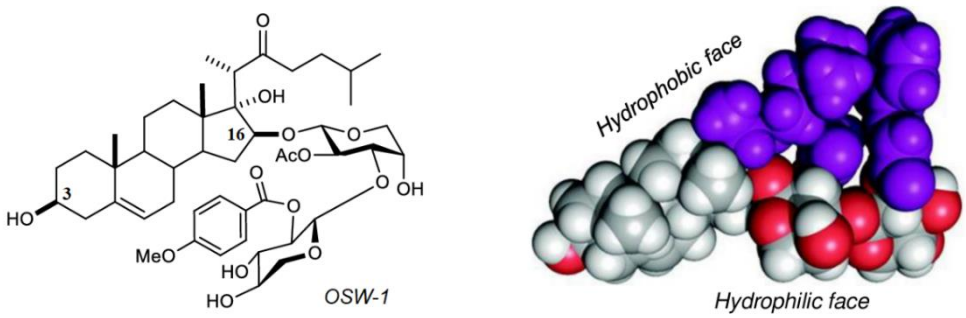

Figure 2-1. Structure of OSW-1 (left); 3D space-filling representation of a derivative of OSW-1[7] (right). Reprinted with permission from *BBA Biomembranes*, **2017**.[20] Copyright © (2017) Elsevier.

Despite the studies conducted on the activities of OSW-1, there were no attempts regarding its mechanism of action towards biological membranes at the atomistic level. Here, the activity of OSW-1 was assessed in comparison with typical 3-*O*-glycosyl saponins, including digitonin, soyasaponin Bb(I) and glycyrrhizin. Numerous saponins have shown membrane permeabilizing and hemolytic properties, which are thought to be sterol-

dependent.[9-11] Chol is a predominant lipid found in the eukaryotic plasma membrane, which is important for membrane stability and permeability of various solutes.[12,13] In the membrane permeabilizing and disrupting activities of various saponins, Chol has been proposed to play a key role by forming complexes in membrane, which leads to hydrophilic interactions between sugar moieties. Furthermore, when this saponin-Chol complex reaches a certain density, membrane defects and creation of spherical buds and/or tubules can be observed, which is likely attributed to the complex formation through interactions of saponin sugar moieties. Membrane disruption could take place due to rearrangement of the membrane.[14-16] Another mechanism involves the formation of saponin-sterol aggregates and toroidal pores as a consequence of hydrophilic interactions between sugar moieties.[11] In some cases, saponins showed concentration-dependent membrane permeabilization based on saponin arrangement and organization. It has been observed that below the critical micelle concentration (CMC), saponins exist as monomers and bind to the external monolayer inducing an area of positive curvature resulting to vesiculation. On the other hand, above CMC, saponins induce direct pore formation leading to a loss of membrane materials.[17,18] The direct interaction of micelles with membrane leads to the deposit of high saponin concentration near the membrane, which causes permeabilization. Moreover, the interaction of saponins with Chol-enriched domains results in immediate permeabilization.[19]

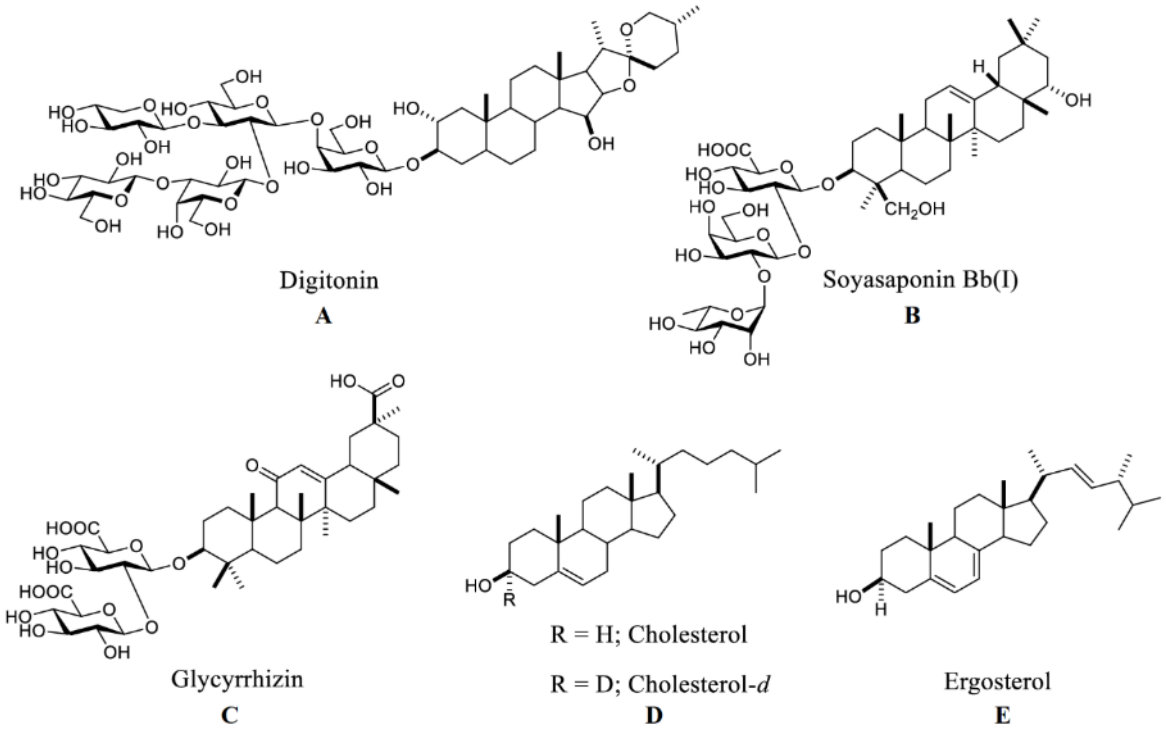

Figure 2-2. Structures of common saponins digitonin (A), soyasaponin Bb(I) (B), glycyrrhizin (C); cholesterol (D) and ergosterol (E).

Mechanism of interactions has been proposed for some of the saponins such as digitonin (Fig.2-2**A**), a typical saponin from the plant *Digitalis purpurea*, which has been classified under the concentration-dependent membrane action model. Digitonin exhibited significant membrane-disrupting properties, which leads to permanent membrane insertion into the membrane due to aggregation and equimolecular complex formation with Chol and surrounding phospholipids.[4,21,22] However, the mechanism of interaction of soyasaponin Bb(I) (Fig. 2-2**B**), isolated from *Glycine max*, has not been completely elucidated although ^{2}H-NMR measurements have been made, which revealed a less ordered and flexible membrane components upon Chol interaction.[23] Similarly, no clear mechanism was established for glycyrrhizin (Fig. 2-2**C**), isolated from *Glycyrrhiza glabra*, probably due to its weak membrane permeabilizing activities. The mechanism of interaction of OSW-1 has not been clearly elucidated, but the unique glycosylation position and presence of hydrophobic caps on the hydroxy groups of the sugar moiety could provide comparable amphiphilic properties with other typical saponins (Fig.2-2**A** to **C**). In this study, the elucidation of the mechanism of interaction of OSW-1, in comparison with other typical saponins, is determined using several spectroscopic approaches. OSW-1 has been known to target specific membrane proteins in order to exert its activity. However, membrane lipid components could also play a key role towards OSW-1's observed pharmacological activity. Furthermore, since most of the saponins studied require Chol interaction, it is also necessary to determine whether the activity of OSW-1 is Chol-dependent or not.

2.2 Aim and significance

The ability of OSW-1 to permeabilize biological membranes and its underlying mechanism could lead to potential development of new pharmacological and pharmaceutical drugs targeting the membrane Chol. One of the most striking discoveries on OSW-1 is its highly potent and selective cytotoxic activity towards tumor cells, and has been found to have higher cytotoxic effects compared to commonly used clinical treatments such as paclitaxel and doxorubicine.[6,8] However, very limited studies have been conducted on the molecular mechanism of OSW-1 towards sterol recognition and membrane permeabilization. This study presents a better understanding on how OSW-1 and other typical saponins recognize sterols and lead to membrane permeabilization using various spectroscopic techniques.

Although several studies have already been carried out on saponins such as digitonin, soyasaponin Bb(I) and glycyrrhizin to postulate models for their possible mechanism of actions, a more comprehensive study on the sterol dependent membrane permeabilizing activity these typical 3-*O*-glycosyl saponins has not been conducted. Furthermore, the focus of the study is on the unique saponin OSW-1 among other saponins. This study aimed to gain a better understanding on the sterol interaction of OSW-1 in order to elucidate a possible mechanism of interaction by using artificial and biological model membranes. Spectroscopic studies, with a main focus on ^{2}H and ^{31}P NMR, were used to provide evidence on the membrane activity of the aforementioned saponins with respect to membrane Chol. By comparing the activity of OSW-1 with those of the usual 3-*O*-glycosyl saponins, the general mechanism of the membrane activity of usual saponins could be studied from a different aspect. Most saponins and amphiphilic drugs require interaction with specific membrane components or receptors such as proteins and lipids in order to exert their cytotoxic activity towards tumor cells. Thus, after binding to the receptor, these compounds must overcome the membrane barrier via adsorption at the surface or partitioning to the bilayer interior to effectively manifest its potent action towards specific cellular target. However, the overall polarity and ionic character of these compounds influence their membrane interaction and permeabilizing effect. A correlation of the membrane activity of OSW-1 with the potent and selective cytotoxic activity towards tumor cells is further established in this study.

2.3 Results

2.3.1 Leakage properties of saponins

The Chol-dependent calcein leakage and pore forming properties of saponins have been determined by utilizing calcein-entrapped liposomes with homogeneous size. In this experiment, the selectivity of these saponins towards membrane composed of ergosterol (Erg) and 3-epicholesterol (Epichol) were also screened by replacing Chol with these sterols. Various saponin concentrations were used (1 μM to 100 μM) to assess the degree of leakage induced via saponin-sterol interactions by monitoring fluorescence changes.[24] OSW-1 exhibited significantly strong permeabilization in Chol-containing liposomes (EC_{50} = 35.4 ± 1.4 μM), but showed weaker effects on Erg-containing liposomes (EC_{50} = ~100 μM) (Fig. 2-3). Interestingly, OSW-1 showed insignificant permeabilizing activity towards Epichol-containing liposomes, which is comparable to the results obtained with pure POPC LUVs. Both digitonin and soyasaponin Bb(I) showed similar membrane permeabilizing activity and sterol selectivity

with OSW-1 (Table 2-1 and Fig. 2-3). The results suggest that initial binding to 3β-hydroxysterols, such as Chol and Erg, is required in order for such saponin-induced permeabilization to proceed. It has been established that both Chol and Erg have membrane-stabilizing properties and that these saponins altered the stability of the membrane and makes it more susceptible to such leakage and membrane disruption via pore formation.[24,25] In addition, soyasaponin Bb(I) showed moderate permeabilization in the presence of Chol and Erg.

Table 2-1. Calcein leakage activity of liposomes in the presence and absence of various sterols.

	EC_{50} (μM)			
Saponin	Pure POPC	POPC/Chol	POPC/Erg	POPC/Epichol
Digitonin	>100	**24.5 ± 1.1**	**70.5 ± 2.4**	>100
OSW-1	>100	**35.4 ± 1.4**	~100	>100
Soyasaponin Bb(I)	>100	~100	~100	>100
Glycyrrhizin	>100	>100	>100	>100

Values are mean ± SEM

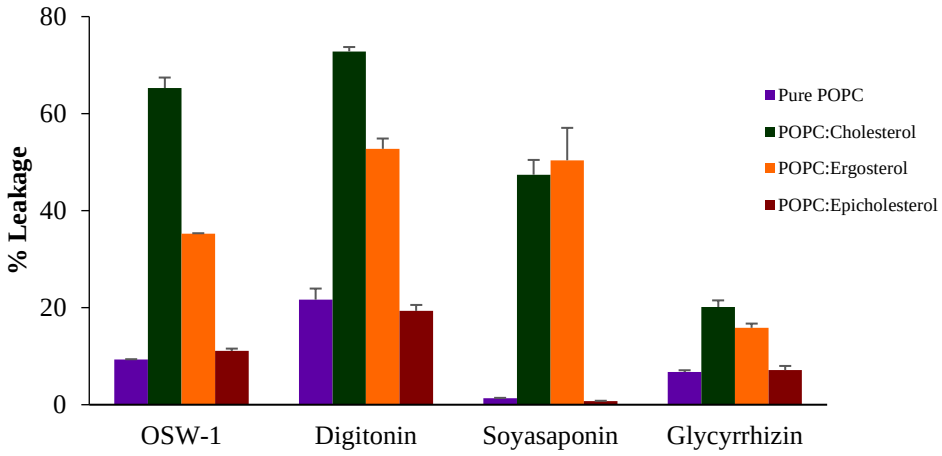

Figure 2-3. Sterol-dependent calcein-leakage from POPC liposomes by various saponins (100 μM). The POPC-sterol molar ratio was set to 9:1 and the final concentration of the phospholipid was 27 μM.

However, glycyrrhizin did not exhibit any leakage at all conditions, noting that it has weak activity towards different membrane components. With the results of this leakage experiment, it is noted that both the type of sapogenin backbone and sugar moiety are important for such membrane interactions.[16]

2.3.2 Hemolysis induced by saponins under Chol-depletion and osmotic protection

Next, the dependence of saponins on Chol content of membrane was assessed using hemolysis assay in Chol-depleted red blood cells (RBCs). Chol-depletion was carried out by treatment of cells with 3.5 mM methyl-β-cyclodextrin (MβCD). In this condition, the Chol content of the erythrocyte membrane was reduced to ~10%.[17,18] To further prove the effect of Chol on hemolysis, the depleted cells were treated with a 7:1 mol ratio of Chol/MβCD[18] to replenish the erythrocyte membrane with Chol. The Chol content of the membrane after replenishment was back to ~90% of the initial Chol in the non-treated cells. It is established that at the optimum concentration of MβCD, Chol depletion/repletion experiments did not cause hemolysis of RBCs during the process. However, this experiment cannot give assurance whether the overall membrane composition and lipid arrangement are not altered during the course of the depletion/repletion process.

The hemolysis assay showed that OSW-1 (EC_{50} = 7.4 ± 0.8 μM) exhibits significant hemolytic activity comparable to digitonin (EC_{50} = 14.3 ± 0.9 μM) as shown in Table 2-2 and Fig. 2-4. However, a loss in hemolytic activity was observed in both saponins when Chol was depleted by MβCD treatment. Repletion of Chol in the erythrocyte membrane restored the hemolytic activity of digitonin (EC_{50} = 25.4 ± 1.2 μM) and OSW-1 (EC_{50} = 12.7 ± 1.1 μM). Soyasaponin Bb(I) showed weaker hemolytic activity as compared to digitonin and OSW-1 but similar hemolytic tendency towards Chol depletion/repletion conditions. As expected, glycyrrhizin exhibited very weak hemolytic activity (EC_{50} > 300 μM) in all the erythrocyte membrane systems (Table 2-2). This assay indicates that Chol plays a key role in the hemolytic activity of OSW-1, digitonin, and soyasaponin Bb(I).[26-28] Similar Chol depletion/repletion studies have also been done on monocytic cells, assessing the degree of cell death induced by saponin addition.[17] It has been confirmed that Chol is an important membrane lipid in order for the saponins to exhibit their biological and membrane activities.

Table 2-2. Hemolytic activity of saponins under Chol depletion/repletion conditions.

	EC_{50} (μM)		
Saponin	Non-Depleted	Chol-Depleted	Chol-Repleted
Digitonin	**14.3 ± 0.9**	>300	**25.4 ± 1.2**
OSW-1	**7.4 ± 0.8**	>300	**12.7 ± 1.1**
Soyasaponin Bb(I)	**155.6 ± 4.2**	>300	>300
Glycyrrhizin	>300	>300	>300

Values are mean ± SEM

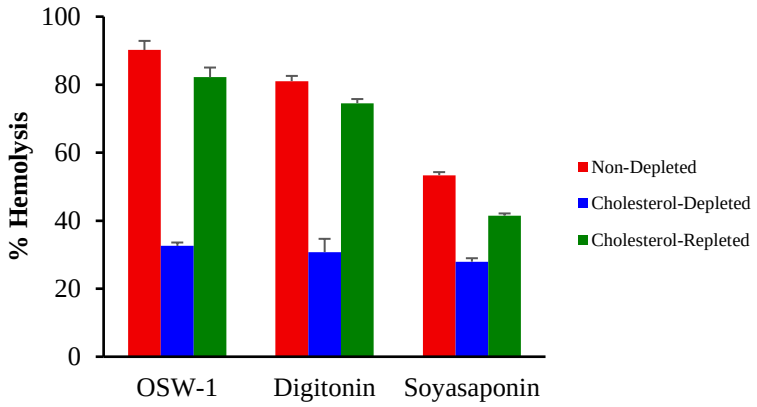

Figure 2-4. Hemolytic activity of saponins (300 μM) using non-depleted, cholesterol-depleted and cholesterol-repleted red blood cells. Human RBC (1%) was incubated for 18 h at 37 °C.

To evaluate the membrane pore size, the hemolytic effects of saponins were assessed in the presence of osmotic protectants with various sizes (Table 2-3). When any size of pore is formed on the living cell membranes, the gap of the osmotic pressures between cytosol and outer cell solutions accelerate equilibrium, which induce increment of cell volume resulting in cell burst. The osmotic protectants with appropriate size can cap the pore, resulting in the protection from cell burst. It was observed that the pore size (~0.9 nm) generated by AmB was consistent with the published data[29], (Fig. 2-5, yellow). Surprisingly, hemolysis by digitonin was not suppressed by any size of protectants (Fig. 2-5, blue). In the presence of OSW-1, suppression of hemolytic activity was observed with PEG-600 and larger protectants. This result indicates that OSW-1 was able to create pores with size of ~1.6 nm (Fig. 2-5, green). Meanwhile, soyasaponin Bb(I) showed a significant decrease in hemolytic activity in the presence of raffinose and thus, the pore size was estimated to be ~1.1 nm (Fig. 2-5, red). The observed hemolytic activity of digitonin, which was independent of the presence of various osmotic protectants, is due to its detergent activity, leading to the direct leakage of hemoglobin as a consequence of membrane disruption and/or cholesterol removal from membrane core.[30] In the case of OSW-1 and soyasaponin Bb(I), leakage of hemoglobin from RBCs could be characterized by saponin-Chol interaction, which results in the invagination of erythrocyte membrane and subsequent formation of distinct pores.[29] In this experiment, glycyrrhizin was not tested due to its weak activity.

Table 2-3. Osmotic protectants utilized for hemolytic assay and their estimated size.

osmotic protectant	molecular size (nm)
glucose	0.7
sucrose	0.9
raffinose	1.1
PEG-600	1.6
PEG-1000	2.0
PEG-1540	2.4
PEG-2000	2.9
PEG-4000	3.8
PEG-6000	5.1

Table 2-4. Estimated size of pores induced by saponin addition.

Compound	Pore size (nm)
Digitonin	>5.1
OSW-1	~1.6
Soyasaponin Bb(I)	~1.1
Amphotericin B	~0.9

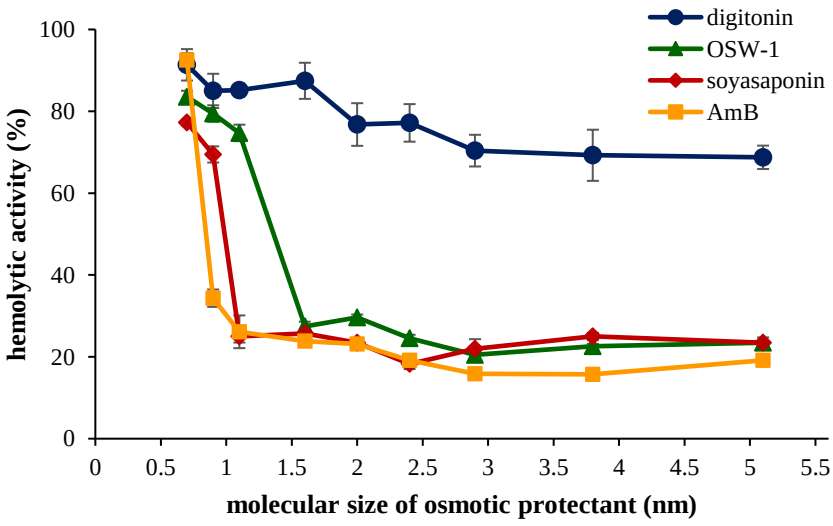

Figure 2-5. Osmotic protection experiments for saponins using 1% (v/v) RBC. Pore size was estimated using various osmotic protectants (30 mM). The concentrations of digitonin, OSW-1, soyasaponin Bb(I) and AmB were 28.7 μM, 14.9 μM, 311.3 μM and 4.0 μM, respectively.

2.3.3 Binding of saponin to Chol in membrane by CTL fluorescence spectroscopy

The ability of saponins to bind with Chol in membrane was further examined by utilizing a fluorescent analog of Chol referred to as cholestatrienol (CTL). Changes in the fluorescence properties of CTL were monitored under aqueous and bilayer environments. In the aqueous environment (above CMC of CTL, 1 nM)[31], CTL fluorescence is normally vanished due to self-quenching, but the fluorescence emission at 396 nm can be recovered when CTL molecules dissociate under the hydrophobic environments, which include aggregation with Chol in membrane. Actually, significant increase of CTL fluorescence was observed with increasing OSW-1 concentrations, indicating a dose-dependent aggregation of OSW-1 with CTL (Fig. 2-6**A**, blue). The observed increase in fluorescence emission at 396 nm upon increase in the concentration of OSW-1 is due to the dissociation of CTL aggregates to form a plausible mixed complex with OSW-1. (Fig. 2-6**C**).[32,33] This experiment indicates that OSW-1 forms a complex with Chol in a similar fashion with digitonin (Fig. 2-6**A**, black) and soyasaponin Bb(I) (Fig. 2-6**A**, red). However, among the saponins tested, glycyrrhizin (Fig. 2-6**A**, green) showed insignificant fluorescence changes indicative of its weak binding affinity with CTL.

The effect of saponins on CTL fluorescence was further assessed in the bilayer environment. In this experiment, LUVs composed of POPC/Chol/CTL (90:9:1 in molar ratio) were incubated with the saponins for 3 h. Fluorescence measurements were done at various saponin concentrations. Fluorescence intensities of CTL were shown to decrease in a concentration dependent manner at lower saponin concentrations in membrane. With 10 μM saponins (except for glycyrrhizin), the lowest intensities (intensities < 496) were observed. The decrease in intensities indicates the reduction in fluorescence lifetime due to the perturbation of the lipid packing by OSW-1 and other saponins.[34] In the higher concentrations of OSW-1, i.e. 30 μM to 100 μM concentrations, an increase in fluorescence intensity was observed (Fig. 2-6**B**, blue). These increase could be due to formation of OSW-1/Chol mixed micelles.[35] The interaction of Chol with large amounts of OSW-1 (OSW-1 > total lipids) leads to the disruption of the bilayer structure and favors formation of micelles in the aqueous phase.[31,32] Therefore, the marked increase of the CTL fluorescence is accounted for by a consequence of tight interaction between CTL and OSW-1 in the micelles.

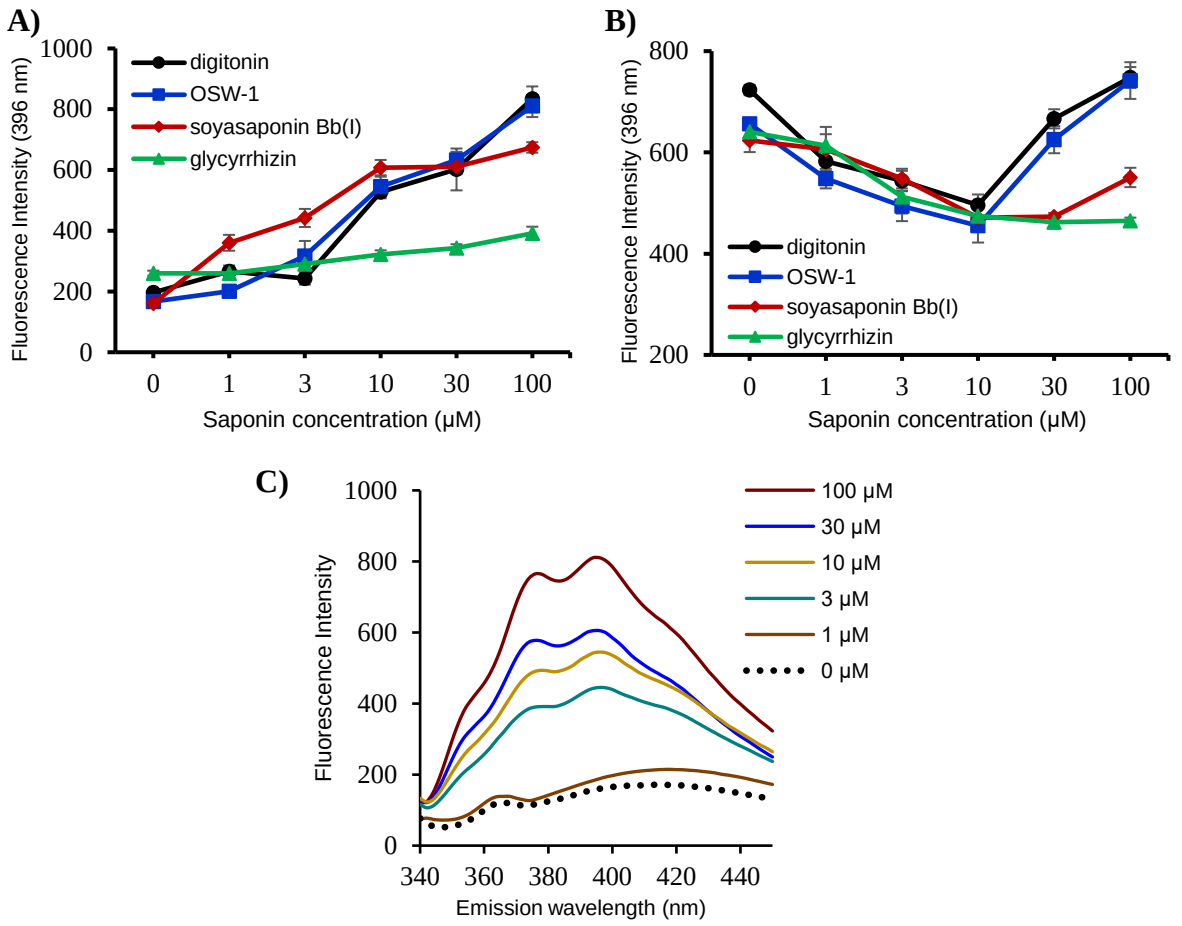

Figure 2-6. Fluorescence intensities of cholestatrienol (CTL) at different saponin concentrations. CTL was excited with 325 nm and the intensities of the emission maximized at 396 nm were plotted in aqueous media (**A**) and in LUV (**B**). Fluorescence emission spectra of increasing concentrations of OSW-1 in aqueous media (**C**). The POPC-Chol-CTL molar ratio was set to 90:9:1 and the final concentration of the phospholipid was 177 μM.

Digitonin exhibited similar properties with OSW-1 (Fig. 2-6**B**, black) while soyasaponin Bb(I) showed significantly weaker effect (Fig. 2-6**B**, red) in comparison with the other two saponins. Moreover, dynamic light scattering (DLS) experiments revealed that the size of the LUVs significantly decreased upon the addition of 30 μM OSW-1 (Table 2-5). Similarly, reduction of the particle size was also observed for digitonin, while soyasaponin Bb(I) showed minimal reduction (Table 2-5).

Table 2-5. Effect of saponin on size of LUVs (9:1 POPC/Chol).

	Average particle size (nm)		
Saponin	Control (0 μM)	30 μM	100 μM
OSW-1	197.6	126.4	11.9
Digitonin	220.4	127.2	7.3
Soyasaponin Bb(I)	212.8	181.8	127.8
Glycyrrhizin	207.8	207.1	180.6

Notes: The final concentration of POPC and Chol were 129 μM and 16 μM, respectively

2.3.4 Solid state ^{2}H NMR for investigating saponin/Chol interaction

The results of the fluorescence experiments revealed that OSW-1/Chol interaction is important for the membrane disrupting activity due to mixed micelle formation. In this section, solid state ^{2}H NMR was employed in order to determine direct molecular interaction between Chol and saponin in membrane. Molecular interaction with the deuterated probes leads to the effect on signal broadening and change of quadrupolar splitting.[36-38] The size of quadrupolar splitting is affected by the molecular mobility and orientation of the molecule (the C─D vector) with respect to the bilayer normal, which is used to detect the direct interaction between Chol and membrane-active compounds. In this study, Chol-*d* was used as the probe to examine the effects of saponin in a POPC/Chol-*d* (9:1 molar ratio) bilayer preparation (Fig. 2-7).[37,38] Without addition of saponins, a typical Pake doublet pattern of Chol-*d* in membrane was observed in POPC-based membrane at 30 °C as shown in Fig. 2-7**A**. As depicted in Fig. 2-7**B**, 2-7**D** and 2-7**E**, OSW-1, glycyrrhizin and soyasaponin Bb(I) showed the markedly reduced splitting of the Pake doublet without affecting the gross signal shape. In contrast, the ^{2}H NMR spectra of digitonin showed the complete disappearance of the Pake doublet (Fig. 2-7**C**) (Fig. 2-7**B**). The disappearance of the Pake doublet signals could be attributed to the direct interaction between digitonin and Chol that results in formation of large aggregates.

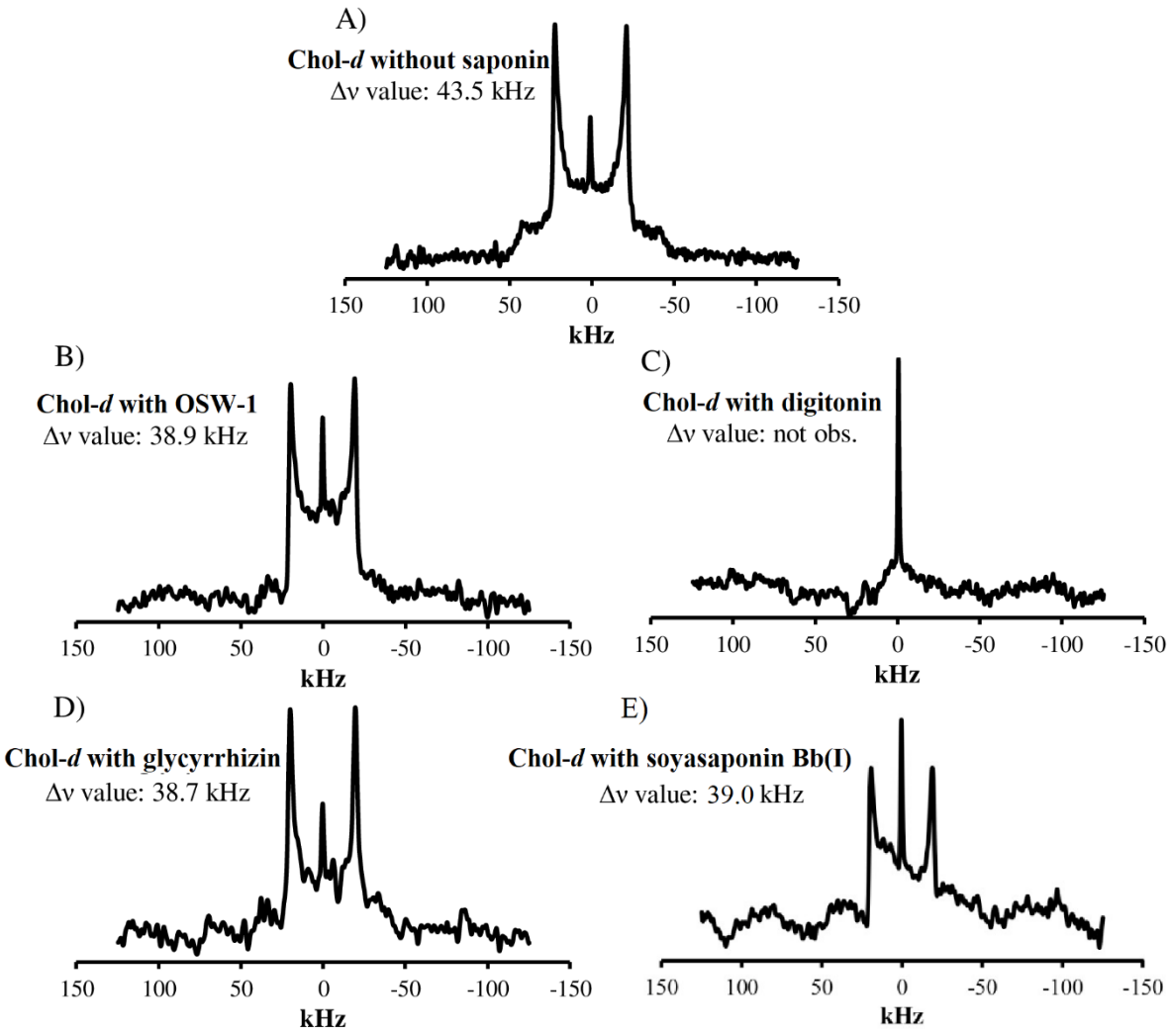

Figure 2-7. ^{2}H NMR spectra of POPC/Chol-*d* bilayers (molar ratio 9:1) in the absence of saponins (**A**) and presence of OSW-1 (**B**); digitonin (**C**); glycyrrhizin (**D**); and soyasaponin Bb(I) (**E**). All the saponin-containing membranes were prepared at the molar ratio of Chol-*d*-saponin, 1:0.5. ^{2}H NMR spectra were measured at 30 °C. The concentrations of POPC, Chol and saponin in the multilamellar vesicles (MLVs) were 47, 5.3, and 2.7 μmol, respectively. Reprinted and modified with permission from *BBA Biomembranes*, **2017**.[20] Copyright © (2017) Elsevier.

2.3.5 Solid state ^{31}P NMR for investigating membrane integrity

Besides ^{2}H NMR, another useful tool used to investigate the effect of saponins on the physical properties of membrane is solid state ^{31}P NMR. This technique could detect changes in the morphological state of the membrane, in which the overall spectral shape and signal width are used to assess the effect of saponins in the surrounding phospholipids. In this

experiment, the ^{31}P spectra are recorded in the absence or presence of saponin. Fig. 2-8**A** shows the axially symmetrical pattern for a typical lamellar structure of the 9:1 POPC/Chol system.

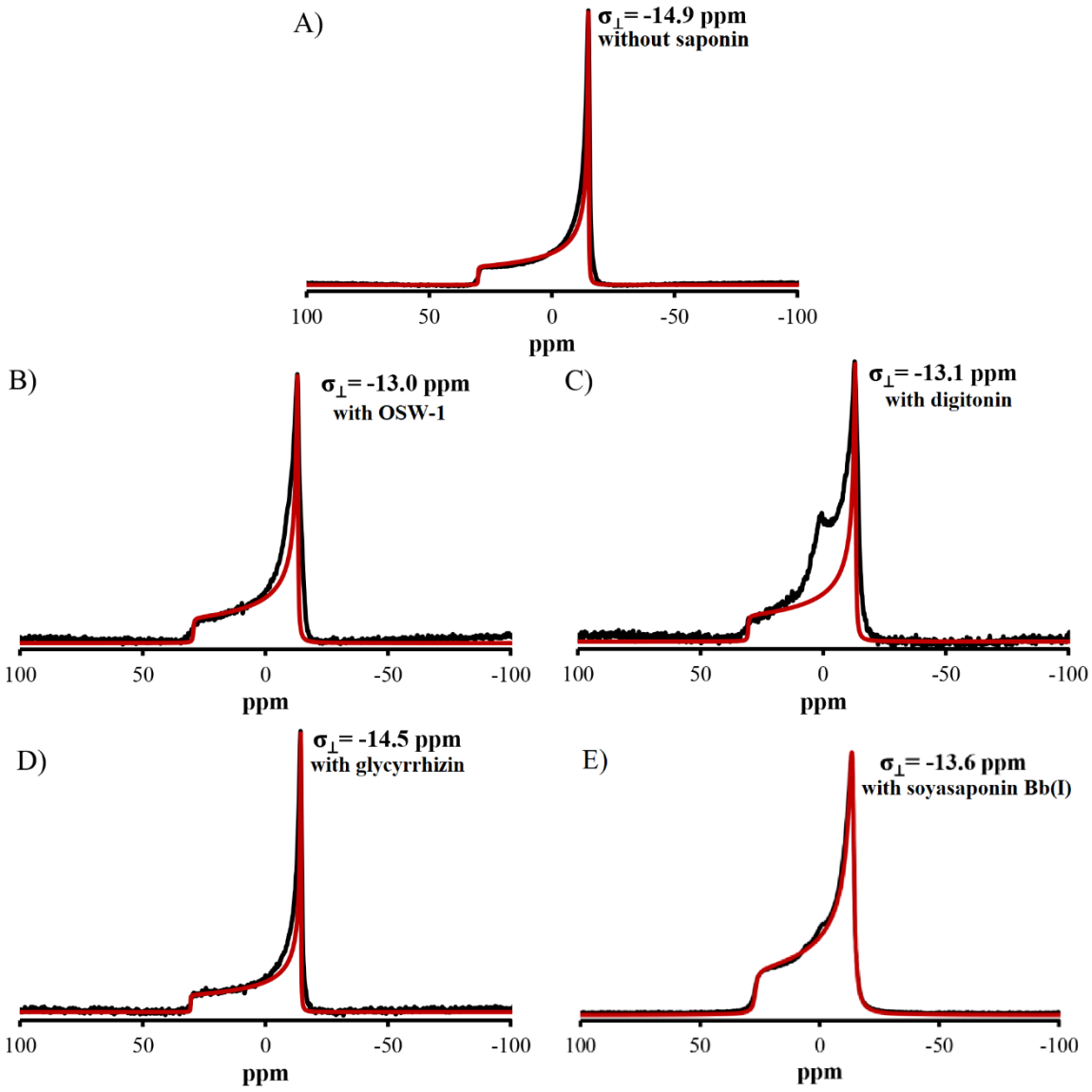

Figure 2-8. ^{31}P NMR spectra (black ─) of MLVs consisting of POPC/Chol (9:1) in the absence of saponins (**A**) and presence of OSW-1 in the Chol/OSW-1 molar ratio of 1:0.5 (**B**); digitonin in the Chol/digitonin molar ratio of 1:0.5 (**C**); glycyrrhizin in the Chol/glycyrrhizin molar ratio of 1:0.5 (**D**); and soyasaponin Bb(I) in the Chol/soyasaponin Bb(I) molar ratio of 1:0.5 (**E**). ^{31}P NMR spectra were measured at 30 °C and referenced from 85% phosphoric acid (H_3PO_4) peak set at 0 ppm. Red (─) spectra corresponds to computer simulation using SIMPSON software.[39] Reprinted and modified with permission from *BBA Biomembranes*, **2017**.[20] Copyright © (2017) Elsevier.

^{31}P spectra in the presence of saponins showed decrease in the signal widths indicating an increase in curvature upon binding of saponin in membrane. This reduction is evident in the presence of OSW-1 (Fig. 2-8**B**) and soyasaponin Bb(I) (Fig. 2-8**E**), as compared to glycyrrhizin (Fig. 2-8**D**). In the addition of digitonin (Fig. 2-8**C**), the spectrum showed the presence of an isotropic peak at around 0 ppm. The appearance of this isotropic signal is due to the formation of small particles in part without affecting the over lamellar structure of the membrane at this saponin/lipid ratio.[17] These results are consistent with the DLS experiment (Table 2-5). DLS experiment revealed that addition of 30 μM digitonin reduced vesicle size to 127.2 nm. Furthermore, addition of 100 μM digitonin induced formation of smaller particles with average size of 7.3 nm. Similarly, OSW-1 and soyasaponin Bb(I) also exhibited a decrease in vesicle size upon increase in the concentration of these saponins.

2.4 Discussion

In this study, various spectroscopic experiments to evaluate the activity of OSW-1 and other usual 3-*O*-glycosyl saponins using artificial and biological membrane models were carried out. The membrane-disrupting activity of OSW-1 in the micromolar range is highly Chol-dependent for both membrane models, despite their large difference in membrane composition and structure. The results of these experiments strongly indicate that OSW-1 and Chol form a complex, which is mainly responsible for the membrane permeabilizing and disrupting activities. Same scenario was observed for digitonin and soyasaponin Bb(I) although the latter showed a weaker activity. Several studies have reported that Chol plays a major role in membrane permeabilization induced by saponins.[11,16-18,40] This study focused on the investigation of the membrane properties and activities of OSW-1 in comparison with usual saponins bearing sugar moieties attached to the C3 of the A ring of steroidal or triterpenic sapogenin. OSW-1 is unique in a way that the partially acylated disaccharide moiety is attached to the hydroxy group at C16 of the steroidal D3 ring. This structural feature brought attention as to how this particular saponin interacts with membrane-bound Chol and induces membrane permeabilization. In particular, the three hydroxy groups of OSW-1 (except for a highly hindered tertiary OH at C17) form a hydrophilic phase, as previously reported by Sakurai et al.[7] (Fig 2-1). The three-dimensional structure of OSW-1 adopts a triangular-like shape secluding the hydrophilic face from the hydrophobic moiety, which could be partly responsible for its potent biological activity.[7] The differences in the amphiphilicity and polarity of OSW-1 with other saponins could indicate differences in the binding mode of these saponins to Chol.

Albeit the differences in the chemical structure between OSW-1 and typical 3-*O*-Glycosyl saponins such as digitonin, the interaction observed in these two saponins is thought to be similarly Chol-dependent.

It is found in this study that Chol is important for hemolysis as induced by OSW-1 and digitonin (Fig. 2-3). This Chol dependence was also seen in the calcein leakage experiments (Fig. 2-4), indicating that membrane permeability enhanced by OSW-1 and by digitonin is highly sterol-dependent. The permeability of OSW-1 and digitonin was also Chol-dependent as evidenced by parallel artificial membrane permeation assay (PAMPA) (Table S1-1, Supporting Information I). This result suggests that OSW-1 and digitonin recognize the sterols, which is the initial step for a permeabilization process. The ability of saponins to bind with CTL was further revealed by monitoring fluorescence changes of CTL in both aqueous and bilayer environments. The high affinity of OSW-1 to Chol observed in the CTL binding assay is comparable to that of digitonin to Chol (Fig. 2-6). Previous studies postulated that digitonin binds to Chol in a face-to-face fashion through the stable hydrophobic interaction between their steroid rings.[41,42] Despite their similarities in membrane activities, OSW-1 is unlikely to be oriented to the membrane in a perpendicular manner due to its unique structure. Specifically, the triangular shape of OSW-1, in which the hydrophilic sugar moiety resides apart from the 3-OH group, does not necessarily lead to parallel interactions with Chol (Fig. 2-1).

Solid-state ^{2}H NMR and ^{31}P NMR revealed remarkable differences in the membrane activity of OSW-1 and digitonin. First, the ^{2}H NMR spectra of Chol-*d* showed that digitonin significantly slows down the rotational motion of Chol, as demonstrated by the complete attenuation of the Pake doublet signals (Fig. 2-7**C**). The signal attenuation observed in the ^{2}H NMR is attributed to the formation of large digitonin/Chol aggregates, which have been previously reported by similar studies.[22,41] Other membrane-active natural products including amphidinol 3 (AM3), amphotericin B (AmB), and theonellamide-A (TNM-A) have shown comparable changes in their ^{2}H NMR spectra, which also greatly reduces the mobility of Chol-*d*.[36-38,43] ^{31}P NMR of POPC in the presence of digitonin showed a broad peak near 0 ppm (Fig. 2-8**C**), which could be partly due to the increase in membrane curvature or reduction in the vesicle size such as micelle formation, without affecting the overall membrane morphology.[17,41] Again, at this particular digitonin/lipid ratio, Chol forms aggregate with digitonin, which could induce membrane deformations. This interaction leads to immobilization of Chol molecules in membrane, as previously reported.[41]

In contrast, OSW-1 showed significant decrease in $\Delta\nu$ of Chol-*d* without a change in ^{2}H NMR signal shape as shown in Fig. 2-7**B**. The incorporation of 5 mol% OSW-1 decreased the $\Delta\nu$ by 4.6 kHz, suggesting that a direct interaction between OSW-1 and Chol-*d* results in the tilting of the Chol axis against the bilayer normal. This interaction could occur to maximize a face-to-face contact between the hydrophobic cores of OSW-1 and Chol in membrane. The interaction with OSW-1 molecule, which has a unique tertiary structure, could contribute to the alteration of the tilting of Chol axis against membrane normal, resulting in the reduction in the $\Delta\nu$ value. In addition, the overall lamellar structure of the POPC/Chol membrane was not greatly affected by saponins including OSW-1, soyasaponin Bb(I) and glycyrrhizin as shown in the ^{31}P NMR. However, a remarkable shift in the $\sigma_{\perp}$ value was observed, which is partly attributed to the gross changes in the membrane curvature.[17] The conserved lamellar structure of the membrane after addition of OSW-1 indicates that there are no significant modifications in the arrangement of the surrounding phospholipids.[36] The similar mechanism would be expected for soyasaponin Bb(I) in terms of the Chol interaction and membrane curvature generation based on their ^{31}P NMR spectra, even though other membrane experiments (Fig 2-7**E and** 2-8**E**) showed weaker activity compared to both OSW-1 and digitonin (Figs. 2-3, 2-4 and 2-6). ^{2}H NMR spectra in Fig. 2-7 showed a significant reduction in the $\Delta\nu$ value induced by glycyrrhizin, despite its weak membrane activity (Figs. 2-3, 2-4 and 2-6). Previous monolayer experiment suggests that glycyrrhizin possibly binds to membrane Chol to a certain extent but does not perturb the membrane integrity, which is consistent with these ^{2}H NMR and ^{31}P NMR data (Fig. 2-8**D**).

The membrane disrupting and permeabilizing activity of various saponins have been published in numerous reports, some of which describe their mechanism of action towards various membrane models.[10,11,15-18,41] In contrast, very few studies have been conducted on saponins with unusual polarity[45] to elucidate their mechanism of action at the molecular level. A structure-activity relationship study has been performed on triterpene saponins containing two sugar moieties attached to A ring and D ring of the triterpene backbone.[46] In this study, the unusual steroidal saponin OSW-1 having sugar moieties at the D ring was investigated using spectroscopic approaches in comparison with typical 3-*O*-glycosyl saponins. In this research, the possible interaction mechanism of OSW-1 was unraveled via spectroscopic experiments. The results gathered highlight that Chol plays a key role in the membrane binding of saponin and following membrane distraction/permeabilization. In more details, OSW-1 accumulates in the surface of the outer membrane leaflet. Bound OSW-1 forms a complex with Chol and further penetrates into the hydrophobic interior of the bilayer (Fig. 2-9**A**). Finally, the deeper

penetration of OSW-1 causes transient pore formation and deformation of the membrane (Fig. 2-9**B**), while maintaining the overall integrity of the bilayer structure.[17-19] In addition, osmotic protection experiments (Table 2-4 and Fig. 2-5) suggest that OSW-1 creates small pores with size of up to 1.6 nm in erythrocyte membrane. With lines of evidence gathered, there is a possibility that OSW-1 acts into the membrane causing the formation of either a toroidal pore or barrel stave pore. However, results of the ^{31}P NMR and the osmotic protection suggest that the mechanism of interaction of OSW-1 is likely to be the barrel stave pore model. Previous studies employed similar NMR-based approach on membrane active natural products including amphidinol 3[36] and theonellamide-A.[43,47,48] The findings of this study were similarly observed in amphidinol 3[36] and alamethicin[49], which have been regarded as membrane active compounds, and are known to form barrel stave pores. This hypothesis could be due to the insignificant changes in the ^{31}P NMR signal shape and the formation of relatively small pores with narrow size distributions as observed in the osmotic protection experiments.

It is also worth mentioning that the concentration to exhibit cytotoxicity by OSW-1 is much smaller than that of the membrane permeabilization in artificial membrane models, as shown in calcein leakage experiments (EC_{50} = 35.4 ± 1.4 μM), as compared to cell-based assays (EC_{50} is around 0.5 nM).[6-8] The higher activity in cytotoxicity can be accounted for by the notion that OSW-1 exerts its potent activity through binding to a target protein; previous study has reported that OSW-1 induces apoptosis via inhibition of the sodium-calcium exchanger[52] and interaction with proteins in the cytoplasm.[53] In addition, it is known that saponins generally interacts with membrane sterols and leads to aggregation and minor alterations in the membrane composition and inclusion/exclusion of Chol could affect the cytotoxic activity of these saponins.[51] It is expected that interactions with other cell components including specific signaling proteins may have contributed to the high cellular toxicity of saponins. The result of PAMPA experiment revealed that permeation of saponin into cell membrane below the membrane-disrupting concentrations is also Chol-dependent, suggesting that OSW-1 can pass through the cellular membrane efficiently and reach the cytoplasmic side in the absence of any transporters and any other biological machineries. Meanwhile, for digitonin and other usual saponins, disruption of the bilayer structure is a prerequisite for membrane penetration. On the other hand, OSW-1 probably passes through the membrane at lower concentrations due to its less hydrophilic structure; this could be attributable to the fewer hydroxy groups present in OSW-1 (5) as compared with those of digitonin (17). These characteristic features of OSW-1 may partly account for its extremely potent cytotoxicity by the rapid membrane permeability,

which makes OSW-1 access the plausible target proteins in cancer cells at very low concentrations.

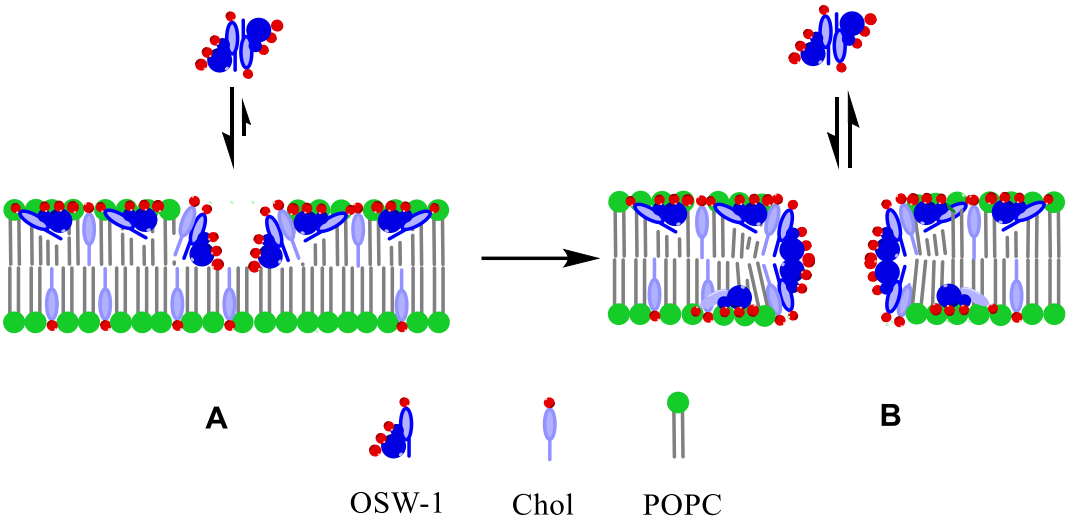

Figure 2-9. Hypothetical mechanism for the membrane-permeabilizing effect of OSW-1 in Chol-containing membranes. (A) Accumulation of OSW-1 in Chol-containing membrane causes small membrane defects. (B) Further binding of OSW-1 results in the formation of a barrel-stave-like assembly.

References

1. Kubo, S. Mimaki, Y., Terao, M., Sashida, M., Nikaido, T., Ohmoto, T., Acylated cholestane glycosides from the bulbs of *Ornithogalum saundersiae*, *Phytochemistry* **1992**, *31*, 3969-3973.

2. Wojtkielewicz, A., Dlugosz, M., Maj, J., Morzycki, J.W., Nowakowski, M., Renkiewicz, J., Strnad, M., Swaczynova, J., Wilczewska, A.Z., Wojcik, J., New analogues of the potent cytotoxic saponin OSW-1, *J. Med. Chem.* **2007**, *50*, 3667-3673.

3. Hostettmann, K., Marston, A., Saponins, Cambridge University Press: Cambridge, **1995**.

4. Akiyama, T., Takagi, S., Sankawa, U., Inari, S., Saito, H., Saponin-cholesterol interaction in the multibilayers of egg yolk lecithin as studied by deuterium nuclear magnetic resonance: digitonin and its analogues, *Biochemistry* **1980**, *19*, 1904-1911.

5. Dembitsky, V.M., Chemistry and biodiversity of the biologically active natural glycosides, *Chem. Biodivers.* **2004**, *1*, 673-781.

6. Sakurai, K., Takeshita, T., Hiraizumi, M., Yamada, R., Synthesis of OSW-1 derivatives by site-selective acylation and their biological evaluation, *Org. Lett.* **2014**, *16*, 6318-6321.

7. Sakurai, K., Fukumoto, T., Noguchi, K., Sato, N., Asaka, H., Moriyama, N., Yohda, M., Three dimensional structures of OSW-1 and its congener, *Org. Lett.* **2010**, *12*, 5732-5735.

8. Zhou, Y., Garcia-Prieto, C., Carney, D.A., Xu, R., Pelicano, H., Kang, Y., Yu, W., Lu, C., Kondo, S., Liu, J., Harris, D.M., Estrov, Z., Keating, M.J., Jin, Z., Huang, P., OSW-1: a natural compound with potent anticancer activity and a novel mechanism of action, *J. Natl. Cancer Inst.* **2005**, *97*, 1781-1785.

9. el Izzi, A., Bennie, T., Thieulant, M.L., Le Men-Olivier, L., Duval, J., Stimulation of LH release from cultured pituitary cells by saponins of *Petersianthus macrocarpus*: a permeabilizing effect, J. *Planta Med.* **1992**, *58*, 229-233.

10. Yeagle, P.L., Cholesterol and the cell membrane, *Biochim. Biophys. Acta Rev. Biomembr.* **1985**, *822*, 267-287.

11. Armah, C.N., Mackie, A.R., Roy, C., Price, K., Osbourn, A.E., Bowyer, P. Ladha, S., The membrane-permeabilizing effect of avenacin A-1 involves the reorganization of bilayer cholesterol, *Biophys. J.* **1999**, *76*, 281-290.

12. Papahadjopoulos, D., Cholesterol and all membrane function: a hypothesis concerning etiology of atherosclerosis, *J. Theor. Biol.* **1974**, *43*, 329-337.

13. Ingolfsson, H.I., Melo, M.N., van Eerden, F.J., Arnarez, C., Lopez, C.A., Wassenaar, T.A., Periole, X., de Vries, A.H., Tielman, D.P., Marrink, S.J., Lipid organization of the plasma membrane, *J. Am. Chem. Soc.* **2014**, *13*, 14554-14559.

14. Shlosser, E., Interaction of saponins with cholesterol, lecithin, and albumin, *Ca. J. Physiol. Pharmacol.* **1969**, *47*, 487-490.

15. Glauert, A.M., Dingle, J.T., Lucy, J.A., Action of saponin on biological cell membranes, *Nature* **1962,** *196*, 953-955.

16. Keukens, E.A., de Vrije, T., van der Boom, C., de Waard, P., Plasman, H.H., Thiel, F., Chupin, V., Jongen, W.M., de Krujiff, B., Molecular basis of glycoalkaloid induced membrane disruption, *Biochim. Biophys. Acta* **1995**, *1240*, 216-228.

17. Lorent, J., Le Duff, C.S., Quetin-Leclercq, J., Mingeot-Leclercq, M.P., Induction of highly curved structures in relation to membrane permeabilization and budding by the triterpenoid saponins, α- and δ-Hederin, *J. Biol. Chem.* **2013**, *288*, 14000-14017.

18. Lorent, J., Lins, L., Domenech, O., Quetin-Leclercq, J., Brasseur, R., Mingeot-Leclercq, M.P., Domain formation and permeabilization induced by the saponin α-hederin and its aglycone hederagenin in a cholesterol-containing bilayer, *Langmuir* **2014**, *30*, 4556-4569.

19. Bottger, S., Hofmann, K., Melzig, M.F., Saponins can perturb biologic membranes and reduce the surface tension of aqueous solutions: a correlation? *Bioorg. Med. Chem.* **2012**, *20*, 2822-2828.

20. Malabed, R., Hanashima, S., Murata, M., Sakurai, K., Sterol-recognition ability and membrane-disrupting activity of *Ornithogalum saponin* OSW-1 and usual 3-*O*-glycosyl saponins, *BBA - Biomembranes* **2017**, *1859*, 2516–2525.

21. Nishikawa, M., Nojima, S., Akiyama, T., Sankawa, U., Inoue, K., Interaction of digitonin and its analogs with membrane cholesterol, *J. Biochem.* **1984**, *96*, 1231-1239.

22. Stockton, G.W., Polnaszek, C.F., Tulloch, A.P., Hassan, F., Smith, I.C.P., Molecular motion and order in single-bilayer vesicles with multilamellar dispersions of egg lecithin and lecithin-cholesterol mixtures. A deuterium nuclear magnetic resonance study of specifically labeled lipids, *Biochemistry* **1976**, *15*, 954-966.

23. Murata, M., Houdai, T., Morooka, A., Matsumori, N., Oishi, T., Membrane interaction of soyasaponins in association with their antioxidation effects, *Soy Protein Research, Japan* **2005**, *8*, 81-85.

24. Weinstein, J.N., Yoshikami, S., Henkart, P., Blumenthal, R., Hagins, W.A., Liposome-cell interaction: transfer and intracellular release of a trapped fluorescent marker, *Science* **1977**, *195*, 489-492.

25. Singer, S.J., Nicolson, G.L., The fluid mosaic model of the structure of cell membranes, *Science* **1972**, *175*, 720-731.

26. Yuldasheva, L.N., Carvalho, E.B., Catanho, M.Y., Krasilnikov, O.V., Cholesterol-dependent hemolytic activity of *Passiflora quadrangularis* leaves. *Braz J Med Biol Res.* **2005**, *38*, 1061-1070.

27. Luckey, M., Structural biology: with biochemical and biophysical foundations, Cambridge University Press, New York, **2008**, pp. 13-41.

28. Lange, Y., Ye, J., Duban, M.E., Steck, T.L., Activation of membrane cholesterol by 63 amphipaths, *Biochemistry* **2009**, *48*, 8505-8515.

29. Houdai, T., Matsuoka, S., Matsumori, N., Murata, M., Membrane-permeabilizing activities of amphidinol 3, polyene-polyhydroxy antifungal from a marine dinoflagellate, *Biochimica et Biophysica Acta (BBA) – Biomembranes* **2004**, *1667*, 91-100.

30. Thelestam, M., Florin, I., Assay of cytopathogenic toxins in cultured cells, *Methods Enzymol.* **1994**, *235*, 679–690.

31. Schroeder, F., Dempsey, M.E., Fischer, R.T., Sterol and squalene carrier protein interactions with fluorescent Δ5,7,9(11)-cholestatrien-3β-ol, *J. Biol. Chem.* **1985**, *260*, 2904-2911.

32. Loura, L.M., Prieto, M., Dehydroergosterol structural organization in aqueous medium and in a model system of membranes, *Biophys. J.* **1997**, *72*, 2226-2236

33. Cheng, K.H., Virtanen, J., Somerharju, P., Fluorescence studies of dehydroergosterol in phosphatidylethanolamine/phosphatidylcholine bilayers, *Biophys. J.* **1999**, *77*, 3108-3119.

34. Seras, M., Gallay, J., Vincent, M., Ollivon, M., Leseiur, S., Micelle-vesicle transition of nonionic surfactant-cholesterol assemblies induced by octyl glucoside: A time-resolved fluorescence study of dehydroergosterol, *J. Colloid Interface Sci.* **1994**, *167*, 159-171.

35. Björkqvist, Y.J., Nyholm, T.K., Slotte, J.P., Ramstedt, B., Domain formation and stability in complex lipid bilayers as reported by cholestatrienol, *Biophys J.* **2005**, *88*, 405440-405463.

36. Espiritu, R.A., Matsumori, N., Tsuda, M., Murata, M., Direct and stereospecific interaction of amphidinol 3 with sterol in lipid bilayers, *Biochemistry* **2014**, *53*, 3287-3293

37. Matsumori, N., Tahara, K., Yamamoto, H., Morooka, A., Doi, M., Oishi, T., Murata, M., Direct interaction between amphotericin B and ergosterol in lipid bilayers as revealed by ^{2}H NMR spectroscopy, *J. Am. Chem. Soc.* **2009**, *131*, 11855-11860.

38. Espiritu, R.A., Matsumori, N., Murata, M., Nishimura, S., Kakeya, H., Matsunaga, S., Yoshida, M., Interaction between the marine sponge cyclic peptide theonellamide A and sterols in lipid bilayers as viewed by surface plasmon resonance and solid-state ^{2}H nuclear magnetic resonance, *Biochemistry* **201**3, *52*, 2410-2418.

39. Bak, M., Rasmusse, J.Y., Nielsen, N.C., SIMPSON: A General Simulation Program for Solid-State NMR Spectroscopy, *J. Mag. Res.* **2000**, *147*, 296-330.

40. Li, X.X., Davis, B., Haridas, V., Gutterman, J.U., Colombini, M., Proapoptotic triterpene electrophiles (avicins) form channels in membranes: cholesterol dependence, *Biophys. J.* **2005**, *88*, 2577-2584.

41. Frenkel, N., Makky, A., Sudji, I.R., Wink, M., Tanaka, M., Mechanistic investigation of interactions between steroidal saponin digitonin and cell membrane models, *J. Phys. Chem.* **2014**, *118*, 14632-14639.

42. Sudji, I.R., Subburaj, Y., Frenkel, N., García-Sáez, A.J., Wink, M., Membrane disintegration caused by the steroid saponin digitonin is related to the presence of cholesterol, *Molecules* **2015**, *20*, 20146–20160.

43. Murata, M., Sugiyama, S., Matsuoka, S., Matsumori, N., Bioactive structure of membrane lipids and natural products elucidated by a chemistry-based approach, *Chem. Rec.* **2015**, *15*, 675-690.

44. Sakamoto, S., Nakahara, H., Uto, T., Shoyama, Y., Shibata, O., Investigation of interfacial behavior of glycyrrhizin with a lipid raft model via a Langmuir monolayer study, *Biochim Biophys Acta.* **2013**, *1828*, 1271-1283.

45. Ohnishi, Y., Tachibana, K., Synthesis of pavoninin-1, a shark repellent substance, and its structural analogues toward mechanistic studies on their membrane perturbation, *Bioorg. Med. Chem.* **1997**, *5*, 2251-2265.

46. Hu, M., Konoki, K., Tachibana, K., Cholesterol-independent membrane disruption cause by triterpenoid saponin, *Biochim. Biophys. Acta* **1996**, *1299*, 252-258.

47. Cornelio, K., Espiritu, R.A., Todokoro, Y., Hanashima, S., Kinoshita, M., Matsumori, N., Murata, M., Nishimura, S., Kakeya, H., Yoshida, M., Matsunaga, S., Sterol-dependent membrane association of the marine sponge derived bicyclic peptide Theonellamide A as examined by ^{1}H NMR, *Bioorg. Med. Chem.* **2016**, *24*, 5235-5242.

48. Espiritu, R.A., Matsumori, N., Murata, M., Nishimura, S., Kakeya, H., Matsunaga, S., Yoshida, M., Interaction between the marine sponge cyclic peptide theonellamide A and sterols in lipid bilayers as viewed by surface plasmon resonance and solid-state ^{2}H nuclear magnetic resonance, *Biochemistry* **2013**, *52*, 2410-2418.

49. He, K., Ludtke, S.J., Worcester, D., Huang, H.W., Neutron scattering in the plane of membranes: structure of alamethicin pores, *Biophys. J.* **1996**, *70*, 2659-2666.

50. Seeman, P., Ultrastructure of membrane lesions in immune lysis, osmotic lysis and drug-induced lysis, *Fed Proc.* **1974**, *33*, 2116-2124.

51. Ashworth, L.A., Green, C., Plasma membranes: phospholipid and sterol content, *Science* **1966**, *151*, 210-211.

52. Garcia-Prieto, C.,, Riaz Ahmed, K.B.,, Chen, Z., Zhou, Y., Hammoudi, N., Kang, Y., Lou, C., Mei, Y., Jin, Z., Huang P., Effective killing of leukemia cells by natural product OSW-1 through disruption of cellular calcium homeostasis, *J. Biol. Chem.* **2013**, *288*, 3240-3250.

53. Burgett, A.W., Poulsen, T.B., Wangkanont, K., Anderson, D.R., Kikuchi, C., Shimada, K., Okubo, S., Fortner, K.C., Mimaki, Y., Kuroda, M., Murphy, J.P., Schwalb, D.J., Petrella, E.C., Cornella-Taracido, I., Schirle, M., Tallarico, J.A., Shair, M.D., Natural products reveal cancer cell dependence on oxysterol-binding proteins, *Nat. Chem. Biol.* **2011**, *7*, 639-647.

Chapter 3

Effect of saponins on membrane permeability and morphology as examined by fluorescence techniques

3.1 Introduction – Utilizing fluorescence probes

Fluorescence probes have been very useful in the determination of membrane related interactions and dynamics. In the previous chapter, fluorescence spectroscopic techniques were employed to study the effect of saponins on membrane permeability and binding. Calcein leakage assays demonstrated that membrane permeabilizing effects were dependent on 3-β-hydroxysterol. Furthermore, the experiments utilizing CTL, a fluorescent Chol analogue, suggested that saponins could directly interact with CTL and formation of aggregates composed of saponin/CTL were observed in higher saponin concentrations. In the first section of this chapter, the details of the saponin-Chol interactions was further assessed through estimation of binding affinity and molar ratio of membrane-bound saponins using time-course and binding isotherm experiments by monitoring leakage of calcein from liposomes.[1,2]

Dynamic behavior of cell membranes including the conformation, arrangement, and interaction of lipids has been extensively studied using variable spectroscopic techniques. Although these spectroscopic technique provides very valuable information, details on membrane organization at the level of single vesicle cannot be provided by spectroscopy alone.[3] To address this problem, fluorescence microscopy has been utilized to visualize biological cells and artificial vesicles to provide information about the shape and size of various lipid domains.[3-7] Membrane model systems such as small unilamellar vesicles (SUVs), large unilamellar vesicles (LUVs) and multilamellar vesicles (MLVs) have been used to examine single vesicles under fluorescence microscopy[8-10], but these attempts have not given suitable results due to the size of vesicles and the resolution of the microscope.[11,12] Giant unilamellar vesicle (GUV) has become a popular artificial membrane model for fluorescence microscopy related experiments[13] because the vesicle size is much higher than the intrinsic resolution limit of most available optical microscopes. Additionally, the average size of the GUV is similar to that of the size of the plasma membrane in variety of cells. The lipid species and compositions of GUVs can be varied and the surrounding environment of these vesicles can also be controlled.[14,15] In order to aid for the visualization of GUVs, fluorescent probes have been developed depending on the nature of the experiment.[9,15-20] These probes contain a fluorescent

moiety that is either attached to the lipid alkyl chain or in the hydrophilic head group of the lipid. The differences in the fluorescent label of these probes vary according to the properties and organization of membrane preparations in terms of the phase and lateral distribution. One of the most widely used probe to label GUVs is TR-DPPE (Texas Red-1,2-dipalmitoyl-sn-glycero-3-phosphoethanolamine, Fig. 3-1**A**), a red fluorophore which has a fluorescence excitation of 560 nm and emission of 595 nm.[19] TR-DPPE contains saturated palmitoyl chains with the fluorophore attached to the head group. This fluorophore prefers partitioning to the L_d phase in both DSPC/DOPC/Chol and SM/DOPC/Chol systems. Similarly, DiI (1,1'-dioctadecyl-3,3,3',3' tetramethylindocarbocyanine perchlorate, Fig. 3-1**B**), a carbocyanine dye containing saturated alkyl chains can be excited at about 549 nm and emits fluorescence at 565 nm. DiI prefers partitioning to the L_d phase in the SM/DOPC/Chol system. In DSPC-containing GUVs (DSPC/DOPC/Chol), DiI partitioning changes to the L_o phase as the length of the alkyl chain in the probe is increased. Other notable probes have also been developed, including NBD-DPPE [N-(7-nitro-2-1,3-benzoxadiazol-4-yl)] and BODIPY-PC N-(4,4-difluoro-5,7-dimethyl-4-bora-3a,4a-diaza-sindacene-3-dodecanoyl), which also prefer partitioning into the L_d phase.

In the middle part of this chapter, the effect of saponins was assessed using fluorescence-labeled GUVs. A synthetic fluorescence analog of OSW-1, DBD-tagged OSW-1 (DBD-OSW-1, Fig. 3-2, **2**) that was synthesized by Sakurai et al. using site-selective acylation was also used for imaging experiments.[21] Preliminary experiments were conducted utilizing this fluorescent OSW-1 analog in HeLa cells for analysis of its cellular localization. It was found that OSW-1 rapidly internalized into the cells and localized primarily around the nucleus but is also distributed in other subcellular organelles.[21,22] To evaluate the effect of OSW-1 on membrane integrity, DBD-OSW-1 was used on TR-DPPE-labeled GUVs. Another method to assess and compare the effect of non-labeled saponins was designed by Sudji et al.;[23] GUVs were labeled with DiI while the solution surrounding the GUVs was labeled by Alexa Fluor 488. Their study highlighted the importance of Chol in membrane interaction of digitonin. They observed a time-dependent membrane permeabilization in GUVs containing Chol, which eventually led to membrane disruption at a prolonged incubation. On the other hand, they reported that digitonin did not show any effect on GUVs in the absence of Chol. In this study, similar preparations were applied except that Rhodamine 6G (Fig. 3-1**C**, Ex: 480; Em: 530) was used in the place of Alexa Fluor 488. The effect of non-labeled saponins including OSW-1, digitonin, soyasaponin Bb(I) and glycyrrhizin on the morphology of GUVs were examined using fluorescence microscopic techniques.

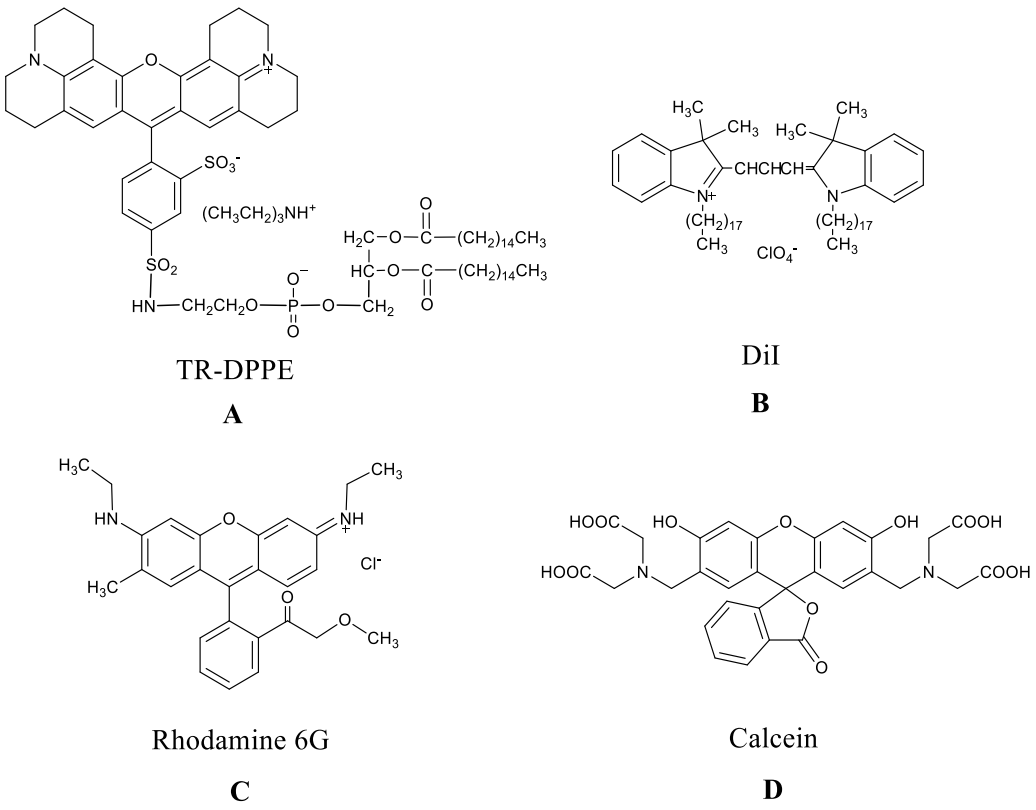

Figure 3-1. Common fluorescent probes, TR-DPPE (A), DiI B), Rhodamine 6G (C) and Calcein (D).

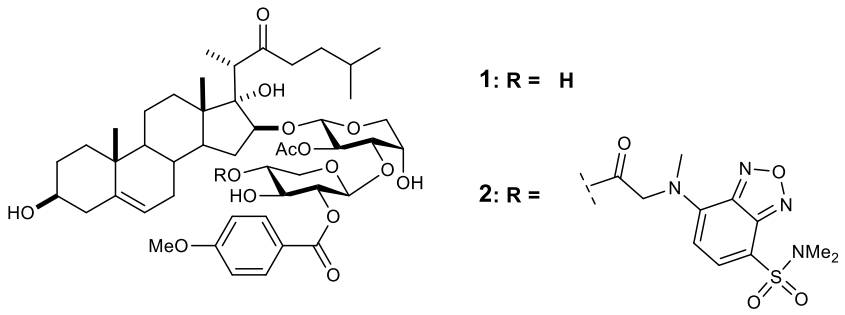

Figure 3-2. Structure of OSW-1 (***1***); and DBD-OSW-1 (***2***) with excitation wavelength of 470 nm and emission wavelength of 529 nm.[21]

3.2 Aim and significance of the study

In the previous chapter, the membrane permeabilizing activity of OSW-1 and typical 3-*O*-glycosyl saponins were evaluated using various spectroscopic approaches. The differences in the mode of action between OSW-1 and digitonin against the membrane have been established by the osmotic protection experiments, DLS spectroscopy, ^{2}H NMR spectroscopy and ^{31}P NMR spectroscopy. It has been revealed that OSW-1 assumes a barrel stave-like pore model in accordance with the results obtained from these experiments and in comparison with the results of other membrane active compounds. In this chapter, the differences in the mechanism between OSW-1 and digitonin were further studied using binding isotherm experiment. Leakage assays were carried out on calcein-entrapped LUVs and the apparent binding and membrane disruptivity of these saponins were evaluated by varying the concentrations of specific membrane components.

In addition, fluorescence microscopic techniques were utilized to examine membrane morphological changes induced by various saponins. GUVs, in the absence or presence of Chol, were used as membrane models. Changes in shape and size, formation of membrane defects (curvature, tubules, pores, buds, etc.), and membrane disruption were monitored upon saponin addition for a certain period. The simplicity of the models used only allows determination of specific interactions of saponins with the components of the membrane, including Chol. Furthermore, the limited availability of fluorescence probes that can be used for this kind of study on saponins only allows us to evaluate certain aspects of the saponin-Chol interaction.

3.3 Results

3.3.1 Time-course leakage assays

In order to investigate the binding and disrupting properties of OSW-1 and digitonin, time-course calcein leakage experiments were conducted on LUVs. LUVs with varying final phospholipid ([L] = 5 μM to 40 μM PL) and Chol concentration were prepared while maintaining 10 mol% of Chol in the system. It was already discussed that OSW-1 and digitonin only induce membrane permeabilization in LUVs containing Chol. The degree of leakage was also monitored at various saponin concentrations from 1 μM up to 100 μM (or up to 300 μM in the case of soyasaponin Bb(I).

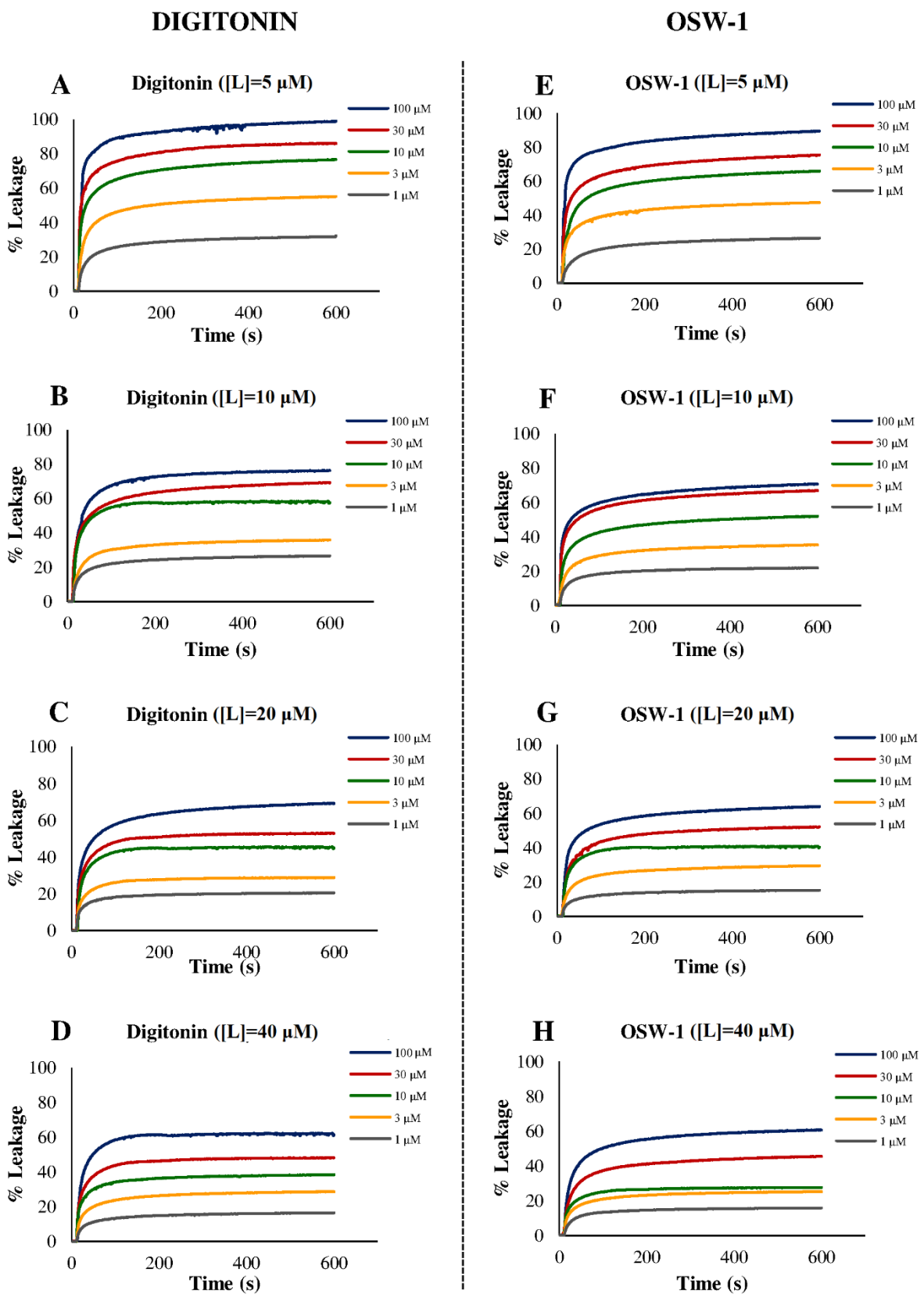

Figure 3-3. Time-course calcein leakage by treatment with digitonin (A to D) or OSW-1 (E to H) in 9:1 POPC/Chol LUVs measured for 10 minutes after saponin addition. 100% leakage was obtained by addition of 10% (v/v) Triton-X. Measurements were monitored at 25 °C.

Time-course calcein leakage data were obtained for 10 minutes upon saponin addition (Fig. 3-3), the increase in the fluorescence intensity is attributed to the dilution of calcein upon rupture of LUVs. As shown in Fig. 3-3, leakage is dependent on the concentration of both digitonin and OSW-1. This result was similarly observed in soyasaponin Bb(I), however, the activity is weaker compared to the other two saponins (Fig. S2-1, Supporting Information II). Previous studies suggested that digitonin exerts stronger leakage properties in comparison with OSW-1.[24] Similar results were observed in this study confirming that among all the saponins tested, digitonin showed the highest activity towards membrane permeabilization.

3.3.2 Binding isotherm experiments

To determine the influence of the affinity of saponins to the membrane and their perturbing properties towards permeability enhancement, a binding isotherm is generated for each saponin from the dose-response curve obtained in the time-course leakage experiments at various final phospholipid concentrations in the presence of ~10 mol% Chol. In addition, the measurement of fluorescence intensity was carried out for 10 minutes after saponin addition to achieve the equilibrium conditions that is characterized by a plateau in the time-course fluorescence plot.

The relative leakage rates were evaluated by using effective concentration of 50% calcein release (EC_{50}) at 2 min upon saponin treatments (Table 3-1 and Fig. 3-4). It was observed that increasing the total phospholipid concentration increases the amount of saponin required to induce 50% leakage in 9:1 POPC/Chol (~10 mol % Chol) LUVs as shown in the increase in the calculated EC_{50} values (Table 3-1 and Figure 3-4). It is also worth mentioning that only single measurement was carried out due to the stability of calcein-entrapped liposomes. Prolonged exposure of calcein-entrapped liposomes could undergo premature leakage; this case can only be prevented by using freshly prepared liposomes. The measurement of one sample takes 17 minutes in total, including 2 minutes of stabilization and baseline correction, 10 minutes of observation upon addition of saponin and 5 minutes of observation after the addition of Triton-X.

Table 3-1. EC_{50} of calcein leakage activity by saponins using liposomes composed of 9:1 POPC/Chol.

	EC_{50} (μM)			
SAPONIN	5 μM [L]	10 μM [L]	20 μM [L]	40 μM [L]
Digitonin	3.63	7.37	12.74	20.49
OSW-1	9.31	14.29	21.71	36.88
Soyasaponin Bb(I)	37.19	46.58	59.84	95.49

Note: Single measurement was carried out due to stability of calcein-entrapped LUVs and limited amount of OSW-1.

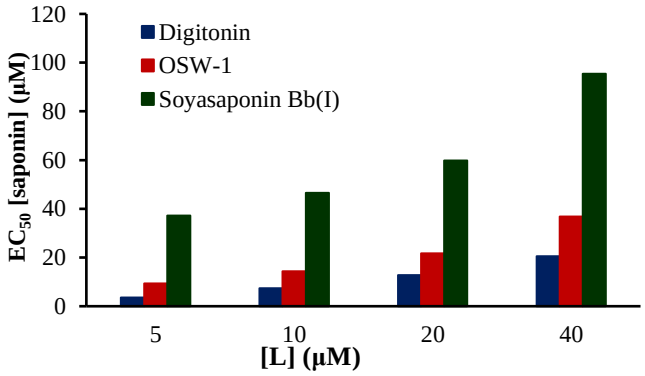

Figure 3-4. Effect of lipid concentration on leakage properties of saponins. LUV consisting of POPC/Chol (9:1) while the amount of phospholipid ([L]) was 5 μM to 40 μM.

The observed membrane-permeabilizing properties of these saponins could be accounted by the differences in their chemical structures, which may also reflect their distinct membrane-binding activities and intrinsic disrupting activities.[2] In addition, the relative increase in the required concentration of these saponins upon higher liposome concentrations could indicate that membrane permeabilization is caused by the concentration of saponin in the membrane. In line with this, the rate of liposome leakage should be determined by the membrane-bound saponin ($[S]_b$) per phospholipid concentration ([L]). The saponin efficacy could be expressed as the ratio r ($r = [S]_b/[L]$) which should be constant for a certain leakage extent (ex. 50% leakage; r_{50}).[1,2] The first-order equation shown (Eq. 1) could be used to determine the r values and free saponin concentrations $[S]_f$. The amount of saponin added, i.e. $[S]_0$ is the sum of the membrane-bound ($[S]_b$) and free ($[S]_f$) saponins at particular % leakages.

$$[S]_0 = [S]_f + [S]_b = [S]_f + r[L] \quad \textbf{(Eq.1)}$$

In Eq. 1, $[S]_0$ and [L] are given as the experimental conditions and the value of $[S]_f$ and r are experimentally determined as the y-intercept and slope, respectively, by linear regression. Different set of r values could be obtained at different %leakage from the dose-response curves generated from four different [L]. Fig. 3-5 shows the $[S]_0$ vs [L] at different leakage extents from 20% to 60% for both digitonin and OSW-1. These values were also calculated for soyasaponin Bb(I) (Fig. S2-2, Supporting Information II).

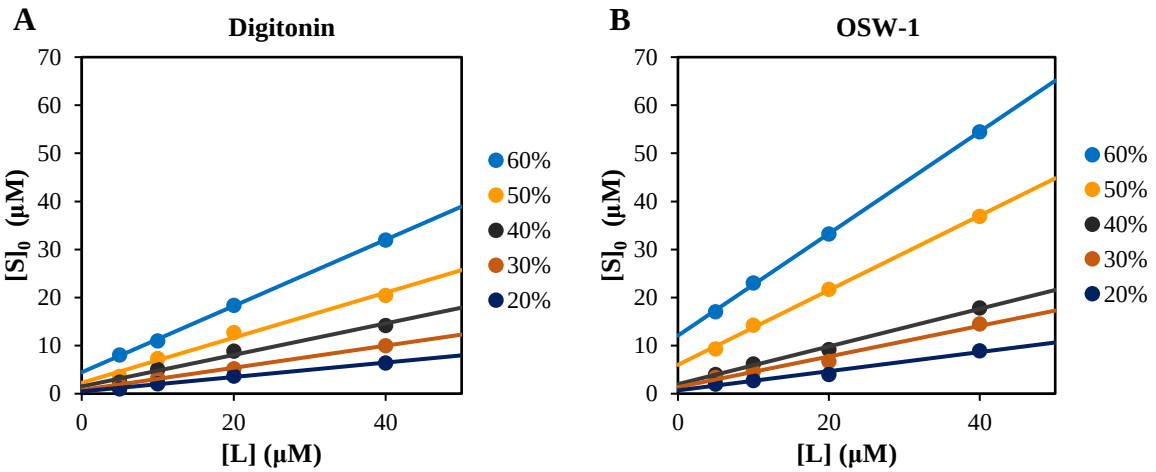

Figure 3-5. Determination of $[S]_f$ and r as intercepts and slopes, respectively, at different leakage extents (20%, 30%, 40%, 50%, and 60%) for digitonin (A) and OSW-1 (B). The concentration of saponin to induce percentage leakage from 20% to 60% taken as the vertical axis were separately determined on the basis of concentration-response curves of each saponin at the incubation time of 10 min (See Fig. S2-4, Supporting Information II for details).

Based on the obtained values for $[S]_f$ and r, the binding isotherm curves could be drawn for both digitonin and OSW-1 as shown in Fig. 3-6 (and for soyasaponin Bb(I) Fig. S2-3, Supporting Information II). By using these isotherms, the apparent association constant K_{app} = [S-L] / ($[S]_f$ •[L]) = $[S]_b$ / ($[S]_f$ •[L]) can be estimated as a ratio between $r/[S]_f$. The K_{app} value at 50% leakage extent is defined as the K_{50}, which describes the affinity of saponin to the membrane under the condition at which saponin permeabilizes 50% of liposomes; as shown in Fig. 3-6, the K_{app} value is constant in the low range of r up to 0.3 to 0.4, but becomes small above r = 0.4. The K_{50} values for both digitonin and OSW-1 and corresponding r value at 50%

leakage, $r_{50,}$ are shown in Table 3-2. Higher K_{50} values indicate that the saponin possess higher affinity to the membrane. Lower r_{50} values indicate stronger disruptivity of the membrane because less amount of the membrane bound saponin is required. Importantly, it should be noted that the action of this saponins are Chol-dependent and that no observed leakage was reported in pure POPC membrane.[24] The results indicate that digitonin showed slightly higher binding affinity (K_{50} = 0.207 μM^{-1}) and stronger membrane disruptivity (r_{50} = 0.469) as compared with OSW-1 (K_{50} = 0.129 μM^{-1}; r_{50} = 0.776), while soyasaponin Bb(I) exhibited the much lower binding affinity and weakest membrane disruptivity (K_{50} = 0.058 μM^{-1}; r_{50} = 1.662) among the three saponins. This result confirms previous data suggesting that digitonin has the strongest activity as compared to other saponins, including OSW-1 and soyasaponin Bb(I).[24]

Table 3-2. Association constant at 50% leakage (K_{50}) and bound saponin/lipid ratio at 50% leakage extent (r_{50}).

	K_{50} (μM^{-1})	r_{50}
Digitonin	0.207	0.469
OSW-1	0.129	0.776
Soyasaponin Bb(I)	0.058	1.662

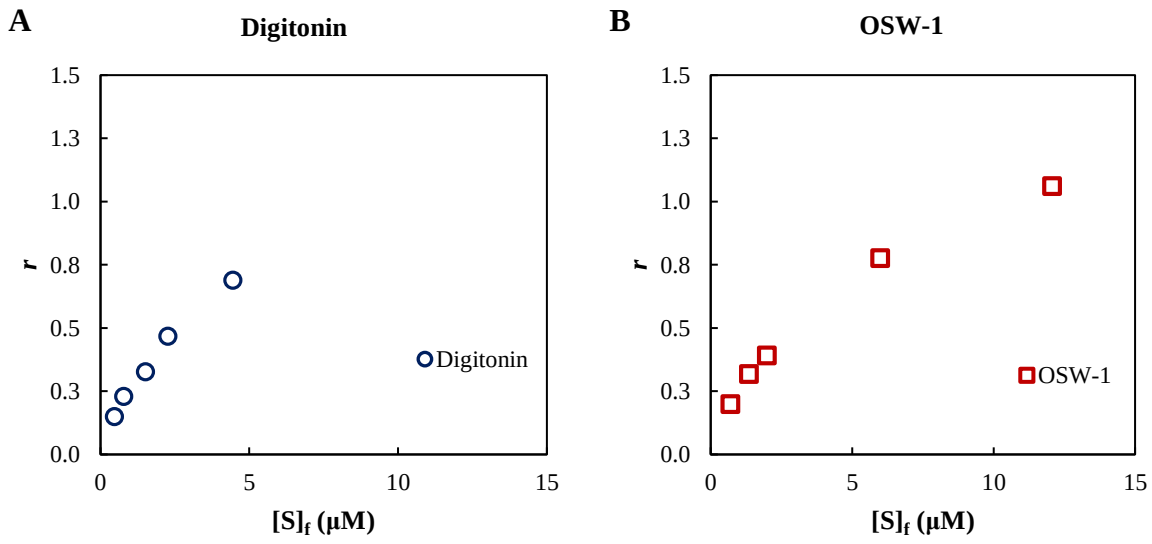

Figure 3-6. Binding isotherms of digitonin and OSW-1 at different leakage extents. Bound saponin/lipid ratio (r) was plotted in each free saponin concentration $[S]_{f.}$

In addition, Fig. 3-7 shows the intrinsic membrane disruptivity at a certain leakage extent, indicating the intrinsic disruptive ability of the membrane-bound saponin. Furthermore, the observed membrane disruptivity at various saponin concentrations, as shown in Fig. 3-6, suggests that the mode of membrane perturbation and interaction are distinct for each saponin. The distinguishable chemical structure and polarity between digitonin and OSW-1 could partly account for this observed difference.

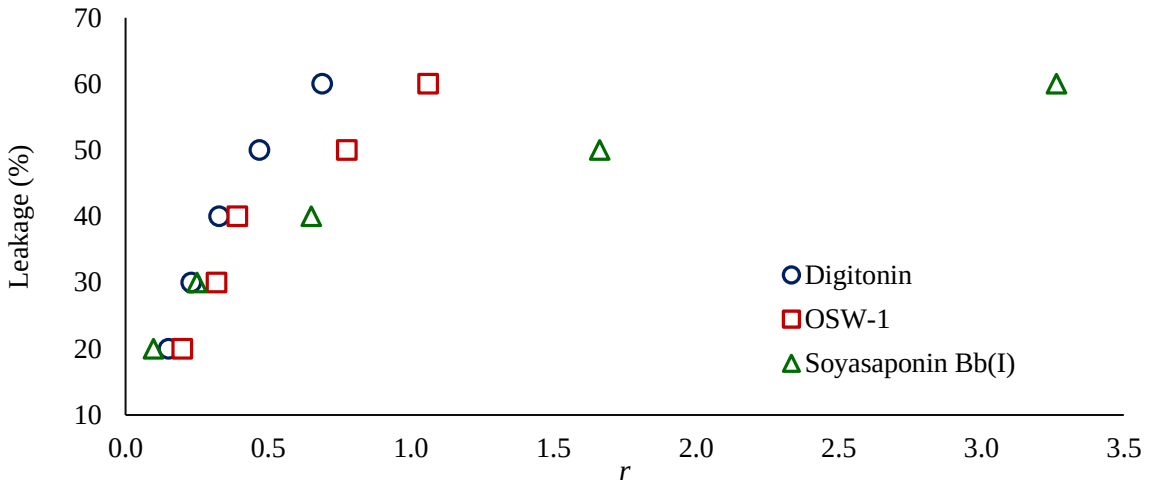

Figure 3-7. Membrane disruptivity of the saponins. Relationship between leakage extent and $[S]_b/[L]$ (r) were plotted.

3.3.3 Membrane permeabilization and morphological changes induced by saponins examined by fluorescence microscopy

To further examine the effects of saponins on membrane, fluorescence microscopic experiments were employed. In this section, natural saponins including OSW-1, digitonin, soyasaponin and glycyrrhizin were used to investigate their effects on GUVs. GUVs composed of 2:2:1 DOPC/DMPC/Chol (20 mol% Chol) labeled with 0.01 mol% DiI (red fluorophore) was used as the model membrane. Initially, this membrane model was chosen to assess the interaction of saponins with membrane phases such as the L_o and L_d phase but the distinction between these phase is not well-defined. Alternatively, microscopic observations utilizing a 9:1 POPC/Chol GUV labelled with a fluorescent probe can also be carried out to examine the

effect of saponins in single phase GUV and to allow a clearer comparison with previous results that used similar membrane system. The GUVs used in the study were prepared via electroformation process as shown in Fig. 5-2 (Methodology section). After electroformation process, aqueous GUV suspension was labeled with Rhodamine 6G (green fluorophore). At this point, the GUV encloses a non-fluorescent environment (black) while the surrounding solution gives a green fluorescence. The ability of the saponins to induce permeabilization and morphological changes can be investigated by the entry of green fluorophore and changes in the GUV integrity, upon addition of 30 μM saponins into the system.[23]

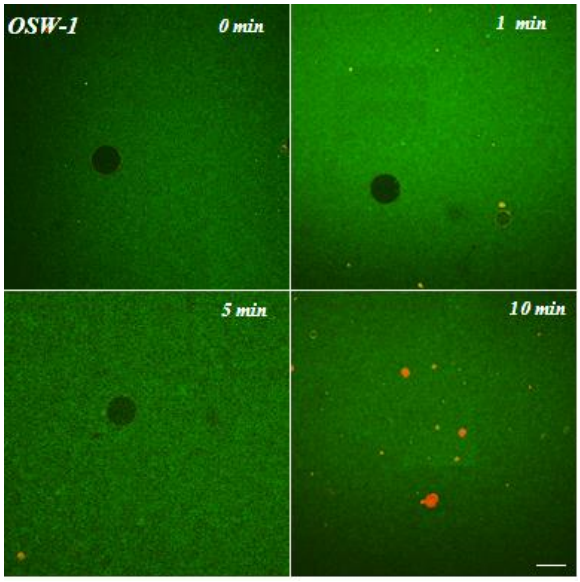

Figure 3-8. Effect of addition of 30 μM OSW-1 in 2:2:1 DOPC/DMPC/Chol GUV (Scale = 10 μm) measured at 37 °C.

In the addition of OSW-1, a rapid membrane permeabilization was observed after 5 minutes of incubation as shown in Fig. 3-8. The effect of OSW-1 was further highlighted at 10 minutes of incubation when the GUV undergoes disruption. This presents that higher OSW-1 concentration (30 μM) promotes membrane disruption. However, this result does not support our previous ^{31}P NMR data, which indicated that OSW-1 increases membrane curvature.[24]

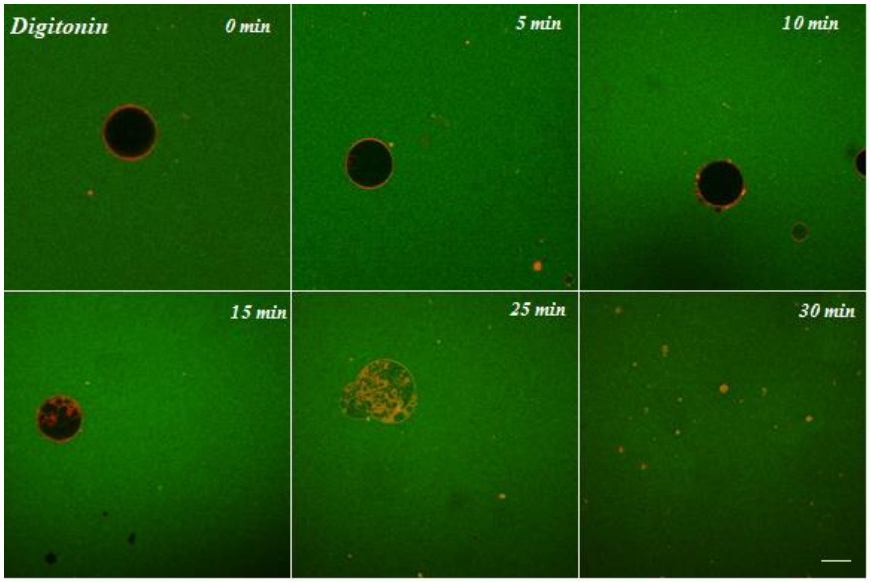

Figure 3-9. Effect of addition of 30 μM digitonin in 2:2:1 DOPC/DMPC/Chol GUV (Scale = 10 μm) measured at 37 °C.

Addition of digitonin promotes membrane disruption (Fig. 3-9) as expected, which was evident after 30 minutes of observation. Furthermore, changes in the integrity of the membrane were clearly observed prior to membrane disruption. Formation of small structures surrounding the GUV was observed at 10 minutes, which could correspond to digitonin/Chol complex. This complex was found to internalize into the GUV after 15 minutes of observation, which could support previous reports stating that digitonin/Chol complex permanently inserts into the membrane.[23,25] Membrane deformations such as positive curvature generation were observed at 25 minutes. This phenomena supports our previous result as illustrated by the ^{2}H NMR and ^{31}P NMR experiments.[24] First, it was reported that digitonin attenuates ^{2}H NMR signal by forming large aggregates with Chol, greatly reducing the mobility of Chol in the membrane. This might be occurring during the 10 minutes of observation. Furthermore, the reduction in signal widths and presence of broad peak at 0 ppm in the ^{31}P NMR suggested that membrane curvature generation and reduction of vesicle size is a consequence of digitonin/Chol interaction. This notion is in line with the results of the microscopic observation. Insertion of digitonin/Chol complex, as well as a slight reduction in the vesicle size was observed at 15 minutes. At 25 minutes, membrane protrusions were observed, which could correspond to positive membrane curvature generation. However, membrane disruption was still observed in the addition of digitonin at 30 minutes. The observed membrane disruption is attributed to the higher concentration of digitonin at 30 μM. The amount of digitonin added is higher than the

final concentration of Chol (18 μM) in the GUV system used. The observed membrane disruption is also true in the case of OSW-1, in which the added concentration is also 30 μM. Furthermore, not all of the saponins bind to the membrane, other saponins may exist in micellar form in equilibrium to the bound state under certain time and conditions. This could also be related by the binding isotherm indicating the affinity of the saponins towards membrane binding, in which unbound saponins also exist under equilibrium conditions. Previous NMR experiments utilized a system with the saponin-Chol ratio of 0.5:1. The differences in the composition of the membrane and the degree of membrane hydration could partly account for these observations. However, it was clear that the mode of action of OSW-1 and digitonin on a single vesicle observation are distinct from one another.

The effects of soyasaponin Bb(I) and glycyrrhizin on GUVs were also examined. As shown in Fig. 3-10, soyasaponin Bb(I) affects the integrity of GUV. This was evident at 50 minutes where soyasaponin Bb(I) allowed permeabilization of the GUV. This further led to membrane disruption at 55 minutes at this concentration. In relation to the previous results suggesting that soyasaponin Bb(I) has a weaker membrane activity compared to OSW-1 and digitonin, higher concentration and longer incubation in the presence of this saponin could be required to exhibit such membrane disrupting effect. It was mentioned in the previous chapter that soyasaponin Bb(I) exerts a similar, but weaker, effect in Chol-containing membranes as described by the corresponding ^{2}H NMR and ^{31}P NMR spectra. Similarly, for both OSW-1 and soyasaponin Bb(I), the permeabilization of the GUV could be brought by the formation of distinct pores as observed in the osmotic protection experiment in RBC. The larger size of pore created by OSW-1 as compared to soyasaponin Bb(I) could partly affect the rate of permeabilization of these saponins towards the membrane. The distinct structures of these saponins could also address the results observed in the experiments that were previously conducted.[24] Furthermore, as expected, glycyrrhizin (Fig. 3-11) did not show any changes in the GUV morphology even after prolonged incubation (90 minutes), suggesting that glycyrrhizin has no effect on the membrane integrity even in the presence of Chol. This supports the results gathered in the previous chapter about the weak activity of glycyrrhizin at all the concentrations tested in the various membrane model preparations.[24] Moreover, the presence of red objects which appeared in Fig. 3-11 do not necessarily correspond to a GUV. The appearance of this structure might have occurred during the electroformation process.

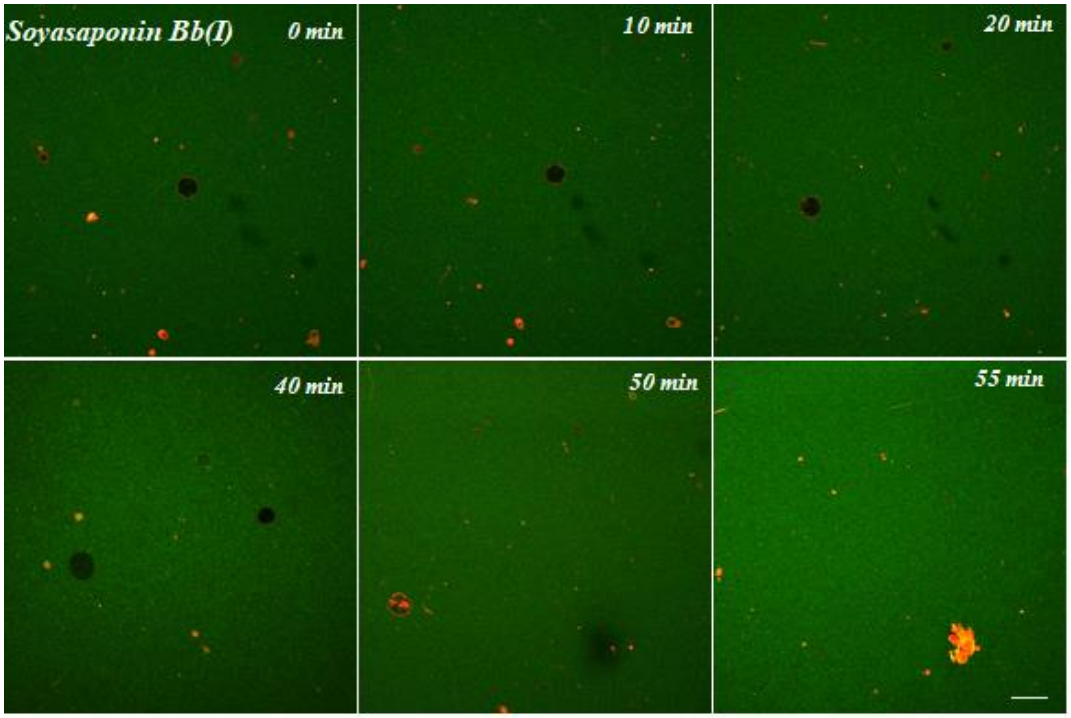

Figure 3-10. Effect of addition of 30 μM soyasaponin Bb(I) in 2:2:1 DOPC/DMPC/Chol GUV (Scale = 10 μm) measured at 37 °C.

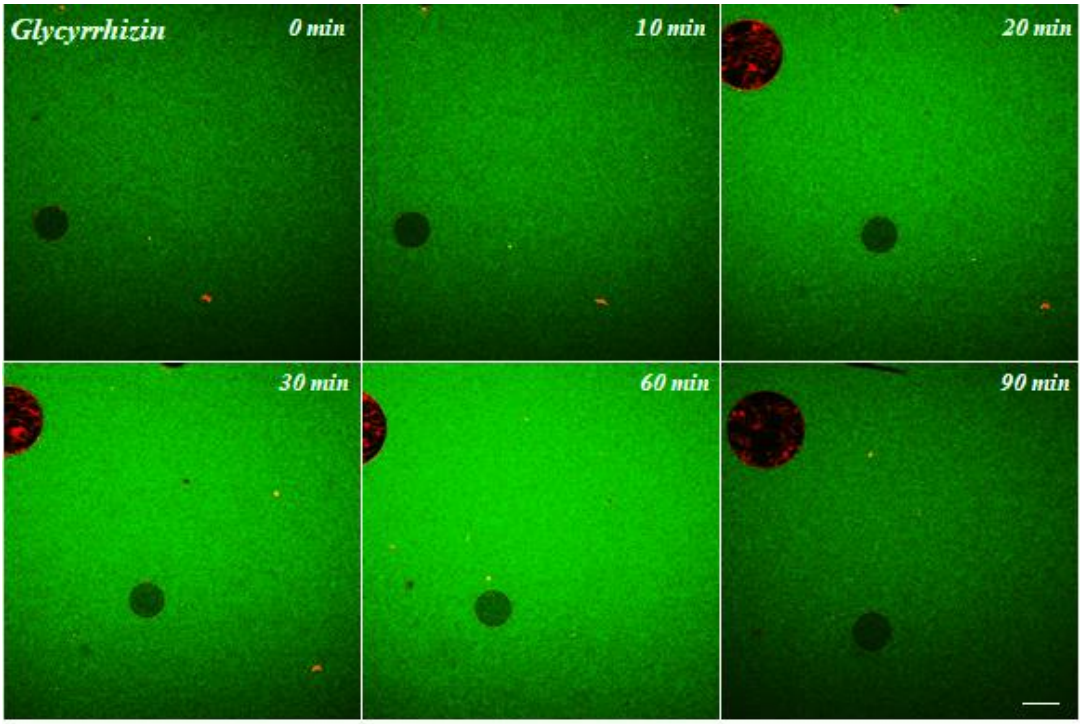

Figure 3-11. Effect of addition of 30 μM glycyrrhizin in 2:2:1 DOPC/DMPC/Chol GUV (Scale = 10 μm) measured at 37 °C.

The differences in the saponin concentrations between the fluorescence and the NMR experiments could also affect the observations; fluorescence experiments used saponin concentrations which is higher than the Chol content of the membrane (30 μM saponin vs. 18 μM Chol) while NMR experiments used 1.0:0.5 Chol/saponin molar ratio indicating that the amount of saponin is less than the amount of Chol used.

Moreover, the hydration of liposomes were different such that liposomes were suspended in aqueous buffer in the fluorescence measurements while in solid-state NMR, the liposomes were only 50% hydrated. Also, the artificial membrane model used for fluorescence measurements were unilamellar (LUV and GUV) while solid-state measurements utilized MLV. The addition of saponins could influence the stability of the membrane model used at varying degrees, as influenced by its size and lamellarity.[3] In the NMR preparation, the saponins were premixed with the phospholipid and Chol while in other experiments, the saponins are added to the liposome under aqueous environment. In addition, the distribution of saponins in the membrane leaflet is very different at the earlier stage of membrane disruption as observed by microscopy. Furthermore, the temperature used for measurements has an effect for these observations. In calcein leakage, the temperature used was 25 °C, while fluorescence microscopy was done at 37 °C. Solid-state NMR was measured at 30 °C. These variations could influence the interaction of saponins in the membrane.

3.3.4 Distribution of DBD-OSW-1 in liposomes and changes in membrane morphology and integrity

The fluorescent analog of OSW-1, DBD-OSW-1, was also utilized to study its effect on Chol dependent change in GUV morphology. In this system, GUVs composed of DOPC/DMPC, in the absence and presence of various Chol mol%, were used. The GUVs were labeled with 0.05 mol% TR-DPPE while the OSW-1 used in this experiment was mixed with DBD-OSW-1 (10 mol%). Upon addition of saponin to GUV in the absence of Chol, green fluorescence from DBD-OSW-1 appeared on the membrane and enhanced in a time dependent manner. However, the morphology of the GUV was not affected regardless of the concentration of OSW-1 (max. at 30 μM), indicating that OSW-1 just binds into the GUV but not exert further activity to cause the membrane deformation without Chol (Fig. 3-12).

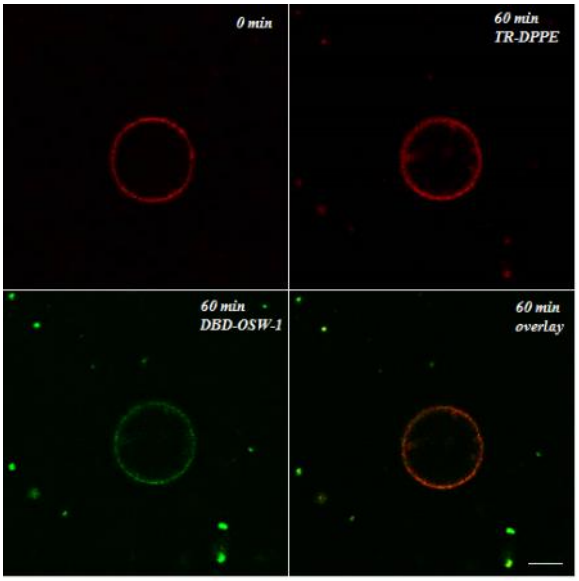

Figure 3-12. Effect of 30 μM OSW-1 in 1:1 DOPC/DMPC GUV (Scale = 10 μm) measured at 37 °C.

Next, GUVs composed of DOPC/DMPC in the presences of different mol% of Chol were treated with various concentrations of OSW-1, and subjected to fluorescence microscopic observations. In GUVs composed of 2:2:1 DOPC/DMPC/Chol (20 mol% Chol), lower concentration of OSW-1 (up to 10 μM) did not induce significant morphological changes as the GUV remained intact up to 60 minutes of incubation (Fig. 3-13**A** to **C**); at 10 μM, a slight deformation of GUV was observed. However, it was evident that higher OSW-1 concentration (30 μM) exhibited marked changes in the morphology of the membrane (Fig. 3-13**D**). This effect was similarly observed in the 9:9:2 DOPC/DMPC/Chol (10 mol% Chol). The effect of OSW-1 in the membrane morphology was only highlighted when the concentration was 30 μM (Fig. 3-14**D**). These observations in the presence of 10 mol% and 20 mol% Chol suggest that OSW-1 exerts its activity at a higher concentration. The GUVs were found to deviate from its spherical shape by slowly shrinking but no further disruption was observed. This result was in contrast to result presented in the non-fluorescent labeled OSW-1 where disruption took place at the same 30 μM concentration (Fig. 3-8, 10 minutes). In addition, presence of a small vesicle residing near the surface of the GUV (Fig. 3-13**D** and Fig. 3-14**D**) could be regarded as small aggregates composed of OSW-1 and Chol (see time lapse images in Figs. S2-5 and S2-6, Supporting Information II). The presence of this structure might be partly responsible for the shrinkage of the membrane. In contrast, in GUVs composed of 19:19:2 DOPC/DMPC/Chol (5 mol% Chol), a significant morphological change was observed upon the addition of 30 μM

concentration (Fig. 3-15**D**). At this condition, a possible disintegration of the membrane took place, as the GUV was no longer intact (see time-lapse images in Fig. S2-7, Supporting Information II).

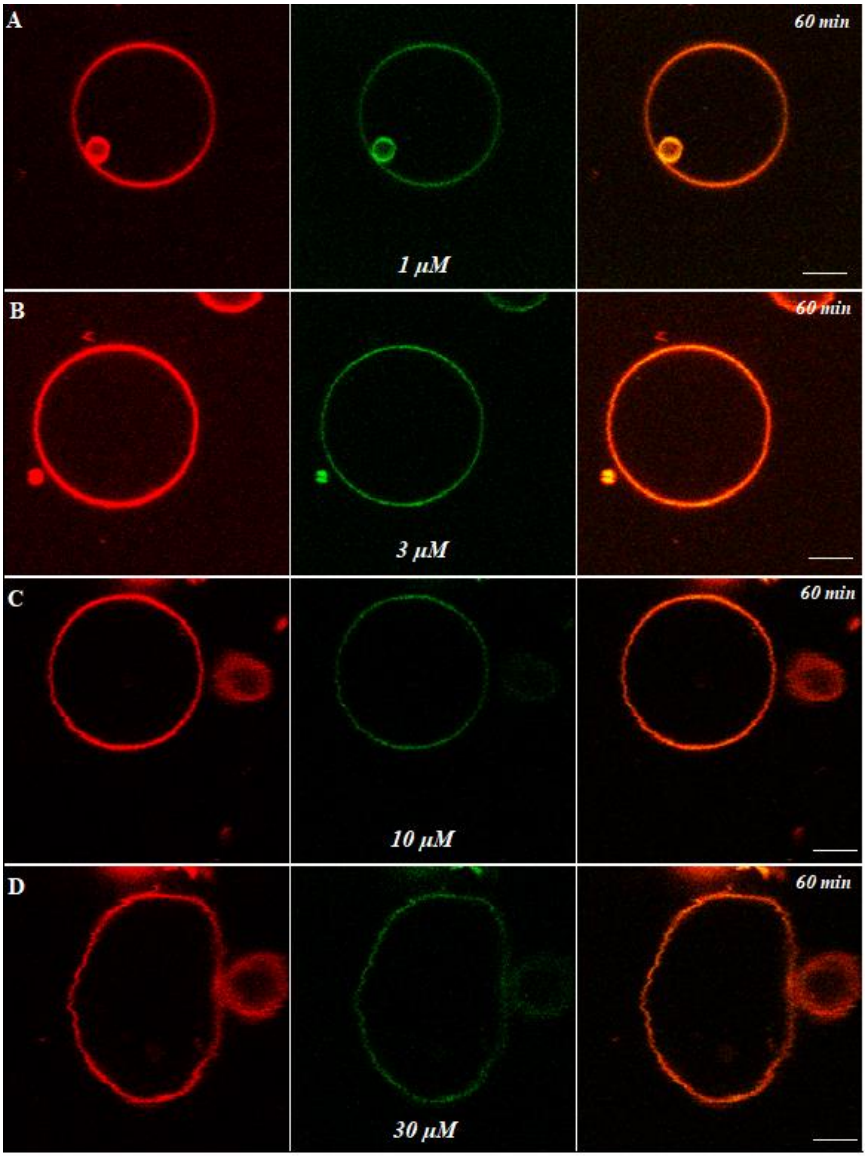

Figure 3-13. Effect of various concentration of OSW-1 in 2:2:1 DOPC/DMPC/Chol (20 mol% Chol) GUV (Scale = 5 μm) at 60 minutes of incubation. The concentrations of OSW-1 used were (A) 1 μM, (B) 3 μM, (C) 10 μM and (D) 30 μM. Measurements were carried out at 37 °C.

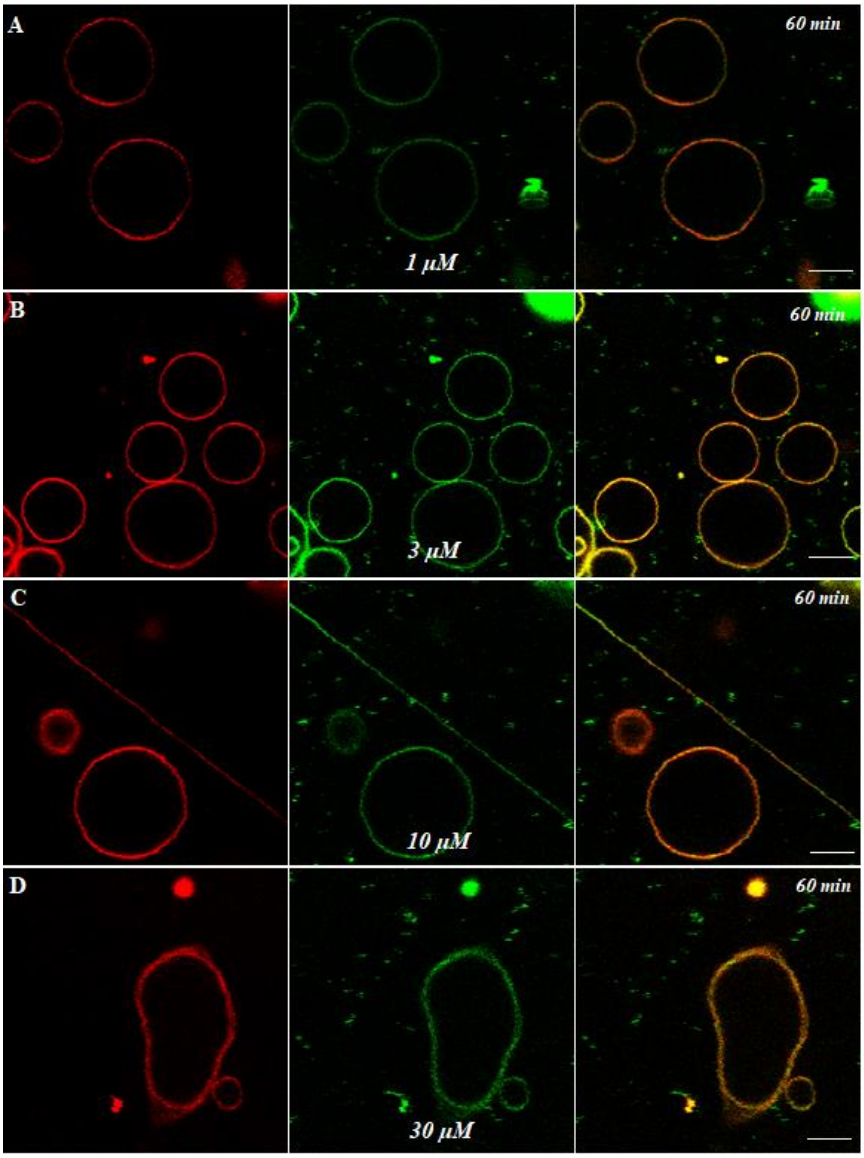

Figure 3-14. Effect of various concentration of OSW-1 in 9:9:2 DOPC/DMPC/Chol (10 mol% Chol) GUV (Scale = 10 μm) at 60 minutes of incubation. The concentrations of OSW-1 used were (A) 1 μM, (B) 3 μM, (C) 10 μM and (D) 30 μM. Measurements were carried out at 37 °C.

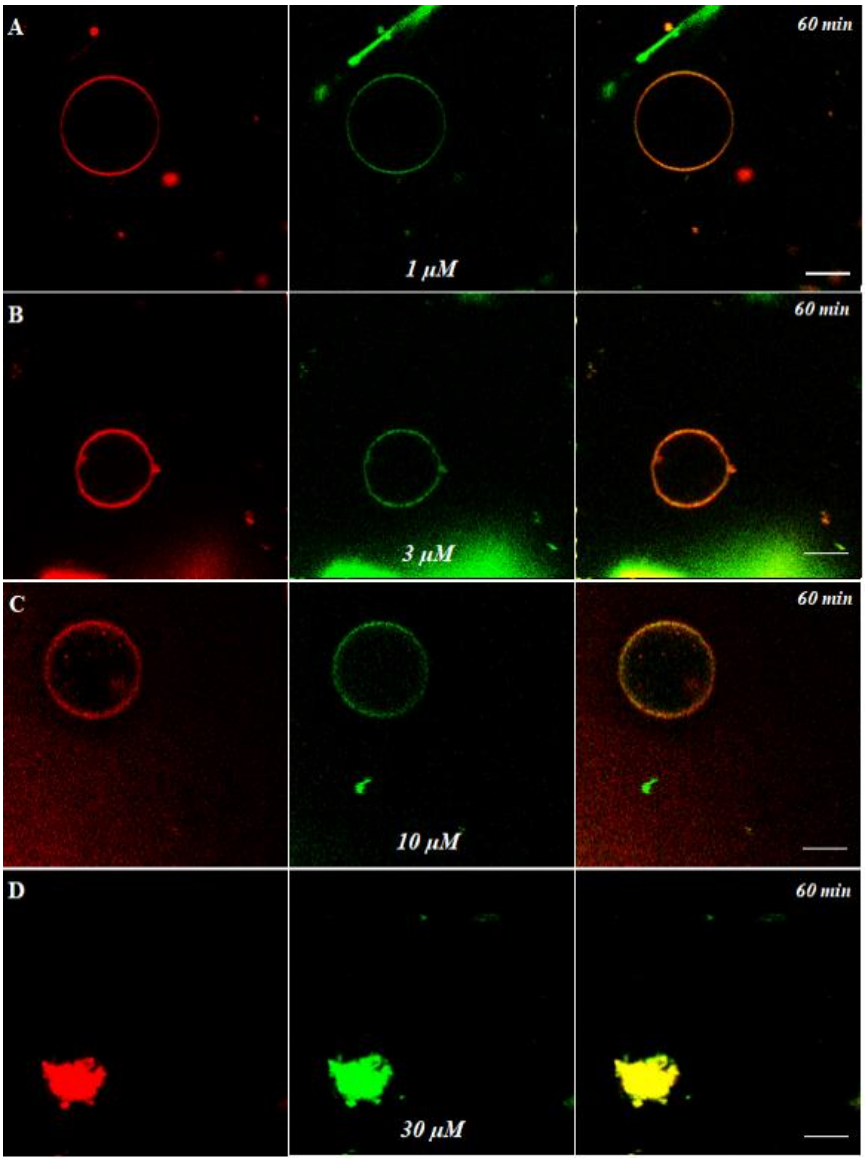

Figure 3-15. Effect of various concentration of OSW-1 in 19:19:2 DOPC/DMPC/Chol (5 mol% Chol) GUV (Scale = 5 μm) at 60 minutes of incubation. The concentrations of OSW-1 used were (A) 1 μM, (B) 3 μM, (C) 10 μM and (D) 30 μM. Measurements were carried out at 37 °C.

3.4 Discussion

Lines of spectroscopic evidence that suggest a sterol-dependent interaction mechanism of saponins including OSW-1, digitonin and soyasaponin Bb(I) were previously presented in this study. In particular, it is highlighted that the formation of Chol/saponin aggregates in membrane is a key factor for the action of their membrane permeabilizing properties.[24] In this chapter, the properties of these saponins were further investigated and their differences in mode of action were established using a time-course fluorescence spectroscopic technique, particularly using calcein leakage assay in LUVs under varying final lipid concentrations while keeping the mol% Chol constant. The binding isotherm experiments revealed their apparent affinities to Chol-membranes and ranks of the disruptive activities. It was earlier confirmed that these saponins did not give rise to the membrane disruption to the liposomes without Chol. Therefore, liposomes carrying calcein was prepared with the membrane composition of POPC/Chol = 9:1. It was observed that the amount of saponin bound in the membrane lipids was crucial to exert their activity towards the membrane. A similar study using pavoninin-1, an unusual steroidal saponin found in *Paradichus* spp., have been reported (Fig. 1-22**A**) to permeabilize Chol-lacking membranes.[1] Increasing the amount of total phospholipid required a higher amount of pavoninin-1 in order to induce the same leakage degree, which is attributed to the dilution of membrane-bound pavoninin-1 due to the increased numbers of the phospholipid molecules. Interestingly, pavoninin-1 showed comparable membrane disruptive properties for the membrane containing Chol, but decreases apparent membrane binding affinity, which might be due to the ability of Chol to produce more rigid membrane.[1,2,26] This observation is in sharp contrast to our study. The membrane disruption effect of OSW-1 and digitonin can only be observed when the membrane is composed of Chol. The modes of action of OSW-1 and digitonin are clearly different from that of pavoninin-1, in terms of its interaction with Chol-containing membrane. Namely, OSW-1 and digitonin disrupt membrane through formation of an aggregate with Chol, while pavoninin-1 solely interacts with phospholipids leading to membrane disruption.

Next, the apparent binding affinity (K_{app}) and the membrane disruptivity (r) values observed for OSW-1 and digitonin were assessed. Digitonin showed a greater affinity towards binding with Chol-containing membrane in comparison with OSW-1. In addition, relatively lower r values indicate its stronger disruptive properties. OSW-1 also exhibited disruptive properties but at a weaker extent compared to digitonin. It is expected that when a critical amount of saponin is bound to the membrane, membrane disruption immediately follow. The

high amount of membrane-bound digitonin directly induced membrane disruption, while a similar but weaker activity was observed in OSW-1. These results could correlate to the differential mode of binding of saponins with Chol, as previously postulated.[23,25] Usual 3-*O*-glycosyl saponins such as digitonin are inserted into the membrane and are thought to interact with the hydrophobic core of Chol in a face-to-face manner. The orientation of the hydrophobic core of digitonin can easily access a Chol molecule residing in the membrane. At a certain threshold, digitonin induces removal of Chol from the membrane core and makes it more susceptible to membrane leakage, as a consequence of its known detergent properties.[27] On the other hand, the shape and orientation of OSW-1 upon membrane interaction may contribute to its affinity and membrane disruptivity. The unusual interaction between the hydrophobic cores of Chol and OSW-1 occurs due to its triangular shape formed by the steroidal aglycone and the acylated disaccharide scaffold.[28] This shape makes OSW-1 access Chol in the different way from other usual saponins. Furthermore, the differences in the overall polarity of digitonin and OSW-1 could also greatly contribute to their observed activity.

The effect of saponins on the morphology of the GUV membrane was examined by using fluorescence microscopy, which allowed observation of the time-dependent membrane interaction of saponins and its consequences on the integrity of the membrane such as possible pore formation, curvature generation, vesicle size reduction and membrane rupture. The GUV models used in this study only allowed determination of specific interactions of saponins with the components of the membrane, including Chol. Moreover, the observed changes in the morphology of the GUVs could be attributed to the interaction of saponins with membrane Chol. As a result, it was confirmed that the membrane disruptions of OSW-1 is Chol-dependent, which is consistent with our previous results. All the saponins exhibited strong disruption activity to the Chol-containing membrane at 30 μM concentration except for glycyrrhizin as presented in Figs. 3-8 to 3-11, while the action of saponins is not efficient in membrane lacking Chol. Furthermore, the excess amount of saponins with respect to Chol content of the GUV could be responsible for the observable membrane disruptions. These results were also confirmed by the spectroscopic experiments in this study, such as Chol depletion/repletion and CTL fluorescence assays.[24,29] Interestingly, it was observed that digitonin altered the morphology of GUVs at various stages of observation, which are somehow consistent with the results of ^{2}H and ^{31}P NMR, indicating that the direct interaction of digitonin with Chol induces the formation of large Chol/digitonin aggregates in the aqueous phase. Curvature generation and vesicle size reduction as a consequence of the strong activity

of digitonin were also observed by ^{31}P NMR and dynamic light scattering experiments, respectively. These observations strongly supported the proposed mechanism of action of digitonin such that Chol/digitonin aggregates are formed and penetrates into the membrane, which cause curvature generation and disruption. In the case of OSW-1 and soyasaponin Bb(I), they essentially require Chol to exhibit membrane interactions, but the molecular mechanism particularly of the membrane permeabilization is not clearly established. In these microscopic observations, membrane disruptions were not observed, like curvature change or budding, depression etc., upon addition of OSW-1 or soyasaponin Bb(I). Thus, it is currently difficult to explain thoroughly about the effect of these two saponins in membrane.

Fluorescence microscopy was similarly conducted on a fluorescently labeled OSW-1 (DBD-OSW-1). In this system, the interaction of OSW-1 with the GUV membrane can be tracked because it also possessed characteristic fluorescence properties. The ability of OSW-1 at various concentrations towards GUVs of different compositions and Chol contents allowed to examine the concentration of both OSW-1 and Chol required inducing changes in GUV morphology. In all the GUV preparations, only 30 μM concentration of OSW-1 exhibited significant membrane alterations. Moreover, an increase in the Chol concentration exhibits a decrease in the activity of OSW-1 towards membrane morphological changes. It is likely due to the contribution of Chol on membrane rigidity. Namely, the higher amount of Chol increase the packing and rigidity of the phospholipids in GUV, which may have minimized the access of OSW-1 to Chol.[30-32] In line with the effect of Chol concentration in GUV, it was clearly observed that GUV containing 5 mol% Chol was significantly affected by the addition of 30 μM OSW-1. The interaction of OSW-1 at this concentration altered the GUV integrity, which led to subsequent membrane disruption and formation of insoluble aggregates composed of OSW-1, Chol and phospholipids as shown as large irregular debris under the microscope (Fig. 3-15**D**). GUVs containing 5 mol% Chol are more labile to the exerted activity of OSW-1. On the other hand, the increasing amount of Chol (10 and 20 mol%) incorporated in the GUV increased the ordering of the membrane towards a more packed and rigid manner. Remarkably, the interaction of OSW-1 under these conditions does not significantly lead to membrane disruption but rather a generation of membrane curvature and shrinking of the GUV. The curvatures observed in microscopy could be supported by the ^{31}P NMR spectra giving a narrower CSA. The orientation of OSW-1 and its triangular shape might have induced this curvature since tilting of membrane components, including Chol, might occur to maximize Chol/OSW-1 interaction.[24,28] Interestingly, small vesicle-like structures were observed near the

GUV. They could be formed due to the removal of Chol and minor membrane components, which induce aggregation with OSW-1. The loss of these membrane components does not necessarily disrupt the membrane but caused the weakening and shrinking of the GUV from its original spherical shape.[25,33,34]

Overall, it was revealed that the amount of both OSW-1 and Chol, added to the surrounding solution and in membrane of the GUV, are critical for the morphological changes. However, it is difficult to establish a correlation between the two since the physical appearance of the membrane was observed under the microscope. With respect to the binding isotherm experiments in this study, the higher propensity of calcein leakage induced by digitonin in Chol-containing membrane is attributed to membrane disruption at a certain amount of membrane-bound digitonin. However, OSW-1 does not follow the membrane disruption mechanism; rather the observed leakage is due to transient pore formation as a consequence of removal of minor membrane components (Fig. 3-13**C** and **D**; Fig 3-14**C** and **D**)

Finally, based on the results of the experiments, the barrel stave-like hypothesis for OSW-1 proposed in the Chapter 2 could be somewhat supported.[24] The fact that in most of the models, OSW-1 interacts with the Chol-containing membrane by forming aggregates that mostly stays in the membrane. The aggregation brought about by the specific Chol/OSW-1 interaction is crucial and is mainly responsible for the observed membrane-permeabilizing property of OSW-1.

References

1. Ohnishi, K., Tachibana, K., Synthesis of pavoninin-1, a shark repellent substance, and its structural analogues toward mechanistic studies on their membrane perturbation, *Bioorg Med Chem.* **1997**, *5*, 2251-2265

2. Hu, M., Konoki, K., Tachibana, K., Cholesterol-independent membrane disruption caused by triterpenoid saponins, *Biochim Biophys Acta.* **1996**, Jan *1299*, 252-258.

3. Bagatolli, L.A., Membrane and fluorescence microscopy, Reviews in Fluorescence, Springer Science, 2007.

4. Munishkina, L.A., Fink, A.L., Fluorescence method to reveal structures and membrane-interactions of amyloidogenic proteins, *Biochim. Biophys. Acta* **2007**, *1768*,1862-1885.

5. Groves, J.T., Parthasarathy, R., Forstner, M.B., Fluorescence imaging of membrane dynamics, *Annual Rev. Biomed. Eng.* **2008**, *10*,311-338.

6. Sezgin, E., Schwille, P., Fluorescence techniques to study lipid dynamics, *Cold Spring Harb Perspect Biol* **2011**, *3*, 1-32.

7. Demchenko, A.P., Mély, Y., Duportail, G., Klymchenko, A.S., Monitoring biophysical properties of lipid membranes by environment-sensitive fluorescent probes, *Biophys. J.* **2009**, *96*, 3461-3470.

8. Ellinger, P., Fluorescence Microscopy in Biology, *Biological Reviews* **1940**, *15*, 323–347.

9. Korlach, J., Schwille, P., Webb, W.W., Feigenson, G.W., Characterization of lipid bilayer phases by confocal microscopy and fluorescence correlation spectroscopy, *Proc. Natl. Acad. Sci. USA* **1999**, *96*, 8461–8466.

10. Bagatolli, L.A., Gratton, E., Two photon fluorescence microscopy of coexisting lipid domains in giant unilamellar vesicles of binary phospholipid mixtures, *Biophys. J.* **2000**, *78*, 290–305.

11. Bagatolli, L.A., Gratton, E., Two-photon fluorescence microscopy observation of shape changes at the phase transition in phospholipid giant unilamellar vesicles, *Biophys. J.* **1999**, *77*, 2090–2101.

12. Kunding, A.H., Mortensen, M.W., Christensen, S.M., Stamou, D., A fluorescence-based technique to construct size distribution from single object measurements, application to the extrusion of lipid vesicles, *Biophys. J.* **2008**, *95*, 1176-1188.

13. Reeves, J.P., Dowben, R.M., Formation and properties of thin-walled phospholipid vesicles, *J. Cell. Physiol.* **1969**, *73*, 49–60.

14. Baumgart, T., Hess, S.T., Webb, W.W., Imaging coexisting fluid domains in biomembranes models coupling curvature and line tension, *Nature* **2003**, *425*, 821–824.

15. Dietrich, C., Bagatolli, L.A., Volovyk, Z.N., Thompson, N.L., Levi, M., Jacobson, K., Gratton, E., Lipid rafts reconstituted in model membranes, *Biophys. J.* **2001**, *80*, 1417–1428.

16. Bagatolli, L.A., Gratton, E., A correlation between lipid domain shape and binary phospholipid mixture composition in free standing bilayers: A two-photon fluorescence microscopy study, *Biophys. J.* **2000**, *79*, 434–447.

17. Kahya, N., Scherfeld, D., Bacia, K., Poolman, B., Schwille, P., Probing lipid mobility of raft exhibiting model membranes by fluorescence correlation spectroscopy, *J. Biol. Chem.* **2003**, *278*, 28109–28115.

18. Bagatolli, L.A., To see or not to see: lateral organization of biological membranes and fluorescence microscopy, *Biochim. Biophys. Acta.* **2006**, *1758*, 1541–1556.

19. Baumgart, T., Hunt, G., Farkas, E.R., Webb, W.W., Feigenson, G.W., Fluorescence probe partitioning between Lo/Ld phases in lipid membranes, *Biochim. Biophys. Acta.* **2007**, *1768*, 2182–2194.

20. Veatch, S.L., Keller, S.L., Seeing spots: complex phase behavior in simple membranes, *Biochim. Biophys. Acta.* **2005**, *1746*, 172–185.

21. Sakurai, K., Takeshita, T., Hiraizumi, M., Yamada, R., Synthesis of OSW-1 derivatives by site-selective acylation and their biological evaluation, *Org. Lett.* **2014**, *16*, 6318–6321.

22. Yamada, R., Takeshita, T., Hiraizumi, M., Shinohe, D., Ohta, Y., Sakurai, K., Fluorescent analog of OSW-1 and its cellular localization, *Bioorganic & Medicinal Chemistry Letters* **2014**, *Volume 24*, 1839-1842.

23. Sudji, I.R., Subbura, Y., Frenkel, N., García-Sáez, A.J., Wink, M., Membrane disintegration caused by the steroid saponin digitonin is related to the presence of cholesterol, *Molecules* **2015**, *20*, 20146-20160.

24. Malabed, R., Hanashima, S., Murata, M., Sakurai, K., Sterol-recognition ability and membrane-disrupting activity of *Ornithogalum saponin* OSW-1 and usual 3-*O*-glycosyl saponins, *BBA - Biomembranes* **2017**, *1859*, 2516–2525.

25. Frenkel, N., Makky, A., Sudji, I.R., Wink, M., Tanaka, M., Mechanistic investigation of interactions between steroidal saponin digitonin and cell membrane models, *J. Phys. Chem.* **2014**, *118*, 14632-14639.

26. Barrow, C.J., Nakanishi, K., Tachibana, K. Structure and activity studies of pardaxin and analogues using model membranes of phosphatidylcholine, *Biochim. Biophys. Acta* **1992**, *1112*, 235-240.

27. Weinstein, J.N., Yoshikami, S., Henkart, P., Blumenthal, R., Hagins, W.A., Liposome-cell interaction: transfer and intracellular release of a trapped fluorescent marker, *Science* **1977**, *195*, 489-492.

28. Sakurai, K., Fukumoto, T., Noguchi, K., Sato, N., Asaka, H., Moriyama, N., Yohda, M., Three dimensional structures of OSW-1 and its congener, *Org. Lett.* **2010**, *12*, 5732-5735.

29. Murata, M., Houdai, T., Morooka, A., Matsumori, N., Oishi, T., Membrane interaction of soyasaponins in association with their antioxidation effects, *Soy Protein Research, Japan* **2005**, *8*, 81-85.

30. van Meer, G., Voelker, D.R., Feigenson, G.W., Membrane lipids: where they are and how they behave, *Nat. Rev. Mol. Cell Biol*. **2008**, *9*, 112–124.

31. Sonnino, S., Prinetti, A., Lipids and membrane lateral organization, *Frontiers in Physiology* **2010**, *1*, 1-9.

32. Karami, L., Jalili S., Effects of cholesterol concentration on the interaction of cytarabine with lipid membranes: a molecular dynamics simulation study, *J Biomol Struct Dyn.* **2015**, *33*, 1254-68.

33. Lorent, J.H., Quetin-Leclercq, J., Mingeot-Leclercq, M.P., The amphiphilic nature of saponins and their effects on artificial and biological membranes and potential consequences for red blood and cancer cells, *Org. Biomol. Chem.* **2014**, *12*, 8803-8822.

34. Lorent, J., Lins, L., Domenech, O., Quetin-Leclercq, J., Brasseur, R., Mingeot-Leclercq, M.P., Domain formation and permeabilization induced by the saponin α-hederin and its aglycone hederagenin in a cholesterol-containing bilayer, *Langmuir* **2014**, *30*, 4556-4569.

Chapter 4

General Discussion and Conclusions

4.1 General Discussion

The elucidation of the atomistic mechanism of cholesterol-dependent membrane activity of saponins was attempted in this study using various spectroscopic and microscopic approaches. This research mainly focused on OSW-1 in comparison with usual 3-*O*-glycosyl saponins including digitonin, soyasaponin Bb(I) and glycyrrhizin. The membrane permeabilizing and disrupting activities of these saponins were assessed using membrane models such as red blood cells and artificially prepared liposomes, which contain various lipid components at a specific molar ratio. Results of the experiments clearly pointed out the dependence of saponins to Chol to induce membrane permeabilization. Several studies have already been conducted on usual 3-*O*-glycosyl saponins pointing out the importance of a sugar moiety attached to C3 of steroidal or triterpenoidal saponins. However, only few studies have been made on saponins with unusual structures such as OSW-1. This saponin is considered unique due to the presence of partially acylated disaccharide moiety attached to C16 of the steroidal sapogenin. Furthermore, its overall triangular shape could account for its potent biological activity. The structural feature of each saponin, such as glycosylation position, size and arrangement of sugar moiety, and the nature of sapogenin ring, suggest difference in the mode of binding to Chol. Apart from these features, the amphiphilic properties and polarity of these saponins could also contribute to the differences in their mode of action. Despite the huge differences in the structure of these saponins, digitonin, soyasaponin Bb(I) and OSW-1 exhibit Chol dependency. However, the strength of membrane activity of OSW-1 is more comparable to digitonin, in which they similarly showed high hemolytic activity and strong permeabilizing properties as revealed by Chol-depletion/repletion and calcein leakage assays, respectively. In addition, the strong binding affinity of OSW-1 towards Chol is also comparable to digitonin, which was suggested by CTL binding and time-course calcein leakage assays. Although in most cases the membrane activity of OSW-1 and digitonin are comparable, difference in the mode of hemolysis could be observed by osmotic protection experiments in such that the hemolytic effect of OSW-1 is likely due to formation of pores, which allow entry of smaller molecules into the cell causing cell lysis. On the other hand, digitonin likely induce hemolysis via direct membrane disruption and/or cholesterol removal in the membrane. This observation could be accounted for by the known detergent property of digitonin. Soyasaponin Bb(I)

similarly induced pore formation prior to hemolysis. Moreover, ^{2}H NMR and ^{31}P NMR showed significant difference between OSW-1 and digitonin. In the ^{2}H NMR experiment, digitonin markedly attenuated the rotational motion of Chol as a consequence of formation of large digitonin/Chol aggregates which immobilizes Chol in membrane. Meanwhile, OSW-1 exhibits a decrease in $\Delta\nu$ probably as a consequence of Chol tilting to maximize interfacial contact between these two molecules. ^{31}P NMR suggests that digitonin induced an increase in membrane curvature and/or vesicle size reduction as indicated by the presence of a broad beak at the origin of the spectra. These changes, however, did not affect the overall morphology of the membrane. On the other hand, OSW-1 did not alter the lamellar structure of the bilayer but a shift in the $\sigma_{\perp}$ value of solid-state ^{31}P NMR was observed, which was attributed to changes in membrane curvature. A similar spectral changes were also manifested by soyasaponin Bb(I) and glycyrrhizin. Based on these observations, soyasaponin Bb(I) has similarities with OSW-1 in terms of mode of action albeit its weaker activity in comparison with other saponins.

Another advantage of this study is the availability of fluorescence probes, which aided on understanding the effect of saponins on membrane morphology using confocal microscopy. It was confirmed that morphological changes observed under a microscope are Chol-dependent but substantial binding to the GUV membrane even in the absence of membrane Chol was also observed without altering the membrane integrity. High amount of saponins directly induced membrane disruption as a consequence of Chol interaction. Although the results of microscopy supports the proposed mechanism of interaction of digitonin, the mechanisms of membrane permeabilization for OSW-1 and soyasaponin Bb(I) were not clearly established at the single vesicle observation. Thus, more thorough experiments should be carried out to establish a reliable mode of membrane permeabilization of the saponins studied.

Basing on the results gathered so far, it is hypothesized that digitonin follows the carpet (or detergent) model due to its known detergent properties, which directly induce membrane disruption and/or cholesterol removal from the membrane core. On the other hand, OSW-1 and soyasaponin Bb(I) shares a similar mechanism of membrane permeabilization in that they form barrel stave-like arrangement in the membrane. This observation could be due to the formation of aggregates with Chol in the membrane. The properties of these saponins may partly account for their reported cytotoxicity by rapid membrane permeability, which enable these saponins access the corresponding target proteins in the cell.

4.2 Conclusions

The unusual structure of OSW-1 has attracted my attention as to whether this large difference could also influence membrane interactions as exhibited by 3-*O*-glycosyl saponins. The fact that most of the naturally occurring saponins of plant and marine origins have exhibited potential pharmaceutical and pharmacological properties, few unique saponins have also shown potential activities especially in cancer research. The data gathered in this research only focused on membrane lipid components as receptors in order for these saponins to manifest their potent activity, although reports mentioned that proteins could also serve as targets to express their activity. This research suggests that OSW-1 and digitonin possess strong hemolytic and liposomal membrane activity attributed to Chol interaction in the membrane. Furthermore, Chol recognition by OSW-1 and digitonin, as well as soyasaponin Bb(I), is important for membrane permeabilization. It was also deduced that OSW-1 and soyasaponin Bb(I) induce membrane permeabilization likely via pore formation in contrast to digitonin, which causes direct membrane lysis via membrane disruption mechanism. Despite of the previous and present results, the concrete mechanism of action of OSW-1 and other saponins with membranes have not been fully elucidated. The proposed mechanism of interaction of OSW-1 can be investigated by future results that might also give a more reliable understanding of its activity. Continuous efforts are being carried out, especially on the conformation of OSW-1 upon binding with membrane Chol by spectroscopic techniques.

Chapter 5

Experimental Section

5.1 Materials

All phospholipids, 1-palmitoyl-2-oleoyl-*sn*-glycero-3-phosphocholine (POPC), 1,2-dimyristoyl-*sn*-glycero-3-phosphocholine (DMPC), and dioleoyl-*sn*-glycero-3-phosphocholine (DOPC) were purchased from Avanti Polar Lipids, Inc. (Alabaster, AL, USA). Cholesterol (Chol) and rhodamine 6G were purchased from Sigma-Aldrich (St. Louis, MO, USA). Ergosterol (Erg) and 3-epicholesterol (Epichol) were purchased from Tokyo Kasei (Tokyo, Japan), and Steraloids (Newport, RI, USA), respectively. Osmotic protectants purchased from Nacalai Tesque (Kyoto, Japan) including glucose, sucrose, raffinose, PEGs 600, 1000, 1540, 2000, 4000 and 6000, were also utilized in this study. Cholesterol-*d* was synthesized according to a previous report.[1] Digitonin, glycyrrhizin, diosgenin, phospholipid C, and cholesterol E test kits were obtained from Wako (Osaka, Japan). Soyasaponin Bb(I) was purified from commercially available soybean saponin, Soy Health SA (Fuji Oil Company Ltd., Tokyo, Japan). Calcein, methyl-β-cyclodextrin (MβCD), verapamil, theophylline, glucose, sucrose, raffinose, and polyethylene glycol (PEG) were purchased from Nacalai Tesque (Kyoto, Japan). The 96-well microplates were purchased from Greener Bio One (Monroe, NC, USA) and Thermo Scientific (Waltham, MA, USA). TR-DPPE and DiI were obtained from Molecular Probes Thermo Fisher Scientific (Waltham, MA, USA). OSW-1 was isolated from the bulbs of *Ornithogalum saundersiae* and purified by HPLC, as previously reported by Kubo et al.[2] Cholestatrienol (CTL) was generously provided by Prof. J Peter Slotte (Åbo Akademi University, Turku, Finland), prepared using a previously published method.[3] All other chemicals used are of standard and analytical quality.

5.2 Instrumentation

The following instruments were used in the course of this study including the brand and the model description:

HPLC	Shimadzu SCL-10AVP
	Hitachi L-7405
UV Spectrophotometer	Shimadzu UV-2500

Fluorescence Spectrofluorometer	Jasco FP-6500
Microplate Reader	Corona Electric Multimode (MTP-800)
Mass Spectrometer	Thermo Scientific LTQ OrbiTrap XL
NMR Spectrometer	JEOL ECA400WB JEOL ECS400 and ECA500 CMX300
Fluorescence Microscope	Olympus FluoView^{TM} FV-1000D
DLS Particle Analyzer	HORIBA LB-550
Lyophilizer	EYELA FDU-1200
Polycarbonate Extruder	LiposoFast Basic (200 nm and 100 nm pore size)

Other instruments used include rotary evaporator, analytical balance, sonicator, vortex mixer, incubator, centrifuge, thermostat and

5.3 Experimental Methods

5.3.1 Calcein leakage assays

The ability of saponins to induce leakage in large unilamellar vesicles (LUVs) was determined by measuring the intensity of calcein. Similarly, time-dependent calcein leakage was done on calcein-loaded LUVs.[4] LUVs were prepared using POPC and various sterols. Pure POPC, 9:1 POPC/Chol, POPC/Erg, and POPC/Epichol were dissolved in chloroform in a round-bottom flask. The solution was dried under reduced pressure at 35 °C and further dried overnight *in vacuo*. The lipid film was resuspended in 60 mM calcein (1 mL) in 10 mM Tris-HCl buffer containing 150 mM NaCl and 1 mM EDTA at pH 7.4 and was mixed using vortex for 1 min. Five cycles of freezing (−20 °C) and thawing (65 °C) were done to produce multilamellar vesicles (MLVs). The MLVs were subjected to extrusion using through LiposoFast Basic extruder (pore size, 200 nm, Avestin Inc., Ottawa, Canada) 19 times to obtain homogeneous LUVs. Excess calcein was removed using Sepharose 4B column (GE Healthcare, Uppsala, Sweden). The lipid and Chol concentrations of the LUV fraction were quantified using the phospholipid C test and cholesterol E test kits, respectively. The final concentrations of the phospholipid and Chol in the resulting LUVs were adjusted depending

on the measurements to be conducted. LUVs were immediately used for measurement to prevent premature vesicle leakage. A 96-well Nunclon Delta Surface (black) F-bottom microplate (Thermo Scientific) used and the initial fluorescence was measured using MTP-800 series, Corona Electric Multimode Microplate Reader at an excitation wavelength of 490 nm and an emission wavelength of 517 nm. Saponins were added to the LUVs, which were mixed at a slow speed for 1 min and were allowed to stand at room temperature for 2 h prior to fluorescent measurement after saponin-induced leakage. 10% Triton-X was added to the mixture to obtain condition of 100% leakage. In the time-course calcein leakage assays, the measurements were carried out using Jasco FP-6500 fluorescence spectrofluorometer. The sample was continuously mixed using a magnetic stirrer and fluorescence was stabilized for 2 min. Saponin was added and fluorescence changes were observed for a total of 10 min. After which, Triton-X was added for the 100% leakage conditions. The % calcein leakage was calculated using the equation:

$$\% \text{ calcein leakage} = \frac{I_S - I_0}{I_T - I_0} \times 100$$

where I_S, I_T, and I_0 are the fluorescence intensities after saponin addition, at 100% LUV leakage, and background, respectively.

5.3.2 Parallel artificial membrane permeation assay (PAMPA)

The absorption of saponins by passive diffusion was determined using parallel artificial membrane permeation assay (PAMPA).[5] A 96-well MultiScreen-IP Acrylic PAMPA plate (Merck Millipore, Germany) with polyvinylidene fluoride membrane (PVDF; pore size, 0.45 μm) was covered with lipid mixtures (POPC, 9:1 POPC/Chol, 1:1 DMPC/DOPC, 2:2:1 DMPC/DOPC/Chol) and was dried for 1 h. while waiting for the complete drying of the lipid layers, test samples were mixed with 10 mM PBS at pH 7.4 to a total volume of 200 μL. The donor wells were filled with the sample solution, and the acceptor wells were filled with 200 μL PBS (pH 7.4), and was sandwiched (Fig. 5-1) to allow the permeation process to proceed for 18 h. The final absorbance of the samples in both plates was measured after the permeation has been completed.[5,6] The experiments were performed in triplicate. Verapamil was used as a high-permeability standard, while theophylline was used as a low-permeability standard. The effective permeability, $\boldsymbol{P_e}$, was calculated using the equation.[7]

$$P_e = -2.303 \frac{V_a V_d}{(V_a+V_d)A(t - t_0)} log\left(1 - \frac{(V_a+V_d)C_a(t)}{V_d S C_d(0)}\right)$$

where V_d and V_a are the volume of donor and acceptor well (cm^3), A is the effective area of membrane (cm^2), t is permeation time (s), $C_a(t)$ and $C_d(0)$ are the concentration (mol/cm^3)of the acceptor well at time t and initial concentration of the donor well, respectively.

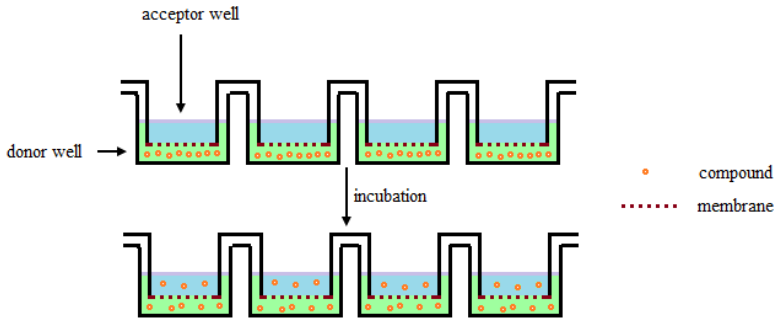

Figure 5-1. PAMPA sandwich set-up

Calcium influx experiment to assess entry of calcium ions through the membrane

The mechanism of permeation of saponins was determined by calcium influx assays. Calcium does not permeate through membrane due to its radius. Calcium can only enter to the cytoplasm by means of pores which size is enough to allow its entry. In this experiment, presence of calcium in the acceptor well indicates entry of calcium through the membrane due to saponin-cholesterol interaction. Membrane deformations could possibly be pores or areas where loss of membrane material occurred.

A simple method for the determination of calcium concentration in the donor and acceptor wells was employed.[8] Calcein was used to detect the presence of calcein. Permeation of calcium carbonate ($CaCO_3$) in PBS with an initial concentration of 3.5 µg/mL per well was monitored using the same PAMPA set up for 18 h. A solution of 100 µL of 5 µM calcein was added to each well followed by careful mixing. The absorbance of the solution per well was read using a microplate reader at 506 nm, and the calcium concentration in the donor and acceptor wells were quantified using a standard curve generated by measuring the absorbance of standard $CaCO_3$ solution with concentrations ranging from 0.5 to 3.5 µg/mL.

Phospholipid C-test

To determine loss of membrane material, the phospholipid content in the acceptor wells was quantified using a commercially available phospholipid C test kit (Wako). A 3 μL solution of phospholipid standard and sample were place into assigned wells using a 96-well polystyrene F-bottom clear microplate (Greener Bio One). A 300 μL of color reagent solution was added to each well followed by incubation at 37 °C for 10 minutes. The absorbance of the solution for each well was measured using a microplate reader at 595 nm and the phospholipid concentration was calculated.

5.3.3 Hemolytic activity under Chol depletion conditions and osmotic protection

Chol depletion/repletion experiment was done in order to determine the effect of Chol in the saponin-induced hemolysis.[9] Human blood samples were collected on the day of the experiment. The blood was washed with 10 mM phosphate buffered saline (PBS) at pH 7.4 and was mixed using vortex. The solution was centrifuged for 5 min at 2000 rpm and the supernatant was carefully discarded. The pellet was resuspended in PBS and labelled as 10% (v/v) red blood cell (RBC) solution. The 10% RBS was divided into three portions. The first portion was mixed with PBS to obtain 1% non-depleted RBC solution. The second portion was incubated with 3.5 mM methyl-β-cyclodextrin (MβCD) at 37 °C for 2 h followed by centrifugation and resuspension in PBS to obtain Chol-depleted red blood cells 1% (v/v) solution. The last portion was treated similarly as the second portion but cells were treated with 7:1 mole ratio of Chol/MβCD at 37 °C for 2 h to restore Chol in the cell membrane. The samples were centrifuged and resuspended in PBS to obtain 1% (v/v) Chol-repleted solution.[10,11]

The cells were seeded into a 96-well microplate and saponins were added to the assigned wells, followed by mixing at moderate speed. The samples were incubated for 18 h at 37 °C followed by centrifugation at 2000 rpm for 5 min. The absorbance of the supernatant was measured at 450 nm using a microplate reader (Corona Electric). A mixture of milliQ water/10% RBC (v/v; 9:1 volume ratio) was used as a positive control, and 1% (v/v) RBC/PBS (18:1 volume ratio) was used as the blank. Triplicate samples were prepared for each saponin concentration. Hemolysis was calculated:

$$\%\ \text{hemolysis} = \frac{A_{sample} - A_{blank}}{A_{positive\ control}} \times 100$$

In addition, osmotic protection experiments under the conditions of hemolysis assays were conducted to estimate the size of pore or channels formed by saponin in lipid bilayers. Red blood cells (RBC, 1% v/v) were prepared as described earlier. Osmotic protectants such as glucose, sucrose, raffinose, PEGs 600, 1000, 1540, 2000, 4000 and 6000, which has estimated molecular size of 0.7, 0.9, 1.1, 1.6, 2.0, 2.4, 2.9, 3.8 and 5.1 nm, respectively, were used in this experiment. Osmotic protectants (30 mM) were added to the RBC solution prior to addition of saponin samples. Amphotericin B, which pore size have been previously reported, was used as control.[12] A rough estimate of the size of the pore or channel can be determined by the size of the protecting agents in which the first significant hemolytic activity is observed. The measurement of saponin-induced hemolytic activity in the presence of various osmotic protectants was done using a microplate reader (Corona Electric) at 450 nm.

5.3.4 CTL fluorescence spectroscopy

The effect of saponins to binding with Chol was determined using a close analog of Chol called cholestatrienol (CTL).[13] The experiment was done in both aqueous and bilayer environment. In aqueous environment, saponins were added to the CTL solutions (4 μg/mL) in 10 mM PBS at pH 7.4, containing 0.1% dimethyl sulfoxide (DMSO) and were incubated at 25 °C for 3 h. On the other hand, in the bilayer environment, CTL was incorporated in LUVs together with Chol. LUVs composed of 90:9:1 POPC/Chol/CTL were prepared by dissolving the lipid mixture in $CHCl_3$, followed by sonication for 1 min. The solvent was dried under reduced pressure and further dried *in vacuo*. The lipid film was rehydrated with 10 mM PBS at pH 7.4, followed by five cycles of freezing (−20 °C) and thawing (65 °C) to obtain the MLVs. To obtain homogeneous LUVs with size of approximately 200 nm, the MLVs were extruded using LiposoFast Basic extruder. The LUV components, POPC, Chol, and CTL were quantified using commercially available test kits referred to as phospholipid C test, cholesterol E test and the CTL UV extinction coefficient at 325 nm (11,000 cm^{-1} M^{-1}), respectively. Various saponin concentration was mixed with the LUVs and was incubated at 25 °C for 3 h. The fluorescence emission of the assay mixture was measured using FP 6500 spectrofluorometer (Jasco Corp., Tokyo, Japan) at 25 °C at an excitation wavelength of 325 nm (5.0-nm slit width) and was scanned at an emission wavelength from 340 nm to 450 nm (1.0-nm slit width). The fluorescence intensity was recorded as a function of emission wavelength.

5.3.5 Dynamic light scattering

Dynamic light scattering (DLS) experiments were performed to determine the effect of saponins on vesicle size. LUVs composed of pure POPC and 9:1 POPC/Chol were prepared as described earlier in the CTL fluorescence assay, with the omission of CTL addition. Saponins with varying concentrations were mixed with the LUVs and were incubated at 25 °C for 3 h. The resultant vesicle size was measured using a dynamic light scattering particle analyzer LB-550 (HORIBA, Ltd. Kyoto, Japan) at 25 °C.

5.3.6 Solid-state ^{2}H NMR

Membrane samples for solid state ^{2}H NMR, composed of various lipid combinations were used for the study of saponins.[14] The lipid mixture was dissolved in 2:1 (v/v) $CHCl_3$/MeOH in a round-bottom flask. The lipid was dried under reduced pressure and further dried overnight *in vacuo*. The lipid film was rehydrated with milliQ water followed by sonication and vortex mixing at 1 min each. The samples were subjected to three cycles of freezing (−20 °C) and thawing (65 °C) to obtain the MLVs. The MLV suspension was lyophilized overnight and rehydrated with deuterium-depleted water (50% hydration). The suspension was homogenized by a cycle of vortex mixing, freezing, and thawing, followed by centrifugation for 5 min at 2000 rpm. The resulting lipid was carefully transferred into a 5-mm glass tube and sealed with epoxy glue. The quadrupolar splitting in liposome is shown as follows:

$$\Delta\nu = \frac{3}{4} Q \times S_{\mathrm{mol}} \times \frac{3\cos^2\theta - 1}{2}$$

where Q is quadrupolar coupling constant, S_{mol} is the order parameter, and θ is the angle between C—D vector and bilayer normal.

All ^{2}H NMR spectra were recorded with a 300 MHz spectrometer (CMX-300, Agilent, Palo Alto, CA, USA) equipped with a 5 mm ^{2}H static probe (Otsuka Electronics, Osaka, Japan) using a quadrupolar echo sequence. The 90° pulse width was 2.5 μs, the interpulse delay was 30 μs, echo delay was 20 μs, and the repetition delay was 0.6 s. The sweep width was 250 kHz covered with 8192 points, and the number of scans ranged from 100,000 to 300,000. The probe

temperature was set at 30 °C. Spectra were processed using Delta NMR Software (Jeol USA, Inc., Peabody, MA, USA), and the plot was generated using Microsoft Excel Software.

5.3.7 Solid-state ^{31}P NMR

Similarly, ^{31}P NMR was done on the membranes previously prepared. The spectra were recorded on a 400 MHz ECA400 (Jeol USA, Inc.) using a 7 mm CP-MAS probe (Doty Scientific, Inc., Columbia, SC, USA) at 30 °C. A single pulse sequence with proton decoupling was employed with the following parameters: acquisition time was 18 ms, 90° pulse width was 7.2 μs, and relaxation delay was 2 s. The sweep width was 113 kHz covered with 8192 points, and the total number of transients per sample was 10,000 to 40,000. All ^{31}P NMR spectra were referenced based on the ^{31}P peak of 85% phosphoric acid (H_3PO_4) standard set at 0 ppm, measured under the same conditions

5.3.8 Fluorescence microscopy

The ability of saponins to induced morphological changes in GUVs was determined using fluorescence microscopy. Giant unilamellar vesicles (GUV) composed of various lipids and Chol were prepared via electroformation method as previously reported.[15] Lipids (1 mg/mL) were dissolved in $CHCl_3$ and were mixed with either Texas Red-DPPE or DiI. The lipid mixture was dried in a glass slide assembled with parallel aligned platinum wires (φ = 100 μm) overnight. Lipids were then enclosed using cut rubber (Fig. 5-2) and rehydrated with milliQ water or sucrose (300 mM) while keeping the wires immersed. The slide was sandwiched by another glass slide and was placed on a temperature-controlled heating mantle. The electroformation was done by applying sinusoidal AC at 10 V and 10 Hz for 50 min at 40 °C, followed by cooling down for 30 min at 25 °C. GUVs were viewed using FluoView FV1000-D scanning unit at an IX81 inverted microscope (Olympus Corp., Tokyo, Japan). A PLAPON 60X universal semiapochromat objective with NA of 1.40 was used for microscopic observations. Acquisition speed was set at 8 μs/pixel and images were captured with FV10-ASW-3.0 software. The sample temperature was kept at 37 ºC for all observations using temperature control objective plate. The effect of various saponins and DBD-OSW-1 was monitored by observing changes in the integrity of the GUVs. In the non-labelled saponins, rhodamine 6G was solubilized in the GUV suspension to make the extravesicular solution fluorescent.

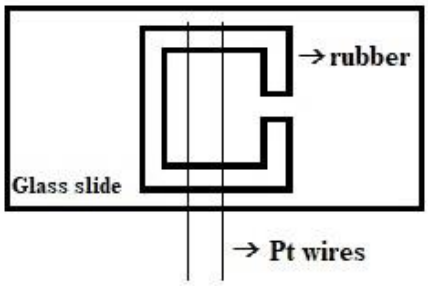

Figure 5-2. Glass slide set-up for electroformation of GUVs

5.3.9 Synthesis of Chol-*d*

Chol-*d* (**3**) was synthesized as previously described ad as shown in Scheme 5-1.[1] Chol (**1**) was dissolved in in CH_2Cl_2 and was subjected to oxidation using pyridinium chlorochromate (PCC) under Ar gas to afford 5-cholesten-3-one (**2**). The desired product was purified by column chromatography using 10:1 hexane/ethyl acetate (H/A) as eluting solvent. The purity was checked by thin layer chromatography (TLC, 4:1 H/A) and characterization was done by ^{1}H NMR (Appendix Fig. 2).

In order to obtain Chol-*d* (**3**), **2** was dissolved in 2:1 MeOH/$CHCl_3$. Sodium borodeuteride ($NABD_4$) in $CeCl_3 \bullet 7H_2O$ was added to allow reduction. The desired product was purified using 4:1 MeOH/CH_2Cl_2 and purity was checked by TLC (4:1 H/A) and characterized by ^{1}H NMR (Appendix Fig. 3). The product (**3**) was kept in solution (dissolved in $CHCl_3$) and was stored at 4 °C prior to usage.

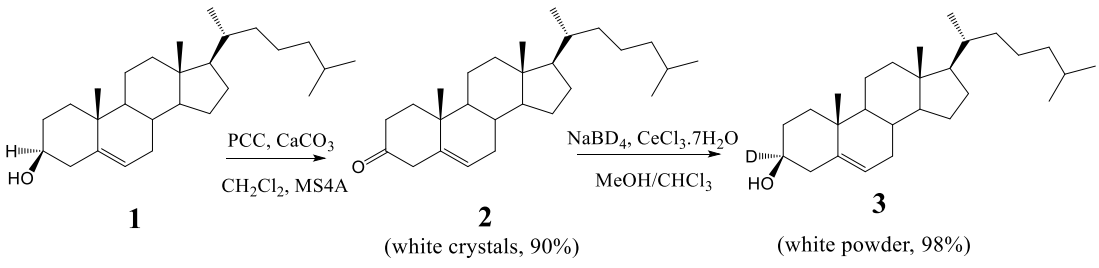

Scheme 5-1. Synthesis of Chol-*d*[1]

References

1. Murari, R., Murari, M.P., Baumann, W.J., Sterol orientations in phosphatidylcholine liposomes as determined by deuterium NMR, *Biochemistry* **1986**, *25*, 1062-1067.

2. Kubo, S., Mimaki, Y., Terao, M., Sashida, Y., Nikaido, T., Ohmoto, T., Acylated cholestane glycosides from the bulbs of Ornithogalum saundersiae, *Phytochemistry* **1992**, *31*, 3969-3973.

3. Fischer, R.T., Stephenson, F.A., Shafiee, A., Schroeder, F., delta 5,7,9(11)-Cholestatrien-3 beta-ol: a fluorescent cholesterol analogue, *Chem. Phys. Lipids* **1984**, *36*, 1-14.

4. Morsy, N., Houdai, T., Konoki, K., Matsumori, N., Oishi, T., Murata, M. Effects of lipid constituents on membrane-permeabilizing activity of amphidinols. *Bioorg. Med. Chem.* **2008**, *16*, 3084-3090.

5. Kansy, M., Senner, F., Gubernator, K., Physicochemical high throughput screening: parallel artificial membrane permeability assay in the description of passive absorption processes, J. *Med. Chem.* **1998**, *41*, 1007-1010.

6. Kerns, E.H., Di, L., Petusky, S., Farris, M., Ley, R., Jupp, P., Combined application of parallel artificial membrane permeability assay and Caco-2 permeability assays in drug discovery, *J Pharm Sci.* **2004**, *93*, 1440-1453.

7. Avdeef, A., Strafford, M., Block, E., Balogh, M.P., Chambliss, W., Khan, I., Drug absorption in vitro model: filter-immobilized artificial membranes: Studies of the permeability properties of lactones in *Piper methysticum* Forst., *Eur. J. Pharm. Sci.* 2001, *14*, 271–280.

8. Robinson, C., Weatherell, J.A., The micro determination of calcium in mammalian hard tissues, *Analyst* **1968**, *93*, 722-728.

9. Lorent, J., Le Duff, C.S., Quetin-Leclercq, J., Mingeot-Leclercq, M.P., Induction of highly curved structures in relation to membrane permeabilization and budding by the triterpenoid saponins, α- and δ-Hederin, *J. Biol. Chem.* **2013**, *288*, 14000-14017.

10. Bignami, G.S., A rapid and sensitive hemolysis neutralization assay for palytoxin, *Toxicon* **1993**, *31*, 817-820.

11. Giddings, K.S., Johnson, A.E., Tweten, R.K., Redefining cholesterol's role in the mechanism of the cholesterol-dependent cytolysins, *PNAS* **2003**, *100*, 11315 -11320.

12. Houdai, T., Matsuoka, S., Matsumori, N., Murata, M., Membrane-permeabilizing activities of amphidinol 3, polyene-polyhydroxy antifungal from a marine dinoflagellate, *Biochimica et Biophysica Acta (BBA) – Biomembranes* **2004**, *1667*, 91-100.

13. Lorent, J., Lins, L., Domenech, O., Quetin-Leclercq, J., Brasseur, R., Mingeot-Leclercq, M.P., Domain formation and permeabilization induced by the saponin α-hederin and its aglycone hederagenin in a cholesterol-containing bilayer, *Langmuir* **2014**, *30*, 4556-4569.

14. Espiritu, R.A., Matsumori, N., Tsuda, M., Murata, M., Direct and stereospecific interaction of amphidinol 3 with sterol in lipid bilayers, *Biochemistry* **2014**, *53*, 3287-3293.

15. Espiritu, R.A., Cornelio, K., Kinoshita, M., Matsumori, N., Murata, M., Nishimura, S., Kakeya, H., Yoshida, M., Matsunaga, S., Marine sponge cyclic peptide theonellamide A disrupts lipid bilayer integrity without forming distinct membrane pores, *Biochimica et Biophysica Acta* **2016**, *1858*, 1373–1379.

Supporting Information I

Sterol recognition and membrane-permeabilizing activity of saponins deduced from spectroscopic evidences

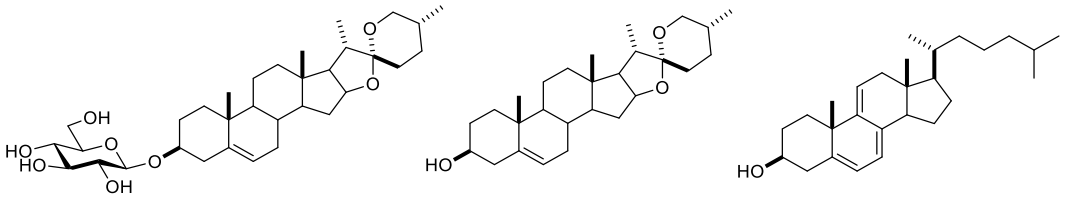

Trillin Diosgenin Cholestatrienol (CTL)

Figure S1-1. Structures of trillin, diosgenin, and cholestatrienol.

Results

PAMPA, calcium influx and phospholipid quantification

PAMPA was used to evaluate the ability of saponins to permeate the membranes by a passive diffusion mechanism.[1-3] Artificial membranes mainly composed of pure phospholipids or with added Chol, were layered on built-in PVDF membranes in the acceptor plate. The permeation rate of saponins into the membrane was measured by the effective permeability (**P_e**) of the compound in comparison with the **P_e** values obtained for both verapamil (high-permeability standard) and theophylline (low-permeability standard).[2] The experiment suggests that the permeation of saponins into the membrane requires Chol, which was highlighted in digitonin and OSW-1 (Table S1-1). Chol significantly contributed to an increase in the **P_e** values of digitonin, OSW-1, and soyasaponin Bb(I), in comparison to the values obtained for membranes in the absence of Chol. However, it is not clearly established whether this process could be accounted by permeation via partitioning of saponins from the bilayer phase to the aqueous phase as observed in the abrupt increase in the **P_e** values. The interaction of saponins with Chol in the artificial membrane could also reflect the observed increase in **P_e** values, as a consequence of pore formation or presence of voids in the membrane, which allows

a rapid transport of saponins from the donor wells to the acceptor wells. In contrast to the other saponins, glycyrrhizin showed low permeability regardless of the type of membrane used.

Table S1-1. Permeation by saponins in various artificial membrane models

Test Sample	Concentration per well	Effective Permeability, $\mathbf{P_e}$ (10^{-6} cm/s)			
		POPC	9:1 POPC/Chol	1:1 DMPC/DOPC	2:2:1 DMPC/DOPC/Chol
OSW-1	1.0 μM	0.43 ± 0.13	1.37 ± 0.60	0.42 ± 0.06	1.83 ± 0.08
Digitonin	1.0 μM	0.40 ± 0.01	1.07 ± 0.28	0.47 ± 0.11	1.60 ± 0.04
Soyasaponin Bb (I)	3.0 μM	0.71 ± 0.13	2.40 ± 0.67	0.92 ± 0.31	3.88 ± 0.48
Glycyrrhizin	3.0 μM	0.79 ± 0.17	0.88 ± 0.04	0.88 ± 0.29	1.05 ± 0.23
Verapamil*	25 μg/mL	16.57 ± 4.18	10.51 ± 1.88	13.52 ± 4.09	8.66 ± 3.52
Theophylline**	25 μg/mL	0.47 ± 0.32	0.40 ± 0.23	0.69 ± 0.45	0.53 ± 0.29

*positive standard; **negative standard

Additionally, determination of calcium influx was carried out to clarify whether saponin-Chol interaction induce the formation of membrane defects which allowed entry of saponins into the membrane. The fluorescence intensity of calcein directly reflects the amount of calcium, which entered through membrane voids and deformations.[4] A rapid entry of calcium into the membrane was detected upon addition of saponin concentrations of 3 μM and higher, which could suggest a possible pore formation or membrane disruption mechanism (Table S1-2).

Table S1-2. Influx of calcium in various membrane models

Test Sample (25 μg/mL per well)	Calcium Concentration (μg/mL)			
	POPC	9:1 POPC/Chol	1:1 DMPC/DOPC	2:2:1 DMPC/DOPC/Chol
OSW-1	-	1.39 ± 0.03	-	1.51 ± 0.01
Digitonin	-	1.35 ± 0.02	-	1.47 ± 0.01
Soyasaponin Bb (I)	-	1.34 ± 0.04	-	1.43 ± 0.03
Glycyrrhizin	-	-	-	-
Verapamil	-	-	-	-
Theophylline	-	-	-	-

Notes: (-) indicates that calcium ions were not detected in the acceptor wells.

Initial concentration of calcium in the donor wells was 3.5 μg/mL.

Furthermore, the amount of free phospholipids was determined to assess the effect of various saponins on the integrity of the membrane. Significant amounts of phospholipids were detected in the Chol-containing wells upon addition of at concentrations of 3 μM or higher, (Table S1-3). The detectable amount of phospholipids observed could be a result of membrane rearrangement likely due to rapid pore formation or loss of membrane material.

Table S1-3. Determination of the presence of phospholipids in the acceptor wells

Test Sample (25 μg/mL per well)	Phospholipid Concentration (μg/mL)			
	POPC	9:1 POPC/Chol	1:1 DMPC/DOPC	2:2:1 DMPC/DOPC/Chol
OSW-1	0.44 ± 0.10	105 ± 4.0	0.38 ± 0.10	114 ± 6.0
Digitonin	0.67 ± 0.18	111 ± 5.4	0.55 ± 0.09	107 ± 4.8
Soyasaponin Bb (I)	0.57 ± 0.18	45 ± 1.9	0.38 ± 0.17	36 ± 1.6
Glycyrrhizin	0.63 ± 0.14	0.37 ± 0.04	0.61 ± 0.17	0.49 ± 0.02
Verapamil	0.34 ± 0.07	0.34 ± 0.10	0.29 ± 0.15	0.24 ± 0.07
Theophylline	0.35 ± 0.10	0.33 ± 0.15	0.28 ± 0.07	0.41 ± 0.01

Note: Final Lipid Concentration = 400 μg/mL per well

The results of the assays conducted to assess permeation of saponins exhibited a concentration-dependent mechanism for the entry of the saponins through the bilayer. The permeation of saponins is greatly affected by the presence of Chol in the membrane. At lower saponin concentration, the permeation process was found to be slower, likely due to the passive diffusion by partitioning through the bilayer to the aqueous phase.[5] On the other hand, at higher saponin concentration, the mechanism could possibly be due to rapid permeation of saponins brought about by the formation of pores or voids larger than the molecular size of the saponins, due to the strong interaction of saponins with membrane sterol. Collectively, these results supported earlier hypothesis suggesting that the membrane composition and saponin concentration plays a major role in the membrane permeabilization process.

DLS spectroscopy

Dynamic light scattering (DLS) spectroscopy was additionally carried out to assess the size of the liposomes before and after addition of saponins (Table S1-4 and Fig. S1-3). Change in vesicle size was observed in pure POPC liposomes and Chol-containing liposomes. The size of the vesicles was found to significantly decrease in addition of 30 μM OSW-1 (Table S1-4). A similar size reduction was observed for digitonin, while in soyasaponin Bb(I), a marginal size reduction was only observed even after the addition of 100 μM concentration, in comparison with OSW-1 and digitonin. These results strongly suggest that the presence of Chol in the membrane induces vesicle size reduction mainly influenced by saponin-Chol interaction. On the other hand, an insignificant change in vesicle size was observed with the addition of glycyrrhizin (Table S1-4). Furthermore, presence of small particles with an average size of ~7 nm for digitonin and ~12 nm for OSW-1 could possibly be attributed to the formation of mixed aggregates composed of Chol, saponin, and phospholipids.[6-8] The formation of pure saponin micelles could also possibly account for the observed average particle size.

Table S1-4. Effect of saponin on size of LUVs (9:1 POPC/Chol)

	Average particle size (nm)		
Saponin	Control (0 μM)	30 μM	100 μM
OSW-1	197.6	126.4	11.9
Digitonin	220.4	127.2	7.3
Soyasaponin Bb(I)	212.8	181.8	127.8
Glycyrrhizin	207.8	207.1	180.6

Notes: The final concentration of POPC and Chol were 129 μM and 16 μM, respectively

A

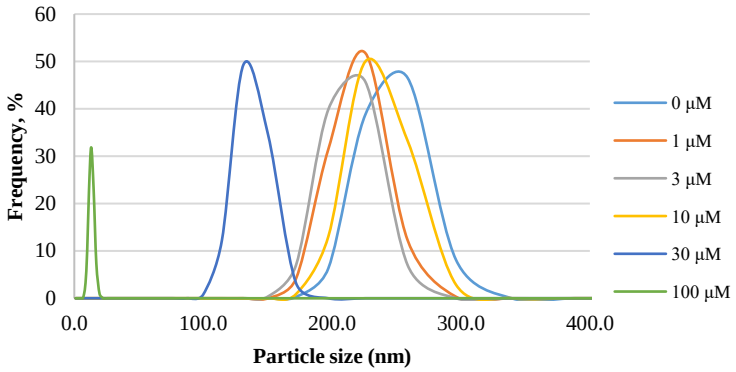
60
50
40
30
20
10
0
Frequency, %
0.0
100.0
200.0
300.0
400.0
Particle size (nm)
0 µM
1 µM
3 µM
10 µM
30 µM
100 µM

B

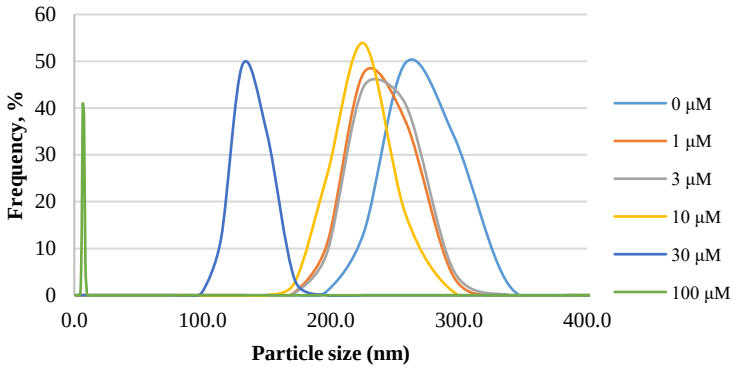
60
50
40
30
20
10
0
Frequency, %
0.0
100.0
200.0
300.0
400.0
Particle size (nm)
0 µM
1 µM
3 µM
10 µM
30 µM
100 µM

C

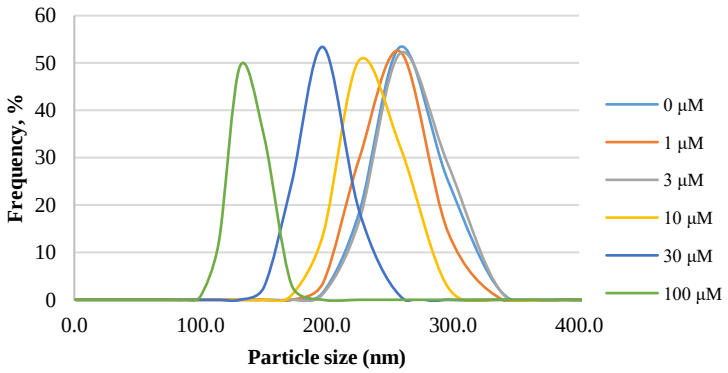
60
50
40
30
20
10
0
Frequency, %
0.0
100.0
200.0
300.0
400.0
Particle size (nm)
0 µM
1 µM
3 µM
10 µM
30 µM
100 µM

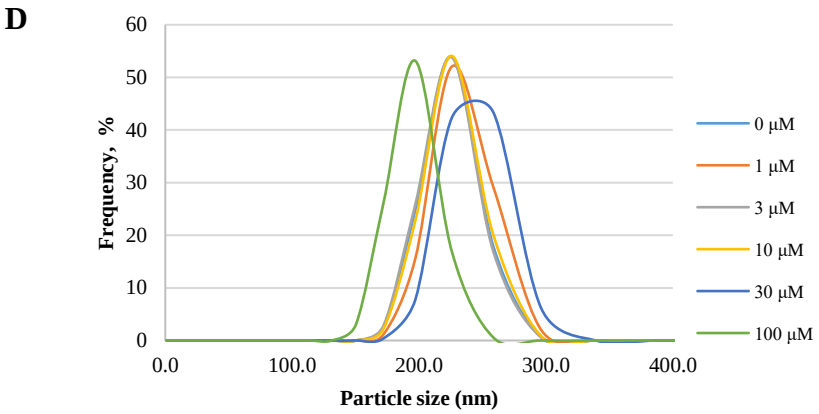

Figure S1-2. Average size of cholesterol-containing liposomes after incubation with various concentrations of OSW-1 (**A**), digitonin (**B**), soyasaponin Bb(I) (**C**), and glycyrrhizin (**D**)

^{2}H NMR spectroscopy

Previously, we discussed that soyasaponin Bb(I) exerts a marginal reduction in the $\Delta\nu$ value comparable with that of OSW-1 and glycyrrhizin at a ratio of 1:0.5 Chol-*d*/saponin (Fig. S1-3**A**). This was attributed to the direct formation of saponin/Chol aggregates that largely stay in the membrane. However, an increase in the amount of soyasaponin, i.e. 1:1 Chol/saponin, induced a significant change in the appearance of the spectra as the Pake doublet signals were significantly attenuated (Fig. S1-3**B**). This could also be accounted by the formation of Chol-*d*/soyasaponin Bb(I) aggregates that are separated from the membrane. The presence of this large aggregated species significantly reduced the motion of Chol-*d* in the same manner with digitonin.[9,10] Moreover, the observed direct interaction between saponin and Chol-*d* is dependent on saponin concentration as a remarkable change was observed when the Chol-*d*/saponin ratio was increased. Likewise, digitonin did not show a significant attenuation of signals at a 1:0.1 Chol-*d*/digitonin ratio (Fig. S1-3**C**).

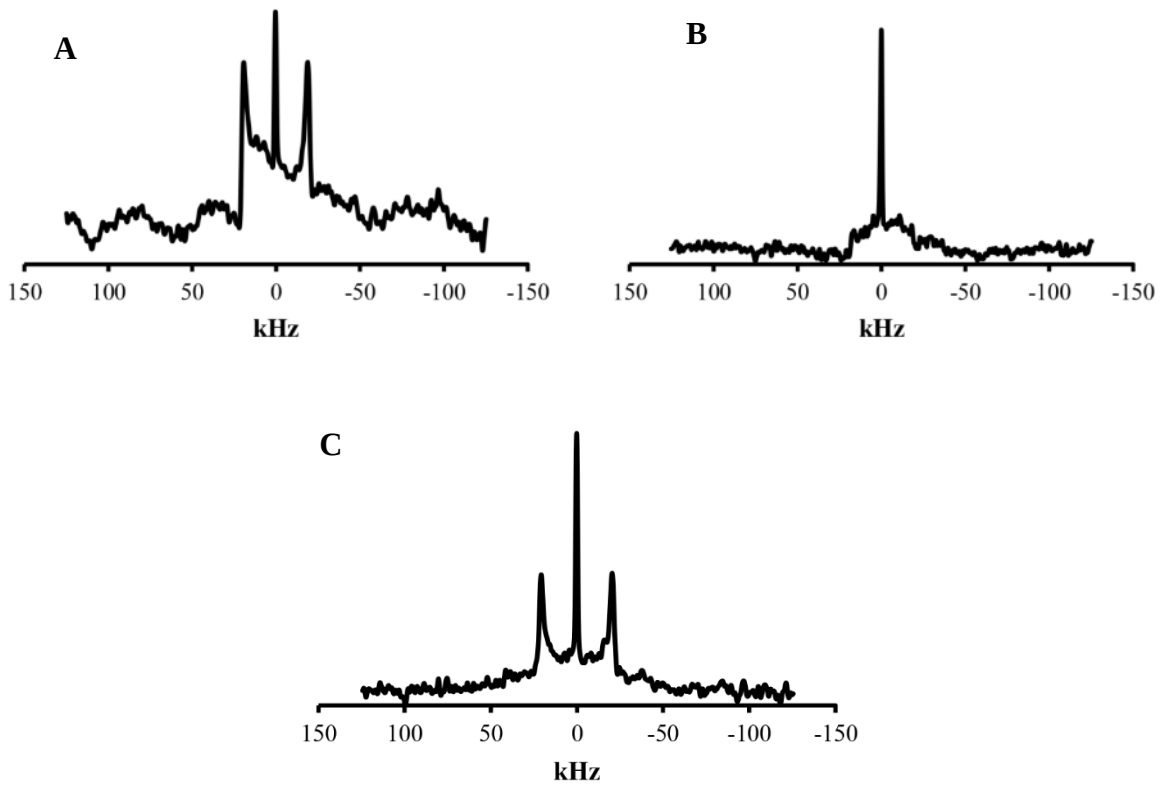

Figure S1-3. ^{2}H NMR spectra of Chol-d in POPC bilayer in the presence of soyasaponin Bb(I) at a molar Chol/saponin ratio of 1:0.5 with the $\Delta\nu$ value of 39.0 kHz (**A**), and at a molar Chol/saponin ratio of 1:1 with the $\Delta\nu$ value of approximately 0 kHz (**B**). ^{2}H NMR spectra of Chol-d in a POPC bilayer in the presence of digitonin at a molar Chol/saponin ratio of 1:0.1 with the $\Delta\nu$ value of 41.2 kHz (**C**). ^{2}H NMR spectra were recorded at 30 °C.

^{31}P NMR spectroscopy

We also clearly established that the interaction of saponins into the membrane did not induce significant morphological changes rather a change in the membrane curvature or vesicle reduction is elicited. This was observed at all saponin concentration tested owing that the interaction between saponin and Chol does not greatly influence the overall membrane morphology (Fig. S1-4).

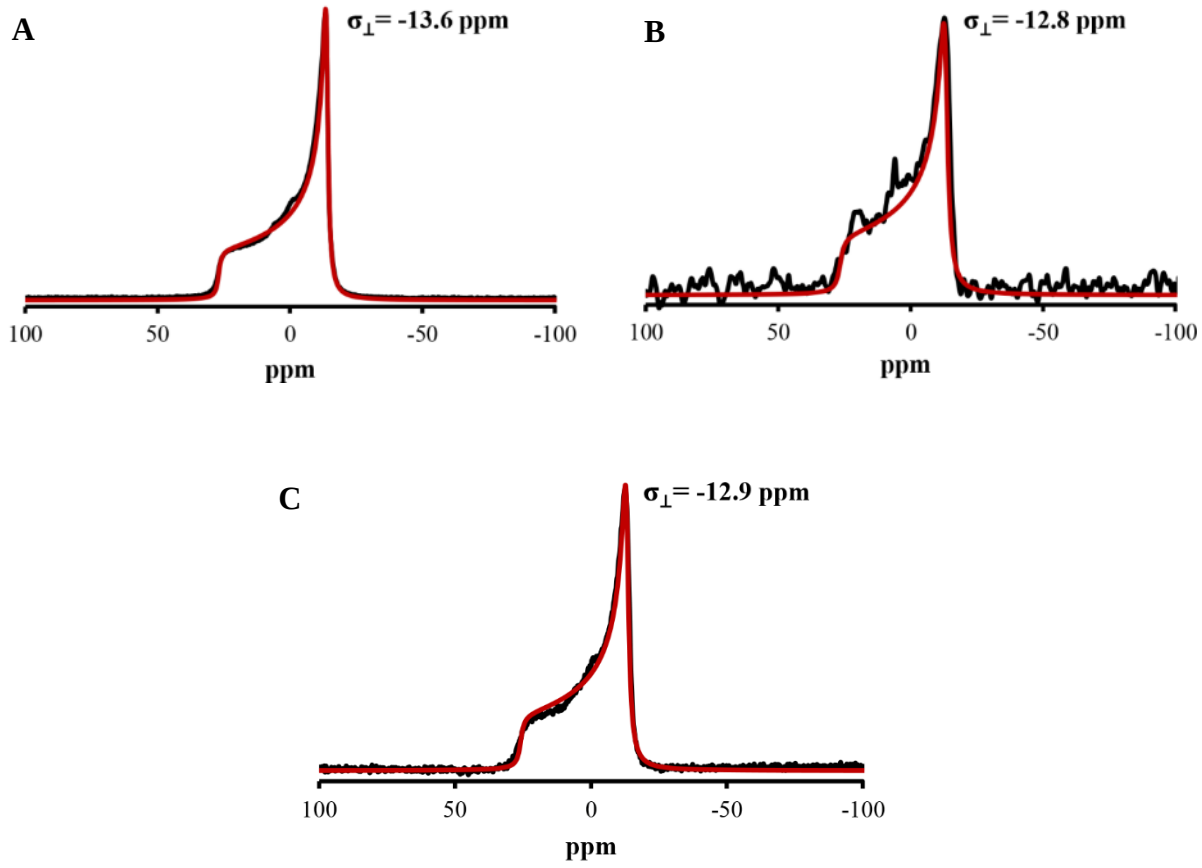

Figure S1-4. ^{31}P NMR spectra (black ─) of POPC in POPC/Chol 9:1 bilayers in the presence of soyasaponin Bb(I) at a molar Chol/saponin ratio of 1:05 (**A**), and at a molar Chol/saponin ratio of 1:1 (**B**). The ^{31}P NMR spectrum (black ─) of the same bilayers in the presence of digitonin at a molar Chol/saponin ratio of 1:0.1 (**C**). All of the ^{31}P NMR spectra were measured at 30 °C and referenced from an 85% phosphoric acid (H_3PO_4) peak set at 0 ppm. Red (─) spectra corresponds to computer simulation using SIMPSON software.[9]

References

1. Kansy, M., Senner, F., Gubernator, K., Physicochemical high throughput screening: parallel artificial membrane permeability assay in the description of passive absorption processes, *J. Med. Chem.* **1998**, *41*, 1007-1010.

2. Kerns, E.H., Di, L., Petusky, S., Farris, M., Ley, R., Jupp, P., Combined application of parallel artificial membrane permeability assay and Caco-2 permeability assays in drug discovery, *J Pharm Sci.* **2004**, *93*, 1440-1453.

3. Avdeef, A., Strafford, M., Block, E., Balogh, M.P., Chambliss, W., Khan, I., Drug absorption in vitro model: filter-immobilized artificial membranes: Studies of the permeability properties of lactones in *Piper methysticum* Forst , *Eur. J. Pharm. Sci.* **2001**, *14*, 271–280.

4. Robinson, C., Weatherell, J.A., The micro determination of calcium in mammalian hard tissues, *Analyst* **1968**, *93*, 722-728.

5. Lodish, H., Berk, A., Zipursky, S.L., Matsudaira, P., Baltimore, D., Darnell, J., Molecular Cell Biology, 4th edition, New York: W. H. Freeman, 2000. Section 15.1, Diffusion of small molecules across phospholipid bilayers. https://www.ncbi.nlm.nih.gov/books/NBK21626/ (accessed 19.12.16)

6. Lorent, J., Le Duff, C.S., Quetin,-Leclercq, J., Mingeot-Leclercq, M.P., Induction of highly curved structures in relation to membrane permeabilization and budding by the triterpenoid saponins, α- and δ-Hederin, *J. Biol. Chem.* **2013**, *288*, 14000-14017.

7. Haslam, R.M., Klyne, W., The precipitation of 3β-hydroxysteroids by digitonin, *Biochem. J.* **1953**, *55*, 340-346.

8. Haslewood, G.A., Digitonides of steroid ketones, *Biochem. J.* **1947**, *41*, xli.

9. Bak, M., Rasmusse, J.Y., Nielsen, N.C., SIMPSON: A General Simulation Program for Solid-State NMR Spectroscopy. *J. Mag. Res.* **2000**, *147*, 296-330.

9. Stockton, G.W., Polnaszek, C.F., Tulloch, A.P., Hassan, F., Smith, I.C.P., Molecular motion and order in single-bilayer vesicles with multilamellar dispersions of egg lecithin and lecithin-cholesterol mixtures. A deuterium nuclear magnetic resonance study of specifically labeled lipids, *Biochemistry* **1976**, *15*, 954-966

10. Frenkel, N., Makky, A., Sudji, I.R., Wink, M., Tanaka, M., Mechanistic investigation of interactions between steroidal saponin digitonin and cell membrane models, *J. Phys. Chem.* **2014**, *118*, 14632-14639

Supporting Information II

Effect of saponins on membrane permeability and morphology as examined by fluorescence techniques

Results

Time-course leakage assay for soyasaponin Bb(I)

A time-course calcein leakage was similarly conducted for soyasaponin Bb(I). Since it was observed that higher amount of soyasaponin Bb(I) is required to induce 50% leakage, 300 μM concentrations was also used to estimate the EC_{50} values at varying phospholipid concentrations (Fig. S2-1). Soyasaponin Bb(I) also required Chol to induce leakage of liposomes, however, it exhibited the weakest binding affinity and membrane disruptivity among the other saponins tested.[1,2]

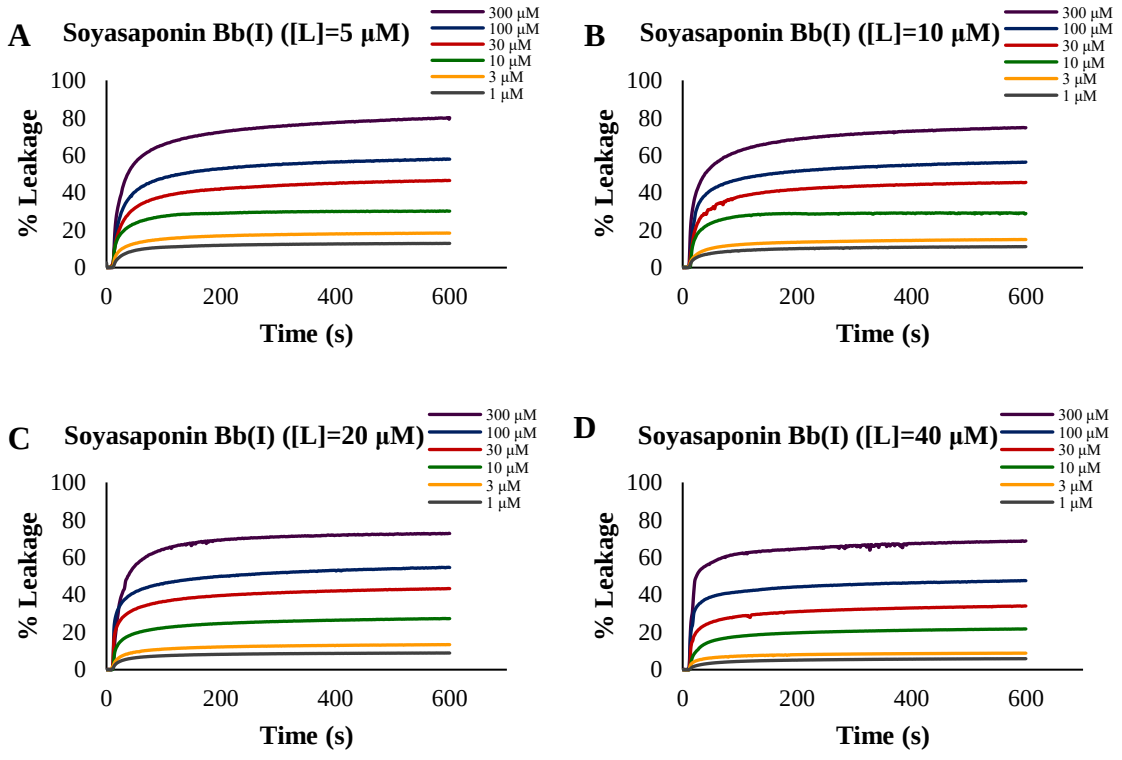

Figure S2-1. Time-course calcein leakage by treatment with soyasaponin Bb(I) (A to D) in 9:1 POPC/Chol LUVs measured for 10 minutes after saponin addition. 100% leakage was obtained by addition of 10% (v/v) Triton-X. Measurements were monitored at 25 °C.

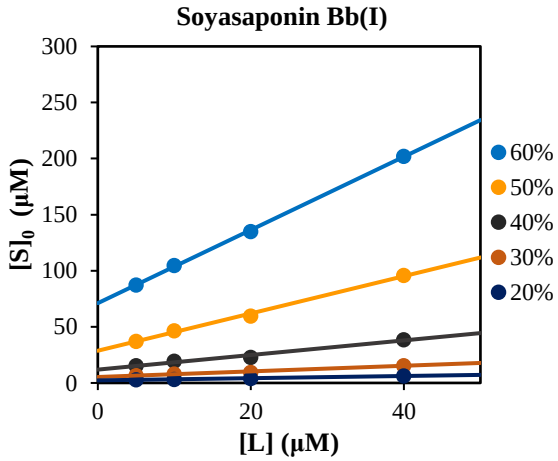

Figure S2-2. Determination of $[S]_f$ and *r* as intercepts and slopes, respectively, at different leakage extents (20%, 30%, 40%, 50%, and 60%) for soyasaponin Bb(I).

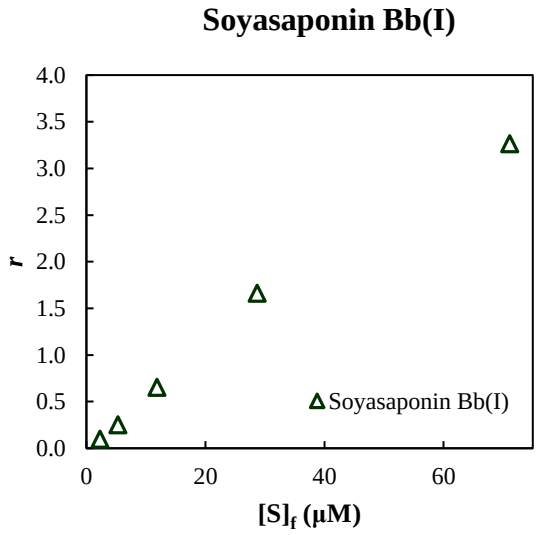

Figure S2-3. Binding isotherm of soyasaponin Bb(I) at different leakage extents. Bound saponin/lipid ratio (*r*) was plotted in each free saponin concentration $[S]_f$.

Concentration-response curves for each saponins

The concentration-response curve was also plotted as shown in Fig S2-4. This was used to determine the concentration of saponin to induce percentage leakage from 20% to 60% taken as the vertical axis separately.

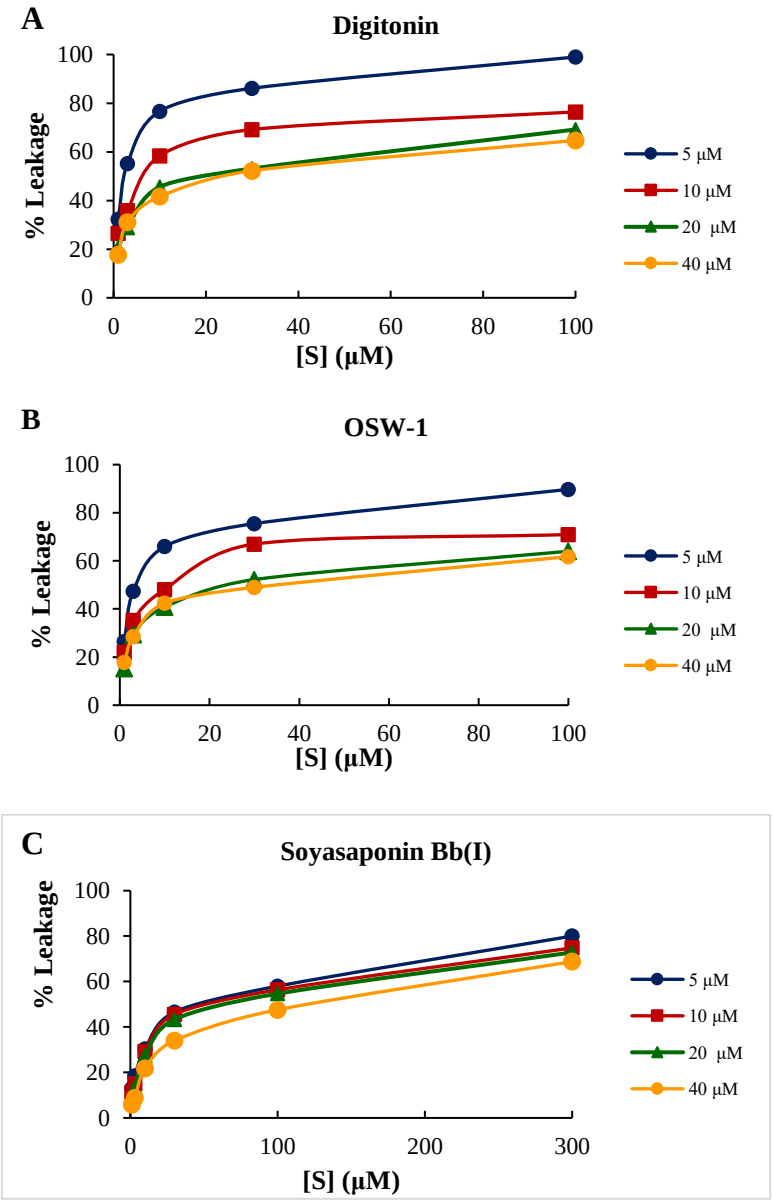

Figure S2-4. Concentration-response curves for digitonin (A), OSW-1 (B) and soyasaponin Bb(I) (C) at the incubation time of 10 min.

Fluorescence Microscopy

The time-lapse images upon addition of 30 μM OSW-1 in GUVs at varying mol% Chol were also recorded up to 60 minutes as shown in Figs. S2-5 to S2-7. The GUV composed of 20 mol% Chol (Fig. S2-5) and 10 mol% Chol (Fig. S2-6) showed significant changes in the shape at 20 min. The GUVs further shrink but remains intact. In the case of GUV composed of 5 mol% Chol (Fig. S2-7) significant changes in the GUV was detected as early as 5 min and completely vanished at 20 min of observation. In this concentration of Chol, OSW-1 exhibited membrane disruption and resulted in the formation of large amount of OSW-1/Chol aggregates.

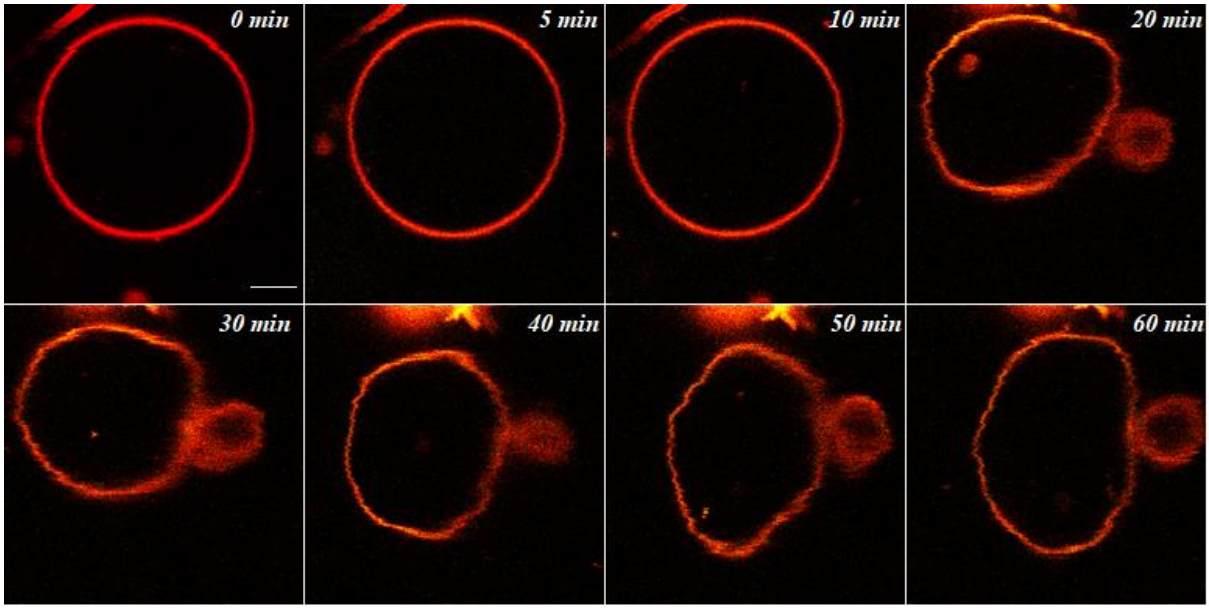

Figure S2-5. Time-lapse image for 30 μM OSW-1 in 2:2:1 DOPC/DMPC/Chol (20 mol% Chol) GUV (Scale = 5 μm) up to 60 minutes of incubation (*overlay*). Measurements were carried out at 37 °C.

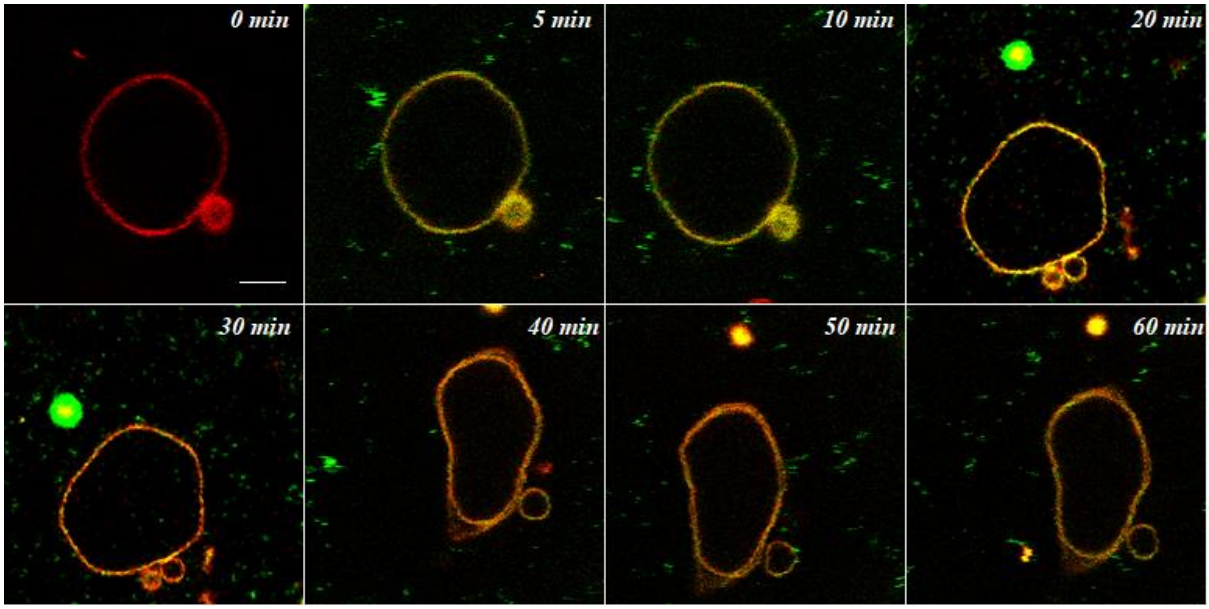

Figure S2-6. Time-lapse image for 30 μM OSW-1 in 9:9:2 DOPC/DMPC/Chol (10 mol% Chol) GUV (Scale = 10 μm) up to 60 minutes of incubation (*overlay*). Measurements were carried out at 37 °C.

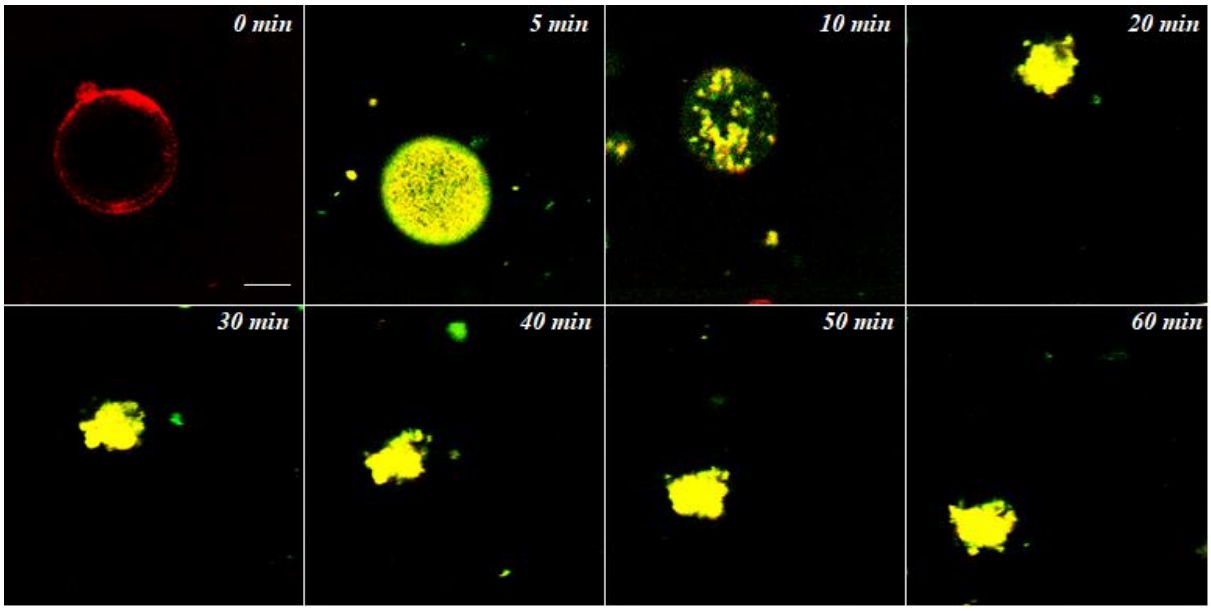

Figure S2-7. Time-lapse image for 30 μM OSW-1 in 19:19:2 DOPC/DMPC/Chol (5 mol% Chol) GUV (Scale = 5 μm) up to 60 minutes of incubation (*overlay*). Measurements were carried out at 37 °C.

References

1. Ohnishi, K., Tachibana, K., Synthesis of pavoninin-1, a shark repellent substance, and its structural analogues toward mechanistic studies on their membrane perturbation, *Bioorg Med Chem.* **1997**, *5*, 2251-2265

2. Hu, M., Konoki, K., Tachibana, K., Cholesterol-independent membrane disruption caused by triterpenoid saponins, *Biochim Biophys Acta.* **1996**, Jan *1299*, 252-258.

Acknowledgment

I would like to express my sincerest gratitude to the persons involved in the fulfillment of my Ph.D. thesis.

First, I would like to thank Professor Michio Murata for the giving me the opportunity to work in his laboratory. His guidance and kindness helped me to pursue my research career. I would also like to thank Dr. Shinya Hanashima and Dr. Hiroshi Tsuchikawa for their valuable assistance in my experiments.

I would also like to extend my gratitude to all my collaborators who also made the research and publications possible most especially to Dr. Kaori Sakurai for providing the OSW-1 sample I used in my experiments. To Dr. Yasuto Todokoro, Dr. Naoya Inazumi and Dr. Tomokazu Yasuda for helping me with the ssNMR measurements. Professor Nobuaki Matsumori and Dr. Masanao Kinoshita for allowing me to use their research facilities.

I would also like to thank my examiners, Professor Yasuhiro Kajihara and Professor Hironobu Hojo for helping me improve my written and oral skills, and for their time in scrutinizing my thesis.

To all Murata lab members, with special mention to Ms. Misaki Yofu, thank you for all your help most especially during those times that I need personal assistance for Japan-related concerns and for making my life in Japan more exciting. Without all of you, I will not be able to finish this degree.

To all of my friends in Osaka thank you for your love and support and for making Japan feels like home. I will definitely miss all of you and all of the happy moments we have shared. Special mention to Kimberly, Juan Lorenzo, Millicent Joyce, Wilfred, Christian David, Jenny Rose, Ivy Grace, Melvin John, Mittsu, Candice and Quang who were always there during these special moments.

To my family, I love you. Thank you for your support and for allowing me to pursue my dreams. For your financial support during the hard times and for your unconditional love and understanding. I will see you soon and we will celebrate this milestone in my life. You are the main reason why I came here. I know three years is long but we made it. To my father Rogelio and mother Alicia, thank you for all your sacrifice. To my sister Rose and brother-in-law Aleen, thank you for taking care of our parents. To my sister Jinky, brother Regidor and his wife Khaye, I know we are different places but your continuous support is never ending.

Lastly, I would like to thank the Lord for all his blessings. For always being with me and for guiding me through my life's choices.

This chapter of my life is full of challenges and a lot of new learnings. My experience here in Japan is very memorable. I will be forever grateful for this once in a lifetime opportunity. I will definitely miss Japan.

Appendix

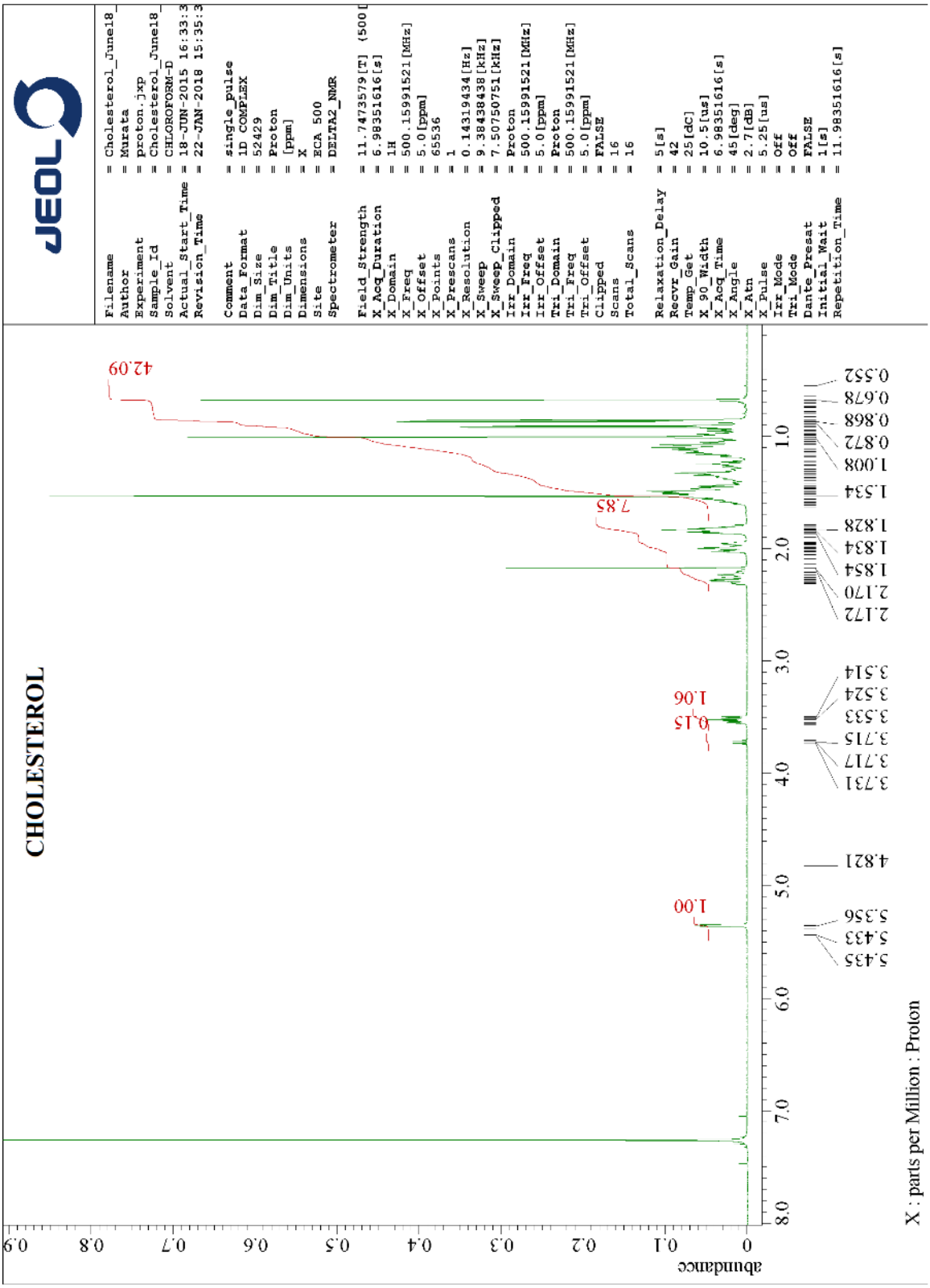

Appendix Figure 1. ^{1}H NMR spectrum of Chol in $CDCl_3$

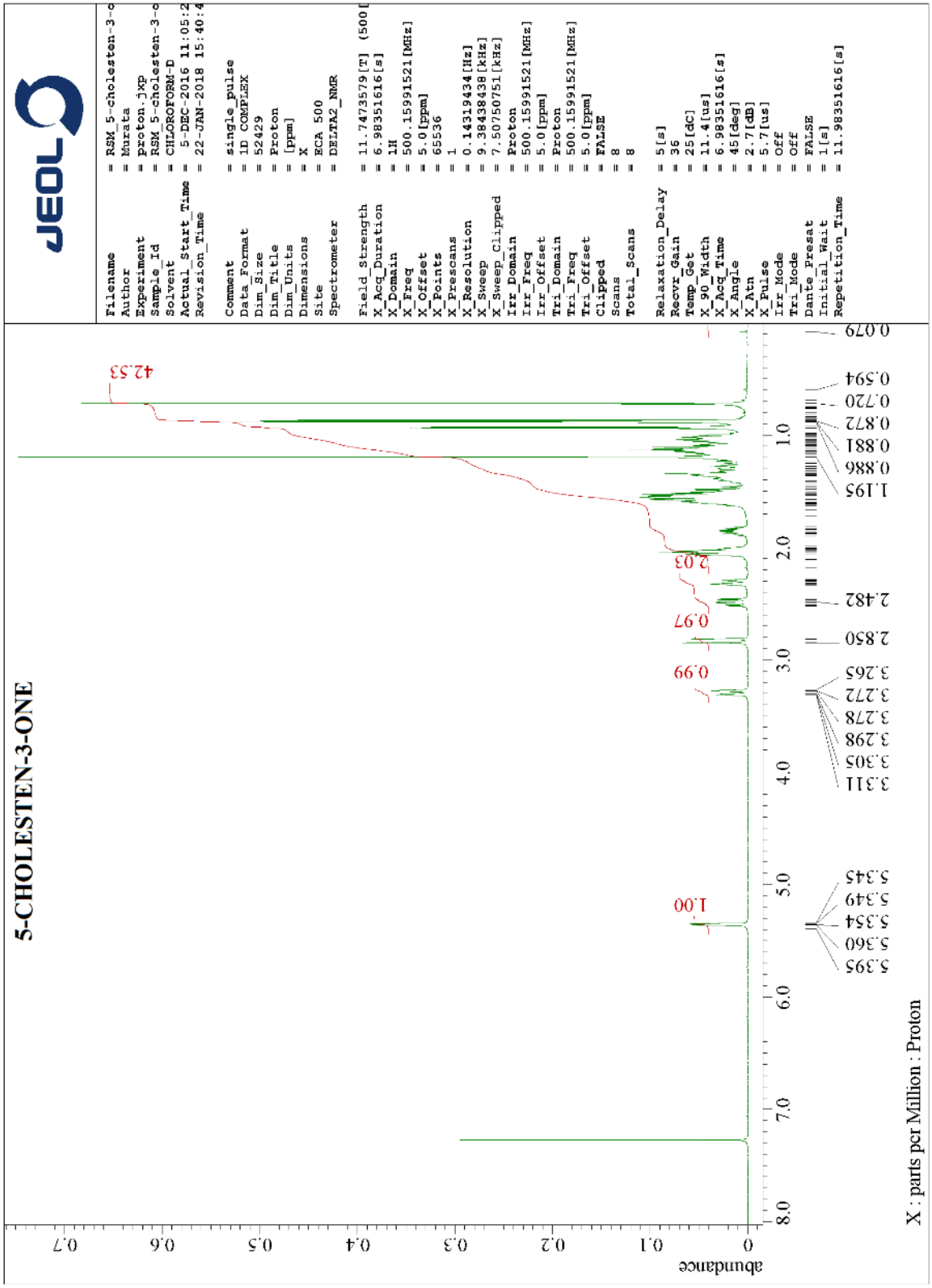

Appendix Figure 2. ^{1}H NMR spectrum of 5-cholesten-3-one in $CDCl_3$

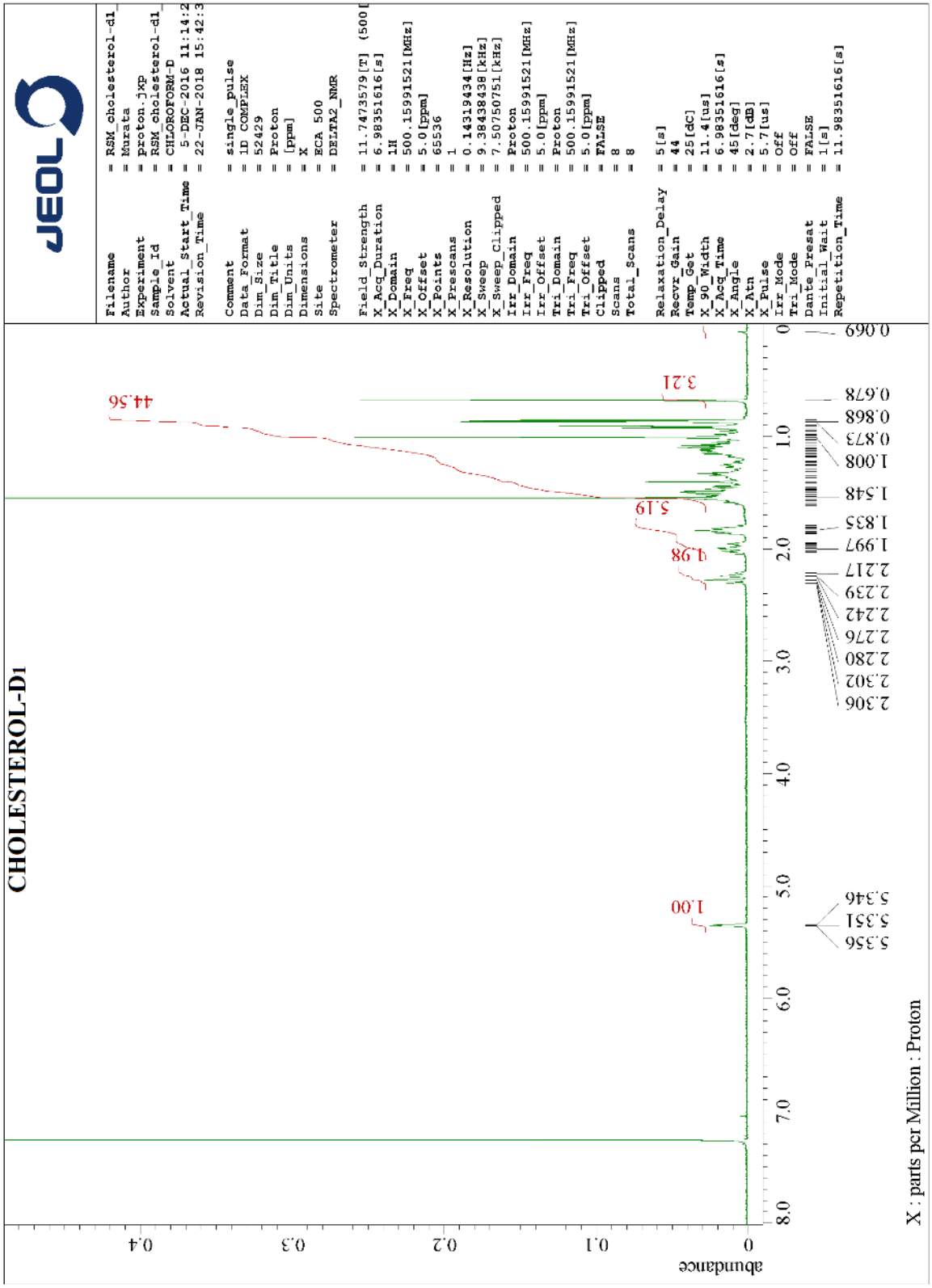

Appendix Figure 3. ^{1}H NMR spectrum of Chol-*d* in $CDCl_3$

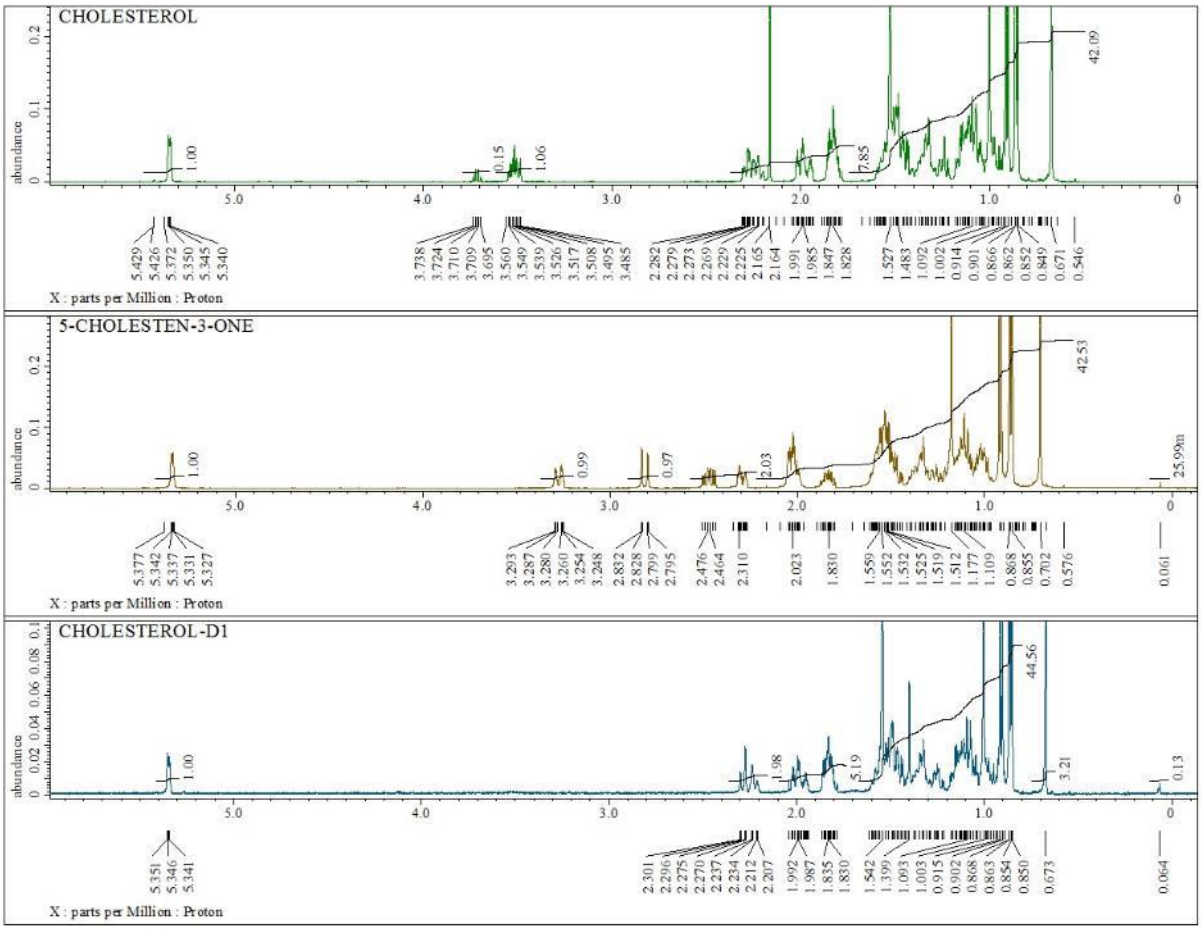

Appendix Figure 4. Summary of ^{1}H NMR spectrum of Chol (**1**), 5-cholesten-3-one (**2**) and Chol-*d* (**3**) in $CDCl_3$

Reprint Permissions

Figures related to this thesis were used with prior consent from the publishers. Permissions were obtained under the author's name. All persons involved in writing of this thesis declare that no copyright infringement was intended for the use of these articles in these publications.

JOHN WILEY AND SONS LICENSE TERMS AND CONDITIONS

Jan 13, 2017

This Agreement between Raymond S. Malabed ("You") and John Wiley and Sons ("John Wiley and Sons") consists of your license details and the terms and conditions provided by John Wiley and Sons and Copyright Clearance Center.

License Number	4026911063666
License date	Jan 13, 2017
Licensed Content Publisher	John Wiley and Sons
Licensed Content Publication	The Chemical Record
Licensed Content Title	Bioactive Structure of Membrane Lipids and Natural Products Elucidated by a Chemistry-Based Approach
Licensed Content Author	Michio Murata,Shigeru Sugiyama,Shigeru Matsuoka,Nobuaki Matsumori
Licensed Content Date	Jun 30, 2015
Licensed Content Pages	16
Type of use	Dissertation/Thesis
Requestor type	University/Academic
Format	Print and electronic
Portion	Figure/table
Number of figures/tables	1
Original Wiley figure/table number(s)	Figure 1
Will you be translating?	No
Title of your thesis / dissertation	Investigation of the Mechanism of Interaction of Saponins with Biological Membranes
Expected completion date	Mar 2018
Expected size (number of pages)	100
Requestor Location	Raymond S. Malabed Osaka-fu, Ikeda-shi Kuko 1-2-13, Kuko Golden House 103 Osaka, 563-0034 Japan Attn: Raymond S. Malabed
Publisher Tax ID	EU826007151
Billing Type	Invoice
Billing Address	Raymond S. Malabed Osaka-fu, Ikeda-shi Kuko 1-2-13, Kuko Golden House 103 Osaka, Japan 563-0034 Attn: Raymond S. Malabed
Total	0 JPY

Copyright permission for Figure 1-1. A representation of biological membrane. Reprinted with permission from *The Chemical Record*, **2015**. Copyright © (2015) John Wiley and Sons.

NATURE PUBLISHING GROUP LICENSE TERMS AND CONDITIONS

May 02, 2017

This Agreement between Raymond S. Malabed ("You") and Nature Publishing Group ("Nature Publishing Group") consists of your license details and the terms and conditions provided by Nature Publishing Group and Copyright Clearance Center.

License Number	4100591066816
License date	May 02, 2017
Licensed Content Publisher	Nature Publishing Group
Licensed Content Publication	Nature Reviews Molecular Cell Biology
Licensed Content Title	Membrane lipids: where they are and how they behave
Licensed Content Author	Gerrit van Meer,Dennis R. VoelkerandGerald W. Feigenson
Licensed Content Date	Feb 1, 2008
Licensed Content Volume	9
Licensed Content Issue	2
Type of Use	reuse in a dissertation / thesis
Requestor type	academic/educational
Format	electronic
Portion	figures/tables/illustrations
Number of figures/tables/illustrations	1
High-res required	no
Figures	1-2
Author of this NPG article	no
Your reference number	8
Title of your thesis / dissertation	Investigation of the Mechanism of Interaction of Saponins with Biological Membranes
Expected completion date	Mar 2018
Estimated size (number of pages)	100
Requestor Location	Raymond S. Malabed Osaka-fu, Ikeda-shi Kuko 1-2-13, Kuko Golden House 103 Osaka, 563-0034 Japan Attn: Raymond S. Malabed
Billing Type	Invoice
Billing Address	Raymond S. Malabed Osaka-fu, Ikeda-shi Kuko 1-2-13, Kuko Golden House 103 Osaka, Japan 563-0034 Attn: Raymond S. Malabed

Copyright permission for Figure 1-2. Representative structures of main classes of lipids. Reprinted and modified with permission from *Nature Reviews Molecular Cell Biology*, **2008**. Copyright © (2008) Nature Publishing Group.

THE AMERICAN ASSOCIATION FOR THE ADVANCEMENT OF SCIENCE LICENSE TERMS AND CONDITIONS

May 02, 2017

This Agreement between Raymond S. Malabed ("You") and The American Association for the Advancement of Science ("The American Association for the Advancement of Science") consists of your license details and the terms and conditions provided by The American Association for the Advancement of Science and Copyright Clearance Center.

License Number	4100651256795
License date	May 02, 2017
Licensed Content Publisher	The American Association for the Advancement of Science
Licensed Content Publication	Science
Licensed Content Title	The Fluid Mosaic Model of the Structure of Cell Membranes
Licensed Content Author	S. J. Singer,Garth L. Nicolson
Licensed Content Date	Feb 18, 1972
Licensed Content Volume	175
Licensed Content Issue	4023
Volume number	175
Issue number	4023
Type of Use	Thesis / Dissertation
Requestor type	Scientist/individual at a research institution
Format	Print and electronic
Portion	Figure
Number of figures/tables	1
Order reference number	
Title of your thesis / dissertation	Investigation of the Mechanism of Interaction of Saponins with Biological Membranes
Expected completion date	Mar 2018
Estimated size(pages)	100
Requestor Location	Raymond S. Malabed Osaka-fu, Ikeda-shi Kuko 1-2-13, Kuko Golden House 103 Osaka, 563-0034 Japan Attn: Raymond S. Malabed
Billing Type	Invoice
Billing Address	Raymond S. Malabed Osaka-fu, Ikeda-shi Kuko 1-2-13, Kuko Golden House 103 Osaka, Japan 563-0034 Attn: Raymond S. Malabed
Total	0 JPY
Terms and Conditions	

Copyright permission for Figure 1-3. The fluid mosaic model of the structure of cell membranes. Reprinted with permission from *Science*, **1972.** Copyright © (1972) The American Association for the Advancement of Science.

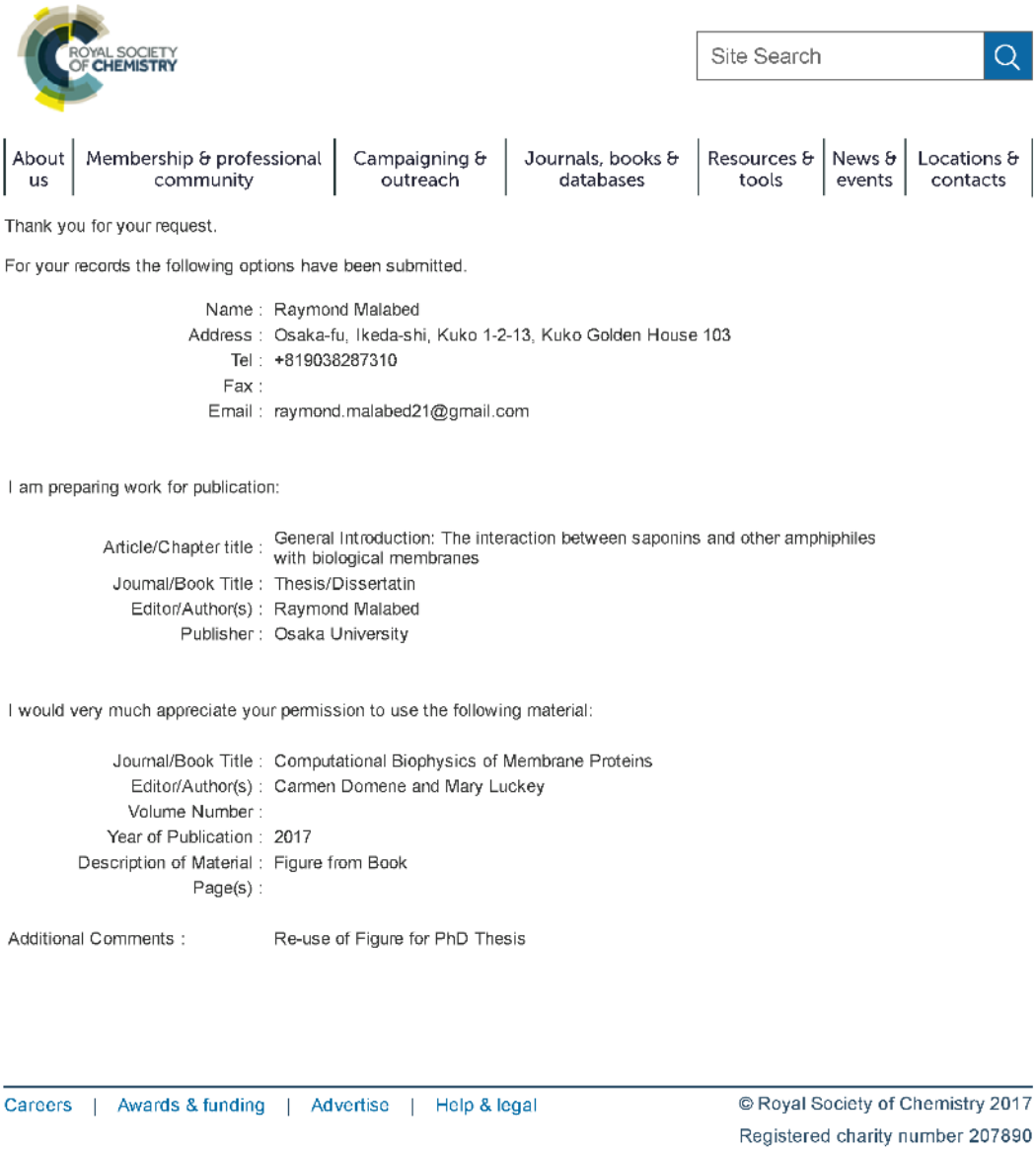

Site Search

About us | Membership & professional community | Campaigning & outreach | Journals, books & databases | Resources & tools | News & events | Locations & contacts

Thank you for your request.

For your records the following options have been submitted.

Name : Raymond Malabed
Address : Osaka-fu, Ikeda-shi, Kuko 1-2-13, Kuko Golden House 103
Tel : +819038287310
Fax :
Email : raymond.malabed21@gmail.com

I am preparing work for publication:

Article/Chapter title : General Introduction: The interaction between saponins and other amphiphiles with biological membranes
Journal/Book Title : Thesis/Dissertatin
Editor/Author(s) : Raymond Malabed
Publisher : Osaka University

I would very much appreciate your permission to use the following material:

Journal/Book Title : Computational Biophysics of Membrane Proteins
Editor/Author(s) : Carmen Domene and Mary Luckey
Volume Number :
Year of Publication : 2017
Description of Material : Figure from Book
Page(s) :

Additional Comments : Re-use of Figure for PhD Thesis

Careers | Awards & funding | Advertise | Help & legal

© Royal Society of Chemistry 2017
Registered charity number 207890

Copyright permission for Figure 1-4. Movements of lipids in biological membrane. Reprinted with permission from *Computational Biophysics of Membrane Proteins*, 2016. Copyright © (2017) Royal Society of Chemistry.

CONTRACTS-COPYRIGHT (shared) <Contracts-Copyright@rsc.org> May 12 (6 days ago)

to me

Dear Raymond

The Royal Society of Chemistry hereby grants permission for the use of the material specified below in the work described and in all subsequent editions of the work for distribution throughout the world, in all media including electronic and microfilm. You may use the material in conjunction with computer-based electronic and information retrieval systems, grant permissions for photocopying, reproductions and reprints, translate the material and to publish the translation, and authorize document delivery and abstracting and indexing services. The Royal Society of Chemistry is a signatory to the STM Guidelines on Permissions (available on request).

Please note that if the material specified below or any part of it appears with credit or acknowledgement to a third party then you must also secure permission from that third party before reproducing that material.
Please ensure that the published article carries a credit to The Royal Society of Chemistry in the following format:
[Original citation] – Reproduced by permission of The Royal Society of Chemistry

and that any electronic version of the work includes a hyperlink to the article on the Royal Society of Chemistry website.

Regards

Gill Cockhead
Publishing Contracts & Copyright Executive

Gill Cockhead
Publishing Contracts & Copyright Executive
Royal Society of Chemistry,
Thomas Graham House,
Science Park, Milton Road,
Cambridge, CB4 0WF, UK
Tel +44 (0) 1223 432134

Winner of The Queen's Award for Enterprise, International Trade 2013

From: Raymond Malabed [mailto:raymond.malabed21@gmail.com]
Sent: 05 May 2017 13:19

To: CONTRACTS-COPYRIGHT (shared) <Contracts-Copyright@rsc.org>
Subject: Re: Permission Request Form: Raymond Malabed

Hello again,

As I have already requested using the instructions in your page, I will be swnding you the details of my request as follows:

Name : Raymond Malabed
Address : Osaka-fu, Ikeda-shi, Kuko 1-2-13, Kuko Golden House 103
Tel : +819038287310
Fax :
Email : raymond.malabed21@gmail.com

I am preparing the following work for publication:

Article/Chapter Title : Investigation of the Mechanism of Interaction of Saponins with Biological Membranes
Journal/Book Title : Thesis/Dissertatin
Editor/Author(s) : Raymond Malabed
Publisher : Osaka University

I would very much appreciate your permission to use the following material:

Journal/Book Title : Computational Biophysics of Membrane Proteins, Chapter 1: Introduction to the Structural Biology of Membrane Proteins
Editor/Author(s) : Carmen Domene and Mary Luckey
Volume Number :
Year of Publication : 2017
Description of Material : Figure from Book (Fig 1.3)
Page(s) :1-18

Any Additional Comments :
On Fri, 5 May 2017 at 9:07 PM CONTRACTS-COPYRIGHT (shared) <Contracts-Copyright@rsc.org> wrote:

Copyright permission for Figure 1-4. Movements of lipids in biological membrane. Reprinted with permission from *Computational Biophysics of Membrane Proteins*, 2016. Copyright © (2017) Royal Society of Chemistry.

NATURE PUBLISHING GROUP LICENSE TERMS AND CONDITIONS

May 03, 2017

This Agreement between Raymond S. Malabed ("You") and Nature Publishing Group ("Nature Publishing Group") consists of your license details and the terms and conditions provided by Nature Publishing Group and Copyright Clearance Center.

License Number	4101230234810
License date	May 03, 2017
Licensed Content Publisher	Nature Publishing Group
Licensed Content Publication	Nature Reviews Molecular Cell Biology
Licensed Content Title	Membrane lipids: where they are and how they behave
Licensed Content Author	Gerrit van Meer,Dennis R. VoelkerandGerald W. Feigenson
Licensed Content Date	Feb 1, 2008
Licensed Content Volume	9
Licensed Content Issue	2
Type of Use	reuse in a dissertation / thesis
Requestor type	academic/educational
Format	print and electronic
Portion	figures/tables/illustrations
Number of figures/tables/illustrations	1
High-res required	no
Figures	Lipid phases in biological membranes
Author of this NPG article	no
Your reference number	8
Title of your thesis / dissertation	Investigation of the Mechanism of Interaction of Saponins with Biological Membranes
Expected completion date	Mar 2018
Estimated size (number of pages)	100
Requestor Location	Raymond S. Malabed Osaka-fu, Ikeda-shi Kuko 1-2-13, Kuko Golden House 103 Osaka, 563-0034 Japan Attn: Raymond S. Malabed
Billing Type	Invoice
Billing Address	Raymond S. Malabed Osaka-fu, Ikeda-shi Kuko 1-2-13, Kuko Golden House 103 Osaka, Japan 563-0034 Attn: Raymond S. Malabed

Copyright permission for Figure 1-5. Lipid phase in biological membranes. Reprinted with permission from *Nature Reviews Molecular Cell Biology*, **2008**. Copyright © (2008) Nature Publishing Group.

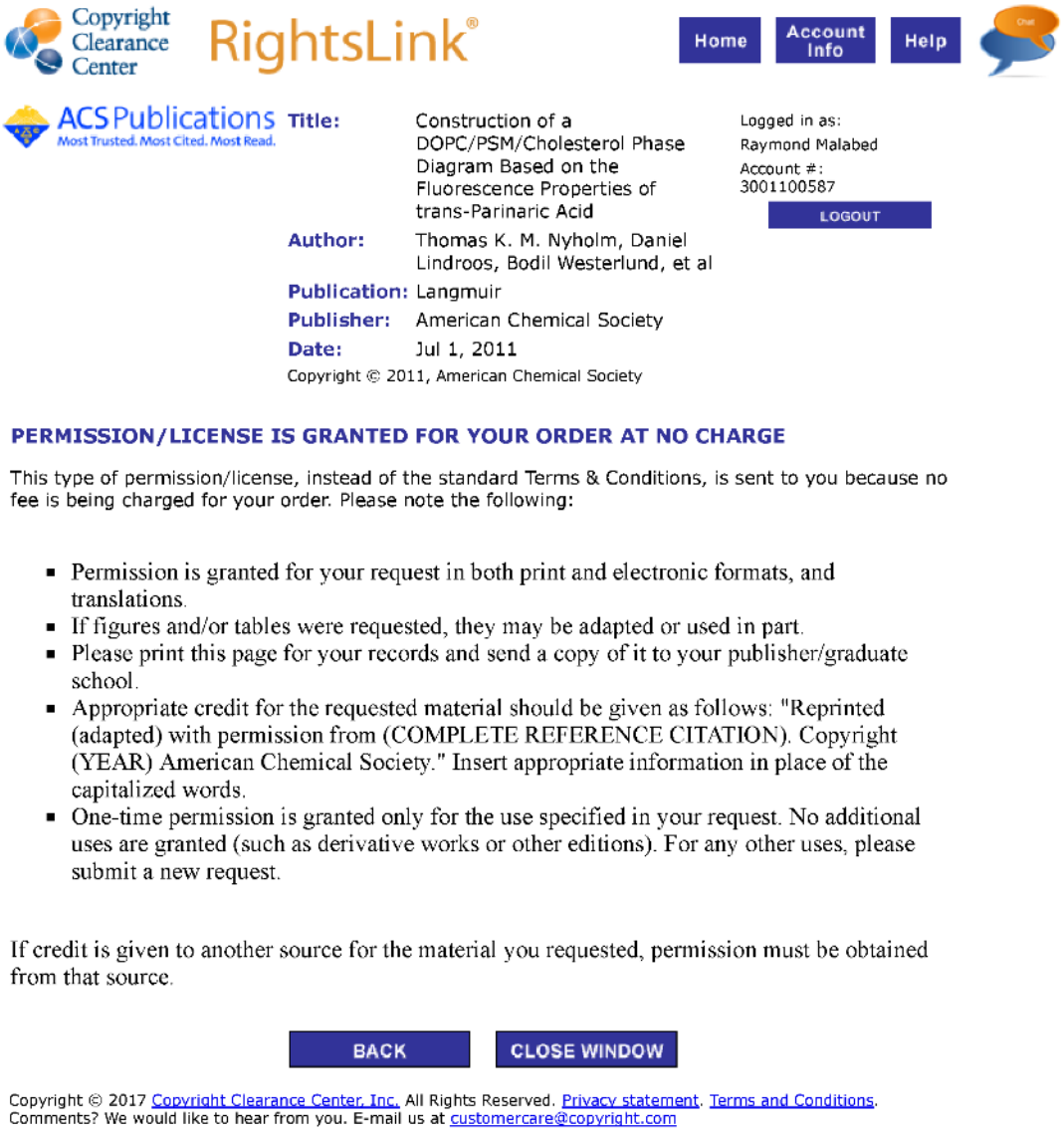

Copyright Clearance Center RightsLink®

Home | Account Info | Help

ACS Publications
Most Trusted. Most Cited. Most Read.

Title: Construction of a DOPC/PSM/Cholesterol Phase Diagram Based on the Fluorescence Properties of trans-Parinaric Acid

Author: Thomas K. M. Nyholm, Daniel Lindroos, Bodil Westerlund, et al

Publication: Langmuir

Publisher: American Chemical Society

Date: Jul 1, 2011

Copyright © 2011, American Chemical Society

Logged in as:
Raymond Malabed
Account #:
3001100587

LOGOUT

PERMISSION/LICENSE IS GRANTED FOR YOUR ORDER AT NO CHARGE

This type of permission/license, instead of the standard Terms & Conditions, is sent to you because no fee is being charged for your order. Please note the following:

- Permission is granted for your request in both print and electronic formats, and translations.
- If figures and/or tables were requested, they may be adapted or used in part.
- Please print this page for your records and send a copy of it to your publisher/graduate school.
- Appropriate credit for the requested material should be given as follows: "Reprinted (adapted) with permission from (COMPLETE REFERENCE CITATION). Copyright (YEAR) American Chemical Society." Insert appropriate information in place of the capitalized words.
- One-time permission is granted only for the use specified in your request. No additional uses are granted (such as derivative works or other editions). For any other uses, please submit a new request.

If credit is given to another source for the material you requested, permission must be obtained from that source.

BACK | CLOSE WINDOW

Copyright © 2017 Copyright Clearance Center, Inc. All Rights Reserved. Privacy statement. Terms and Conditions.
Comments? We would like to hear from you. E-mail us at customercare@copyright.com

Copyright permission for Figure 1-6. Phase diagram for co-existence of phase separated lipids in ternary system composed of DOPC/CHOL/PSM. Reprinted with permission from *Langmuir*, **2011**. Copyright © (2011) American Chemical Society.

NATURE PUBLISHING GROUP LICENSE TERMS AND CONDITIONS

May 05, 2017

This Agreement between Raymond S. Malabed ("You") and Nature Publishing Group ("Nature Publishing Group") consists of your license details and the terms and conditions provided by Nature Publishing Group and Copyright Clearance Center.

License Number	4102360953603
License date	May 05, 2017
Licensed Content Publisher	Nature Publishing Group
Licensed Content Publication	Nature Reviews Microbiology
Licensed Content Title	Antimicrobial peptides: pore formers or metabolic inhibitors in bacteria?
Licensed Content Author	Kim A. Brogden
Licensed Content Date	Mar 1, 2005
Licensed Content Volume	3
Licensed Content Issue	3
Type of Use	reuse in a dissertation / thesis
Requestor type	academic/educational
Format	print and electronic
Portion	figures/tables/illustrations
Number of figures/tables/illustrations	3
High-res required	no
Figures	Figure 1-13 Figure 1-14 Figure 1-15
Author of this NPG article	no
Your reference number	
Title of your thesis / dissertation	Investigation of the Mechanism of Interaction of Saponins with Biological Membranes
Expected completion date	Mar 2018
Estimated size (number of pages)	100
Requestor Location	Raymond S. Malabed Osaka-fu, Ikeda-shi Kuko 1-2-13, Kuko Golden House 103 Osaka, 563-0034 Japan Attn: Raymond S. Malabed
Billing Type	Invoice
Billing Address	Raymond S. Malabed Osaka-fu, Ikeda-shi Kuko 1-2-13, Kuko Golden House 103 Osaka, Japan 563-0034 Attn: Raymond S. Malabed

Copyright permission for Figure 1-13 to 1-15. Mechanism of interaction of antimicrobial peptides (AMPs). Reprinted with permission from *Nat. Rev. Microbiol.*, **2005**. Copyright © (2005) Nature Publishing Group.

ROYAL SOCIETY OF CHEMISTRY LICENSE TERMS AND CONDITIONS

May 05, 2017

This Agreement between Raymond S. Malabed ("You") and Royal Society of Chemistry ("Royal Society of Chemistry") consists of your license details and the terms and conditions provided by Royal Society of Chemistry and Copyright Clearance Center.

License Number	4102471212376
License date	May 05, 2017
Licensed Content Publisher	Royal Society of Chemistry
Licensed Content Publication	Organic & Biomolecular Chemistry
Licensed Content Title	The amphiphilic nature of saponins and their effects on artificial and biological membranes and potential consequences for red blood and cancer cells
Licensed Content Author	Joseph H. Lorent,Joëlle Quetin-Leclercq,Marie-Paule Mingeot-Leclercq
Licensed Content Date	Sep 15, 2014
Licensed Content Volume	12
Licensed Content Issue	44
Type of Use	Thesis/Dissertation
Requestor type	academic/educational
Portion	figures/tables/images
Number of figures/tables/images	1
Format	print and electronic
Distribution quantity	6
Will you be translating?	no
Order reference number	
Title of the thesis/dissertation	Investigation of the Mechanism of Interaction of Saponins with Biological Membranes
Expected completion date	Mar 2018
Estimated size	100
Requestor Location	Raymond S. Malabed Osaka-fu, Ikeda-shi Kuko 1-2-13, Kuko Golden House 103 Osaka, 563-0034 Japan Attn: Raymond S. Malabed
Billing Type	Invoice
Billing Address	Raymond S. Malabed Osaka-fu, Ikeda-shi Kuko 1-2-13, Kuko Golden House 103 Osaka, Japan 563-0034 Attn: Raymond S. Malabed
Total	0 JPY

Copyright permission for Figure 1-16. Mechanism of interaction of α-hederin. Reprinted with permission from *Org. Biomol. Chem.*, **2014**. Copyright © (2014) Royal Society of Chemistry.

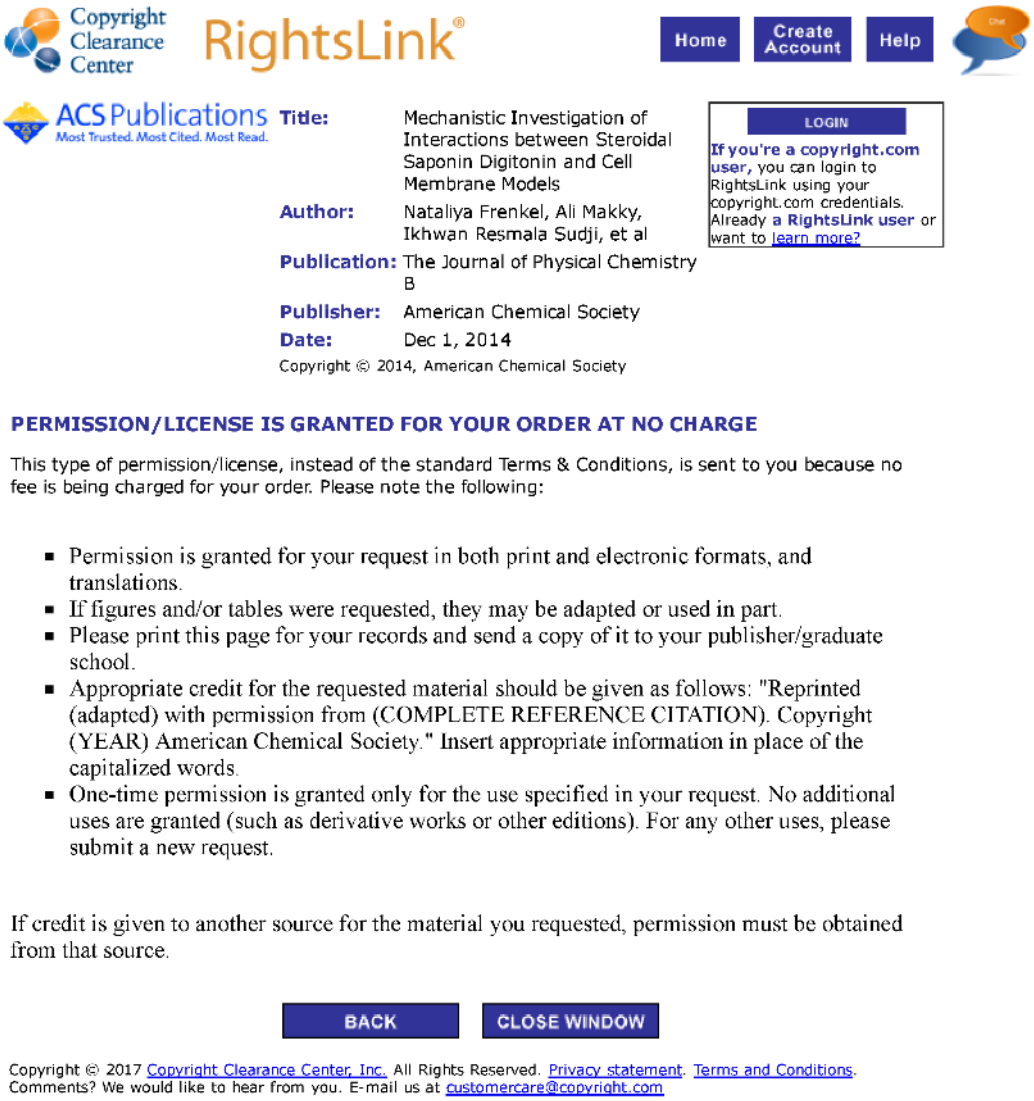

Copyright permission for Figure 1-17. Mechanism of interaction of 50 μM digitonin at various Chol concentration. Reprinted with permission from *J. Phys. Chem. B,* **2014**. Copyright © (2014) American Chemical Society.

Copyright permission for Figure 1-19. Images of *Ornithogalum saundersiae*. Reprinted and modified with permission from *Chem. Rev.*, **2013**. Copyright © (2013) American Chemical Society.

Copyright permission for Figure 1-20. Structure-activity relationship of OSW-1 towards tumor cells. Reprinted with permission from *Chem. Rev.*, **2013**. Copyright © (2013) American Chemical Society.

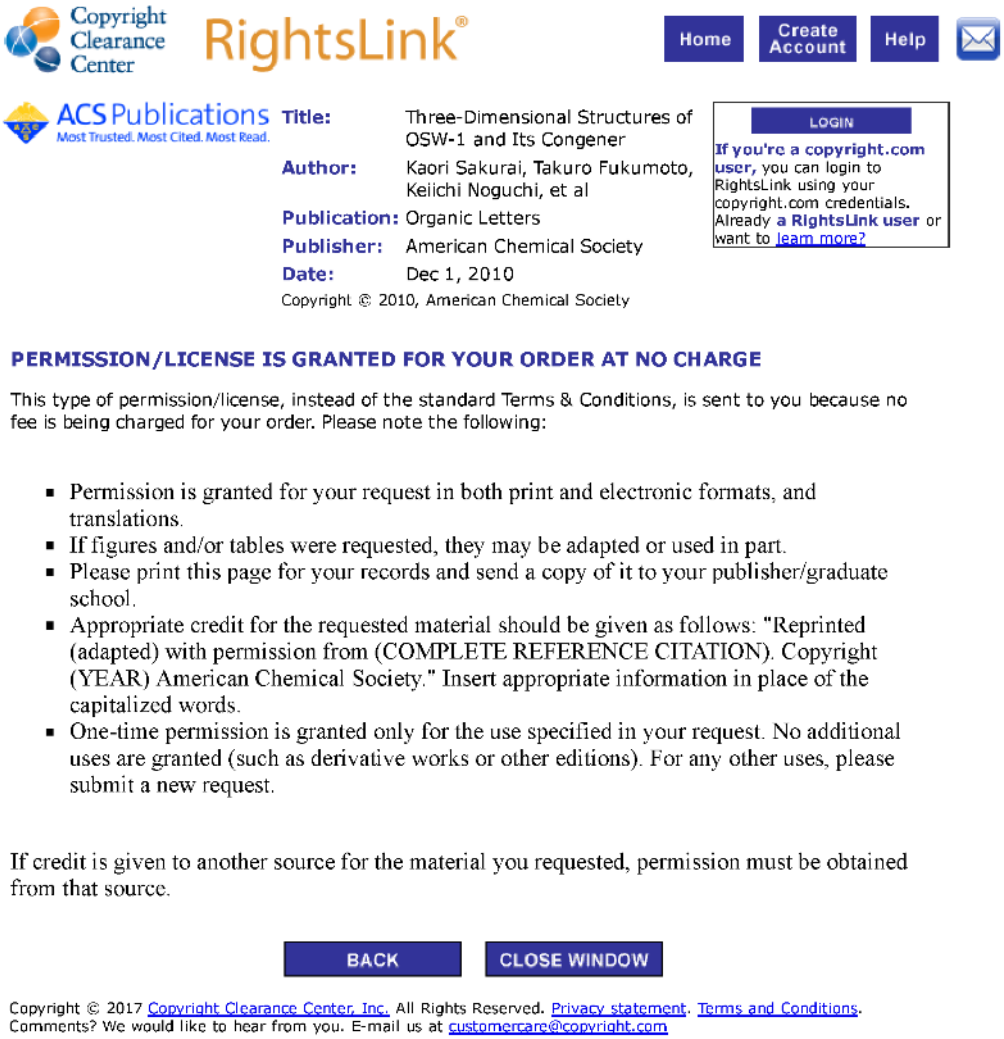

Copyright Clearance Center RightsLink®

Home | Create Account | Help

ACS Publications
Most Trusted. Most Cited. Most Read.

Title: Three-Dimensional Structures of OSW-1 and Its Congener
Author: Kaori Sakurai, Takuro Fukumoto, Keiichi Noguchi, et al
Publication: Organic Letters
Publisher: American Chemical Society
Date: Dec 1, 2010
Copyright © 2010, American Chemical Society

LOGIN
If you're a copyright.com user, you can login to RightsLink using your copyright.com credentials. Already a RightsLink user or want to learn more?

PERMISSION/LICENSE IS GRANTED FOR YOUR ORDER AT NO CHARGE

This type of permission/license, instead of the standard Terms & Conditions, is sent to you because no fee is being charged for your order. Please note the following:

- Permission is granted for your request in both print and electronic formats, and translations.
- If figures and/or tables were requested, they may be adapted or used in part.
- Please print this page for your records and send a copy of it to your publisher/graduate school.
- Appropriate credit for the requested material should be given as follows: "Reprinted (adapted) with permission from (COMPLETE REFERENCE CITATION). Copyright (YEAR) American Chemical Society." Insert appropriate information in place of the capitalized words.
- One-time permission is granted only for the use specified in your request. No additional uses are granted (such as derivative works or other editions). For any other uses, please submit a new request.

If credit is given to another source for the material you requested, permission must be obtained from that source.

BACK | CLOSE WINDOW

Copyright © 2017 Copyright Clearance Center, Inc. All Rights Reserved. Privacy statement. Terms and Conditions.
Comments? We would like to hear from you. E-mail us at customercare@copyright.com

Copyright permission for Figure 1-21. Three-dimensional structure of OSW-1. Reprinted with permission from *Org. Lett.*, **2010**. Copyright © (2010) American Chemical Society.

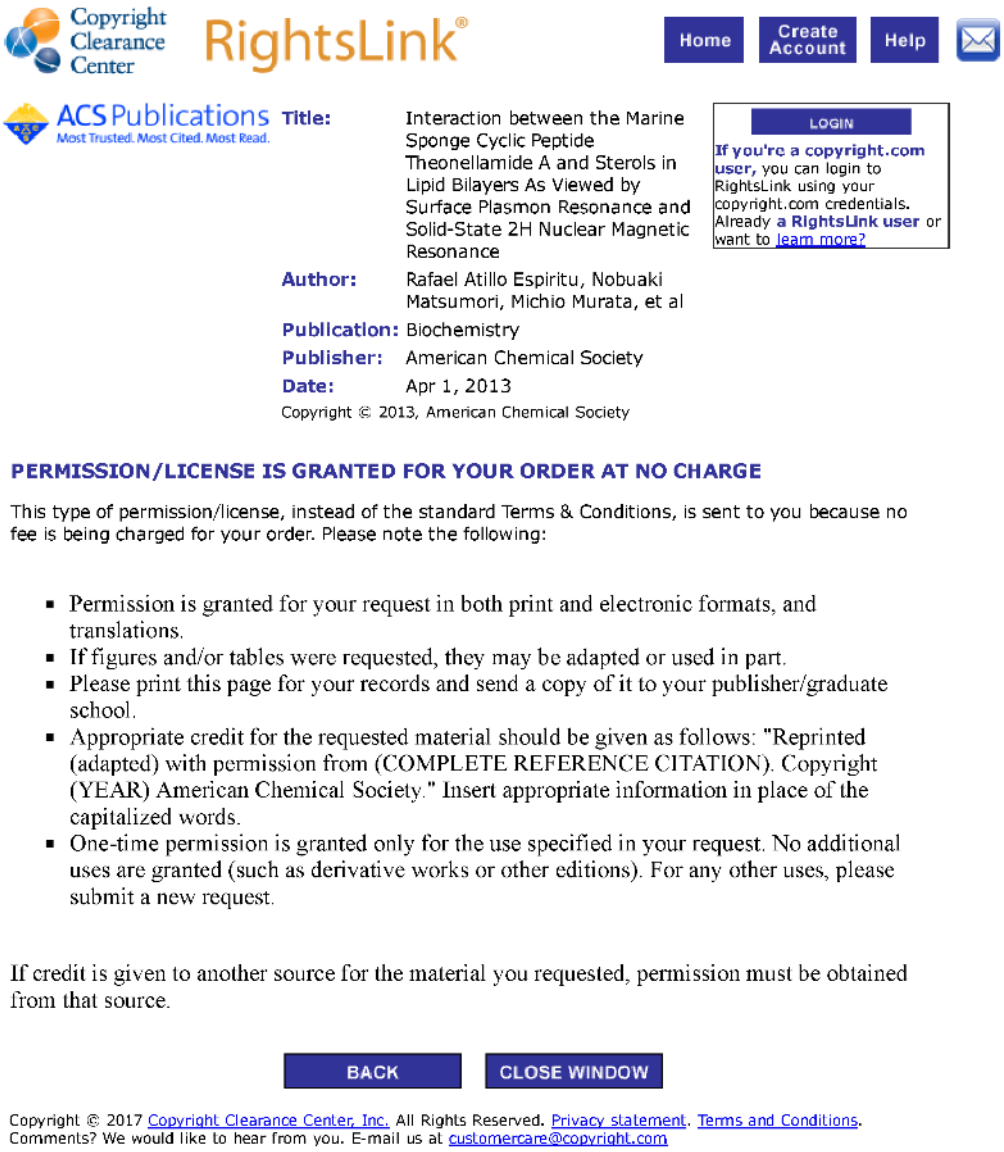

Copyright Clearance Center RightsLink®

Home | Create Account | Help

ACS Publications
Most Trusted. Most Cited. Most Read.

Title: Interaction between the Marine Sponge Cyclic Peptide Theonellamide A and Sterols in Lipid Bilayers As Viewed by Surface Plasmon Resonance and Solid-State 2H Nuclear Magnetic Resonance

Author: Rafael Atillo Espiritu, Nobuaki Matsumori, Michio Murata, et al

Publication: Biochemistry

Publisher: American Chemical Society

Date: Apr 1, 2013

Copyright © 2013, American Chemical Society

LOGIN

If you're a copyright.com user, you can login to RightsLink using your copyright.com credentials. Already a RightsLink user or want to learn more?

PERMISSION/LICENSE IS GRANTED FOR YOUR ORDER AT NO CHARGE

This type of permission/license, instead of the standard Terms & Conditions, is sent to you because no fee is being charged for your order. Please note the following:

- Permission is granted for your request in both print and electronic formats, and translations.
- If figures and/or tables were requested, they may be adapted or used in part.
- Please print this page for your records and send a copy of it to your publisher/graduate school.
- Appropriate credit for the requested material should be given as follows: "Reprinted (adapted) with permission from (COMPLETE REFERENCE CITATION). Copyright (YEAR) American Chemical Society." Insert appropriate information in place of the capitalized words.
- One-time permission is granted only for the use specified in your request. No additional uses are granted (such as derivative works or other editions). For any other uses, please submit a new request.

If credit is given to another source for the material you requested, permission must be obtained from that source.

BACK | CLOSE WINDOW

Copyright © 2017 Copyright Clearance Center, Inc. All Rights Reserved. Privacy statement. Terms and Conditions.
Comments? We would like to hear from you. E-mail us at customercare@copyright.com

Copyright permission for Figure 1-23. ^{2}H NMR spectra of sterol probes in in absence (and presence of marine sponge cyclic peptide Theonellamide A (TNM-A). Reprinted with permission from *Biochemistry*, **2013**. Copyright © (2013) American Chemical Society.

SPRINGER LICENSE
TERMS AND CONDITIONS

May 10, 2017

This Agreement between Raymond S. Malabed ("You") and Springer ("Springer") consists of your license details and the terms and conditions provided by Springer and Copyright Clearance Center.

License Number	4105200326209
License date	May 10, 2017
Licensed Content Publisher	Springer
Licensed Content Publication	Springer eBook
Licensed Content Title	The Structures and Properties of Membrane Lipids
Licensed Content Author	Robert B. Gennis
Licensed Content Date	Jan 1, 1989
Type of Use	Thesis/Dissertation
Portion	Figures/tables/illustrations
Number of figures/tables/illustrations	1
Author of this Springer article	No
Order reference number	
Original figure numbers	Figure 2.8
Title of your thesis / dissertation	Investigation of the Mechanism of Interaction of Saponins with Biological Membranes
Expected completion date	Mar 2018
Estimated size(pages)	100
Requestor Location	Raymond S. Malabed Osaka-fu, Ikeda-shi Kuko 1-2-13, Kuko Golden House 103 Osaka, 563-0034 Japan Attn: Raymond S. Malabed
Billing Type	Invoice
Billing Address	Raymond S. Malabed Osaka-fu, Ikeda-shi Kuko 1-2-13, Kuko Golden House 103 Osaka, Japan 563-0034 Attn: Raymond S. Malabed
Total	0 JPY
Terms and Conditions	

Introduction
The publisher for this copyrighted material is Springer. By clicking "accept" in connection with completing this licensing transaction, you agree that the following terms and conditions apply to this transaction (along with the Billing and Payment terms and conditions

Copyright permission for Figure 1-24. ^{31}P NMR spectra of phospholipids at different phase. Reprinted with permission from *The Structures and Properties of Membrane Lipids*, **1989**. Copyright © (1989) Springer.

11200 Rockville Pike
Suite 302
Rockville, Maryland 20852

August 19, 2011

American Society for Biochemistry and Molecular Biology

To whom it may concern,

It is the policy of the American Society for Biochemistry and Molecular Biology to allow reuse of any material published in its journals (the Journal of Biological Chemistry, Molecular & Cellular Proteomics and the Journal of Lipid Research) in a thesis or dissertation at no cost and with no explicit permission needed. Please see our copyright permissions page on the journal site for more information.

Best wishes,

Sarah Crespi

American Society for Biochemistry and Molecular Biology
11200 Rockville Pike, Rockville, MD
Suite 302
240-283-6616
JBC | MCP | JLR

Copyright permission for Figure 1-25. Pore-forming properties of α-hederin (40 μM) on GUVs composed of DMPC/Chol (3:1) incubated with of α-hederin. Reprinted and modified with permission from *Journal of Biological Chemistry*, **2013**. Copyright © (2013) The American Society for Biochemistry and Molecular Biology.

Copyright permission for Figure 1-26. Effect of addition of 20 µM digitonin in GUVs composed of PC/Chol (80:20) at different incubation period. Reprinted with permission from *Molecules*, **2015**. Copyright © (2015) Multidisciplinary Digital Publishing Institute (MDPI).

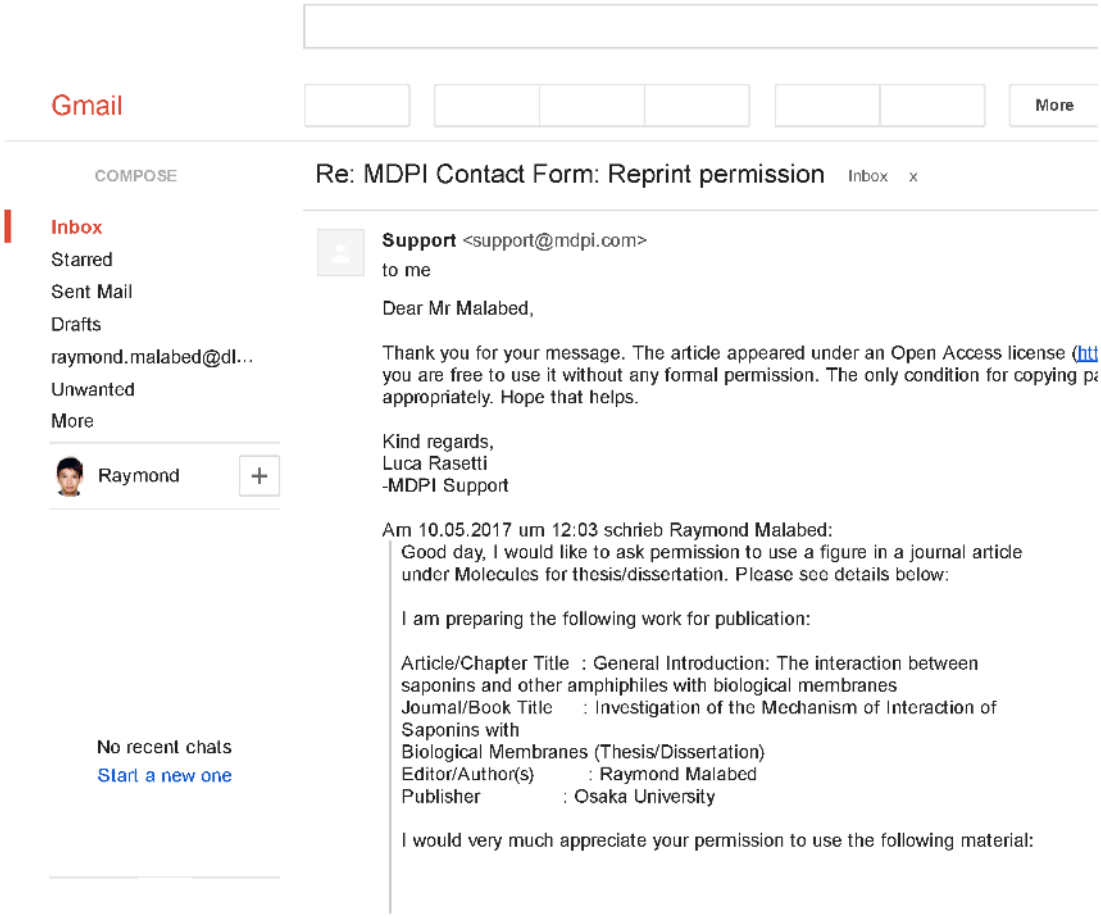

Copyright permission for Figure 1-26. Effect of addition of 20 µM digitonin in GUVs composed of PC/Chol (80:20) at different incubation period. Reprinted with permission from *Molecules*, **2015**. Copyright © (2015) Multidisciplinary Digital Publishing Institute (MDPI).

ELSEVIER LICENSE
TERMS AND CONDITIONS

Oct 10, 2017

This Agreement between Raymond S. Malabed ("You") and Elsevier ("Elsevier") consists of your license details and the terms and conditions provided by Elsevier and Copyright Clearance Center.

License Number	4205700887685
License date	Oct 10, 2017
Licensed Content Publisher	Elsevier
Licensed Content Publication	Biochimica et Biophysica Acta (BBA) - Biomembranes
Licensed Content Title	Sterol-recognition ability and membrane-disrupting activity of Ornithogalum saponin OSW-1 and usual 3-O-glycosyl saponins
Licensed Content Author	Raymond Malabed,Shinya Hanashima,Michio Murata,Kaori Sakurai
Licensed Content Date	Available online 22 September 2017
Licensed Content Volume	n/a
Licensed Content Issue	n/a
Licensed Content Pages	1
Start Page	0
End Page	0
Type of Use	reuse in a thesis/dissertation
Portion	figures/tables/illustrations
Number of figures/tables/illustrations	9
Format	both print and electronic
Are you the author of this Elsevier article?	Yes
Will you be translating?	No
Original figure numbers	Figures 1 to 9 and Supplementary Figures
Title of your thesis/dissertation	Investigation of the Mechanism of Interaction of Saponins with Biological Membranes
Expected completion date	Mar 2018
Estimated size (number of pages)	100
Requestor Location	Raymond S. Malabed Osaka-fu, Ikeda-shi Kuko 1-2-13, Kuko Golden House 103 Osaka, 563-0034 Japan Attn: Raymond S. Malabed
Publisher Tax ID	JP00022
Total	0 JPY
Terms and Conditions	

Copyright permission for Figure 2-1 to 2-9. Sterol-recognition ability and membrane-disrupting activity of *Ornithogalum saponin* OSW-1 and usual 3-*O*-glycosyl saponins. Reprinted with permission from *BBA Biomembranes*, **2017**. Copyright © (2017) Elsevier.

Publications Related to Thesis

Thesis-related publication is listed below and a copy of the corresponding full text are attached from the next page onwards.

1. Malabed, R., Hanashima, S., Murata, M., Sakurai, K., Sterol-recognition ability and membrane-disrupting activity of *Ornithogalum saponin* OSW-1 and usual 3-*O*-glycosyl saponins, *BBA - Biomembranes* **2017**, *1859*, 2516–2525.

BBA - Biomembranes 1859 (2017) 2516–2525

Contents lists available at ScienceDirect

BBA - Biomembranes

journal homepage: www.elsevier.com/locate/bbamem

Sterol-recognition ability and membrane-disrupting activity of *Ornithogalum* saponin OSW-1 and usual 3-*O*-glycosyl saponins

Raymond Malabed[a,b], Shinya Hanashima[a,*], Michio Murata[a,b,*], Kaori Sakurai[c]

[a] Department of Chemistry, Graduate School of Science, Osaka University, 1-1 Machikaneyama, Toyonaka, Osaka 560-0043, Japan
[b] ERATO, Lipid Active Structure Project, Japan Science and Technology Agency, 1-1 Machikaneyama, Toyonaka, Osaka 560 0043, Japan
[c] Department of Biotechnology and Life Science, Tokyo University of Agriculture and Technology, Koganei shi, Tokyo 184 8588, Japan

ARTICLE INFO

Keywords:
Saponin
OSW-1
Plant saponin
Cholesterol
Membrane permeabilization
Solid state NMR

ABSTRACT

OSW-1 is a structurally unique steroidal saponin isolated from the bulbs of *Ornithogalum saundersiae*, and has exhibited highly potent and selective cytotoxicity in tumor cell lines. This study aimed to investigate the molecular mechanism for the membrane-permeabilizing activity of OSW-1 in comparison with those of other saponins by using various spectroscopic approaches. The membrane effects and hemolytic activity of OSW-1 were markedly enhanced in the presence of membrane cholesterol. Binding affinity measurements using fluorescent cholestatrienol and solid-state NMR spectroscopy of a 3-*d*-cholesterol probe suggested that OSW-1 interacts with membrane cholesterol without forming large aggregates while 3-*O*-glycosyl saponin, digitonin, forms cholesterol-containing aggregates. The results suggest that OSW-1/cholesterol interaction is likely to cause membrane permeabilization and pore formation without destroying the whole membrane integrity, which could partly be responsible for its highly potent cell toxicity.

1. Introduction

Saponins are a class of amphiphilic compounds that possess one or more hydrophilic sugar moieties attached to a hydrophobic steroid or triterpenoid backbone. A wide variety of saponins have been isolated and characterized from diverse terrestrial plants and some marine organisms such as sea cucumbers and starfish. The chemical structure of saponins varies greatly due to the types of sugars attached, branching and positioning of sugar chains, and the nature of the sapogenin backbone [1–8]. Several saponins have long been used in Chinese medicine because of their pharmacological actions such as anti-inflammation [9], fatigue reduction [10], and improved blood circulation [11]. Some saponins also have promising anticancer properties; *e.g.*, angiogenesis inhibition, cell cycle arrest, and apoptosis induction [11,12].

OSW-1 is a member of the steroidal saponins, first isolated in 1992 from the bulbs of *Ornithogalum saundersiae* by Sashida's group [13,14]. This saponin is structurally unique in that it contains an acylated disaccharide moiety attached to the C16β-OH position on the D ring of sapogenin aglycone; these structural features are markedly different from most saponins, which bear sugar moieties substituted at the 3β-OH position on A ring [4,15–18] (Fig. 1). OSW-1 has exhibited highly potent and selective anticancer activities in several human cancer cell lines including HeLa cells (IC_{50} = 0.5 nM) and HL-60 cells (IC_{50} = 0.25 nM) [17–20]. Structure and activity relationship (SAR) studies have shown that the presence of the acyl groups on the sugar moiety is required to exhibit significant biological activity. In fact, removal of the methoxybenzoyl group on the D-xylose moiety caused a ~40-fold drop in the cytotoxicity index, and successive removal of the acetyl group in the L-arabinose moiety caused a ~800-fold decrease in cytotoxicity [13].

Several saponins have been found to exhibit membrane permeabilization activities and hemolytic effects [21] in a sterol-depending manner [22–24]. Cholesterol (Chol) is a major (20 to 50%) lipid component of the mammalian plasma membrane that provides stability to the membrane and controls permeability to various solutes [25–27]. Some possible molecular mechanisms have been proposed to explain the membrane permeabilization and breaking-down activities of the saponins [28,29]. Previous studies have proposed that the saponins and membrane sterols form equimolecular complexes in the membrane,

Abbreviations: OSW-1, 3β,16β,17α-trihydroxycholest-5-en-22-one 16-*O*-(2-*O*-4-methoxybenzoyl-β-D-xylopyranosyl)-(1 → 3)-2-*O*-acetyl-α-L-arabinopyranoside; POPC, 1-palmitoyl-2-oleoyl-*sn*-glycero-3-phosphocholine; DOPC, dioleoyl-*sn*-glycero-3-phosphocholine; DMPC, 1,2-dimyristoyl-*sn*-glycero-3-phosphocholine; CTL, cholestatrienol; Chol, cholesterol; Erg, ergosterol; Epichol, 3-epicholesterol; PBS, phosphate buffered saline; LUVs, large unilamellar vesicles; MLVs, multilamellar vesicles; MβCD, methyl-β-cyclodextrin; PVDF, polyvinylidene fluoride; EDTA, ethylenediaminetetraacetic acid; RBC, red blood cells/erythrocytes

* Corresponding authors at: Department of Chemistry, Graduate School of Science, Osaka University, 1-1 Machikaneyama, Toyonaka, Osaka 560-0043, Japan.
E-mail addresses: hanashimas13@chem.sci.osaka-u.ac.jp (S. Hanashima), murata@chem.sci.osaka-u.ac.jp (M. Murata).

http://dx.doi.org/10.1016/j.bbamem.2017.09.019
Received 12 June 2017; Received in revised form 5 September 2017; Accepted 18 September 2017
Available online 22 September 2017

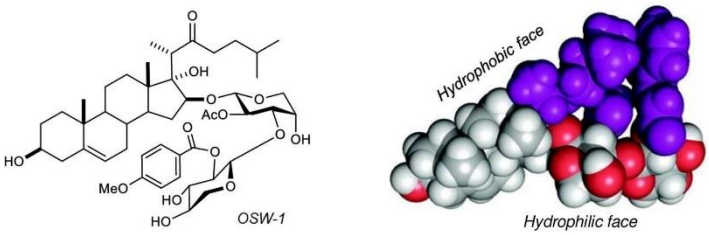

Fig. 1. Structure of OSW-1 (*left*); 3D space-filling representation [18] (*right*).

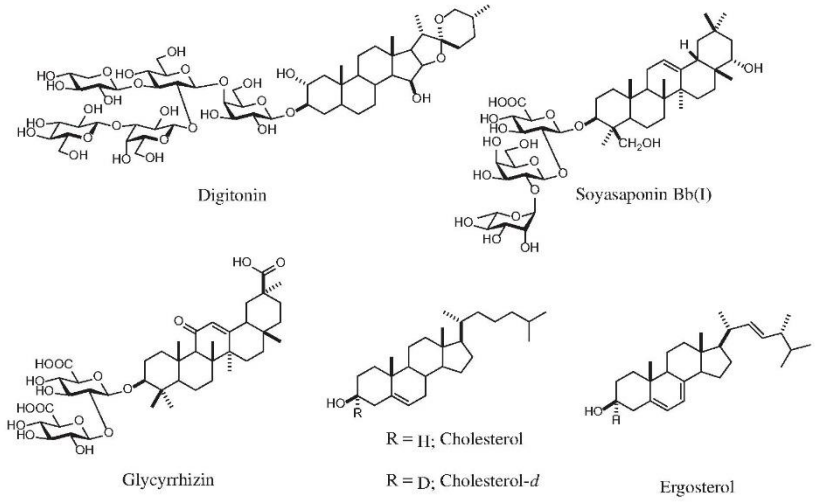

Fig. 2. Structures of digitonin, soyasaponin Bb(I), glycyrrhizin, cholesterol, and ergosterol.

resulting in hydrophilic interactions between the sugar moieties, creating defects in the lamellar structure in the form of spherical buds and/or tubules [30,31]. Another study has proposed a mechanism based on the formation of toroidal pores in which hydrophilic interactions between sugar moieties lead to saponin-sterol aggregates and formation of pores [23]. A separate study proposed that some saponins showed concentration-dependent membrane permeabilization based on the organization and arrangement of the saponins. Below the critical micelle concentration (CMC), saponin monomers bind to the external monolayer to induce an area difference and curvature, which results in vesiculation. Above the CMC, saponins induce direct pore formation and a loss of membrane materials [32,33]. Permeabilization is an effect of direct interactions of micelles with the cell membrane, which leads to the deposit of high amounts of saponins near the membrane. In addition, immediate membrane permeabilization was observed upon the interaction of saponins with Chol-enriched domains [1]. With these proposed mechanisms, digitonin (Fig. 2A), a typical saponin isolated from *Digitalis purpurea*, can be classified into the concentration-dependent membrane action model. Digitonin has shown significant membrane-disrupting activity, leading to a permanent insertion into the membrane because of aggregation and equimolecular complex formation with Chol and phospholipids [15,34,35]. On the other hand, the mechanism of interaction of soyasaponin Bb(I) (Fig. 2B), isolated from soy bean, has not been completely elucidated although ^{2}H NMR measurements revealed that the interaction of soyasaponin with membrane Chol renders less ordered and more flexible membrane constituents [36]. The membrane-interaction mechanism of OSW-1 remains unclear because of the unique glycosylation position as well as the hydrophobic caps on the sugar hydroxy groups, which likely provide distinguishable amphiphilic properties from other saponins.

This study aimed to gain insights into the sterol interactions of the unique steroidal saponin OSW-1 to elucidate possible molecular mechanisms of membrane permeabilization by using model lipid bilayers. Membrane interactions with OSW-1 are thought to be very important to gain a deeper understanding of the mechanism of action in potent and selective cytotoxic activity. Spectroscopic studies, including solid state ^{2}H and ^{31}P NMR, provided evidence of the ability of OSW-1 to permeabilize artificial and biological membranes in a sterol-dependent manner. Digitonin (Fig. 2**A**), as a strong membrane-disrupting steroidal saponin, soyasaponin Bb(I) and glycyrrhizin (Fig. 2**B** and **C**), as weakly permeabilizing triterpene saponins, were adopted as examples of the well-known saponins to evaluate the membrane activity of OSW-1 [1]. By comparing the activities of these typical 3-*O*-glycosyl saponins with those of OSW-l, the general mechanism underlying the membrane activity of typical saponins could also be investigated from a different viewpoint.

2. Materials and methods

2.1. Materials

All phospholipids, 1-palmitoyl-2-oleoyl-*sn*-glycero-3-phosphocholine (POPC), 1,2-dimyristoyl-*sn*-glycero-3-phosphocholine (DMPC), and dioleoyl-*sn*-glycero-3-phosphocholine (DOPC) were purchased from

Avanti Polar Lipids, Inc. (Alabaster, AL, USA). Cholesterol (Chol), ergosterol (Erg) and 3-epicholesterol (Epichol) were purchased from Sigma-Aldrich (St. Louis, MO, USA), Tokyo Kasei (Tokyo, Japan), and Steraloids (Newport, RI, USA), respectively. Cholesterol-*d* was synthesized according to a previous report [37]. Digitonin, glycyrrhizin, diosgenin, phospholipid C, and cholesterol E test kits were obtained from Wako (Osaka, Japan). Soyasaponin Bb(I) was purified from commercially available soybean saponin, Soy Health SA (Fuji Oil Company Ltd., Tokyo, Japan). Calcein, methyl-β-cyclodextrin (MβCD), verapamil, theophylline, glucose, sucrose, raffinose, and polyethylene glycol (PEG) were purchased from Nacalai Tesque (Kyoto, Japan). The 96-well microplates were purchased from Greener Bio One (Monroe, NC, USA) and Thermo Scientific (Waltham, MA, USA). OSW-1 was isolated and purified from the bulbs of *Ornithogalum saundersiae* belonging to the Aparagaceae family, originating from South Africa, as previously reported by Kubo et al. with modifications [13,18]. Cholestatrienol (CTL) was generously provided by Prof. J Peter Slotte (Åbo Akademi University, Turku, Finland), prepared using a previously published method [38]. All other chemicals used are of standard and analytical quality.

2.2. Calcein leakage assays

The extent of saponin-induced leakage was determined by measuring the intensity of calcein fluorescence released from large unilamellar vesicles (LUVs) [39]. LUVs composed of pure POPC, 9:1 POPC/Chol, POPC/Erg, and POPC/Epichol were dissolved in $CHCl_3$ in a round-bottom flask. The solvent was removed under reduced pressure at 35 °C and further dried overnight *in vacuo*. The lipid film was rehydrated with 60 mM calcein (1 mL) in 10 mM Tris-HCl buffer containing 150 mM NaCl and 1 mM EDTA at pH 7.4. The solution was vortexed for 1 min and subjected to five cycles of freezing (−20 °C) and thawing (65 °C) to obtain multilamellar vesicles (MLVs). The suspension was allowed to pass through LiposoFast Basic extruder (pore size, 200 nm, Avestin Inc., Ottawa, Canada) 19 times to obtain homogeneous LUVs. Homogeneous LUVs were purified using a Sepharose 4B column (GE Healthcare, Uppsala, Sweden). The lipid and Chol concentrations of the LUV fraction were quantified using the phospholipid C test and cholesterol E test kits, respectively. The final concentrations of the phospholipid and Chol in the resulting LUVs were 27 μM and 3.1 μM, respectively. Prepared LUVs were immediately used for measurement to avoid premature vesicle leakage. LUVs were placed in a 96-well Nunclon Delta Surface (black) F-bottom microplate (Thermo Scientific), and the initial fluorescence was measured using a fluorescence microplate reader (MTP-800 series, Corona Electric Multimode Microplate Reader) with an excitation wavelength of 490 nm and an emission wavelength of 517 nm. Saponins were added to the LUVs which were mixed at a slow speed for 1 min. The mixture was allowed to stand at room temperature for 2 h. To obtain the condition of 100% leakage, 10% Triton-X was finally added to each well, subsequently followed by fluorescence measurements. All experiments were performed in triplicate, and the % calcein leakage was calculated using the equation:

$$\%\text{calcein leakage} = \frac{I_S - I_0}{I_T - I_0} \times 100$$

where I_S, I_T, and I_0 are the fluorescence intensities after saponin addition, at 100% LUV leakage, and background, respectively.

2.3. Hemolytic activity under Chol depletion conditions and osmotic protection experiments

The effect of Chol on the hemolytic activity of saponins was investigated using a Chol depletion/repletion experiment [32]. Freshly obtained human blood samples were washed with 10 mM phosphate buffered saline (PBS) at pH 7.4 and centrifuged at 2000 rpm for 5 min. The pellet was resuspended in PBS to obtain a 10% (v/v) red blood cell (RBC) solution. The solution was divided into three portions. The first portion was resuspended with PBS to obtain 1% (v/v) solution of non-depleted RBCs. The second portion was treated with 3.5 mM methyl-β-cyclodextrin (MβCD) at 37 °C for 2 h, and the cells were centrifuged and then resuspended with PBS to obtain Chol-depleted red blood cells 1% (v/v) solution. The third portion was treated similarly as the second portion, but in addition, the cells were incubated with 7:1 mol ratio of Chol/MβCD at 37 °C for 2 h to replenish Chol in the cell membrane. The samples were centrifuged and resuspended with PBS to obtain 1% (v/v) Chol-repleted solution [40,41].

The cells were transferred into a 96-well microplate and saponins with concentrations ranging from 0 to 300 μM were added to the assigned wells, followed by mixing at moderate speed. The samples were incubated for 18 h at 37 °C, and then centrifuged at 2000 rpm for 5 min. The supernatants were carefully transferred to a separate 96-well microplate. The absorbance of the samples was measured at 450 nm using a microplate reader (Corona Electric). A mixture of milliQ water/10% RBC (v/v; 9:1 volume ratio) was used as a positive control, and 1% (v/v) RBC/PBS (18:1 volume ratio) was used as the blank. Triplicate samples were prepared for each saponin concentration. The degree of hemolysis was calculated using the absorption at 450 nm (A) according to the formula:

$$\%\text{hemolysis} = \frac{A_{sample} - A_{blank}}{A_{positive\ control}} \times 100$$

2.4. Osmotic protection against hemolysis

Osmotic protection experiments under the conditions of hemolysis assays were also conducted to estimate the size of pore or channels formed by saponin in lipid bilayers. Red blood cells (RBC, 1% v/v) were prepared as described earlier. Osmotic protectants purchased from Nacalai Tesque (Kyoto, Japan) including glucose, sucrose, raffinose, PEGs 600, 1000, 1540, 2000, 4000 and 6000, which has the estimated molecular diameters of 0.7, 0.9, 1.1, 1.6, 2.0, 2.4, 2.9, 3.8 and 5.1 nm, respectively, were utilized in this experiment. A concentration of 30 mM of osmotic protectants was added to the RBC solution prior to addition of saponin samples. In this experiment we used twice the concentration of the reported EC_{50} values (2 x EC_{50}) of digitonin and OSW-1 as the basis for measurement. Amphotericin B (AmB, EC_{50} = 2.0 μM) which pore size has been reported, was used as control [42]. The information obtained from this assay is described by the ability of the saponins to induce hemolysis in the presence of various osmotic protectants. If the protecting agent added to the assay mixture is too large to pass through the pore or channel formed in the membrane of erythrocytes, no hemolysis should be observed, which indicates that there is a balance between the osmotic pressure of the intracellular hemoglobin and that of the protecting agent in the extracellular solution. Therefore, we can give a rough estimate of the size of the pore or channel using these protecting agents. The measurement of saponin-induced hemolytic activity in the presence of various osmotic protectants was done using a microplate reader (Corona Electric) at 450 nm. Experiments were performed in triplicate.

2.5. CTL fluorescence spectroscopy in solution and with liposomes

In solution experiments, saponins with varying concentrations were added to the CTL solutions (4 μg/mL) in 10 mM PBS at pH 7.4, containing 0.1% dimethyl sulfoxide (DMSO) and incubated at 25 °C for 3 h. In liposome experiments, CTL was incorporated in LUVs to examine the effect of saponins on Chol incorporated in a lipid environment. LUVs composed of 90:9:1 POPC/Chol/CTL were prepared by dissolving the lipid mixture in $CHCl_3$, which was sonicated for 1 min. The solvent was dried under reduced pressure and further dried *in vacuo*. The lipid film was rehydrated with 10 mM PBS at pH 7.4 and subjected to five cycles of freezing (−20 °C) and thawing (65 °C) to obtain the MLVs. The MLVs

were extruded 31 times to obtain homogeneous LUVs with size of approximately 200 nm. The LUV components, POPC, Chol, and CTL were quantified using phospholipid C test, cholesterol E test and the CTL UV extinction coefficient at 325 nm (11,000 cm^{-1} M^{-1}), respectively. Saponin, at varying concentrations, was incubated with the LUVs in PBS at 25 °C for 3 h. The fluorescence emission of the assay mixture was measured using FP 6500 spectrofluorometer (Jasco Corp., Tokyo, Japan) at 25 °C. The excitation wavelength was set to 325 nm (5.0-nm slit width), and the emission was scanned from 340 nm to 450 nm (1.0-nm slit width). The fluorescence intensity was recorded as a function of emission wavelength. Experiments were performed in triplicate.

2.6. Solid-state ^2H NMR

Membrane samples for solid state ^2H NMR, composed of POPC (47 μmol), Chol-*d* (5.3 μmol), and saponin (0 and 0.5 to 5.3 μmol) were prepared as previously published [43]. The lipid mixture was dissolved in 2:1 (v/v) $CHCl_3$/MeOH in a round-bottom flask and sonicated for 2 min. The solvent was removed under reduced pressure and further dried overnight *in vacuo*. The lipid film was rehydrated with milliQ water and was sonicated and vortexed for 1 min each. The samples were subjected to three cycles of freezing (−20 °C) and thawing (65 °C) to obtain the MLVs. The MLV suspension was lyophilized overnight and rehydrated with deuterium-depleted water (50% hydration). The suspension was subjected to homogenization by a cycle of vortex mixing, freezing, and thawing. The samples were centrifuged for 5 min at 2000 rpm and transferred into a 5-mm glass tube and sealed with epoxy glue. The quadrupolar splitting in liposome is shown as follows:

$$\Delta\nu = \frac{3}{4} Q \times S_{mol} \times \frac{3\cos^2\theta - 1}{2}$$

where Q is quadrupolar coupling constant, S_{mol} is the order parameter, and θ is the angle between C–D vector and bilayer normal.

All ^2H NMR spectra were recorded with a 300 MHz spectrometer (CMX-300, Agilent, Palo Alto, CA, USA) equipped with a 5 mm ^2H static probe (Otsuka Electronics, Osaka, Japan) using a quadrupolar echo sequence. The 90° pulse width was 2.5 μs, the interpulse delay was 30 μs, echo delay was 20 μs, and the repetition delay was 0.6 s. The sweep width was 250 kHz covered with 8192 points, and the number of scans ranged from 100,000 to 300,000. The probe temperature was set at 30 °C. Spectra were processed using Delta NMR Software (Jeol USA, Inc., Peabody, MA, USA), and the plot was generated using Microsoft Excel Software.

2.7. Solid-state ^{31}P NMR

The membrane preparations in ^2H NMR measurements were used for ^{31}P NMR. The spectra were recorded on a 400 MHz ECA400 (Jeol USA, Inc.) using a 7 mm CP-MAS probe (Doty Scientific, Inc., Columbia, SC, USA) at 30 °C. A single pulse sequence with proton decoupling was employed with the following parameters: acquisition time was 18 ms, 90° pulse width was 7.2 μs, and relaxation delay was 2 s. The sweep width was 113 kHz covered with 8192 points, and the total number of transients per sample was 15,000 to 25,000. All ^{31}P NMR spectra were referenced based on the ^{31}P peak of a 85% phosphoric acid (H_3PO_4) standard set at 0 ppm, measured under the same conditions.

3. Results

3.1. Calcein leakage assays

Chol-dependent membrane permeability and pore formation due to saponins were examined by calcein leakage assays using liposomes (Fig. 3). In this assay, sterol selectivity was also screened using ergosterol (Erg) and 3-epicholesterol (Epichol) in place of Chol. The calcein-entrapped LUVs were treated with varying saponin concentrations and

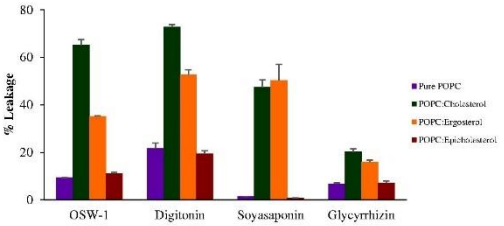

Fig. 3. Sterol-dependent calcein-leakage from POPC liposomes by various saponins (100 μM). The POPC-sterol molar ratio was set to 9:1 and the final concentration of the phospholipid was 27 μM.

the degree of leakage was measured by the increase in fluorescence (Fig. 3) [44]. Calcein leakage assays revealed that OSW-1 exhibited significantly strong permeabilization of Chol-containing liposomes (EC_{50} = 35.4 ± 1.4 μM), but weaker permeabilization of Erg-containing liposomes (EC_{50} = ~100 μM). Furthermore, in the Epichol-containing liposomes, OSW-1 showed insignificant permeabilization, which is almost identical to the result obtained using pure POPC LUVs. Similar results were observed with digitonin and soyasaponin Bb(I) (Table 1 and Fig. 3). These data suggest that initial binding to 3β-hydroxysterols, *i.e.* Chol and Erg, is required for saponin-induced permeabilization to proceed. Chol and Erg are believed to have membrane-stabilizing properties [45]. The saponins may affect this membrane stability and make it more susceptible to leakage by forming pores or inducing membrane disruptions. Soyasaponin Bb(I) showed moderate permeabilization of both 3β-hydroxysterol membranes. The result of this leakage experiment may also imply the importance of the type of sapogenin backbone and the sugar moiety of saponins for membrane interaction [30].

3.2. Saponin-induced hemolysis in usual and Cho-depleted erythrocytes

The dependence of saponins on membrane Chol was assessed by hemolysis tests on RBCs. RBCs were treated with 3.5 mM MβCD to reduce the Chol content to ~10% of the erythrocyte membrane [32,33]. To back up the Chol selectivity, the assay also used RBCs with replenished Chol upon the treated with 7:1 mol ratio of Chol/MβCD [33]. The Chol content of the replenished erythrocytes was found to increase back to ~90% of the initial Chol content of the non-depleted cells.

The result of this assay showed that OSW-1 possesses strong hemolytic activity, which is comparable to that of digitonin (Table 2 and Fig. 4). However, a significant decrease in hemolytic activity by both saponins was observed when Chol was depleted by MβCD treatment. The repletion of Chol in the erythrocyte membrane restored the hemolytic activity of these two saponins. A similar trend was observed with soyasaponin Bb(I), although it shows weaker hemolytic activity than digitonin or OSW-1. Glycyrrhizin showed very weak hemolytic activity (EC_{50} > 300 μM) in all the erythrocyte membrane systems

Table 1
Calcein leakage activity of liposomes in the presence and absence of various sterols.

Saponin	EC_{50} (μM)			
	Pure POPC	POPC/Chol	POPC/Erg	POPC/Epichol
Digitonin	> 100	24.5 ± 1.1	70.5 ± 2.4	> 100
OSW-1	> 100	35.4 ± 1.4	~100	> 100
Soyasaponin Bb(I)	> 100	~100	~100	> 100
Glycyrrhizin	> 100	> 100	> 100	> 100

Values are mean ± SEM.

Table 2
Hemolytic activity of saponins under Chol depletion/repletion conditions.

Saponin	EC_{50} (μM)		
	Non-Depleted	Chol-Depleted	Chol-Repleted
Digitonin	14.3 ± 0.9	> 300	25.4 ± 1.2
OSW-1	7.4 ± 0.8	> 300	12.7 ± 1.1
Soyasaponin Bb(I)	155.6 ± 4.2	> 300	> 300
Glycyrrhizin	> 300	> 300	> 300

Values are mean ± SEM.

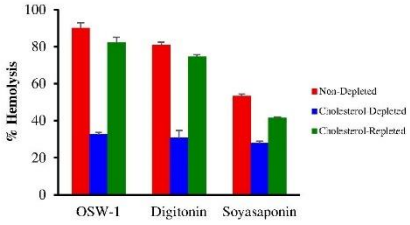

Fig. 4. Hemolytic activity of saponins (300 μM) using non-depleted, cholesterol-depleted and cholesterol-repleted red blood cells. Human RBC (1%) was incubated for 18 h at 37 °C.

(Table 2). The results of this assay suggest that Chol plays an important role in the hemolytic activity of OSW-1, digitonin, and soyasaponin Bb (I) [46–49].

3.3. Osmotic protection experiments

The osmotic protection experiment yielded information on the pore size created by saponins as a consequence of hemolysis. First, the result for AmB was consistent with published data [42] in which the estimated pore diameter was ~0.9 nm (Fig. 5, yellow). Surprisingly in digitonin, hemolysis did not suppress in all conditions (Fig. 5, blue). For OSW-1, hemolytic activity started to suppress in the addition of PEG-600 and did not exhibit hemolytic activity in the presence of PEGs with larger size. This shows that OSW-1 was able to create pores with diameter of ~1.6 nm (Fig. 5, green). In digitonin, the observed hemolytic activity in the presence of the osmotic protectants is attributed to its detergent activity that caused direct leakage of hemoglobin *via* membrane disruption or cholesterol removal from membrane core [50]. In the case of OSW-1, release of hemoglobin could be characterized by

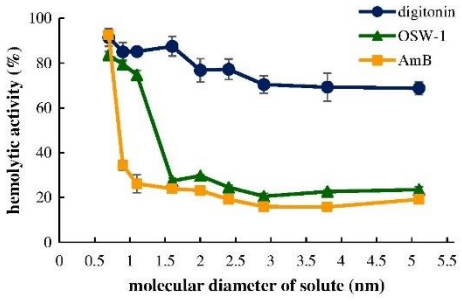

Fig. 5. Osmotic protection experiments for saponins using 1% (v/v) RBC. Pore size was estimated using various osmotic protectants (30 mM). The concentrations of digitonin, OSW-1, and AmB were 28.7 μM, 14.9 μM, and 4.0 μM, respectively.

saponin-Chol interaction that leads to invagination of red blood cells and subsequent formation of distinct pores [42].

3.4. Binding of saponin to membrane Chol, measured by fluorescence spectroscopy using CTL

In order to investigate the ability of saponins to bind to Chol, cholestatrienol (CTL), a structurally close analog of Chol, was employed. In an aqueous environment (above CMC of CTL, 1 nM) [51], a significant increase in CTL fluorescence intensity was observed with increasing OSW-1 concentration, which is attributed to the dose-dependent aggregation of OSW-1 with CTL (Fig. 6**A**, blue). The increasing intensity of emission (396 nm) as OSW-1 concentration increases indicates that the aggregates of CTL, where the self-quenching of its fluorescence occurs, are dissociated upon interacting with the saponin, which causes CTL to partition to a more hydrophobic environment [52,53] (Fig. 6**C**). The result suggests that the aggregated structure of CTL is separated into a monomeric state to favor interaction and formation of mixed aggregates with OSW-1. The result of this experiment shows that OSW-1 tends to form a complex with Chol. Likewise, digitonin (Fig. 6**A**, black) showed a similar pattern to OSW-1. On the other hand, glycyrrhizin (Fig. 6**A**, green) showed no significant changes in fluorescence intensity with increasing concentration, indicative of its weak binding affinity with CTL.

The effect of saponins on CTL fluorescence in a bilayer environment was assessed by using LUVs composed of POPC/Chol/CTL (molar ratio of 90:9:1). A similar study had previously been performed for triterpene saponins by using MLVs [32]. CTL in LUVs was incubated with saponins for 3 h and subjected to fluorescence measurements. In the bilayer environment, the fluorescence intensities of CTL decreased in a concentration dependent manner at lower concentrations and showed the lowest average intensity at 10 μM saponins except for glycyrrhizin. In contrast, fluorescence intensities increased when saponins' concentrations were 30 μM and further increased at 100 μM (Fig. 6**B**, blue). The observed decrease in fluorescence intensities could be attributed to the reduction in fluorescence lifetime due to the perturbation of the lipid packing by OSW-1 and other saponins [54]. The prominent increase in the fluorescence intensity above 30 μM OSW-1 could be attributed to formation of OSW-1/Chol mixed micelles [55]. Interaction of Chol with a very high content of OSW-1, where the saponin concentration was higher than lipid concentration, causes a disruption of the bilayer structure and leads to the formation of the micelles largely in the aqueous phase [51,52,56], which significantly increases fluorescence life time due to the tight interaction of OSW-1/CTL in the micelles. Comparable results were observed with digitonin (Fig. 6**B**, black). Soyasaponin Bb(I) showed slightly weaker effect (Fig. 6**B**, red). In addition, dynamic light scattering (DLS) experiments demonstrated that the size of the LUVs significantly decreased upon the addition of 30 μM OSW-1 (Table S4 and Fig. S2). A similar reduction in particle size was observed for digitonin, while soyasaponin Bb(I) showed only a marginal reduction (Table S4).

3.5. Solid state ^2H NMR for examining saponin/Chol interaction

The results described in the previous sections implied that the direct molecular interaction of OSW-1/Chol is important for membrane disruption activity partly due to formation of mixed micelles. Thus, we next measured solid-state ^2H NMR spectra to determine the molecular interaction between sterol and saponins in bilayer membranes through signal broadening and splitting [43,57,58]. The quadrupolar splitting pattern is greatly influenced by the molecular mobility and orientation (the C–D vector) with respect to the bilayer normal and thus, is often used to detect the direct interaction between membrane active compounds and Chol-*d* in membrane. We used a 9:1 POPC/Chol-*d* system to examine saponin/Chol interaction (Fig. 7) [57,58]. A typical Pake doublet shown in Fig. 7**A** represents the usual molecular mobility of

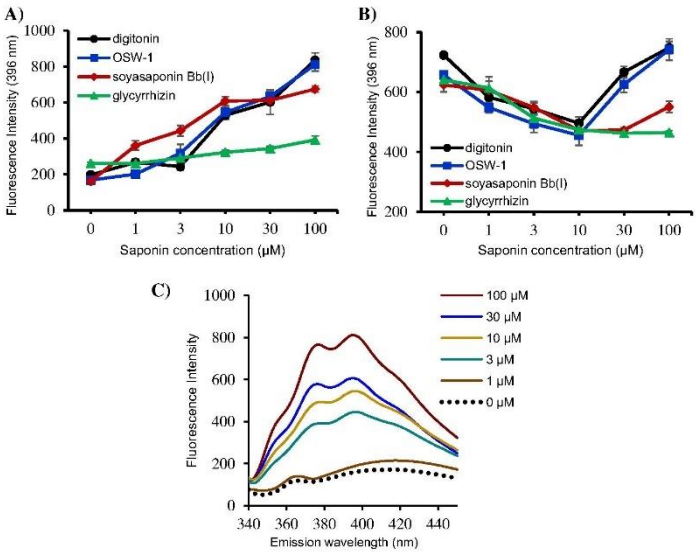

Fig. 6. Fluorescence intensities of cholestatrienol (CTL) at different saponin concentrations. CTL was excited with 325 nm and the intensities of the maximum emission (396 nm) were plotted in aqueous media (**A**) and in LUV (**B**). Fluorescence emission spectra of increasing concentrations of OSW-1 in aqueous media (**C**). The POPC-Chol-CTL molar ratio was set to 90:9:1 and the final concentration of the phospholipid was 177 μM.

Chol-*d* in POPC membranes at 30 °C. As depicted in Fig. 7**B** and **D**, OSW-1 and glycyrrhizin significantly reduced the splitting width of the Pake doublet without affecting the gross signal shape. On the other hand, the ^{2}H NMR spectra of digitonin showed the complete disappearance of the Pake doublet (Fig. 7**C**), which is in sharp contrast to the OSW-1 spectra (Fig. 7**B**). The disappearance of the signals could be attributed to the direct interaction between digitonin and Chol that results in formation of large aggregates.

3.6. Solid state ^{31}P NMR for examining membrane integrity

To further examine the effect of saponins on the physical properties

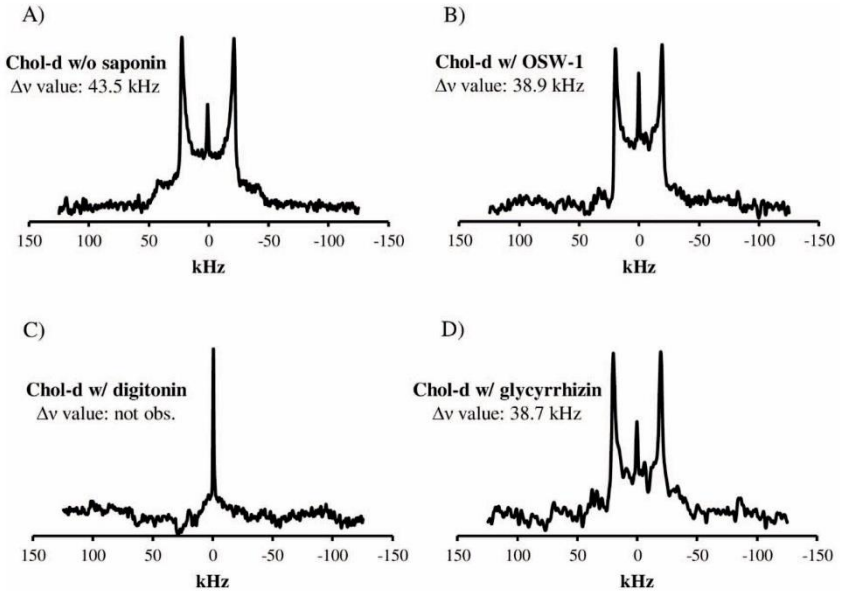

Fig. 7. ^{2}H NMR spectra of Chol-*d*/POPC bilayers (molar ratio 1:9) in the absence of saponins (**A**) and presence of OSW-1 (**B**); digitonin (**C**); and glycyrrhizin (**D**). All the saponin-containing membranes were prepared at the molar ratio of Chol-*d*-saponin, 1:0.5. ^{2}H NMR spectra were measured at 30 °C. The isotropic signals at 0 ppm are due to the presence of residual deuterium water in the prepared samples. The concentrations of POPC, Chol and saponin in the multilamellar vesicles (MLVs) were 47, 5.3, and 2.7 μmol, respectively.

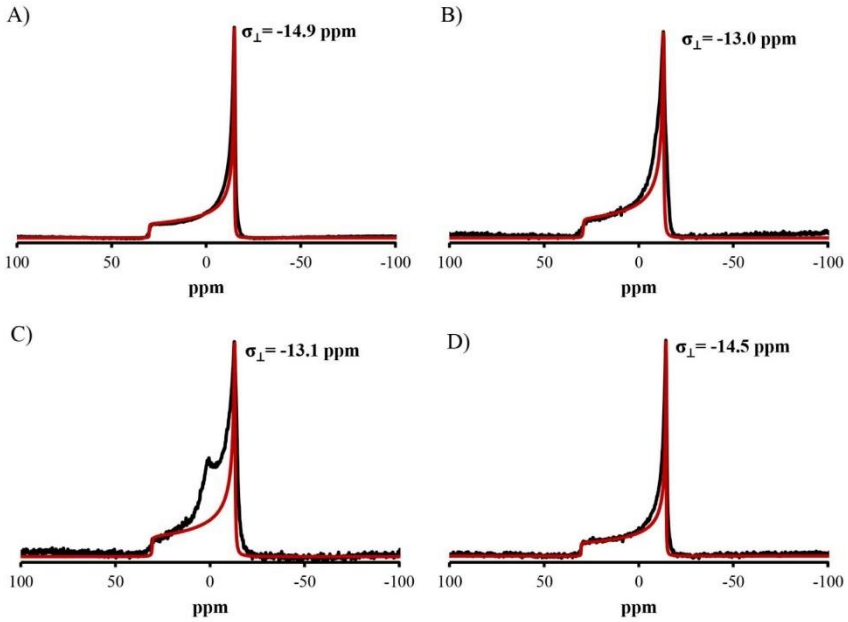

Fig. 8. ^{31}P NMR spectra (black —) of MLVs consisting of POPC/Chol (9:1) in the absence of saponins (**A**) and presence of OSW-1 in the Chol/OSW-1 M ratio of 1:0.5 (**B**); digitonin in the Chol/digitonin molar ratio of 1:0.5 (**C**); glycyrrhizin in the Chol/glycyrrhizin molar ratio of 1:0.5 (**D**). ^{31}P NMR spectra were measured at 30 °C and referenced from 85% phosphoric acid (H_3PO_4) peak set at 0 ppm. Red (—) spectra corresponds to computer simulation using SIMPSON software [59].

of membrane such as a morphological change, ^{31}P NMR spectra were recorded in the presence and absence of a saponin. The spectra in Fig. 8**A** show the axially symmetrical pattern for a typical lamellar structure. The spectra of saponins show the reductions in the signal widths, which can be attributed to the increased curvature due to binding of saponin on membrane; the effect is more evident for OSW-1 than for glycyrrhizin, which is consistent with the results of DLS (Table S4 and Fig. S2). In the spectrum of digitonin, an isotropic peak is observed at 0 ppm (Fig. 8**C**). The presence of the isotropic signal is attributed partly to formation of small particles, while the large portion of membrane stays in the lamellar structure at this saponin/lipid ratio, as shown by gross overlap with the red trace of the axially symmetrical pattern [32].

4. Discussion

In the present study, we have carried out several experiments on the membrane interactions and disrupting activities of OSW-1 and 3-*O*-glycosyl saponins using both erythrocyte and model membranes. For both of the membrane systems, we observed that the membrane-disrupting activity of OSW-1 is markedly Chol-dependent and the potency of the activities in EC_{50} values is in the tens of micromolar range in both systems, albeit their large differences in membrane composition. These results suggest that formation of OSW-1/Chol complexes is mainly responsible for its membrane disruption activity as is the case with digitonin; several studies on saponins have established the importance of Chol in their membrane permeabilization [23,24,30,32–34,60]. In our study, we scrutinized the membrane activity of OSW-1 in comparison with well-known saponins to deduce a possible mechanism of action for its membrane-permeabilizing activities. The unique structure of OSW-1, in which the partially acylated sugar chain is attached at the D ring of the steroidal aglycone, intrigued us to investigate its interaction with Chol and the mode of membrane activity. The hydrophilic face of the OSW-1 molecule due to the presence of three hydroxy groups resides near a side chain, as shown in Fig. 1 according to the previous report by Sakurai et al. [18]. Moreover, the overall three-dimensional structure of OSW-1 was found to have a flat triangular shape, which could play a role in exerting its potent bioactivity [18]. This characteristic amphiphilic polarity likely differentiates the binding mode of OSW-1 to Chol from that of usual saponins such as digitonin that bears a 3-*O*-sugar chain. However, even though it possesses such a unique chemical structure, OSW-1 showed Chol-dependent membrane activity comparable with digitonin.

First, we found that Chol is crucial for the potent hemolytic activity of OSW-1 as is the case with digitonin, as seen in the hemolysis and calcein leakage experiments (Figs. 3 and 4). Moreover, the membrane permeability caused by the two saponins is highly sterol-dependent, as observed in the calcein leakage assays (Fig. 3) and PAMPA permeation (Table S1). These data indicate that OSW-1, as well as digitonin, preferentially recognize a sterol core. We further assessed the ability of saponins to bind to CTL by measuring its fluorescence in aqueous and bilayer environments. The high affinity of OSW-1 to Chol observed in the CTL binding assay (Fig. 6) is thought to be attributable to the stable hydrophobic interaction between the steroid rings of both molecules in a face-to-face manner (Fig. 1). Although OSW-1 and digitonin showed similarities in membrane-disrupting activities, OSW-1 is unlikely to be oriented perpendicular to membrane as observed in digitonin upon binding to Chol with the face-to-face interaction [61,62]. This is because such a parallel interaction with the head groups of Chol and lipids is hampered by the triangular shape of OSW-1 in which the hydrophilic sugar moiety resides apart from the 3-OH group (Fig. 1).

In contrast to the close similarity between OSW-1 and digitonin in the membrane activity, solid-state ^{2}H NMR and ^{31}P NMR spectra showed marked differences between the two compounds. The ^{2}H

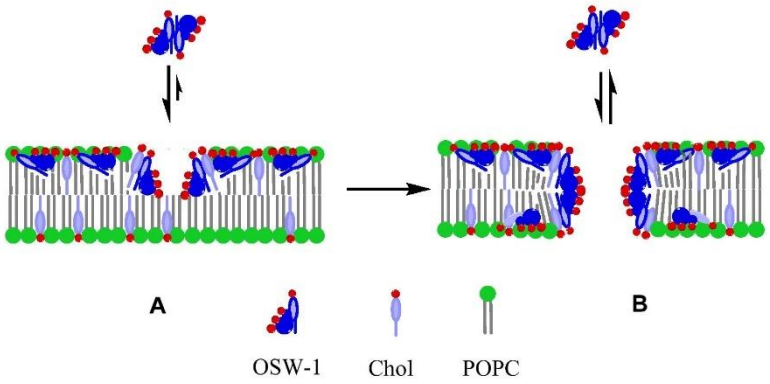

Fig. 9. Hypothetical mechanism for the membrane-permeabilizing effect of OSW-1 in Chol-containing membranes. (A) Accumulation of OSW-1 in Chol-containing membrane causes small membrane defects. (B) Further binding of OSW-1 results in the formation of a barrel-stave-like assembly.

Table 3
Estimated size of pores induced by saponin addition.

Saponin	Pore diameter (nm)
Digitonin	> 5.1
OSW-1	~1.6
Amphotericin B	~0.9

spectra of Chol-*d* revealed that digitonin significantly slows down the rotational motion of Chol, which resulted in a complete broadening of the Pake doublet (Fig. 7**C**). The disappearance of the ^{2}H NMR signal induced by digitonin suggests that saponin forms large aggregates with Chol as reported previously [35,61], which greatly reduce the mobility of Chol-*d* as seen for the other membrane-active compounds [43,58,63]. The ^{31}P NMR spectra of POPC with digitonin showed the presence of a broad peak near 0 ppm (Fig. 7**C**), which could be attributed to an increase in membrane curvature or a reduction in the vesicle size without greatly affecting the overall morphology of the membrane [32,61]. Appearance of the small isotropic peak in the ^{31}P NMR implies that digitonin at this saponin/lipid ratio partly induces membrane deformation [32] while the mobility of Chol in the deformed area is markedly restricted. This notion indicates that the tight interaction between digitonin and Chol in large aggregates immobilizes Chol molecules, supporting the previous report by Frenkel et al. [61]. On the other hand, OSW-1 did not reduce the ^{2}H NMR signal intensity but rather elicited a change in $\Delta\nu$ of Chol-*d*, as shown in Fig. 7**B**. The decrease in $\Delta\nu$ by 4.6 kHz after incorporation of 5 mol% OSW-1 suggests that the direct interaction between OSW-1 and Chol-*d* results in the tilt of the Chol axis against the bilayer normal. The molecular interaction between OSW-1 and Chol could partly be attributed to the face-to-face contact between their hydrophobic cores in the membrane. Additionally, the presence of the unusual sugar moiety and the orientation of OSW-1 [18] may have induced changes in the packing of the membrane and contributed to the observed reduction in the $\Delta\nu$ value. Furthermore, the ^{31}P NMR showed that, except for digitonin, the overall lamellar structure of the membrane was not significantly affected by saponins including OSW-1 at 1:0.5 Chol/saponin ratio, but a noticeable shift of the $\sigma_{\perp}$ value was observed, probably due to the gross changes in membrane curvature [32]. The conservation of the basic lamellar structure of the membrane after addition of OSW-1 clearly shows that there are no significant modifications in the arrangement of the surrounding phospholipids [43]. In the ^{2}H NMR spectra in Fig. 7, glycyrrhizin induced significant reduction in the $\Delta\nu$ value while it showed very weak membrane activity (Figs. 3, 4 and 6). It is worth noting that glycyrrhizin possibly binds to membrane Chol to a certain extent as previously suggested by monolayer experiments [64] but hardly perturbs the membrane integrity as revealed by the ^{31}P signal (Fig. 7**D**).

The ability of saponins to disrupt the bilayer structure and cause membrane permeabilization has already been described in several reports [22–24,28–33,61]. However, a very few mechanistic studies [65] have been carried out on saponins with unusual polarity such as OSW-1; the structure-activity relationship study has been reported for triterpene saponins bearing two sugar chains at rings A and D [66]. Hereon, we attempted to deduce the possible mechanism of interaction by OSW-1 towards membrane permeabilization. The present results particularly highlight the important role of Chol in membrane-permeabilization; we have conducted similar NMR-based studies on membrane active natural products such as amphidinol 3 [43] and theonellamide-A [63,67,68]. At the first step, OSW-1 molecules bind to Chol in the membrane, leading to an accumulation of OSW-1 on the surface of the outer leaflet. Next, the binding of the saponin leads to the formation of an OSW-1/Chol complex, followed by penetration into the hydrophobic interior of a bilayer (Fig. 9**A**). Lastly, Chol leads OSW-1 to a deeper insertion into the membrane core and causes transient pore formation and subsequent membrane deformations (Fig. 9**B**), without greatly affecting the overall bilayer structure [1,32,33]. Osmotic protection experiments (Table 3 and Fig. 5) suggest that OSW-1 was able to create small pores with diameter of up to 1.6 nm in erythrocyte membrane. With the present results, the mode of action of OSW-1 can use either the toroidal pore or barrel stave pore. When we look closer at the results of the ^{31}P NMR and the osmotic protection, the mechanism of OSW-1 may be directed towards the barrel stave model. Amphidinol 3 [43] and alamethicin [69], which are thought to form barrel-stave pore, hardly elicit ^{31}P spectral changes and form relatively small pores with narrow size distributions.

In calcein leakage experiments using artificial model membranes, the membrane-permeabilizing activity of OSW-1 (EC_{50} = 35.4 ± 1.4 μM) is much weaker than the reported EC_{50} values in cell-based assays (EC_{50} is around 0.5 nM) [17–20]. Saponins have been generally found to interact with membrane sterols and promote aggregation [70], where slight changes in the composition of membrane lipids and cholesterol could alter the susceptibility of membrane to saponin-induced cytotoxicity [24,71]. More importantly, interactions with other cell components including specific signaling proteins may contribute to the high cellular toxicity of saponins; OSW-1 has been reported to induce apoptosis through inhibition of the sodium-calcium exchanger [72] and interaction with cytoplasmic proteins [73]. The present PAMPA results in the present study revealed that OSW-1 far below the membrane-disrupting concentration permeates a Chol-containing POPC membrane, indicating that OSW-1 can rapidly pass through cellular membrane to reach the cytoplasmic side without transporters or endocytosis. In the case of digitonin and other usual saponins, disruption of

the bilayer structure is a prerequisite for membrane penetration while OSW-1 probably passes through the membrane at lower concentrations with its less hydrophilic structure; the number of hydroxy groups in OSW-1 is 5 while that of digitonin is 17. These characteristic features of OSW-1 may partly account for its extremely potent cytotoxicity.

5. Conclusion

Our present work aimed to elucidate the mechanism of interaction of OSW-1 with membranes in the presence or absence of Chol and its membrane-permeabilizing properties through the use of spectroscopic methodologies. Results of the experiments suggest a strong and highly Chol-dependent OSW-1 interaction with membranes, as determined by the hemolysis under Chol depletion/repletion assays, and calcein leakage and PAMPA experiments. Solid-state ^{2}H NMR measurements revealed that OSW-1 induces the mobility changes and/or the tilt of Chol against the bilayer normal, as reflected by the decrease in $\Delta\nu$. Moreover, ^{31}P NMR showed that the overall lamellar structure of the membrane is not greatly affected by the OSW-1/Chol interaction. Finally, we deduced a possible mechanism of interaction of OSW-1 with Chol-containing membranes, which could be the key point for the subsequent mechanism, inducing membrane permeabilization *via* possible pore formation. Furthermore, increased interactions between OSW-1 and Chol caused partial membrane deformation, but did not significantly affect the overall membrane integrity. The proposed model in this study needs to be verified by further investigations by means of additional spectroscopic and microscopic experiments.

Transparency document

The https://dx.doi.org/10.1016/j.bbamem.2017.09.019 associated with this article can be found, in online version.

Acknowledgments

We thank Prof. J.P. Slotte of Åbo Akademi University, Turku, Finland, for providing CTL samples used for spectroscopic measurements; Prof. N. Matsumori and Dr. M. Kinoshita for assisting in the DLS measurements, Dr. N. Inazumi and Dr. Y. Todokoro for the assistance of NMR measurements. This work is supported in part by JST ERATO Lipid Active Structure project (Grant Number JPMJER1005) and JSPS KAKENHI Grant Numbers JP16H06315, JP26560448, JP25242073, and JP15K01801.

Appendix A. Supplementary data

Supplementary data to this article can be found online at https://doi.org/10.1016/j.bbamem.2017.09.019.

References

[1] S. Bottger, K. Hofmann, M.F. Melzig, Saponins can perturb biologic membranes and reduce the surface tension of aqueous solutions: a correlation? Bioorg. Med. Chem. 20 (2012) 2822–2828.
[2] J.P. Vincken, L. Heng, A. de Groot, H. Gruppen, Saponins, classification and occurrence in the plant kingdom, Phytochemistry 68 (2007) 275–297.
[3] M. Thakur, M.F. Melzig, H. Fuchs, A. Weng, Chemistry and pharmacology of saponins: special focus on cytotoxic properties, Botanics 1 (2011) 19–29.
[4] K. Hostettmann, A. Marston, Saponins, Cambridge University Press, Cambridge, 1995.
[5] S. van Dyck, P. Flammang, C. Meriaux, D. Bonnell, M. Salzet, I. Fournier, M. Wisztorski, Localization of secondary metabolites in marine invertebrates: contribution of MALDI MSI for the study of saponins in Cuvierian tubules of *H. forskali*, PLoS One 5 (2010) 1–10.
[6] H.W. Liu, J.K. Li, D.W. Zhang, J.C. Zhang, N.L. Wang, G.P. Cai, Isolation of a new glycoside from starfish, *Asterias amurensis* Lutken, and its stimulation activity on the proliferation of the UMR106 cell, J. Asian Nat. Prod. Res. 10 (2008) 521–529.
[7] J. Bruneton, Pharmacognosy, Phytochemistry, Medicinal Plants, Lavoisier, Paris, 4th edn, (2009).
[8] B. Dinda, S. Debnath, B.C. Mohanta, Y. Harigaya, Naturally occurring triterpenoid saponins, Chem. Biodivers. 7 (2010) 2327–2580.
[9] S. Sun, Y. Li, W. Fang, P. Cheng, L. Liu, F. Li, Effect and mechanism of AR-6 in experimental rheumatoid arthritis, Clin. Exp. Med. 10 (2010) 113–121.
[10] X. Yong-xin, Z. Jian-jun, Evaluation of anti-fatigue activity of total saponin *Radix notoginseng*, Indian J. Med. Res. 137 (2013) 151–155.
[11] X. Yang, X. Xiong, H. Wang, J. Wang, Protective effects of *Panax notoginseng* saponins on cardiovascular diseases: a comprehensive overview of experimental studies, Evid. Based Complement. Alternat. Med. 2014 (2014) 1–13.
[12] C. Bachran, S. Bachran, M. Sutherland, D. Bachran, H. Fuchs, Saponins in tumor therapy, Mini-Rev. Med. Chem. 8 (2008) 575–584.
[13] S. Kubo, Y. Mimaki, M. Terao, Y. Sashida, T. Nikaido, T. Ohmoto, Acylated cholestane glycosides from the bulbs of *Ornithogalum saundersiae*, Phytochemistry 31 (1992) 3969–3973.
[14] A. Wojtkielewicz, M. Dlugosz, J. Maj, J.W. Morzycki, M. Nowakowski, J. Renkiewicz, M. Strnad, J. Swaczynova, A.Z. Wilczewska, J. Wojcik, New analogues of the potent cytotoxic saponin OSW-1, J. Med. Chem. 50 (2007) 3667–3673.
[15] T. Akiyama, S. Takagi, U. Sankawa, S. Inari, H. Saito, Saponin-cholesterol interaction in the multibilayers of egg yolk lecithin as studied by deuterium nuclear magnetic resonance: digitonin and its analogues, Biochemistry 19 (1980) 1904–1911.
[16] V.M. Dembitsky, Chemistry and biodiversity of the biologically active natural glycosides, Chem. Biodivers. 1 (2004) 673–781.
[17] K. Sakurai, T. Takeshita, M. Hiraizumi, R. Yamada, Synthesis of OSW-1 derivatives by site-selective acylation and their biological evaluation, Org. Lett. 16 (2014) 6318–6321.
[18] K. Sakurai, T. Fukumoto, K. Noguchi, N. Sato, H. Asaka, N. Moriyama, M. Yohda, Three dimensional structures of OSW-1 and its congener, Org. Lett. 12 (2010) 5732–5735.
[19] J. Zhu, L. Xiong, B. Yu, J. Wu, Apoptosis induced by a new member of saponin family is mediated through caspase-8-dependent cleavage of bcl-2, Mol. Pharmacol. 68 (2005) 1831–1838.
[20] Y. Zhou, C. Garcia-Prieto, D.A. Carney, R. Xu, H. Pelicano, Y. Kang, W. Yu, C. Lu, S. Kondo, J. Liu, D.M. Harris, Z. Estrov, M.J. Keating, Z. Jin, P. Huang, OSW-1: a natural compound with potent anticancer activity and a novel mechanism of action, J. Natl. Cancer Inst. 97 (2005) 1781–1785.
[21] A. el Izzi, T. Bennie, M.L. Thieulant, L. Le Men-Olivier, J. Duval, Stimulation of LH release from cultured pituitary cells by saponins of *Petersianthus macrocarpus*: a permeabilizing effect, J. Plant Med. 58 (1992) 229–233.
[22] P.L. Yeagle, Cholesterol and the cell membrane, Biochim. Biophys. Acta Rev. Biomembr. 822 (1985) 267–287.
[23] C.N. Armah, A.R. Mackie, C. Roy, K. Price, A.E. Osbourn, P. Bowyer, S. Ladha, The membrane-permeabilizing effect of avenacin A-1 involves the reorganization of bilayer cholesterol, Biophys. J. 76 (1999) 281–290.
[24] H. Gogelein, A. Huby, Interaction of saponin and digitonin with black lipid membranes and lipid monolayers, Biochim. Biophys. Acta 773 (1984) 32–38.
[25] D. Papahadjopoulos, Cholesterol and all membrane function: a hypothesis concerning etiology of atherosclerosis, J. Theor. Biol. 43 (1974) 329–337.
[26] H.I. Ingolfsson, M.N. Melo, F.J. van Eerden, C. Arnarez, C.A. Lopez, T.A. Wassenaar, X. Periole, A.H. de Vries, D.P. Tielman, S.J. Marrink, Lipid organization of the plasma membrane, J. Am. Chem. Soc. 13 (2014) 14554–14559.
[27] G. van Meer, A.I.P. de Kroon, Lipid map of the mammalian cell, J. Cell Sci. 124 (2011) 5–8.
[28] E. Shlosser, Interaction of saponins with cholesterol, lecithin, and albumin Ca, J. Physiol. Pharmacol. 47 (1969) 487–490.
[29] A.M. Glauert, J.T. Dingle, J.A. Lucy, Action of saponin on biological cell membranes, Nature 196 (1962) 953–955.
[30] E.A. Keukens, T. de Vrije, C. van der Boom, P. de Waard, H.H. Plasman, F. Thiel, V. Chupin, W.M. Jongen, B. de Krujiff, Molecular basis of glycoalkaloid induced membrane disruption, Biochim. Biophys. Acta 1240 (1995) 216–228.
[31] P.M. Elias, D.S. Friend, J. Goerke, Membrane sterol heterogeneity: freeze-fracture detection with saponins and filipin, J. Histochem. Cytochem. 27 (1979) 1247–1260.
[32] J. Lorent, C.S. Le Duff, J. Quetin-Leclercq, M.P. Mingeot-Leclercq, Induction of highly curved structures in relation to membrane permeabilization and budding by the triterpenoid saponins, α- and δ-hederin, J. Biol. Chem. 288 (2013) 14000–14017.
[33] J. Lorent, L. Lins, O. Domenech, J. Quetin-Leclercq, R. Brasseur, M.P. Mingeot-Leclercq, Domain formation and permeabilization induced by the saponin α-hederin and its aglycone hederagenin in a cholesterol-containing bilayer, Langmuir 30 (2014) 4556–4569.
[34] M. Nishikawa, S. Nojima, T. Akiyama, U. Sankawa, K. Inoue, Interaction of digitonin and its analogs with membrane cholesterol, J. Biochem. 96 (1984) 1231–1239.
[35] G.W. Stockton, C.F. Polnaszek, A.P. Tulloch, F. Hassan, I.C.P. Smith, Molecular motion and order in single-bilayer vesicles with multilamellar dispersions of egg lecithin and lecithin-cholesterol mixtures. A deuterium nuclear magnetic resonance study of specifically labeled lipids, Biochemistry 15 (1976) 954–966.
[36] M. Murata, T. Houdai, A. Morooka, N. Matsumori, T. Oishi, Membrane Interaction of Soyasaponins in Association With Their Antioxidation Effects, 8 Soy Protein Research, Japan, 2005, pp. 81–85.
[37] R. Murari, M.P. Murari, W.J. Baumann, Sterol orientations in phosphatidylcholine liposomes as determined by deuterium NMR, Biochemistry 25 (1986) 1062–1067.
[38] R.T. Fischer, F.A. Stephenson, A. Shafiee, F. Schroeder, delta 5,7,9(11)-cholestatrien-3 beta-ol: a fluorescent cholesterol analogue, Chem. Phys. Lipids 36 (1984) 1–14.
[39] N. Morsy, T. Houdai, K. Konoki, N. Matsumori, T. Oishi, M. Murata, Effects of lipid constituents on membrane-permeabilizing activity of amphidinols, Bioorg. Med.

Chem. 16 (2008) 3084–3090.
[40] G.S. Bignami, A rapid and sensitive hemolysis neutralization assay for palytoxin, Toxicon 31 (1993) 817–820.
[41] K.S. Giddings, A.E. Johnson, R.K. Tweten, Redefining cholesterol's role in the mechanism of the cholesterol-dependent cytolysins, PNAS 100 (2003) 11315–11320.
[42] T. Houdai, S. Matsuoka, N. Matsumori, M. Murata, Membrane-permeabilizing activities of amphidinol 3, polyene-polyhydroxy antifungal from a marine dinoflagellate, Biochim. Biophys. Acta Biomembr. 1667 (2004) 91–100.
[43] R.A. Espiritu, N. Matsumori, M. Tsuda, M. Murata, Direct and stereospecific interaction of amphidinol 3 with sterol in lipid bilayers, Biochemistry 53 (2014) 3287–3293.
[44] J.N. Weinstein, S. Yoshikami, P. Henkart, R. Blumenthal, W.A. Hagins, Liposome-cell interaction: transfer and intracellular release of a trapped fluorescent marker, Science 195 (1977) 489–492.
[45] S.J. Singer, G.L. Nicolson, The fluid mosaic model of the structure of cell membranes, Science 175 (1972) 720–731.
[46] L.N. Yuldasheva, E.B. Carvalho, M.Y. Catanho, O.V. Krasilnikov, Cholesterol-dependent hemolytic activity of *Passiflora quadrangularis* leaves, Braz. J. Med. Biol. Res. 38 (2005) 1061–1070.
[47] M. Luckey, Structural Biology: With Biochemical and Biophysical Foundations, Cambridge University Press, New York, 2008, pp. 13–41.
[48] Y. Lange, J. Ye, M.E. Duban, T.L. Steck, Activation of membrane cholesterol by 63 amphipaths, Biochemistry 48 (2009) 8505–8515.
[49] Y. Lange, J. Ye, T.L. Steck, Activation of membrane cholesterol by displacement from phospholipids, J. Biol. Chem. 280 (2005) 36126–36131.
[50] M. Thelestam, I. Florin, Assay of cytopathogenic toxins in cultured cells, Methods Enzymol. 235 (1994) 679–690.
[51] F. Schroeder, M.E. Dempsey, R.T. Fischer, Sterol and squalene carrier protein interactions with fluorescent $\Delta^{5,7,9(11)}$-cholestatrien-3β-ol, J. Biol. Chem. 260 (1985) 2904–2911.
[52] L.M. Loura, M. Prieto, Dehydroergosterol structural organization in aqueous medium and in a model system of membranes, Biophys. J. 72 (1997) 2226–2236.
[53] K.H. Cheng, J. Virtanen, P. Somerharju, Fluorescence studies of dehydroergosterol in phosphatidylethanolamine/phosphatidylcholine bilayers, Biophys. J. 77 (1999) 3108–3119.
[54] M. Seras, J. Gallay, M. Vincent, M. Ollivon, S. Leseiur, Micelle-vesicle transition of nonionic surfactant-cholesterol assemblies induced by octyl glucoside: a time-resolved fluorescence study of dehydroergosterol, J. Colloid Interface Sci. 167 (1994) 159–171.
[55] Y.J. Björkqvist, T.K. Nyholm, J.P. Slotte, B. Ramstedt, Domain formation and stability in complex lipid bilayers as reported by cholestatrienol, Biophys. J. 88 (2005) 405440–405463.
[56] G. Smutzer, B.F. Crawford, P.L. Yeagle, Physical properties of the fluorescent sterol probe dehydroergosterol, Biochim. Biophys. Acta 862 (1986) 361–371.
[57] N. Matsumori, K. Tahara, H. Yamamoto, A. Morooka, M. Doi, T. Oishi, M. Murata, Direct interaction between amphotericin B and ergosterol in lipid bilayers as revealed by ^{2}H NMR spectroscopy, J. Am. Chem. Soc. 131 (2009) 11855–11860.
[58] R.A. Espiritu, N. Matsumori, M. Murata, S. Nishimura, S.H. Kakeya, S. Matsunaga, M. Yoshida, Interaction between the marine sponge cyclic peptide theonellamide A and sterols in lipid bilayers as viewed by surface plasmon resonance and solid-state ^{2}H nuclear magnetic resonance, Biochemistry 52 (2013) 2410–2418.
[59] M. Bak, J.Y. Rasmusse, N.C. Nielsen, SIMPSON: a general simulation program for solid-state NMR spectroscopy, J. Magn. Reson. 147 (2000) 296–330.
[60] X.X. Li, B. Davis, V. Haridas, J.U. Gutterman, M. Colombini, Proapoptotic triterpene electrophiles (avicins) form channels in membranes: cholesterol dependence, Biophys. J. 88 (2005) 2577–2584.
[61] N. Frenkel, A. Makky, I.R. Sudji, M. Wink, M. Tanaka, Mechanistic investigation of interactions between steroidal saponin digitonin and cell membrane models, J. Phys. Chem. 118 (2014) 14632–14639.
[62] I.R. Sudji, Y. Subburaj, N. Frenkel, A.J. García-Sáez, M. Wink, Membrane disintegration caused by the steroid saponin digitonin is related to the presence of cholesterol, Molecules 20 (2015) 20146–20160.
[63] M. Murata, S. Sugiyama, S. Matsuoka, N. Matsumori, Bioactive structure of membrane lipids and natural products elucidated by a chemistry-based approach, Chem. Rec. 15 (2015) 675–690.
[64] S. Sakamoto, S.H. Nakahara, T. Uto, Y. Shoyama, O. Shibata, Investigation of interfacial behavior of glycyrrhizin with a lipid raft model via a Langmuir monolayer study, Biochim. Biophys. Acta 1828 (2013) 1271–1283.
[65] Y. Ohnishi, K. Tachbana, Synthesis of pavoninin-1, a shark repellent substance, and its structural analogues toward mechanistic studies on their membrane perturbation, Bioorg. Med. Chem. 5 (1997) 2251–2265.
[66] M. Hu, K. Konoki, K. Tachibana, Cholesterol-independent membrane disruption cause by triterpenoid saponin, Biochim. Biophys. Acta 1299 (1996) 252–258.
[67] K. Cornelio, R.A. Espiritu, Y. Todokoro, S. Hanashima, M. Kinoshita, N. Matsumori, M. Murata, S. Nishimura, H. Kakeya, M. Yoshida, S. Matsunaga, Sterol-dependent membrane association of the marine sponge derived bicyclic peptide Theonellamide A as examined by ^{1}H NMR, Bioorg. Med. Chem. 24 (2016) 5235–5242.
[68] R.A. Espiritu, N. Matsumori, M. Murata, S. Nishimura, S.H. Kakeya, S. Matsunaga, M. Yoshida, Interaction between the marine sponge cyclic peptide theonellamide A and sterols in lipid bilayers as viewed by surface plasmon resonance and solid-state ^{2}H nuclear magnetic resonance, Biochemistry 52 (2013) 2410–2418.
[69] K. He, S.J. Ludtke, D. Worcester, H.W. Huang, Neutron scattering in the plane of membranes: structure of alamethicin pores, Biophys. J. 70 (1996) 2659–2666.
[70] P. Seeman, Ultrastructure of membrane lesions in immune lysis, osmotic lysis and drug-induced lysis, Fed. Proc. 33 (1974) 2116–2124.
[71] L.A. Ashworth, C. Green, Plasma membranes: phospholipid and sterol content, Science 151 (1966) 210–211.
[72] C. Garcia-Prieto, K.B.R. Ahmed, Z. Chen, N. Hammoudi, Y. Kang, C. Lou, Y. Mei, Z. Jin, P. Huang, Effective killing of leukemia cells by natural product OSW-1 through disruption of cellular calcium homeostasis, J. Biol. Chem. 288 (2013) 3240–3250.
[73] A.W. Burgett, T.B. Poulsen, K. Wangkanont, D.R. Anderson, C. Kikuchi, K. Shimada, S. Okubo, K.C. Fortner, Y. Mimaki, M. Kuroda, J.P. Murphy, D.J. Schwalb, E.C. Petrella, I. Cornella-Taracido, M. Schirle, J.A. Tallarico, M.D. Shair, Natural products reveal cancer cell dependence on oxysterol-binding proteins, Nat. Chem. Biol. 7 (2011) 639–647.